

University of Alberta

Titanacyclobutene and Cobalt(II) Phosphinimide Complexes

by

Jeremy Michael Anthony Gauthier

A thesis submitted to the Faculty of Graduate Studies and Research
in partial fulfillment of the requirements for the degree of

Doctor of Philosophy

Department of Chemistry

©Jeremy Michael Anthony Gauthier

Fall 2012

Edmonton, Alberta

Permission is hereby granted to the University of Alberta Libraries to reproduce single copies of this thesis and to lend or sell such copies for private, scholarly or scientific research purposes only. Where the thesis is converted to, or otherwise made available in digital form, the University of Alberta will advise potential users of the thesis of these terms.

The author reserves all other publication and other rights in association with the copyright in the thesis and, except as herein before provided, neither the thesis nor any substantial portion thereof may be printed or otherwise reproduced in any material form whatsoever without the author's prior written permission.

Abstract

This dissertation describes some advances that were made in the field of paramagnetic first-row transition metal complexes. Two independent topics will be discussed.

The first topic that will be discussed is the preparation and reactivity of titanacyclobutene complexes. Initially, the Stryker group discovered that titanacyclobutenes can be prepared by the SmI_2 -mediated coupling of propargyl halides, $[\text{Cp}_2\text{TiCl}]_2$, and alkyl halides. We have since improved on this procedure; this involves replacing $[\text{Cp}_2\text{TiCl}]_2$ with titanocene(IV) dichloride, and replacing SmI_2 with activated manganese powder. These conditions now give chemists the ability to prepare titanacyclobutenes from reagents that do not have to be kept under an inert atmosphere.

The second part of this topic discusses the conversion of titanacyclobutenes into 5-membered α -iminoenamine carbocycles. It has been demonstrated that titanacyclobutenes undergo double-insertion reactions with organic isonitriles which form carbocyclic-titanium enediamidate complexes however, successful reaction conditions for obtaining the titanium-free 5-membered carbocycles were unknown. We now report that 5-membered α -iminoenamine carbocycles can be obtained from carbocyclic-titanium enediamidate complexes through protonation, using 2,4,6-collidine hydrochloride.

The last part of this topic discusses our attempts to prepare titanacyclobutenes from titanium(IV) precursors which contain alternative ligands than cyclopentadienyl ligands. Trialkyl-phosphoranimide and diphenyl-sulfimide ligands are ideal candidates

for this chemistry, because the imide nitrogen of both ligands acts as a six-electron donor to the titanium(IV) center and the alkyl or aryl substituents provide suitable steric shielding to the metal center. This section discusses both the preparation and reactivity of three precursors: $((t\text{-bu})_3\text{PN})_2\text{TiCl}_2$, $\text{Cp}(\text{Ph}_2\text{SN})\text{TiCl}_2$ and $\text{Cp}^*(\text{Ph}_2\text{SN})\text{TiCl}_2$.

The second half of this document discusses our attempts to prepare late transition metal phosphinimide complexes; we were particularly interested in preparing analogues of cobaltocene (Cp_2Co) and half-sandwich cobalt(I) (CpCo) analogues. A series of new cobalt(II) phosphinimide complexes were prepared by the addition of lithium di(*i*-propyl)amide (LDA) to cobalt(II) phosphinimine coordination complexes. Continuing studies in this area revealed that cobalt(II) phosphinimide complexes are reactive towards electrophilic and acidic compounds; this led to the isolation of other new cobalt(II) phosphinimide clusters and cobalt(II) phosphinimine complexes.

Acknowledgements

The problem I always find with writing acknowledgements is that I always forget to mention everybody who has helped me in some fashion along my academic path, so my apologies if you are absent from this list.

I would like to begin by thanking my boss Dr. Jeff Stryker, who has not only given me enough freedom to explore the realm of organometallic chemistry in my own way, but has always been there to knock some sense into me before I take the wrong turn and accidentally drive off an “academic cliff”. In addition, I would also like to thank my committee members past and present: Dr. Josef Takats, Dr. Fred West, Dr. Martin Cowie, Dr. Rik Tykwinski, Dr. Natalia Semagina, Dr. Dennis Hall and Dr. Stephen MacNeil. To the past and present members of the Stryker group (a.k.a. the Stryker Bullies): thanks for making the work environment fun and enjoyable. From this list, I’d like to especially thank especially Bryan, Ross, Robin, Owen, Jeff Q., Houston, Kirsten, Devin and Colin. I’d also like to thank Dr. Masaki Morita for teaching me a lot about organometallic chemistry during my first two years.

To the members of the Gauthier clan: Mom, Dad and Andrew, you guys have been there for me more times that I can even think about, I love you all very much. I also appreciate your efforts in pretending to understand me when I talk about my research during family dinners on Sunday nights. I also want to acknowledge my Papa, John Howell, for being one of the first people to show me that taking an interest in how the world works (aka. being a nerd) is not exactly a bad thing. To the rest of my close immediate family: Uncle Leigh and Auntie Sheila, Uncle Leigh and Auntie Di, Nick and Emily, my Nana (R.I.P.), and Grandma G., you guys have been great! From the long list of close family friends, I would like to especially thank Neil Adesky, Len O’Connor and Jack Madro for helping me out when I needed that extra support. Of course I cannot forget my beautiful Sara! You have been a constant joy in my life over the past few years.

Finally to my closest friends: Andy T., Beck, Par, Jess, Alison, Matt L., Rich P., Nate and Lisel G., Ted. B, Mike R., Ed. H., Mary K., Katie B., Leo W., Matt B., Andy K., Paul

B., Bryan C., Albert Y., Blair B., Jessie Li, Scott A., Jesse H., Greg K., Andy D. and Sumayr S., and Mike and Sara W., you guys are alright I guess.

Table of Contents

Chapter 1: Synthesis, Reactivity and Characterization of Titanacyclobutene Complexes

1.1 Introduction	1
1.2 Physical Characteristics of titanacyclobutene complexes	1
1.2.1 Nomenclature	1
1.3 Characterization of titanacyclobutenes.....	2
1.4 Synthesis of titanacyclobutenes	
1.4.1 Titanacyclobutenes by [2+2] cycloaddition between alkynes and titanium alkylidene or vinylidene complexes	4
1.4.2 Preparation of titanacyclobutenes by γ -elimination of vinyl titanium complexes by concerted σ -bond metathesis or by 4π cyclization of titanium- vinylcarbene complexes.....	10
1.4.3 Addition of organic radicals to (η^3 -propargyl/allenyl)titanocene(III) complexes	14
1.5 Titanacyclobutene reactivity.....	20
1.5.1 Protonation.....	21
1.5.2 Transmetallation with organo main-group dihalide complexes.....	21
1.5.3 Reactivity of titanacyclobutene complexes with carbon-heteroatom multiple bonds	22
1.5.4 Retro [2+2] cycloaddition	29
1.5.5 4π electrocyclic ring opening.....	29
1.5.6 β -hydride elimination of titanacyclobutene complexes.....	32
1.6 Conclusions.....	32

Chapter 2: Advances in the Synthesis of Titanacyclobutene Complexes Prepared by Radical Alkylation of (η^3 -allenyl/propargyl)titanocene(III) Complexes

2.1 Introduction	34
2.2 Activated manganese powder as an alternative reductant to samarium(II) iodide	34

2.2.1 Evolution of the use of samarium(II) iodide in titanacyclobutene synthesis	34
2.2.2 Development of optimized reaction conditions using activated manganese powder	36
2.2.3 The role of activated manganese powder	42
2.2.4 Conclusions	47
2.3 Preparation of five-membered carbocycles from titanacyclobutene complexes	
2.3.1 Introduction	48
2.3.2 Results.....	50
2.3.3 Conclusions	55
2.4 Investigations into the preparation of bicyclic titanacyclobutene complexes using bi-functional substrates containing cyclic ethers as alkyl radical precursors.....	56
2.4.1 Introduction	56
2.4.2 Intermolecular radical coupling of oxetanes with (η^3 -propargyl)titanocene	58
2.4.3 Construction of the epoxide-containing substrates	62
2.4.4 Construction of the oxetane-containing bi-functional substrate	63
2.4.5 Attempted preparation of bicyclic titanacyclobutene complexes by intramolecular cyclizations involving oxirane and oxetane containing bi-functional substrates	65
2.4.6 Discussion	68
2.4.7 Conclusions	69

Chapter 3: A Review of Phosphinimide Containing Transition Metal Complexes

3.1 Introduction. The stabilizing capability of electron-rich transition metal ligands	72
3.2 Physical Characteristics of Phosphinimide ligands	73
3.2.1 Electronic properties of phosphinimide ligands.....	73

3.2.2 Steric and electronic properties of phosphinimide ligands	77
3.2.3 Physical methods for characterizing transition metal phosphinimide complexes	78
3.3 Synthetic methodologies towards preparing transition metal phosphinimide complexes	79
3.3.1 Phosphinimide complexes from phosphine addition to metal-nitrogen multiple bonds	79
3.3.2 Transition metal phosphinimide complexes by phosphine induced rearrangement of nitrogen containing ligands.....	82
3.3.3 Transition metal phosphinimide complexes by neutral σ -bond metathesis	84
3.2.4 Transition metal phosphinimide complexes by anionic σ -bond metathesis	94
3.2.5 Transition metal phosphinimide complexes from low-valent metals	95
3.3 Chelating bis(phosphinimide) complexes	98
3.4 Conclusions	99

Chapter 4: Alternatives to Cyclopentadienyl Ligands: Preparation of Titanium Phosphinimide and Sulfimide Compounds

4.1 Introduction to the use of titanium phosphinimide precursors to titanacyclobutene complexes	101
4.2 The chemistry of bis[tri(tert-butyl)phosphinimide]titanium(IV) dichloride	104
4.2.1 Preparation of bis[tri(tert-butyl)phosphinimide]titanium(IV) dichloride	104
4.3 Reactivity of bis[tri(t-butyl)phosphinimide]titanium(IV) dichloride	108
4.3.1 Attempted reduction of bis[tri(t-butyl)phosphinimide]titanium(IV) dichloride	108
4.3.2 Attempted preparation of titanacyclobutene complexes	109

4.3.3 Attempted preparation of titanacyclobutenes using samarium(II)-mediated coupling conditions.....	110
4.3.4 Attempted preparation of cationic titanium(IV) propargyl complexes	112
4.3.5 Conclusions	116
4.4 Sulfimide ligands as Cp mimics	117
4.4.1 Introduction to sulfimide ligands.....	117
4.4.2 Preparation of transition metal sulfimide complexes	118
4.4.3 Preparation of half-sandwich titanium(IV) sulfimide complexes	119
4.5 Reactivity of half-sandwich titanium(IV) sulfimide complexes	123
4.5.1 Reduction of 313 and 314	123
4.5.2 Attempted preparation of titanacyclobutene complexes	124
4.5.3 Alkylation of half-sandwich titanium(IV) sulfimide complexes	125
4.5.4 Addition of MeMgCl to 313 and 314	125
4.5.5 Addition of (allyl)magnesium chloride to 313 and 314	126
4.5.6 Addition of benzylmagnesium chloride.....	128
4.5.7 Conclusions	131
4.6 Conclusions and insights.....	132

Chapter 5: Preparation of Cobalt (II) Phosphinimide Compounds: Dehydrohalogenation of Cobalt(II) Phosphinimine Complexes

5.1 Introduction to selected uses of cobalt(I) cyclopentadienyl complexes	134
5.2 Introduction to cobalt(II) phosphinimide complexes	136
5.3 Preparation of bis(phosphinimine)- and mono(phosphinimide)cobalt(II) halide complexes	139
5.3.1 Cobalt(II) phosphinimine complexes from cobalt(II) halides and cobalt(II) acetate	139

5.3.2 Deprotonation of bis(phosphinimine)cobalt(II) halide and acetate complexes	145
5.3.3 Double deprotonation of bis(phosphinimine)cobalt(II) bromide complexes	150
5.3.4 Conclusions	151
5.4 Preparation of mono(phosphinimine)cobalt(II) acetylacetonate complexes	152
5.4.1 Preparation of mono(phosphinimine)cobalt(II) acetylacetonate precursors	152
5.4.2 Deprotonation of (triphenylphosphinimine)cobalt(II) acetylacetonate	155
5.4.3 Preparation of mono(tricyclohexylphosphinimide)- and mono(tri(t-butyl)phosphinimide)cobalt(II) complexes	158
5.5 Reactivity of mono(phosphinimide)cobalt(II) acetylacetonate complexes	159
5.5.1 Reduction using various low-valent metals	159
5.5.2 Thermal decomposition of the linear tri-cobalt(II) phosphinimide complex 366	160
5.5.3 Addition of electrophilic compounds to the linear tri-cobalt phosphinimide complex 366	162
5.5.4 Reactivity between acetoacetatocobalt(II) phosphinimide complexes and H-X bonds	166
5.6 Preparation of (phosphinimine)- and (phosphinimide)cobalt(II) thiolate complexes	170
5.7 Conclusions and future work	176

Chapter 6: Experimental section

6.1 General procedures	179
6.2 Instruments used	180

6.3 Materials used	180
6.4 Annotation of acyclic and cyclic assignments.....	181
6.5 Procedures	
6.5.1 Chapter 2 experimental section	181
6.5.2 Chapter 4 experimental section	211
6.5.3 Chapter 5 experimental section	217
Notes and References	232

Table of Figures

Figure 1.1: Labeling of the titanacyclobutene core	1
Figure 1.2: Common crystallographic properties and ^1H , and ^{13}C NMR chemical shifts of titanacyclobutene complexes	2
Figure 1.3: Calculated (top) and representative depictions (bottom) of the bonding EHMO's of "bent metallocenes"	17
Figure 1.4: EHMO diagram of (η^3 -allyl)titanocene(III)	18
Figure 1.5: Hypothetical EHMO diagram of (η^3 -propargyl)titanocene(III)	18
Figure 2.1: Selected ^1H and ^{13}C NMR chemical shifts of 144	42
Figure 2.2: Selected ^1H and ^{13}C NMR chemical shifts of 155 and 156	51
Figure 2.3: Selected ^1H and ^{13}C NMR chemical shifts of 160	54
Figure 2.4: Representation of the steric interactions between o-phenyl and o-methyl substituents of 160 that result in broadening of the corresponding ^1H NMR signals by restricting rotation	54
Figure 2.5: Comparison of the selected ^1H and ^{13}C NMR chemical shifts of 160 and 171	61
Figure 2.6: Synthetic targets	61
Figure 2.7: ^1H and ^{13}C NMR chemical shifts of compounds 191 and 192	66
Figure 3.1: Calculated molecular orbitals of CpTiCl_3	72
Figure 3.2: Alternative ligand systems investigated as isolobal analogues for Cp ligands	73
Figure 3.3: Bonding molecular orbitals associated with dipolar resonance of phosphinimide ligands	73
Figure 3.4: Calculated molecular orbital diagram of $\text{H}_3\text{P}=\text{N}-\text{TiCl}_3$	74
Figure 3.5: Different bridging modes of phosphinimide ligands in bi- and tri-molecular complexes	76

Figure 3.6: A comparison between the Tolman’s cone angles, plus the measured distances between the titanium atom and the steric bulk of tri(<i>t</i> -butyl)phosphinimide ligands, and the unsubstituted Cp ligand	77
Figure 3.7: Selected bond lengths and angles of half-sandwich titanium phosphinimide complexes 204 to 210	78
Figure 3.8: Proposed mechanism of pseudo-Hoffmann rearrangement	98
Figure 4.1: Perspective view of 296 showing selected atom labelling scheme.....	106
Figure 4.2: Selected bond distances and angles of 296	106
Figure 4.3: Phosphinimide and sulfimide ligands as isolobal analogues to Cp ligands	118
Figure 4.4: Synthetic targets 313 , 314 , 315 and 316	118
Figure 4.5: Perspective view of 313 showing selected atom labelling scheme.....	122
Figure 4.6: Perspective view of 314 showing selected atom labelling scheme.....	122
Figure 4.7: Selected bond distances of 313 , 314 , and 204	123
Figure 4.8: Selected ¹ H NMR data from 328 , 329 and 330	129
Figure 4.9: Perspective view of 329 showing selected atom labelling scheme.....	130
Figure 4.10: Perspective view of 330 showing selected atom labelling scheme.....	130
Figure 4.11: Selected interatomic distances and angles of 329 and 330	131
Figure 5.1: Selected interatomic distances and angles of complete cobalt(II) phosphinimide heterocubane clusters 344 to 349	137
Figure 5.2: Perspective view of 356 with key atoms labelled	140
Figure 5.3: Perspective view of 357 with key atoms labelled	140
Figure 5.4: Perspective view of 358 with key atoms labelled	142
Figure 5.5: Perspective view of 359 with key atoms labelled	142
Figure 5.6: Selected interatomic distances and angles of cobalt(II) phosphinimine complexes 356-359 and “free” phosphinimine ligands, with standard deviations in parentheses	143
Figure 5.7: Perspective view of 361 with key atoms labelled	147

Figure 5.8: Selected interatomic distances and angles of 361	147
Figure 5.9: Perspective view of 363 with key atoms labelled	149
Figure 5.10: Selected interatomic distances and angles of 363	149
Figure 5.11: Perspective view of 365 with key atoms labelled	154
Figure 5.12: Selected Interatomic distances and angles of 365	154
Figure 5.13: Perspective view of 366 with key atoms labelled	156
Figure 5.14: Selected interatomic distances and angles of 366	156
Figure 5.15: Perspective view of 371 with key atoms labelled	161
Figure 5.16: Selected interatomic distances and angles of 371	161
Figure 5.17: Perspective view of 373 with key atoms labelled	165
Figure 5.18: Selected interatomic distances and angles of 373	165
Figure 5.19: Perspective view of 374 with key atoms labelled	167
Figure 5.20: Selected interatomic distances and angles of 374	167
Figure 5.22: Perspective view of 376 with key atoms labelled	168
Figure 5.23: Selected interatomic distances and angles of 376	169
Figure 5.24: Perspective view of 383 with key atoms labelled	174
Figure 5.25: Selected interatomic distances and angles of 383	175

Table of Schemes

Scheme 1.1	3
Scheme 1.2	4
Scheme 1.3	5
Scheme 1.4	6
Scheme 1.5	7
Scheme 1.6	7
Scheme 1.7	8
Scheme 1.8	9
Scheme 1.9	9
Scheme 1.10.....	11
Scheme 1.11.....	11
Scheme 1.12.....	12
Scheme 1.13.....	13
Scheme 1.14.....	13
Scheme 1.15.....	19
Scheme 1.16.....	20
Scheme 1.17.....	21
Scheme 1.18.....	22
Scheme 1.19.....	23
Scheme 1.20.....	23
Scheme 1.21.....	24
Scheme 1.22.....	25
Scheme 1.23.....	25
Scheme 1.24.....	26

Scheme 1.25	27
Scheme 1.26	28
Scheme 1.27	29
Scheme 1.28	30
Scheme 1.29	31
Scheme 1.30	32
Scheme 2.1	37
Scheme 2.2	38
Scheme 2.3	38
Scheme 2.4	39
Scheme 2.5	40
Scheme 2.6	41
Scheme 2.7	44
Scheme 2.8	45
Scheme 2.9	46
Scheme 2.10	47
Scheme 2.11	48
Scheme 2.12	49
Scheme 2.13	52
Scheme 2.14	52
Scheme 2.15	55
Scheme 2.16	56
Scheme 2.17	57
Scheme 2.18	57
Scheme 2.19	60

Scheme 2.20	62
Scheme 2.21	63
Scheme 2.22	64
Scheme 2.23	64
Scheme 2.24	68
Scheme 3.1	71
Scheme 3.2	80
Scheme 3.3	82
Scheme 3.4	83
Scheme 3.5	84
Scheme 3.6	85
Scheme 3.7	86
Scheme 3.8	86
Scheme 3.9	87
Scheme 3.10	90
Scheme 3.11	93
Scheme 3.12	96
Scheme 3.13	99
Scheme 4.1	101
Scheme 4.2	102
Scheme 4.3	103
Scheme 4.4	105
Scheme 4.5	110
Scheme 4.6	113
Scheme 4.7	115

Scheme 4.8	115
Scheme 4.9	119
Scheme 4.10	120
Scheme 4.11	121
Scheme 4.12	125
Scheme 4.13.....	126
Scheme 4.14	126
Scheme 4.15	128
Scheme 4.16	132
Scheme 5.1	135
Scheme 5.2	137
Scheme 5.3	138
Scheme 5.4	145
Scheme 5.5	148
Scheme 5.6	162
Scheme 5.7	171
Scheme 5.8	172
Scheme 5.9	174

List of Common Abbreviations

Å	Angstroms
acac	Acetylacetonate
APT	Attached Proton Test
Ar	Aryl
atm	Atmospheres
Bn	Benzyl
Bu	Butyl
Chloramine-T	Sodium N-chloro-tosylamide
cm ⁻¹	Wavenumbers
COD	Cyclooctadiene
collidine	2,4,5-trimethylpyridine
COSY	Correlated Spectroscopy
Cp	Cyclopentadienyl
Cp*	Pentamethylcyclopentadienyl
Cy	Cyclohexyl
°C	Degrees celcius
d	Days
d	Doublet
DABCO	1,4-diazabicyclo[2.2.2]octane
dba	Dibenzylideneacetone
dd	Doublet of doublets

ddd	Doublet of doublet of doublets
dddd	Doublet of doublet of doublet of doublets
ddt	Doublet of doublet of triplets
DFT	Density functional theory
DMDO	Dimethyldioxirane
DME	Dimethoxyethane
dq	Doublet of quartets
dsept	Doublet of septets
dt	Doublet of triplets
dtd	Doublet of triplet of doublets
e ⁻	Electron
EHMO	Extended Huckel molecular orbital
EI-MS	Electron-impact mass-spectrometry
equiv.	Equivalents
ESI-MS	Electrospray-ionization mass-spectrometry
Et	Ethyl
η	Eta (Hapticity)
g	Grams
h	Hours
HMBC	Heteroatom multiple bond coherence
HMPA	Hexamethylphosphoramide
HMQC	Heteroatom multiple quantum coherence

Hz	Hertz
<i>l</i> or <i>i</i> -	Iso-
IMes	N,N'-di(2,4,6-trimethylbenzyl)imidazole
IR	Infrared
kcal	Kilocalories
L	Litres
L _n	Ligand
LDA	Lithium di- <i>i</i> -propylamide
M	Metal
μ	Mu (Bridging mode)
<i>m</i> -CPBA	<i>meta</i> -Chloroperbenzoic acid
MAO	Methylaluminoxane
Me	Methyl
mg	Milligrams
MHz	Megahertz
min	Minutes
mL	Millilitre
μL	Microliters
mmHg	Millimeters of mercury
mmol	Millimoles
mol	Moles
ⁿ or <i>n</i> -	Linear chain

NHC	N-heterocyclic carbene
NMR	Nuclear magnetic resonance
ν	Nu (Frequency cm^{-1})
<i>o</i> -	<i>Ortho</i> -
OAc	Acetate
pent	pentet
ppm	Parts per million
Ph	Phenyl
pm	Picometers
Pr	Propyl
psig	Pounds per square inch gauge
q	quartet
R	Generic alkyl or aryl substituent
[R]	Reducing agent
rt	Room temperature
sept	Septet
SOMO	Semi-occupied molecular orbital
^t or <i>tert</i> -	Tertiary
THF	Tetrahydrofuran
TMS	Trimethylsilyl
X	Halide

Chapter 1: Synthesis, Reactivity and Characterization of Titanacyclobutene Complexes

1.1 Introduction

The use of titanacyclobutene complexes as intermediates in organic synthesis is rather undeveloped; this is because of the limited methodologies that are reported for converting titanacyclobutene complexes into useful organic substrates. Various methods of preparing titanacyclobutene complexes are known, and demonstrate that these potentially important intermediates can be obtained from simple starting materials. The *chemistry* of titanacyclobutene complexes has been one of the topics included in a recent review.¹ This chapter provides a general introduction to the physical characteristics, methods of preparation and modes of reactivity of titanacyclobutene complexes.

1.2 Physical characteristics of titanacyclobutene Complexes

1.2.1 Nomenclature

The nomenclature for titanacyclobutene complexes, according to IUPAC rules, is the same used for heterocyclic compounds (Figure 1.1).² The titanium is considered highest priority and is labeled as the one-position; this is followed by the olefinic carbons and finally the aliphatic carbon. A less formal set of nomenclature is also used by assigning a letter of the Greek alphabet to the relative position the carbon atoms from the titanium atom in order of connectivity. Using this nomenclature, the C2-, C3- and C4- carbons atoms are referred to as the α , β and γ -carbons.

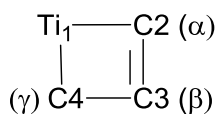


Figure 1.1: Labelling of the titanacyclobutene core.

A number of titanacyclobutene complexes are characterized by X-ray crystallography (see Figure 1.2). An obtuse C-C bond angle is observed for the ring carbons; this might be considered strange due to unfavorable ring strain gained by this geometric arrangement in cyclobutene compounds. Titanacyclobutene complexes are often drawn in an almost perfect square appearance, but in reality, most metallacyclobutene complexes favorably adopt this distorted geometry. Typical structural data of metallacyclobutenes reveals long metal-carbon bond lengths and a smaller C-M-C bond angle; this compensates for the large C-C-C bond angle, which is close to ideal for olefinic carbons.

1.3 Characterization of titanacyclobutenes

The purpose of this section is to highlight some of the modern techniques used to identify titanacyclobutene complexes. The results discussed in this section are based on a selection of reported titanacyclobutene complexes from several references and are summarized in Figure 1.2.³⁻⁷

Hard mass spectrometric methods such as electron impact ionization are used to obtain the molecular ion and conversely the molecular formula of titanacyclobutene complexes. Surprisingly enough, the molecular ion or evidence of titanacyclobutene fragmentation has not been detected when using softer volatilization methods such as chemical ionization or electrospray.

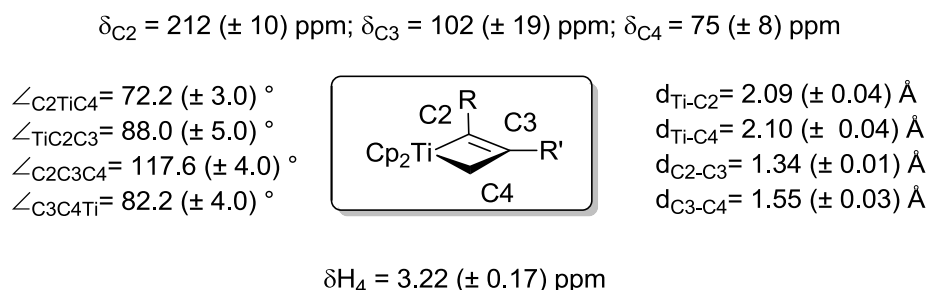
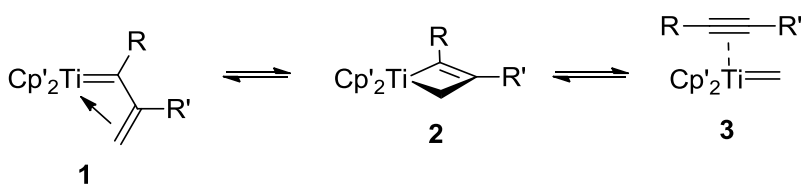


Figure 1.2: Common Crystallographic Properties and ^1H , and ^{13}C NMR chemical shifts of titanacyclobutene complexes.

NMR spectroscopy is also a valuable tool in identifying titanacyclobutene complexes; this is because unique chemical shifts are observed for both the carbon and hydrogen atoms in the ring. The methylene protons on the saturated γ -carbon are typically observed by ^1H NMR spectroscopy between 3.0-3.3 ppm; the downfield shift is attributed to the protons being both allylic and adjacent to the electronically deficient titanium center. Geminal coupling between the methylene protons is not typically observed because of the symmetry of the planar titanacyclobutene ring. Long range “W-coupling” is often observed between the methylene group and protons on the α -carbon substituent. Long range coupling is not observed to substituents on the β -carbon.

Titanacyclobutene complexes are identified by ^{13}C NMR spectroscopy, where the chemical shifts of the C2, C3 and C4-carbons are characteristically observed between 205-213, 91-98, and 69-76 ppm respectively. The chemical shift of the α -carbon appears significantly downfield, closer to the chemical shift of isolated titanium alkylidene complexes, which are typically observed around 280 ppm.⁸ The downfield chemical shift is attributed to contributions from a titanium-vinylcarbene resonance structure **1** (Scheme 1.1). The chemical shift of the β -carbon is also interesting because this signal can be mistaken for an alkyne carbon also observed in this range. Significant contributions from the alkyne-coordinated titanium alkylidene complex **3**, provides an oversimplified rationale for why the β -carbon is found in this range (Scheme 1.1).

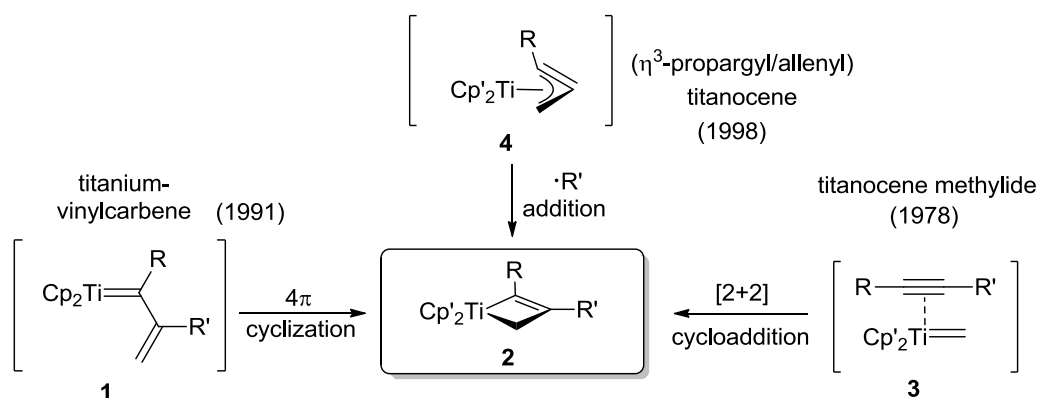
Scheme 1.1



1.4 Synthesis of titanacyclobutenes

Titanacyclobutene complexes were first reported in 1969;⁹ various groups have since explored different approaches for preparing these four-membered titanium-containing rings (Scheme 1.2).¹ In general, titanacyclobutenes are prepared through three main organotitanium intermediates: titanium alkylidenes (**3**), titanium-vinylcarbenes (**1**) and (η^3 -propargyl)titanocene (**4**) complexes. In addition to isolable examples, the organic products obtained from reactions involving transient titanacyclobutene complexes are also discussed.

Scheme 1.2



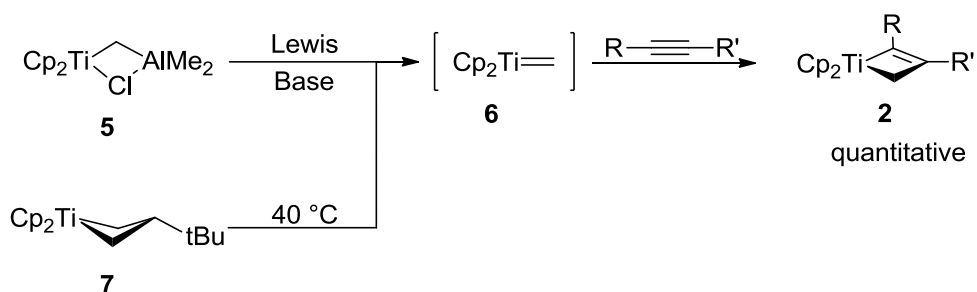
1.4.1 Titanacyclobutenes by [2+2] cycloaddition between alkynes and titanium alkylidene or vinylidene complexes

Titanium alkylidene complexes are reactive intermediates in many titanium-mediated organic transformations,^{10,11} which include olefin metathesis, carbonyl methylenation, ring-opening polymerization of olefins and generation of titanium enolates.

Various attempts to intercept the highly reactive titanium alkylidene intermediates led to the addition of internal alkynes, affording titanacyclobutene complexes in near quantitative yields (Scheme 1.3). Initial investigations performed

using the methylene bridged bimetallic species **5**, commonly known as “Tebbe’s reagent”, was the earliest example of an isolated and characterized monomeric titanacyclobutene complex.^{12,13} It was later discovered by Grubbs, that gentle thermolysis of β -substituted titanacyclobutane complexes such as **7** affords titanacyclobutenes by generation of the titanium alkylidene intermediate **6** by [2+2] cyclo-reversion.¹⁴

Scheme 1.3

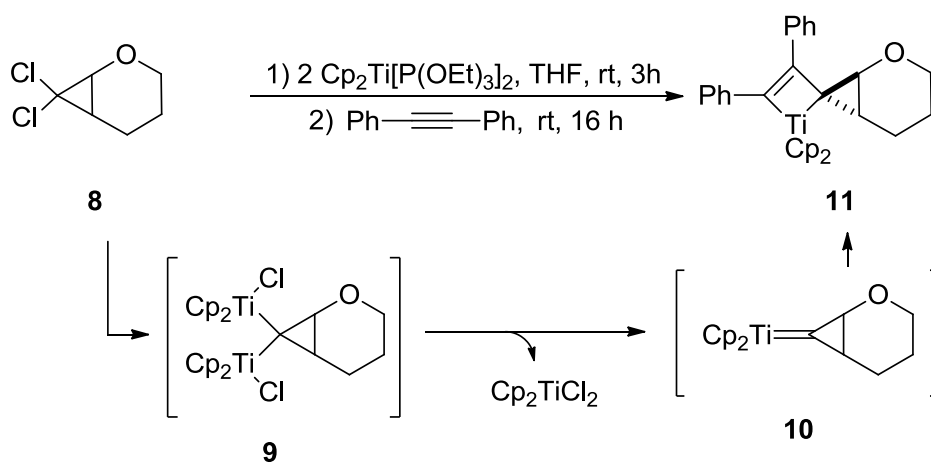


The accepted mechanism for the formation of titanacyclobutenes from titanium alkylidene complexes and alkynes is by a formal [2+2] cycloaddition. This process occurs because of correct symmetry overlap between filled titanium alkylidene orbitals and the anti-bonding orbitals of the alkyne.¹⁵ The word “formal” is used because the reaction proceeds in a step-wise process initiated by coordination of the alkyne to the titanium center, whereas traditional [2+2] cycloaddition reactions do not involve pre-coordination of the independent substrates before cyclization.¹⁶

Takeda reported that 4,4-spirocyclopropyl titanacyclobutene complexes such as **11** are obtained by adding two equivalents of titanocene(II) bis(triethylphosphite) to a solution containing 3,3-dichlorocyclopropane **8** and an internal alkyne (Scheme **1.4**).¹⁷ The proposed mechanism of this reaction occurs through two intermediates. The first intermediate is the methylene bridged bis(titanocene(IV) chloride) intermediate **9**, which is formed through the oxidative insertion of the low-valent titanium(II) species into the two carbon-chloride bonds. The second intermediate in this reaction is the

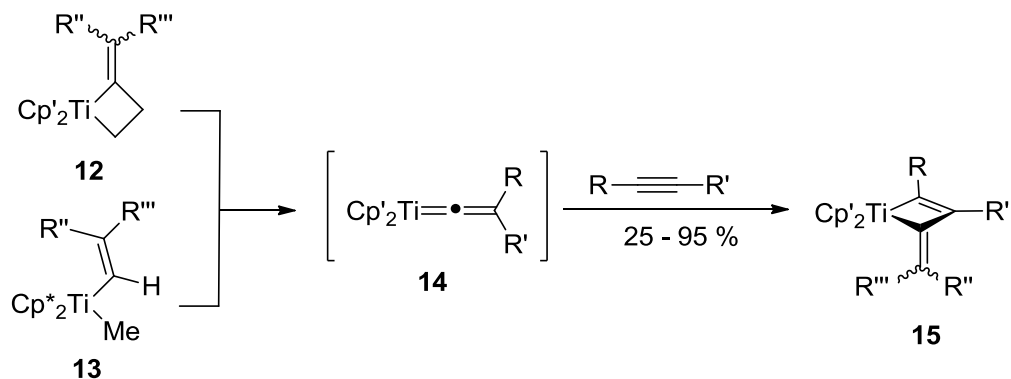
titanium alkylidene **10**, which is formed through the collapse of **9** by expelling titanocene(IV) dichloride; this intermediate then undergoes the formal [2+2] cycloaddition with diphenylacetylene and yield the desired titanacyclobutene product **11**. Takeda and co-workers proposed a similar mechanism when studying the reactivity between titanocene(II) bis(triethylphosphite) (2 equivalents), cyclobutyl-1,1-thioacetal compounds, and internal alkynes. Although only vinylcyclobutenes were obtained, Takeda *et al.*, proposed that the products arose from the decomposition of putative titanacyclobutene intermediates by β -hydride elimination;¹⁸ this however will be discussed later.

Scheme 1.4



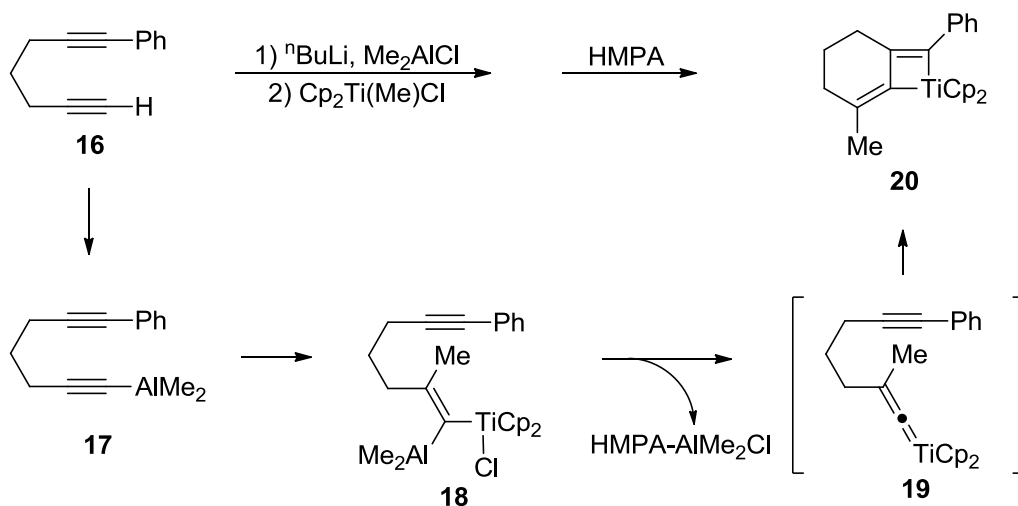
α -Methylenetitanacyclobutene complexes (**15**) have been prepared similarly by the [2+2] cycloaddition between titanium vinylidene intermediate **14** and internal alkynes (Scheme **1.5**). Titanium vinylidene intermediates (**14**) are generated by three methods, the first two involve thermal [2+2] cyclo-reversion of α -methylenetitanacyclobutane complexes¹⁹ (**12**) and α -elimination from alkylvinyltitanocene complexes (**13**).²⁰

Scheme 1.5



The third method involves elimination of dimethylaluminum chloride from (dimethylaluminovinyl)titanium chloride complexes (**18**) by addition of Lewis Bases; these reactions also occur by a α -elimination (Scheme **1.6**).²¹ This method was used to construct the bicyclic α -methylene-titanacyclobutene complex **20** from bi-functional substrate **16**. In this example, HMPA forms an insoluble Lewis acid-base adduct with dimethylaluminum chloride; thus promoting the elimination of dimethylaluminum chloride from intermediate **18**.

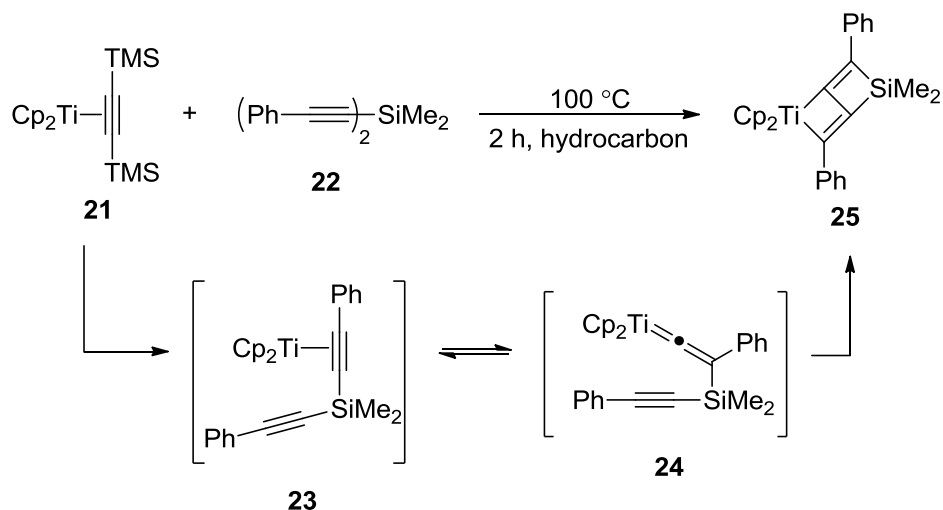
Scheme 1.6



Other examples of α -methylene-titanacyclobutenes are “zig-zag” complexes which incorporate two fused titanacyclobutene rings, or a titanacyclobutene ring that is fused to a silacyclobutene ring such as compound **25** (Scheme 1.7). These complexes were obtained from either oxidative dimerization of titanocene(II) alkyne complexes,^{9,22} or oxidative insertion of low valent titanocene(II) precursors into di(ethynyl)silanes²³ and 1,3-butadiynes.²⁴

Various mechanisms have been proposed to explain the formation of these products, but none have been proven experimentally. A relevant mechanism proposed for the formation of **25** involves a titanium vinylidene intermediate (**24**), which is generated *in situ* by a titanium-mediated alkyne-vinylidene rearrangement from **23**.^{25,26}

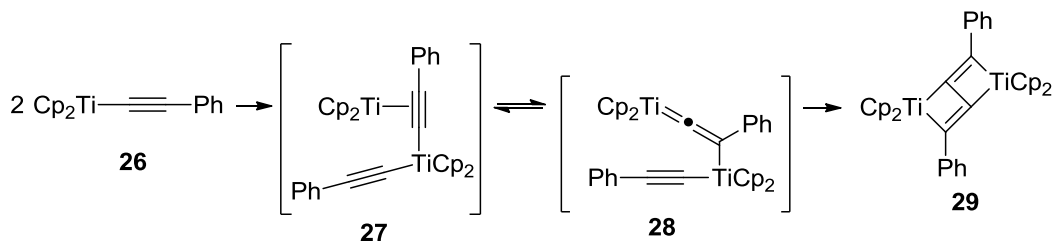
Scheme 1.7



The above pathway can also be used to rationalize the formation of the “zig-zag” complex **29** from 2 equivalents of titanocene(III) acetylide **26**. One can speculate that a redox driven disproportionation of the titanium acetylide **26** would initially afford the titanocene-coordinated titanocene(IV) bis(acetylide) intermediate **27**. Subsequent titanium-mediated alkyne-vinylidene rearrangement and [2+2] cycloaddition would then afford the desired product **29** (Scheme 1.8). This mechanism is of course only speculative at this point, however, this pathway is considered because of 1) the

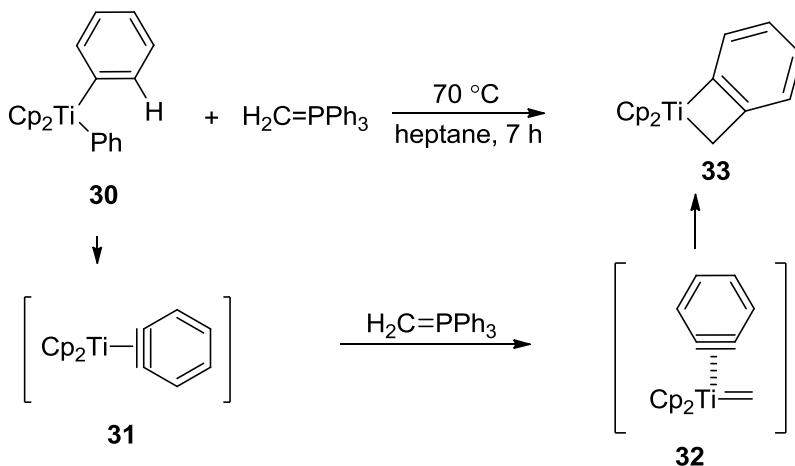
relevance to this section, and 2) the reports of transition metal mediated acetylene-
vinylidene arrangements that are present in the literature.^{24,25}

Scheme 1.8



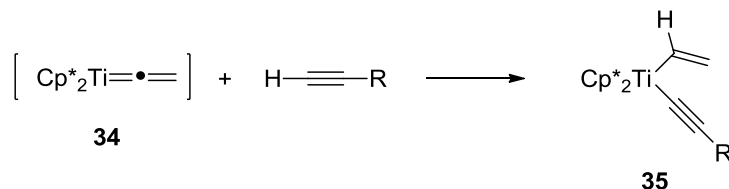
Titanacyclobutabenzene complexes such as **33** have been isolated from mixtures containing diphenyltitanocene (**30**) and triphenylphosphine methylene (Scheme 1.9).²⁷ The mechanism of this reaction involves a (η^2 -benzyne)titanocene intermediate (**31**) that is generated by the liberation of benzene from **30** by β -hydride elimination. Transfer of the methylene group from triphenylphosphine methylene then occurs forming the (η^2 -benzyne)titanium alkylidene intermediate **32** that cyclizes affording **33**. Evidence supporting the aryne mechanism in this example has been supported by mixtures of regiomer titanacyclobutabenzene products that were obtained when using bis(*p*-tolyl)titanocene(IV). Titanacyclobutabenzene complexes such as **33** have also been prepared by addition of double Grignard reagents derived from *ortho*-bromobenzyl chloride to titanocene dichloride.²⁷

Scheme 1.9



A few limitations exist when using this methodology to prepare titanacyclobutene complexes. The first limitation is that complete control over the regioselectivity in the formal [2+2] cycloaddition addition is difficult, as unsymmetrical alkynes often give mixtures of titanacyclobutene complexes at the C2 and C3-positions. The second limitation is that terminal alkynes are not generally compatible with titanium alkylidene or vinylidene complexes, which results in the deprotonation of the alkyne and subsequent formation of vinyltitanocene acetylide complexes (**35**) (Equation 1.1).²⁰ Despite these limitations, titanium alkylidene intermediates constitute an effective method for preparing a wide variety of substituted titanacyclobutene complexes.

Equation 1.1



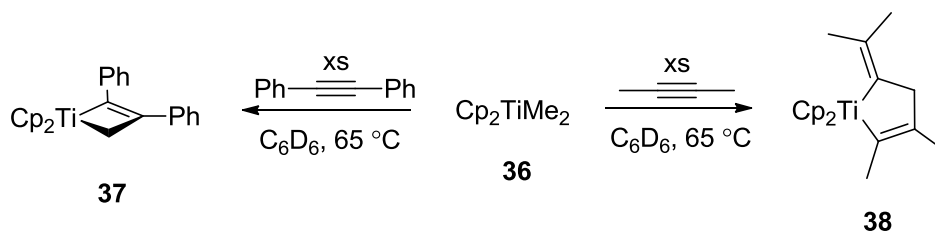
1.4.2 Preparation of titanacyclobutenes by γ -elimination of vinyl titanium complexes, by concerted σ -bond metathesis, or by 4π cyclization of titanium-vinylcarbene complexes

Titanacyclobutene complexes have been obtained from titanium alkylvinyl complexes that have readily accessible γ -hydrogen atoms on the vinyl substituent, as well as titanium-vinylcarbene complexes. Both processes discussed in this section are similar because titanium-vinylcarbenes are the intermediates formed by step-wise γ -elimination reactions of titanium alkylvinyl complexes. In most cases, it is difficult to differentiate between the two mechanisms.

Titanacyclobutene complexes can be obtained by addition of internal alkynes to dimethyltitanocene (**26**), commonly known as the "Petasis' reagent" (Scheme 1.10).²⁸ Although initially proposed to occur through a titanium alkylidene intermediate, an

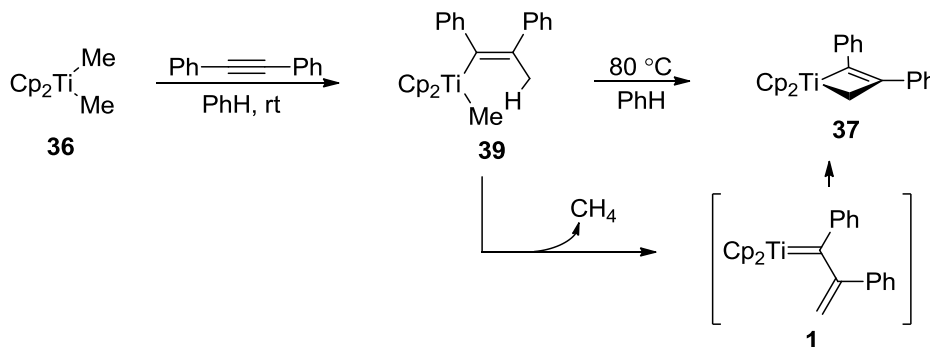
alternative product **38** obtained by the use of 2-butyne established that the reaction is occurring by another pathway.²⁹

Scheme 1.10



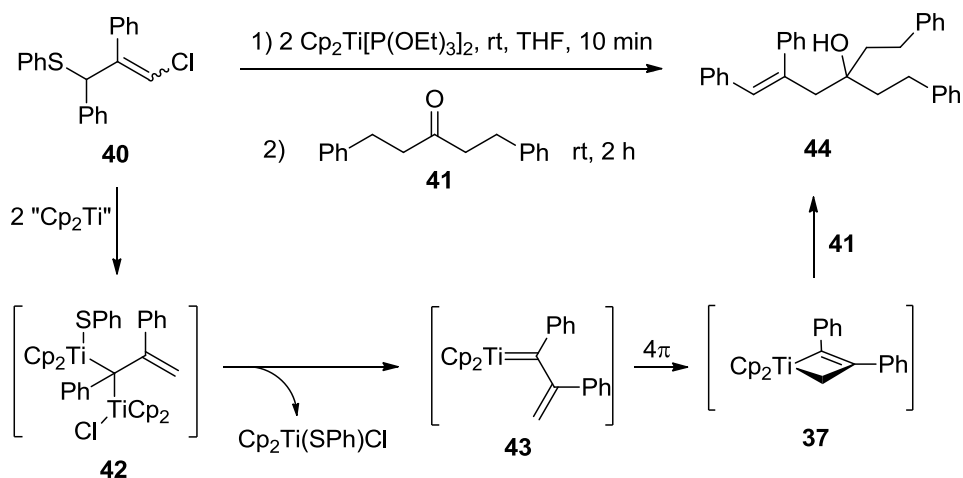
In order to probe the mechanism, diphenylacetylene was added to **36** at room temperature, which afforded a titanium alkylvinyl complex **39** almost quantitatively. This was presumably formed by carbometallation of diphenylacetylene (Scheme 1.11). Upon treatment of **39** at elevated temperatures, titanacyclobutene **37** was obtained quantitatively.³⁰ Based on this evidence, the conversion of **39** to **37** can proceed by either concerted γ -hydride elimination, or through a titanium-vinylcarbene intermediate (**1**); however, no mechanistic evidence is provided that supports either pathway.

Scheme 1.11



Takeda and co-workers were able to isolate homoallylic alcohols through the combination of titanocene(II) bis(triethylphosphite) (2 equivalents), γ -chloroallylic sulfides, and symmetrical ketone **41** (Scheme 1.12).³¹ Similar to the example in Scheme 1.4, Takeda proposes that the homoallylic alcohol **44** is formed from the insertion of the saturated carbon (C2) of putative titanacyclobutene intermediate (**37**) to ketone **41**; the reactivity between titanacyclobutenes and carbonyl compounds will be discussed later. Although Takeda provides no mechanistic insight for this transformation, previous evidence suggests that the two equivalents of titanocene(II) bis(triethylphosphite) will oxidatively insert into both C-S and C-Cl bonds of the γ -chloroallylic sulfide **40**, thus generating a methylene bridged bis(titanocene(IV) chloride) complex (**42**). This intermediate then collapses to titanium-vinylcarbene intermediate (**43**) by extruding $\text{Cp}_2\text{Ti}(\text{SPh})\text{Cl}$; subsequent 4π electrocyclization then affords the titanacyclobutene **37**.

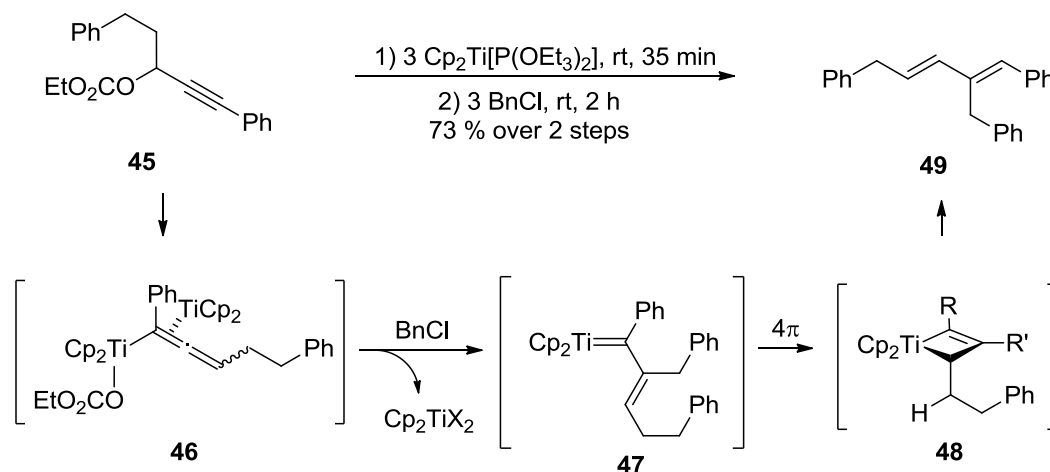
Scheme 1.12



Another class of organic compounds that is obtained from titanacyclobutene intermediates is conjugated dienes. These are obtained using a two-step procedure involving first, the addition of two equivalents of titanocene(II) bis(triethylphosphite) to a solution containing a propargyl carbonate; and second the addition of an alkyl halide (Scheme 1.13). The conjugated diene products are generated through β -hydride

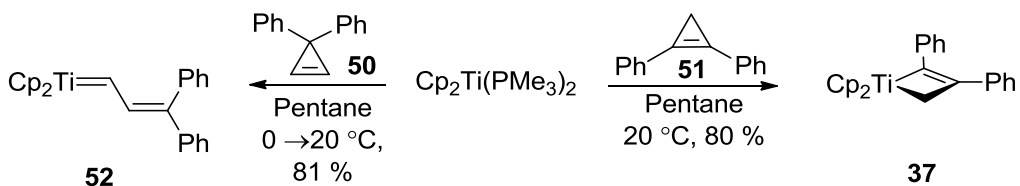
elimination of the putative titanacyclobutene intermediate. Similar to Scheme 1.12, a titanium-vinylcarbene intermediate (**47**) is generated during the reaction. However, this intermediate is formed by the addition of the alkyl halide to the initial titanocene-coordinated titanium(VI) allene complex (**46**).

Scheme 1.13



One final example involving the formation of titanium-vinylcarbene complexes is via the reactivity between titanocene(II) bis(trimethylphosphine) and disubstituted cyclopropenes **50** and **51** (Scheme 1.14).^{8,32} The mechanism of this reaction is not fully understood; however, a low valent titanocene(II) precursor is required because no reaction occurs in its absence. The formation of both products however, suggests that the mechanism involves a titanium-vinylcarbene intermediate.

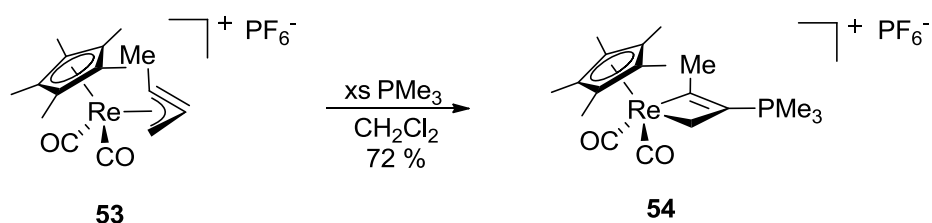
Scheme 1.14



1.4.3 Addition of organic radicals to (η^3 -propargyl/allenyl)titanocene(III) complexes

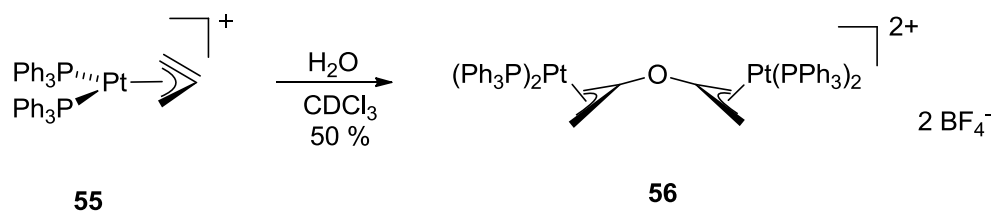
The addition of nucleophiles to the central carbon of (η^3 -propargyl/allenyl) transition metal complexes of platinum,³³ rhenium,³⁴⁻³⁶ molybdenum,³⁷ chromium³⁶ and titanium³⁸ is known. Similar reactivity has also been observed in (η^3 -allyl) metal complexes of molybdenum,³⁹ tungsten,³⁹ rhodium,^{40,41} iridium,^{41,42} zirconium⁴³ and titanium;⁴³ in the majority of cases however, addition to the terminal end of the allyl ligands is highly favored. In some cases, uncharged nucleophiles will attack (η^3 -propargyl/allenyl) transition metal complexes; one example by Casey (Equation 1.2) involves the addition of trimethyl phosphine to the central carbon of a cationic (η^3 -propargyl/allenyl)rhenium complex **53**.³⁵

Equation 1.2



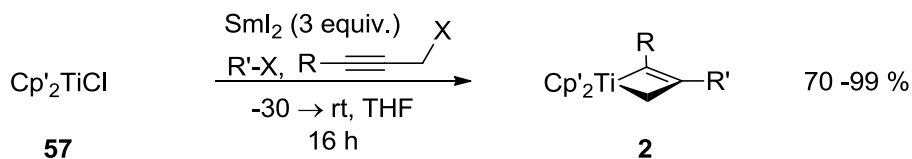
Nucleophiles bearing acidic protons react with (η^3 -propargyl/allenyl) metal complexes to afford β -substituted (η^3 -allyl) transition metal complexes (Equation 1.3). An example of this reactivity is the formation of the oxo-bridged bis(β -allyl)platinum complex **56** by the addition of water to (η^3 -propargyl/allenyl)platinum bis(triphenylphosphine) **55**.⁴⁴

Equation 1.3



The addition of organic radicals to (η^3 -propargyl/allenyl) metal complexes was exceptionally rare (Equation 1.4). This methodology is one of the main focuses of the Stryker group as is the study of radical additions to (η^3 -allyl)titanocene(III) complexes.⁴⁵⁻
⁴⁷ A variety of isolable titanacyclobutene complexes with the general formula **2** are prepared in good to exceptional yields via a one-pot, samarium(II)-mediated coupling of substituted titanocene(III) chlorides **57**, propargyl halides, and alkyl halides.^{6,48} Initial investigations performed used (decamethyl)titanocene(III) chloride as the titanium(III) precursor, where titanacyclobutene complexes are obtained in spectroscopic purity and in high yields. Earlier attempts to use either Cp or ^tBuCp ligands results in impure products and are obtained in poor yields, however, a modified procedure was developed to obtain titanacyclobutene complexes in good yield using titanocene dichloride. The details regarding the modified reaction conditions will be discussed in greater detail in Chapter 2.

Equation 1.4



Cp' = Cp*, ^tBuCp, Cp

R = Ph, (4-OMe)Ph, ^tBu, TMS, Me, H

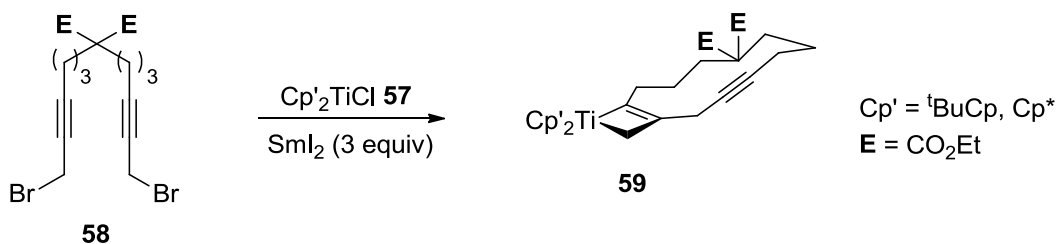
R' = alkyl = Bn, ⁱPr, Cy, ^tBu, CH₂TMS, CH₂C≡CPh,

allyl = CH₂C(Me)CH₂, CH₂CHC(Me)₂

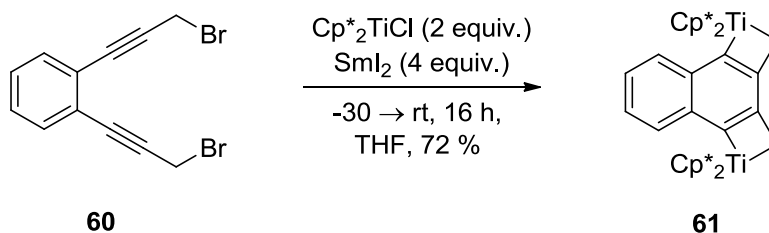
alkynyl = CH₂C≡CPh, CH₂C≡CMe

alkenyl = C(Ph)CH₂, C(Me)CH₂, C(Me)CH(Me)

Bicyclic-titanacyclobutene complexes are obtained when using bi-functional propargyl halides bearing halo-alkyl tethers of various lengths (Equation 1.5). Bicyclic titanacyclobutenes with B-ring sizes as large as twelve carbons such as **59** were isolated and characterized using ^tBuCp and Cp* ligands; although the full series is not complete.^{4,49} Thus far when using Cp ligands, bicyclic titanacyclobutene complexes with B-rings as large as eight carbons have been prepared, but expansion of the substrate scope is being investigated by use of alternative reaction conditions.

Equation 1.5

Titanacyclobutabenzene complexes such as compound **61** have also been prepared by this methodology through the dimerization of two tethered (η^3 -propargyl)titanocene(III) complexes (Equation 1.6).⁴⁸ The formation of titanacyclobutabenzene complexes is attributed to the stabilization gained by formation of an extended naphthalene π -system. The dimerization of acyclic (η^3 -propargyl)titanocene(III) complexes has only been observed in specific cases, but was recently discovered to be favored at low temperature.⁴⁹

Equation 1.6

To understand the regioselectivity of radical additions to the central carbon of the propargyl ligand, a discussion based on the calculated molecular orbitals of (η^3 -allyl)titanocene complexes by Hoffmann, and later by Green, must first be presented.^{50,51} Based on computational results, the calculated $4a_1$, $2b_1$ and $3a_1$ frontier orbitals of bent titanocene compounds (Figure 1.3) are of correct symmetry to interact with the π -system of allyl ligands.

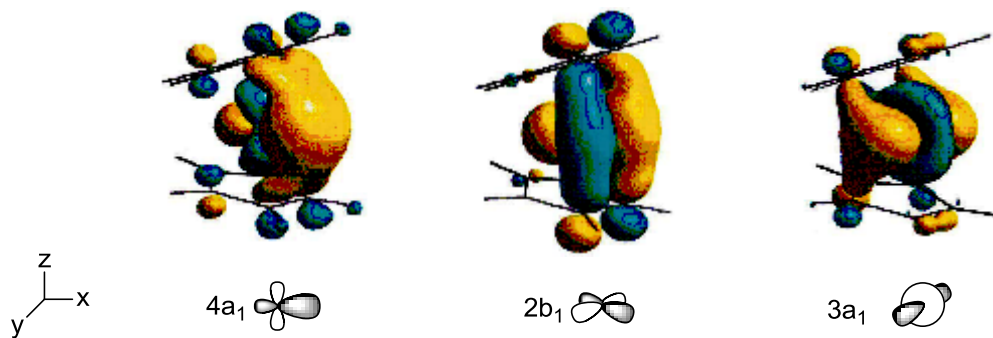


Figure 1.3: Calculated (top) and representative depictions (bottom) of the bonding EHMO's of "bent metallocenes".

The frontier molecular orbitals of (η^3 -allyl)titanocene(III) **62** have been calculated at the Extended Huckel molecular orbital (EHMO) level of theory (Figure 1.4). A low lying semi-occupied molecular orbital (SOMO) at the bond frontier is reported to consist of a combination of the 3a₁ orbital from the bent titanocene and the ψ_3^* anti-bonding orbital of the allyl ligand. A closer examination of the SOMO reveals that significant orbital coefficient is located at the central carbon of the allyl ligand; this is essential as the regioselectivity of the radical attack on the propargyl ligand depends on the site of greatest orbital density. The SOMO however, is mostly metal in character because of the closer proximity to the titanocene 3a₁ orbital. The site of reactivity can be altered in favor of interacting at the central carbon by effectively blocking the interaction between radical species and the titanium based orbital. Cyclopentadienyl ligands are crucial by providing a sterically encumbering environment around the titanium center that prevents radical reactivity at the titanium based SOMO. This explanation has also been used to explain the regioselectivity of the nucleophilic attack on (η^3 -allyl)molybdenum complexes.⁵²

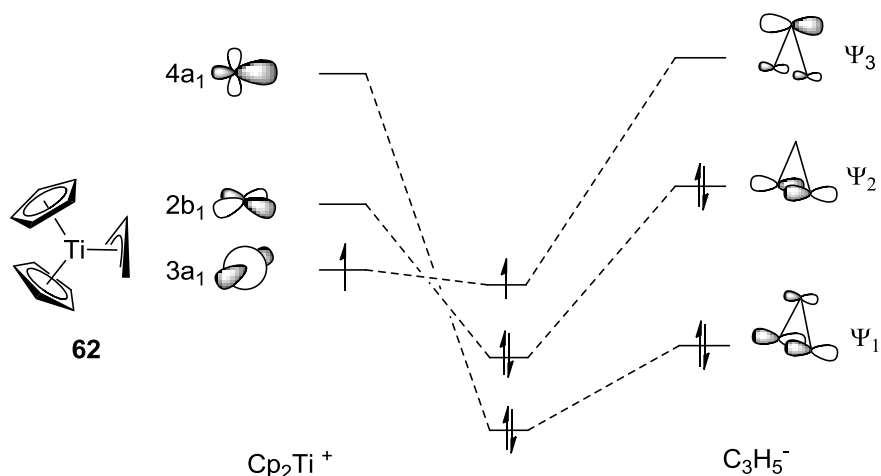


Figure 1.4: EHMO diagram of (η^3 -allyl)titanocene(III) (**62**).

Similar hypothetical molecular orbitals are constructed for (η^3 -propargyl)titanocene(III) **63** (Figure 1.5). One important feature to note is the greater geometrical overlap between the $3a_1$ and ψ_3 orbitals. The second important feature to note in this diagram is that the ψ_3^* orbital is higher in energy when compared to the ψ_3^* orbital of (η^3 -allyl)titanocene(III); this is attributed to the presence of two orthogonal pi-orbitals in the propargyl ligand, which makes the ψ_3^* orbital effectively a higher energy LUMO. The consequence of having a higher energy LUMO (ψ_3^*) is that the resulting SOMO of (η^3 -propargyl)titanocene(III) will be higher in energy in comparison to **62** because of a greater difference in orbital energy.

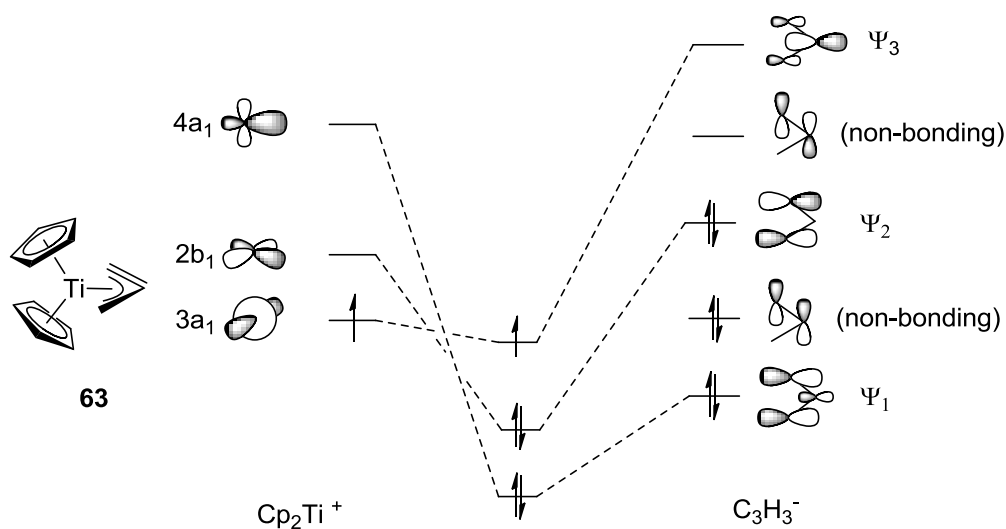
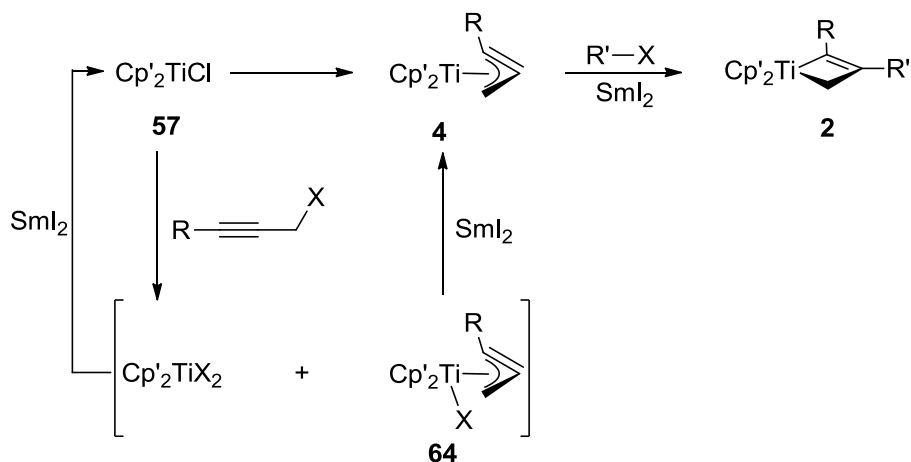


Figure 1.5: Hypothetical EHMO diagram of (η^3 -propargyl)titanocene(III) (**63**).

The advantage of having a higher energy SOMO in **63** is that the close relative energies of both the central carbon on the propargyl ligand and incoming alkyl radicals will be closer; thus a more stable C-C bond will be formed as result of the greater orbital interactions. This suggests that (η^3 -propargyl)titanocene(III) is effectively a better radical trap than (η^3 -allyl)titanocene(III). It should be noted that the orbitals constructed are only speculative and computational studies are required to determine more accurate relative energy levels.

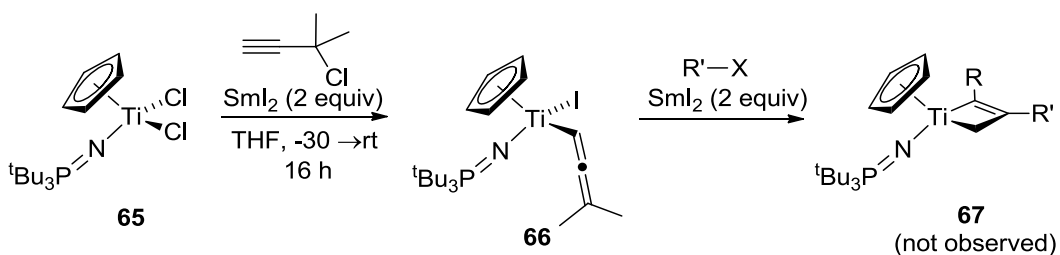
The proposed mechanism describing the formation of titanacyclobutene complexes is divided into two parts (Scheme 1.15); the first is the formation of the (η^3 -propargyl)titanocene(III) intermediate **4**, and the second is the addition of alkyl radicals that afford the titanacyclobutene product **2**. The formation of (η^3 -propargyl)titanocene(III) (**4**) from propargyl halides occurs first by halide abstraction and trapping of the propargyl radical by two equivalents of titanocene(III) monochloride. Reduction of the two titanium(IV) species to **4** and **57** occurs via halide abstraction through the use of two equivalents of samarium(II) iodide. The second part involves addition of alkyl radicals to (η^3 -propargyl)titanocene(III) (**4**) resulting in titanacyclobutene products. The alkyl radicals are generated by a samarium(II) iodide mediated halide abstraction and occurs without interference from **4**, which is also a one-electron radical-type species.

Scheme 1.15



This methodology is presently limited to propargyl halides lacking substituents at the propargylic position (Scheme 1.16). Based on titanium(IV) complexes that are obtained from various substituted propargyl halides, substitution at the propargylic position favors the formation of the (η^1 -allenyl)titanocene(IV) halide complexes **66**.³⁸ Propargyl halides that do not have substituents at the propargylic position form (η^1 -propargyl)- or (η^3 -propargyl)titanocene(IV) halide complexes. The inability of the η^1 -allenyl ligand to isomerize to an η^3 -propargyl ligand explains why titanacyclobutene complexes are not formed from titanium (III) intermediates; as failure to adopt this geometry results in an insufficient amount of overlap between the titanocene $3a_1$ and propargyl ψ_3 orbitals (see Figure 1.5). The resulting orbital density on the central carbon by adopting an alternative geometrical rearrangement is greatly reduced or non-existent.

Scheme 1.16



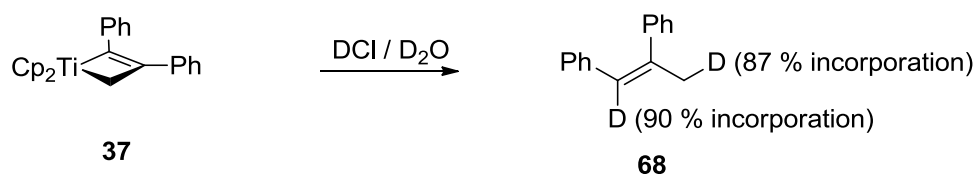
1.5 Titanacyclobutene reactivity

The reactivity of the titanium-carbon bonds of titanacyclobutene complexes presents an opportunity for organic chemists to obtain valuable organic compounds from a single intermediate. This section discusses the products that are obtained as a result of titanacyclobutene reactivity. Similar reactivity patterns are also observed in titanacyclobutane complexes, some of which are discussed in this chapter; a more in-depth discussion regarding this topic can be found in a comprehensive review.¹

1.5.1 Protonation

Protonation of titanacyclobutene complexes occurs with retention of stereochemistry about the olefin (Equation 1.7). This was determined through the addition of DCl in D₂O to the titanacyclobutene complex **37**, where near quantitative incorporation of deuterium occurs at the unsaturated and saturated carbons (C2 and C4 respectively) in the allyl product **68**.⁵³

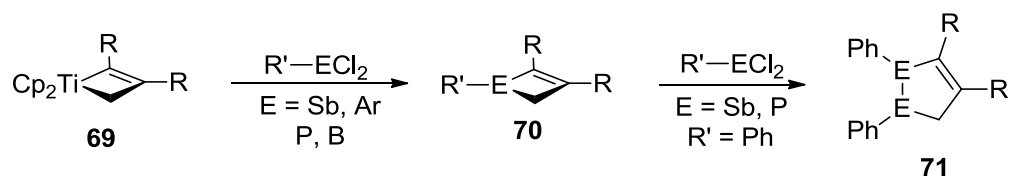
Equation 1.7



1.5.2 Transmetalation with organo main-group dihalide complexes

A variety of phospho-,⁵⁴ arseno-⁵⁴ and boracyclobutene^{4,6,55} complexes of the general formula **70** as well as 1,2-diphosphacyclopentene⁵⁶ and 1,2-distibacyclopentene⁵⁶ complexes with the general formula **71** have been prepared by the addition of organo-main group dihalides to titanacyclobutenes (Scheme 1.17).

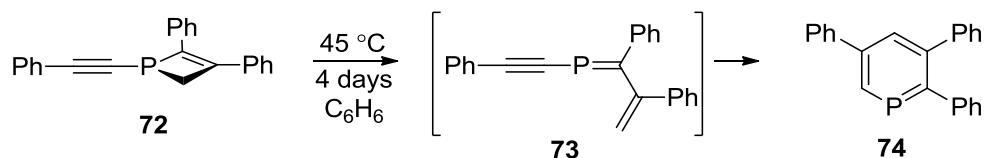
Scheme 1.17



In some cases the nature of the organic main-group substituent affords alternative products. For example, phosphacyclobutenes (Scheme 1.18) with alkynyl

substituents such as **72** rearrange to form phosphabenzenes (**74**). The formation of **74** occurs by 4π electrocyclic ring opening of **72**, which generates a transient phosphorous (vinyl)alkylidene species (**73**) and undergoes subsequent 6π electrocyclization and re-aromatization.⁵⁷

Scheme 1.18

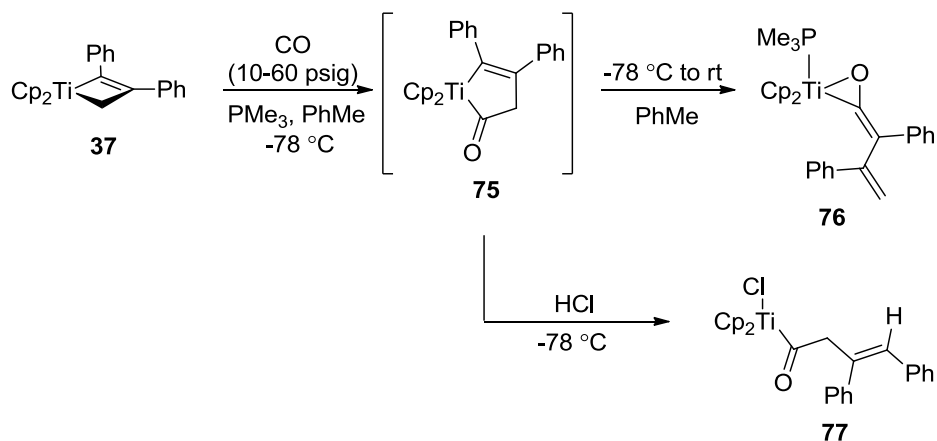


1.5.3 Reactivity of titanacyclobutene complexes with carbon-heteroatom multiple bonds

Carbon-heteroatom multiple bonds will insert into either titanium-carbon bond of titanacyclobutenes, which furnish one or two atom expanded titanacyclopentenones or titanacyclohexenes. Organic products have been also obtained from these expanded titanacycles through demetallation, or by decomposition in the case of unstable products.

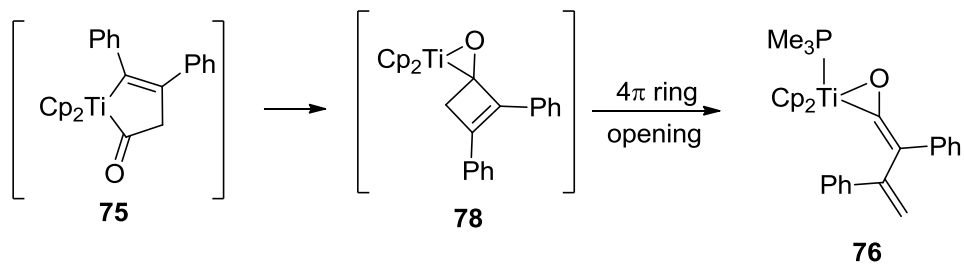
Carbon monoxide reacts reversibly with titanacyclobutene complexes to afford ligand stabilized (η^2 -acyl)titanium(vinyl)ketene⁵⁸ and (η^1 -acyl)titanacyclopentenone complexes (Scheme **1.19**).⁵⁵ What is interesting about these transformations, is that mechanistic evidence by Grubbs reveals that both products arise from carbon monoxide insertion into the saturated carbon (C4) of titanacyclobutenes. This is surprising as the connectivity within the (η^2 -acyl)titanium(vinyl)ketene **76** implies that the product is formed by insertion of carbon monoxide into the unsaturated carbon (C2). Evidence supporting this pathway was provided by the isolation and characterization of an (η^1 -acyl)titanocene(IV) chloride complex **77**, which was obtained from the protonation of **75** at low temperature.

Scheme 1.19



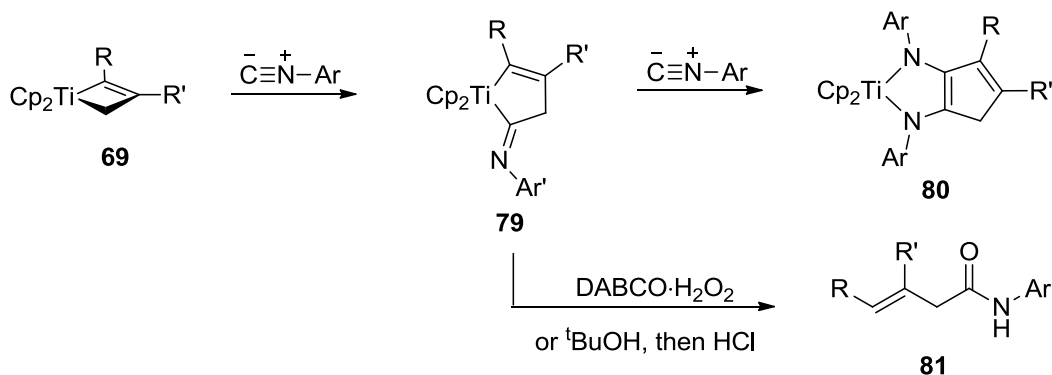
Based on this experimental evidence, it was determined that the skeletal rearrangement responsible for the formation of **76** occurs at elevated temperatures (Scheme 1.20). The rearrangement is proposed to proceed through the titanium (η^2 -acyl)cyclobutenone intermediate **78**, which then undergoes a 4π cycloreversion affording the (η^2 -acyl)titanium(vinyl)ketene **76**. The (η^1 -acyl)titanacyclopentenone complex **75** in Scheme 1.19 could not be isolated; however, stable (η^1 -acyl)titanacyclopentenone complexes can be isolated when bulkier, and more electron donating Cp^* and $^t\text{BuCp}$ ligands are used as ancillary ligands. Presently, titanacyclobutene complexes will not insert more than one equivalent of carbon monoxide; titanacyclobutanes on the other hand insert two equivalents of carbon monoxide which affords carbocyclic titanium(IV) enediolates.^{59,60}

Scheme 1.20



Isonitriles insert into the saturated carbon (C4) of titanacyclobutenes, and afford (η^1 -acyl)iminotitanacyclopentene complexes (**79**) (Scheme 1.21).^{6,55} Demetallation procedures have been developed which effectively convert (η^1 -acyl)iminotitanacyclopentene complexes (**79**) into unsaturated amides (**81**) by addition of *t*-butanol, followed by an acidic workup,⁶¹ or by adding anhydrous DABCO·H₂O₂.⁶ Unlike the case with carbon monoxide, two equivalents of isonitrile inserts twice into both titanacyclobutene **69** and once into (η^1 -acyl)iminotitanacyclopentene (**79**) complexes, furnishing carbocyclic-titanium(IV) enediamidate complexes (**80**).⁶ Obtaining the titanium-free carbocyclic-enediamidates is problematic however, as an effective demetallating procedure has not been reported.

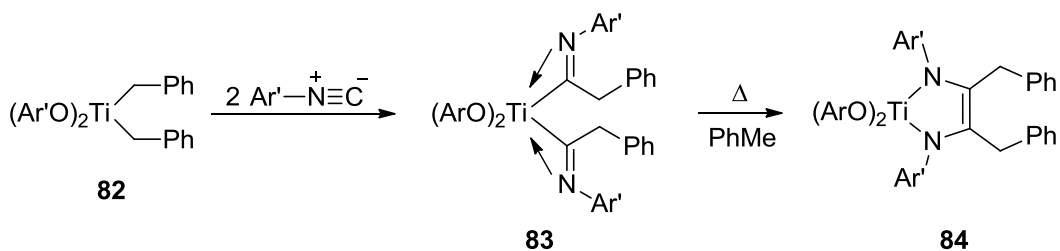
Scheme 1.21



The mechanistic understanding as to the conversion of titanacyclobutenes into carbocyclic-titanium(IV) enediamidates is presently unknown, but experimental evidence suggests that this can occur through two potential pathways. The first proposed mechanism is based on investigations conducted on acyclic-titanium(IV) enediamidates by Chamberlain, et al. (Scheme 1.22). In this case, acyclic-titanium(IV) enediamidate complexes are formed through a titanium bis(η^2 -iminoacyl) intermediate **83**. This occurs by insertion of the second equivalent of isonitrile into the unsaturated carbon (C2) of the initial (η^1 -acyl)iminotitanacyclopentene product such as complex **79** in Scheme 1.21. The formation of the acyclic-titanium enediamidate **84** from the bis(η^2 -iminoacyl) intermediate **83** then occurs by coupling the two titanium-iminoacyl substituents in refluxing hydrocarbon solvents.⁶² If such a mechanism applies to

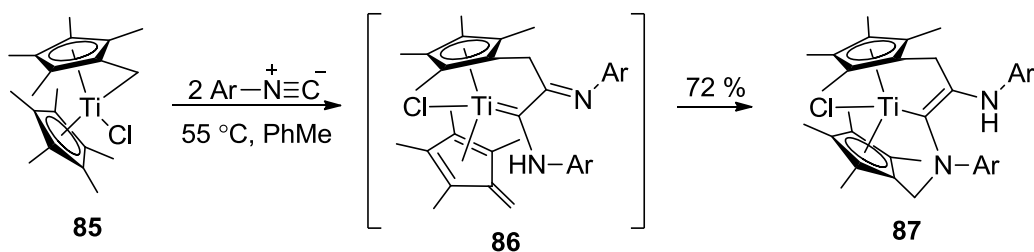
titanacyclobutene complexes, the coupling of the iminoacyl substituents occurs at significantly lower temperatures.

Scheme 1.22



A second mechanism arose from experimental results by Teuben and co-workers who demonstrated that titanium enediamidate complexes arise from the insertion of the second isonitrile into the titanium iminoacyl bond of the $(\eta^1\text{-acyl})\text{iminotitanacyclopentene}$ **79** (Scheme 1.23). This type of reactivity was observed in systems such as the titanium fulvene complex **85**, where only one titanium-carbon bond is present.⁶³

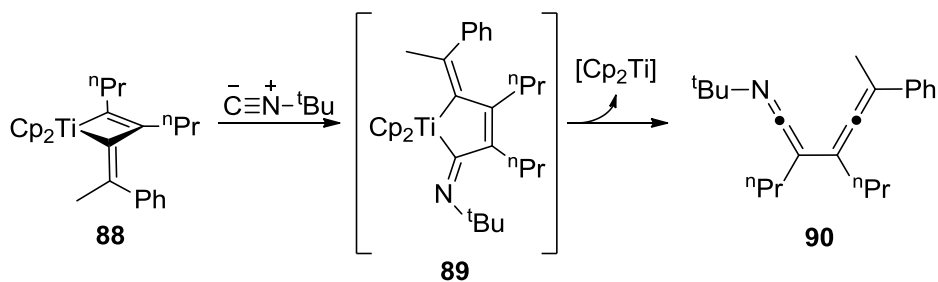
Scheme 1.23



α -Methylenetitanacyclobutene complexes will also insert isonitriles into its unsaturated carbon (C2), which furnishes allenylketenimine compounds (Scheme 1.24).⁶¹ The authors propose that a $(\eta^1\text{-iminoacyl})\text{titanacyclopentene}$ intermediate **89** is

initially formed in the reaction which then extrudes an equivalent of titanocene to afford the allenylketenimine product (**90**). Similar to carbon monoxide insertions, the (η^1 -iminoacyl)titanacyclopentene **89** is generated through the skeletal rearrangement of a putative (η^2 -iminoacyl)titanium(IV) iminocyclobutenone intermediate. This intermediate is not displayed but is structurally similar to complex **78** in Scheme 1.20.

Scheme 1.24

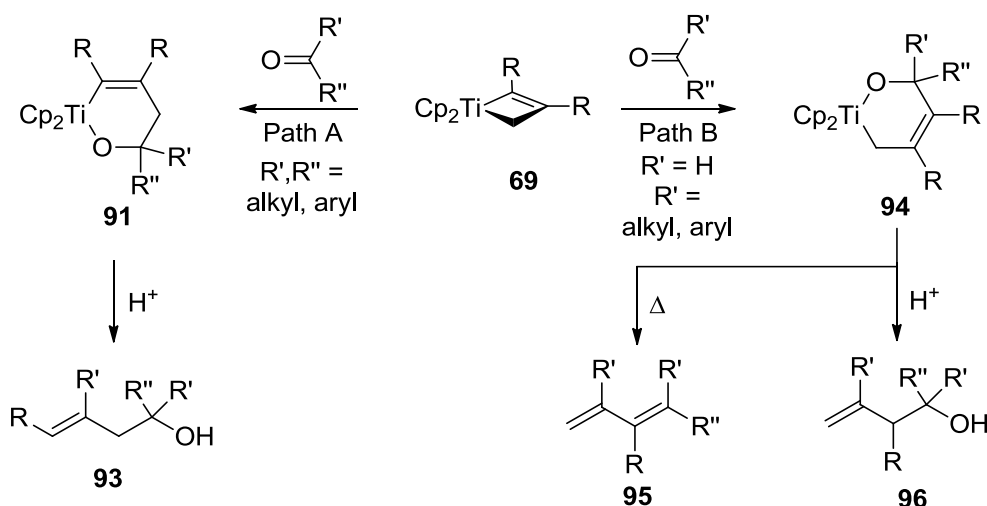


Carbonyl compounds insert into titanacyclobutene complexes at both saturated (C4), and unsaturated carbons (C2); the products formed are one of two oxa-titanacyclohexene complexes **91** (Path A) and **94** (Path B) (Scheme 1.25). In this case, the regioselectivity of carbonyl insertions are influenced by the steric nature of the substituents at the unsaturated carbon (C2), as well as the nature of the carbonyl group. Typically, insertion of carbonyl compounds into the saturated (C4) carbon (Path A) occur when either the C2-substituents are large (R = Ph), or if the added carbonyl compounds are ketones. These factors furnish oxa-titanacyclohexenes (**91**) almost exclusively. In contrast, the addition of aldehydes to titanacyclobutenes bearing smaller alkyl substituents at the unsaturated carbon (C2) (R= Et, Me) furnishes oxa-titanacyclohexenes (**94**) exclusively (Path B). A combination of any of these factors however, affords mixtures of oxa-titanacyclohexenes **91** and **94**.

Oxa-titanacyclohexenes **91** and **94** are synthetically useful, as protonation of these complexes furnishes regiomerically homoallylic alcohols **93** and **96** respectively.⁶⁴ Conjugated dienes **95** have also been obtained from oxa-titanacyclohexenes (**94**) (Path

B) by thermal [4+2] cycloreversion which expels titanium oxide.⁶⁵ The formation of conjugated dienes depends on the thermal stability of the oxa-titanacyclohexene complex that is formed; as temperatures required for the [4+2] cycloreversion often range from room temperature to 80 °C.

Scheme 1.25

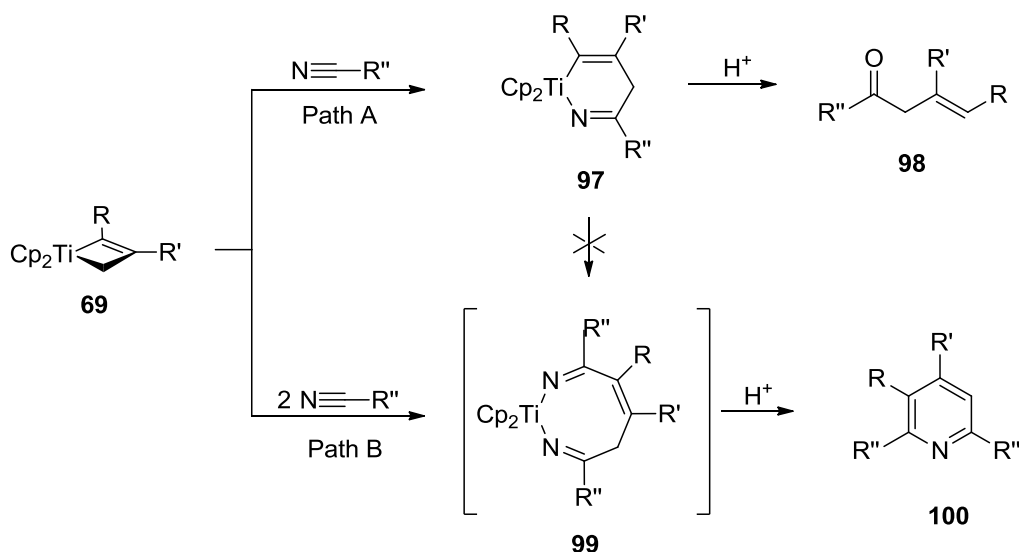


Organic nitriles insert into the unsaturated- (C2), or unsaturated carbons (C4) of titanacyclobutenes (Scheme 1.26). These insertions furnish either aza-titanacyclohexadiene complexes (**97**) (Path A) which can be converted to either β,γ -unsaturated ketones (**98**) by protonolysis,⁶⁶ or substituted pyridines (**100**) (Path B).⁶⁶ Similar to carbonyl insertions, the formation of either organic products is dependent on the size of the substituents at the unsaturated carbon (C2) of the titanacyclobutene. In cases where large C2-substituents ($\text{R} = \text{Ph}$) are present, only aza-titanacyclohexadienes (**97**) are formed (Path A). When smaller substituents are present at the saturated carbon (C2) ($\text{R} = \text{Me, Et}$), mixtures of **97** and **100** were obtained.

Subsequent attempts were made to prepare substituted pyridines through the addition of excess organic nitriles to aza-titanacyclohexene intermediates, but were unsuccessful. These results establish that both products **97** and **100** arise from

separate, non-interconverting pathways. Therefore it is assumed that substituted pyridines are obtained by the initial formation of the other metastable aza-titanacyclohexadiene reimer which will incorporate a second equivalent of nitrile to form the double insertion intermediate **99** and then decompose to the substituted pyridine.

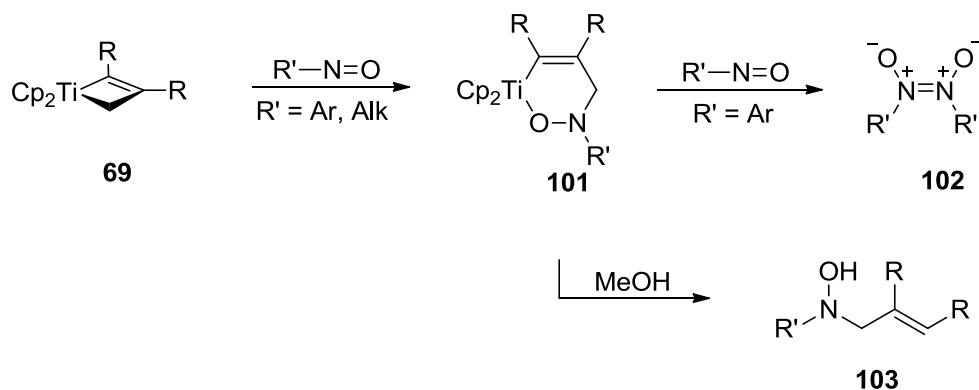
Scheme 1.26



Unlike nitriles, imides were expected to react with titanacyclobutene complexes, however, only tetramethyl urea was found to insert into the saturated carbon (C4); this afforded a aza-titanacyclohexene complex.⁶⁴

The insertion of alkyl- and aryl-nitroso compounds occurs at the saturated carbon (C4) of titanacyclobutenes, where upon protonation affords N-(allyl)-hydroxylamines (**103**) (Scheme 1.27).⁶⁷ The addition of excess aryl-nitroso compounds results in the formation of azoxyarene products **102**; however, these are not synthetically useful considering the initial three titanacyclobutene carbons are not incorporated in the azoxyarene product **102**.⁶⁷

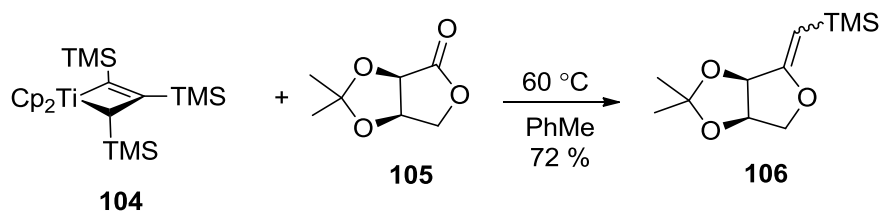
Scheme 1.27



1.5.4 Retro [2+2] cycloaddition

Titanacyclobutene complexes bearing trimethylsilyl- substituents at the two unsaturated carbons (C2, and C3 respectively) will readily expel bis(trimethylsilyl)acetylene via thermal [2+2] cycloreversion; this generates a titanium alkylidene intermediate.^{12,68} Petasis established that the 2,3,4-tris(silyl)-titanacyclobutene complex **104** is very effective at converting carbonyl functionalities into vinyl silanes (**106**) under mild thermal conditions (Equation **1.8**).⁶⁸

Equation 1.8

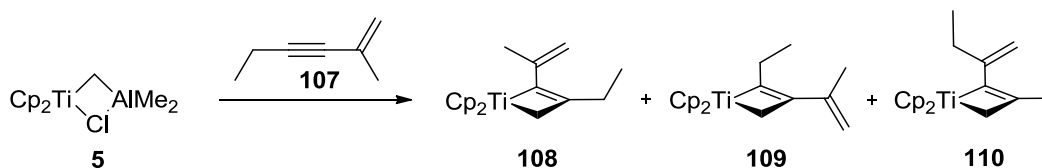


1.5.5 4π electrocyclic ring opening

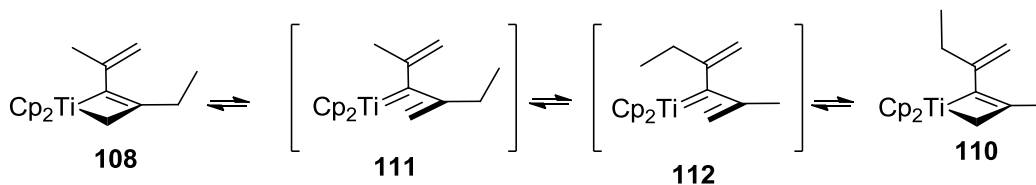
Titanacyclobutenes undergo reversible 4π electrocyclic ring openings to generate titanium-vinylcarbene intermediates. Such reactivity was used by Tebbe to explain the presence of a third titanacyclobutene complex (**110**) obtained by adding unsymmetrical en-yne **107** to Tebbe's reagent (**5**) (Equation **1.9**).⁶⁹ According to this

proposal (Scheme **1.28**) the initial titanacyclobutene **108** first converts to the titanium-vinylcarbene by 4π electrocyclic ring opening. This intermediate then undergoes subsequent rotation about the two pendant vinyl groups then reforms the titanacyclobutene **110** by 4π electrocyclic ring closure.

Equation 1.9

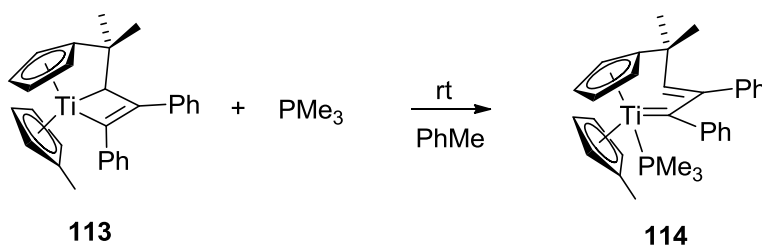


Scheme 1.28



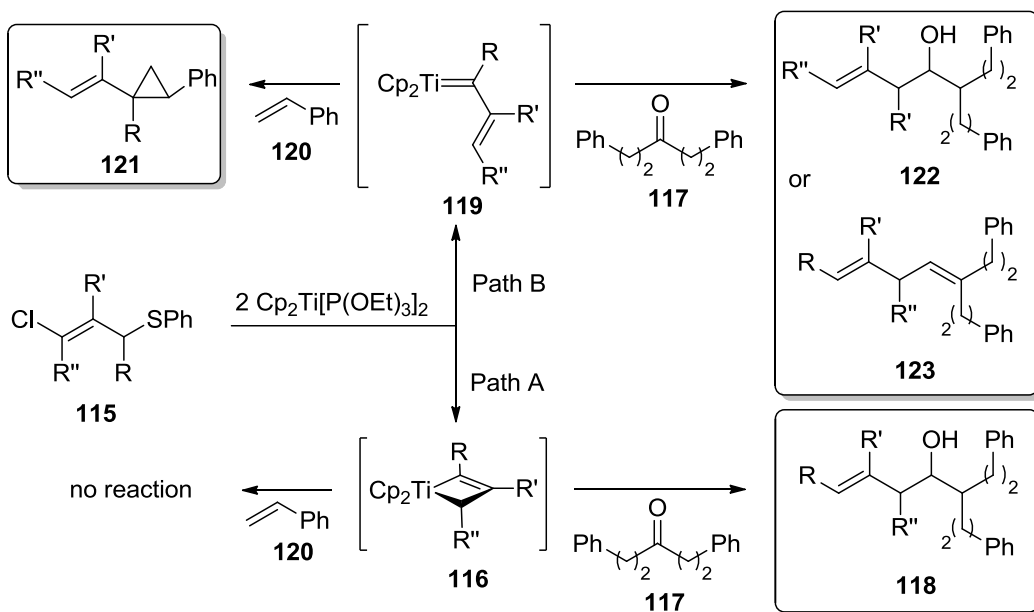
In most cases, titanium-vinylcarbenes are transient intermediates which cyclize to form titanacyclobutene complexes, however, stabilized examples are reported when strongly coordinating Lewis Bases are used such as trimethylphosphine (Equation **1.10**).⁷⁰ Titanium-vinylcarbene complexes are also formed preferentially to titanacyclobutenes when the C-4 position is highly substituted. Such an example was discussed earlier in Scheme **1.14** where the addition of titanocene(II) bis(trimethylphosphine) to 3,3-cyclopropene **50** which furnished the titanium-vinylcarbene **52**.

Equation 1.10



Takeda recently studied the interconversion between titanacyclobutene and titanium-vinylcarbene complexes (Scheme 1.29). This was accomplished by identifying the organic products obtained from adding the symmetrical ketone **117** or styrene **120** to independent reaction mixtures containing two equivalents of bis(triethylphosphite)titanocene and a substituted γ -chloroallylic sulfide **115**.^{31,71} This study is useful in assessing the effect of substitution patterns on titanacyclobutene complexes as substituted γ -chloroallylic sulfides afford the corresponding titanacyclobutene (**116**) (Path A) or titanium-vinylcarbene (**119**) (Path B) intermediates which will react differently with **117** and **120**. These results suggested that both titanacyclobutene complexes and titanium-vinylcarbene complexes are relatively similar in energy with a low energy barrier for interconversion as the majority of substituted γ -chloroallylic precursors yield products from both pathways.

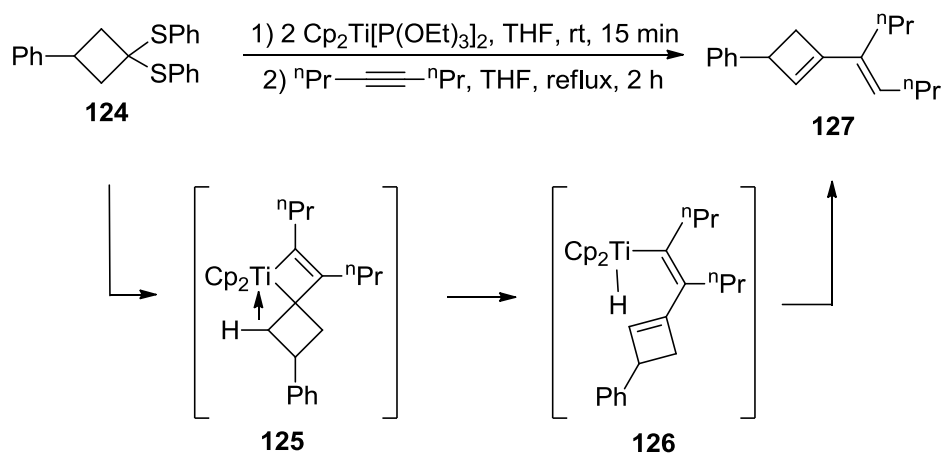
Scheme 1.29



1.5.6 β -Hydride elimination of titanacyclobutene complexes

Titanacyclobutene complexes with substituents at the C4-carbon are prone to β -hydride elimination; this results in the formation of conjugated dienes (Scheme 1.30). Some examples of this reactivity were presented earlier (see Scheme 1.13), where titanocene(II) bis(triethylphosphite) was added to substituted propargyl carbonates.⁷² Takeda has reported other examples depicting this reactivity, as the addition of bis(triethylphosphite)titanocene to cyclobutyl-1,1-thioacetal **124**¹⁸ affords the conjugated vinyl-cyclobutene **127**. Presumably, the reaction proceeds by β -hydride elimination on the metastable titanacyclobutene **125**, which affords a transient vinyltitanium hydride **126**. The putative vinyltitanium(IV) hydride intermediate then collapses by expelling vinylcyclobutene **127** and an unknown titanocene containing by-product.

Scheme 1.30



1.6 Conclusions

A great amount of effort has been devoted to understanding the preparation and reactivity of titanacyclobutene complexes. The results from these investigations by various groups had demonstrated the titanacyclobutenes are useful through further transformation into organic molecules. Future developments should be devoted to

developing methodologies where titanacyclobutene complexes can be converted into organic substrates which is crucial in order for organic chemists to take notice.

A few areas were addressed in this thesis with regards to the chemistry developed in the Stryker group (See Section 1.4.3). The first area focuses on the development of reaction conditions that will allow chemists to prepare titanacyclobutene complexes on large scale. One of the most important advances is finding an alternative to samarium(II) diiodide as the stoichiometric reducing agent. The second significant advance made to this field is finding a method for converting titanacyclobutenes into 5-membered carbocycles. This area of research has also been investigated by the Stryker group where titanium enediamidates have been prepared by the double insertion of isonitriles into titanacyclobutene complexes (See Section 1.5.3). The present issue with this methodology is the lack of reagents which are effective in protonating the enediamidate fragment. This topic will also be discussed in Chapter 2.

Chapter 2: Advances in the Synthesis of Titanacyclobutene Complexes Prepared by Radical Alkylation of (η^3 -allenyl/propargyl)titanocene(III) Complexes

2.1 Introduction

Titanacyclobutene complexes have been transformed into a range of functionalized organic compounds.^{1,18,53,54,56-58,62-69,73} The Stryker group is one of the groups involved in developing this chemistry for the benefit of synthetic organic chemistry as a potentially powerful tool for preparing complex organic products.^{4,6,49,55} This chapter highlights the author's advances in this area that addresses problems associated with substrate specificity and cost efficiency in preparing titanacyclobutene complexes. This chapter also introduces new reaction conditions for the conversion of titanacyclobutene complexes into demetallated carbocycles.

2.2 Activated manganese powder as an alternative reductant to samarium(II) iodide

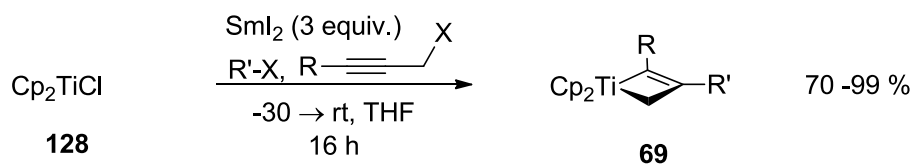
2.2.1 Evolution of the use of samarium(II) iodide in titanacyclobutene synthesis

Samarium(II) iodide is a THF-soluble one-electron reductant that finds many uses in a broad range of organic transformations.⁷⁴ Of particular interest to the Stryker group is the ability of samarium(II) iodide to generate alkyl or vinyl radicals by halogen abstraction from primary, secondary, and tertiary alkyl, and vinyl halides.^{75,76} The advantage of using samarium(II) iodide in this methodology is that carbon-centered radicals can be generated cleanly in the presence of the odd-electron (η^3 -allenyl/propargyl)titanocene(III) complexes.

More recently, concentrated suspensions of solid samarium(II) iodide in THF, were used to prepare titanacyclobutene complexes bearing unsubstituted, and (*t*-butyl) cyclopentadienyl ligands;⁶ these complexes were previously not isolable when using the commercially-available 0.1 mol/L solutions of samarium(II) iodide in THF.⁴ The divergent reactivity observed between solid suspensions and dilute solutions of samarium(II) iodide is attributed to the higher overall reaction concentration, which favours

intermolecular radical coupling. This development has allowed titanacyclobutene complexes **69** to be prepared using the readily available and cost-effective parent titanocene(III) monochloride (**128**) starting material (Equation **2.1**). Solid samarium(II) iodide is also useful because it can be effectively prepared on a large scale⁶ and can be stored for extended periods under an inert atmosphere.

Equation 2.1

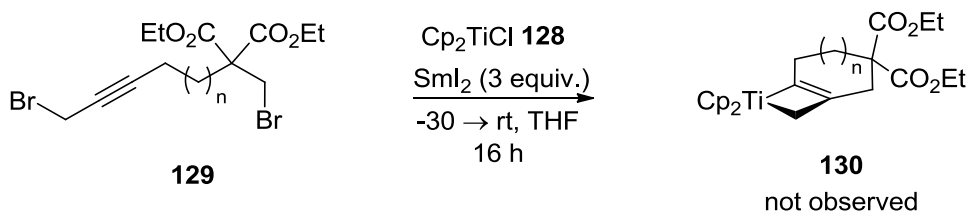


R = Me, Ph, TMS, *t*-Bu; R' = alkyl

Though the use of samarium(II) iodide has been pivotal to the preparation of titanacyclobutene complexes, there are substantial issues that remain to be addressed. First, a large mass of samarium reagent is required for each reaction, rendering it largely ineffective for large scale reactions. This is due to the high molecular weight of samarium(II) iodide (>404 g/mol), and also the stoichiometric requirement of three or four equivalents of the reagent per reaction. The cost associated with using this reagent is also high, as samarium(II) iodide powder can be purchased for \$80/g or in THF solutions (0.1 M) for \$49.70 per 100 mL.

Secondly, both samarium(II) and samarium(III) salts are Lewis acidic, and can form adducts with heteroatom-containing substrates.^{77,78} This was determined to be the contributing factor to the failure of previous investigations into making bicyclic titanacyclobutene complexes from malonate-bearing propargyl halide **129** (Equation **2.2**).⁴⁹

Equation 2.2



Due to the disadvantages of using samarium(II) iodide as a reductant, inexpensive first-row transition metal powders were investigated as alternatives. Early reports showed that a variety of metal powders were inferior to samarium(II) iodide,⁶ however, the reinvestigation of manganese metal proved fortuitous and resulted in the development of new reaction conditions that omit samarium(II) iodide from the reaction. This will be discussed in the following section.

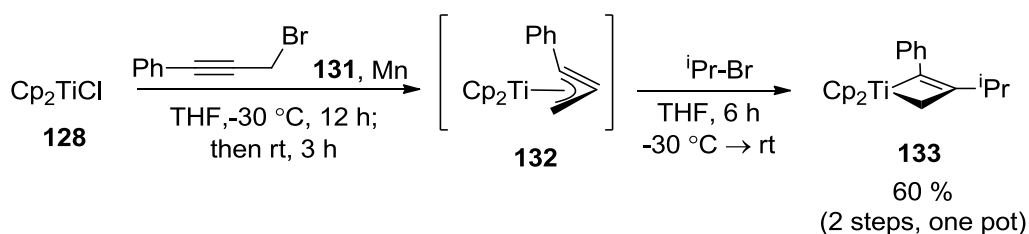
Although relatively new to the preparation of titanacyclobutene complexes, manganese metal has been used in a variety of titanium-mediated organic coupling reactions which involve radical activation of alkyl halides,^{79,80} carbonyl compounds^{81,82} and strained cyclic ethers.^{83,84} The use of manganese powder was first reported by Fürstner, who demonstrated its utility as a stoichiometric reductant in the chromium-catalyzed Nozaki-Hiyama-Kishi reaction.⁸⁵

2.2.2 Development of optimized reaction conditions using activated manganese powder

We envisioned that metal powders could function either to reduce samarium(III) back to samarium(II) iodide and have an overall reaction that is catalytic in samarium, or could replace samarium(II) iodide completely as the stoichiometric reductant. In order to deduce if metal powders can fully replace samarium(II) iodide, aluminum, zinc, manganese and magnesium metal powders were all assessed because of the known ability to reduce titanium(IV) complexes to titanium(III) complexes.⁸⁶⁻⁸⁸ Treatment of titanocene(III) monochloride (**128**) with a 1-bromo-3-phenyl-2-propyne (**131**) and either excess zinc or aluminum powders, afforded insoluble green complexes, while magnesium powder yielded a black intractable solid. The intractable product

mixtures likely arise from the formation of insoluble titanium(III) complexes (Zn, Al) or by reduction of the $[\text{Cp}_2\text{TiCl}]_2$ to Ti(II) complexes (Mg).⁸⁹⁻⁹² When excess manganese powder was used under similar reaction conditions, however, the crude titanacyclobutene complex **133** was isolated in 60 % yield (Scheme 2.1). This was promising, but improved conditions were needed in order to prepare titanacyclobutene **133** in the same yield as with samarium(II) iodide (82 %).⁶

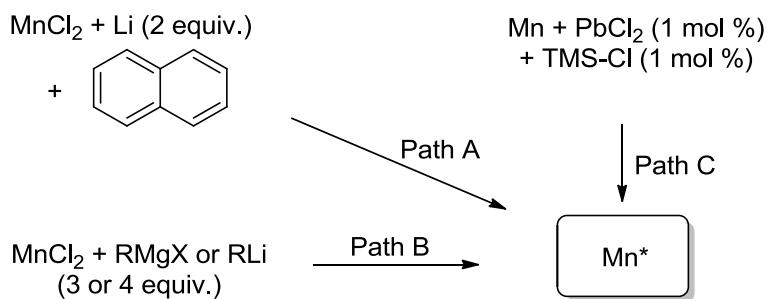
Scheme 2.1



Initial attempts to optimize this reaction by using a catalytic amount of samarium(II) iodide (5 to 20 %), afforded titanacyclobutene **133** in a similar yield to that obtained using manganese powder. An exhaustive optimization of the reaction conditions revealed highly variable activity of the manganese powder which prompted an investigation into the use of “activated” sources of manganese metal.

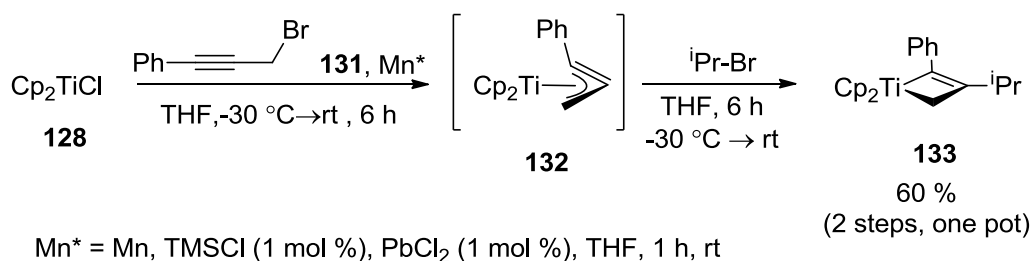
Activated manganese metal can be obtained by one of three methods (Scheme 2.2): reduction of manganese(II) salts to colloidal manganese (Path A),⁹³ generation of trialkylmanganate complexes whose reactivity closely resemble that of low valent manganese (Path B),⁹⁴ or by removal of surface contaminants from the bulk by addition of substoichiometric amounts of lead(II) chloride and chlorotrimethylsilane, as first reported by Takai (Path C).⁹⁵

Scheme 2.2



Treatment of a THF solution containing titanocene(III) monochloride and either version of the activated manganese in THF with propargyl bromide **131** and *i*-propyl bromide did not result in a significant increase in yield of the desired titanacyclobutene **133** (Scheme 2.3). Takai's procedure (path C) however, was the most effective method of the three for preparing titanacyclobutene complex **133**, as the least amount of contamination in the crude products was observed.⁹⁵

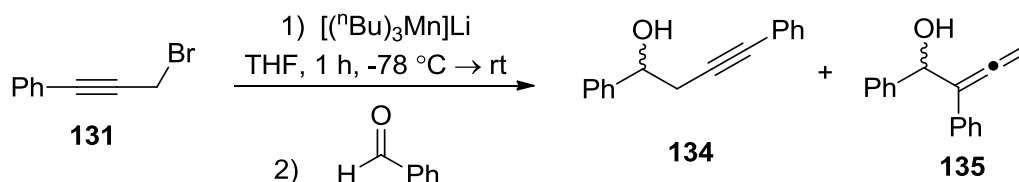
Scheme 2.3



The generation of a "propargylmanganese" reagent had not been considered at this point, as the manganese powder was originally thought to serve as an external reductant to the titanium(IV) intermediates. Hosomi has demonstrated however that propargylmanganese reagents that are prepared at low temperature will react with

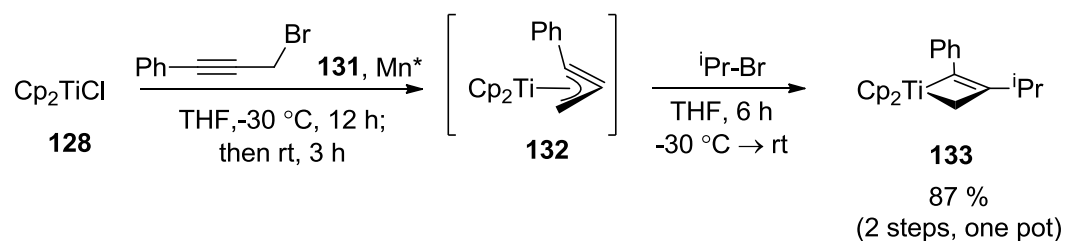
benzaldehyde, which affords homo-propargyl and homo-allenyl alcohols **134** and **135** respectively (Equation 2.3).⁹⁶

Equation 2.3



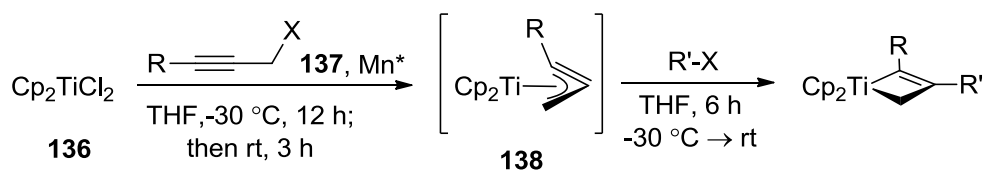
Although the activated manganese used in our investigation is different than that reported by Hosomi,⁹⁶ similar low temperature reaction conditions were used for preparing the (η^3 -allenyl/propargyl)titanocene(III) intermediate **132**; these conditions would allow the alleged “propargylmanganese” reagent to be generated. When allowing a solution of titanocene(III) monochloride (**128**), propargyl halide **131**, and Takai’s activated manganese⁹⁵ to stand at $-30\text{ }^\circ\text{C}$ for eight hours, then adding *i*-propyl bromide at room temperature, the titanacyclobutene **133** was obtained in higher yield (75 %). In subsequent trials (Scheme 2.4), the highest yield of **133** (87 %) was obtained when the reaction titanocene(III) halide, propargyl halide and activated manganese mixture was kept at $-30\text{ }^\circ\text{C}$ for twelve hours, giving the same yield as reported previously using stoichiometric samarium(II) iodide.⁶

Scheme 2.4



Another successful alteration to the reaction was to use titanocene(IV) dichloride (**136**) as the titanium reagent, a cheaper and air-stable alternative to titanocene(III) monochloride. This affords titanacyclobutene **133** in a greater yield (87 %) than when using samarium(II) iodide. This result was significant because although titanacyclobutene complexes have been prepared from titanocene(IV) dichloride using samarium(II) iodide, a decrease in yield was often observed.⁶ In addition to eliminating samarium(II) iodide completely, this also demonstrates a second major advantage, that titanacyclobutene complexes can now be prepared using reagents that do not need to be stored under an inert atmosphere. The newly developed reaction conditions have now been used to prepare five titanacyclobutene complexes **133**, and **139** to **142** that were previously reported by Bauer,⁶ in order to determine the effectiveness for a broad range of substrates (Scheme 2.5). The titanacyclobutene complexes obtained by the new manganese method were isolated in very similar yields to those obtained by using samarium(II) iodide. The crude products were also obtained in near-spectroscopic (NMR) purity.

Scheme 2.5

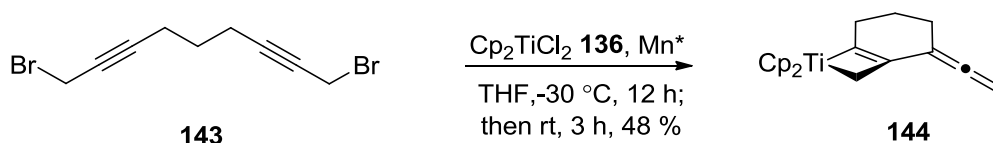


Product	R	R'	Yield (Mn) %	Yield (SmI ₂) %
133	Ph	ⁱ Pr	87	82
139	Ph	^t Bu	78	76
140	Ph	Bn	75	75
141	Me	ⁱ Pr	80	79
142	Me	Bn	85	78

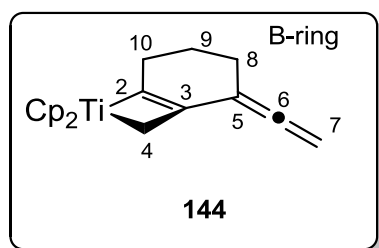
Cyclization of bis-propargyl halide⁴ **143** was also evaluated under the new reaction protocols, which constructed bicyclic titanacyclobutene complex **144** in

moderate yield (Equation 2.4). This result was significant because a previous attempt to generate the same bicyclic complex using samarium(II) iodide instead of manganese, was completely unsuccessful for unknown reasons.⁴ It is apparent from this result that samarium(II) iodide was detrimental in the product outcome, however the reasons for this are unknown.

Equation 2.4



Bicyclic titanacyclobutene **144** was characterized by 1D and 2D NMR spectroscopy; the titanacyclobutene moiety was identified by characteristic ¹³C NMR chemical shifts of the C2-, C3-, and C4-carbons, at 220.0, 88.5, and 70.3 ppm, respectively (Figure 2.1). The signals in the ¹H NMR spectrum of **144** were also broad, which indicates that paramagnetic impurities were still present. The protons on the saturated titanacyclobutene carbon are located at 3.21 ppm in the ¹H NMR spectrum. These titanacyclobutene protons are correlated (COSY) to the exocyclic methylene protons at the C10- position, as well as the exo-cyclic allenic protons. The connectivity of the carbon skeleton in the B-ring was deduced by 2D NMR techniques involving proton-proton (COSY) and proton-carbon (HMQC, HMBC) correlations. The exocyclic allene was identified by the characteristic chemical shifts of the vinyl protons (4.96 ppm) in the ¹H NMR spectrum, as well as the downfield chemical shift (210.0 ppm) of the central allenic carbon in the ¹³C NMR spectrum.



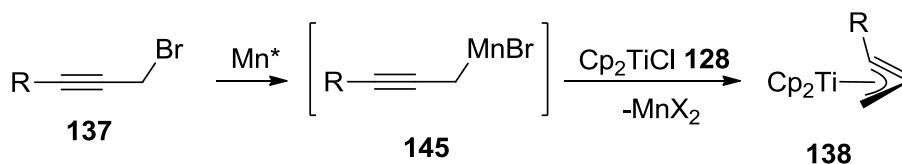
Atom	¹³ C NMR	¹ H NMR
2	224.0	
3	88.5	
4	70.3	3.21
5	99.7	
6	210.1	
7	76.3	4.96
8	28.3	2.38
9	24.3	1.58
10	35.3	2.50

Figure 2.1: Selected ¹H and ¹³C NMR chemical shifts of **144**.

2.2.3 The role of activated manganese powder

Elucidating the role of activated manganese powder in the preparation of titanacyclobutene complexes is significant, considering the major mechanistic “blackbox” that remains in the absence of samarium(II) iodide. A tentative mechanism can be proposed in which the formation of (η^3 -allenyl/propargyl)titanocene(III) intermediate **138** occurs by transmetallation between titanocene(III) monochloride (**128**) and propargylmanganese intermediate **145** (Scheme 2.6). Evidence supporting this theory was the increase in yield of titanacyclobutene **133**, which was obtained from conducting the reaction at low temperature (see Scheme 2.4); such observations parallel Hosomi’s results,⁹⁶ as propargylmanganese reagents were also generated at low temperature (see Equation 2.3). Evidence can also be inferred from the use of organomanganese reagents as transmetallating reagents in iron, and copper cross-coupling reactions.⁹⁷⁻¹⁰⁰ This proposal is very different than the classical mechanism, which invokes titanocene(III) monochloride as the reducing reagent for the propargyl halide, and the activated manganese powder to be responsible for reducing the two titanium(IV) species to the corresponding titanium(III) complexes.

Scheme 2.6



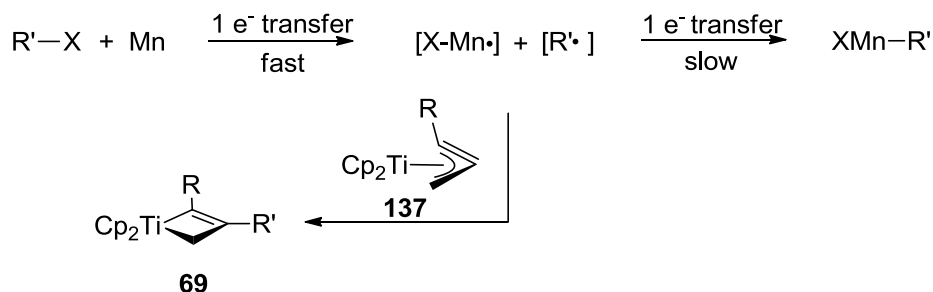
Control experiments were performed in order to differentiate between the two plausible mechanisms. The first experiment involved the addition of stoichiometric titanocene(IV) dichloride (**136**) to a colorless THF solution containing activated manganese powder and propargyl halide **131**, which had been kept at $-30\text{ }^\circ\text{C}$ for 17 hours. This resulted in a slow change in color to dark purple suggesting that a mechanism involving a propargylmanganese reagent is plausible.

Subsequent experiments however, strongly suggest that titanocene(III) monochloride (**128**) is the reducing agent that reacts with the propargyl halide. In the second experiment the activated manganese powder was omitted, in which the green color of the solution containing titanocene(III) monochloride changed to a dark purple almost simultaneously with the addition of propargyl halide **131**. The same observation was made in a third experiment, where the colorless solution containing propargyl halide **131** and activated manganese powder immediately changed to dark purple upon addition of titanocene(III) monochloride. A fourth experiment demonstrated that titanocene(III) monochloride is generated rapidly from the reduction of titanocene(IV) dichloride with activated manganese metal, even at $-30\text{ }^\circ\text{C}$. Therefore, the role of the activated manganese powder in these reactions is the same as that of samarium(II) iodide, which is to reduce the titanium(IV) intermediates to their analogous titanium(III) complexes.⁴⁸

The second part of the proposed mechanism involves the generation of free alkyl radicals from the alkyl halide component; both titanocene(III) monochloride and manganese powder have been reported to be useful reagents for this purpose. Manganese is an effective reagent for generating alkyl radicals,^{26,27} even though it is a two-electron reducing species (Scheme **2.7**). The reason for why manganese is effective

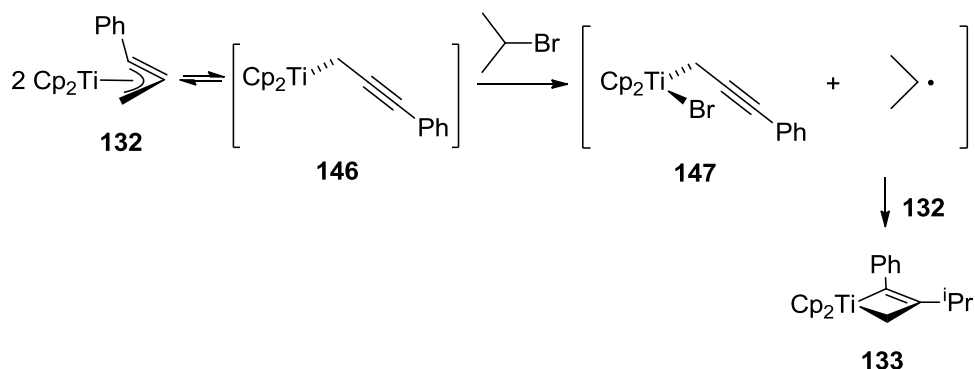
for generating radicals is because manganese metal undergoes rapid one-electron transfer to alkyl halides, but the second electron transfer that leads to the organomanganese reagent is very slow.^{29,30}

Scheme 2.7



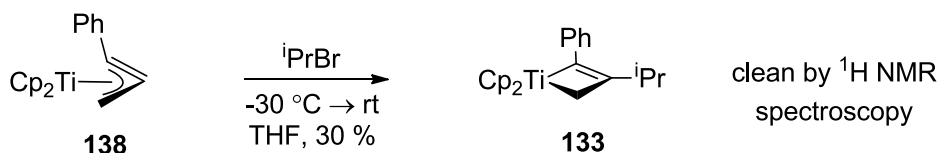
A second case involving titanium-promoted alkyl radical generation was also considered, however, titanocene(III) monochloride (**128**) is presumably consumed during the generation of the (η^3 -propargyl)titanocene(III) intermediate **138**. Therefore, we needed to establish whether the (η^3 -propargyl)titanocene(III) intermediate **138** present at the time of alkyl halide addition is also capable of generating alkyl radicals (Scheme **2.8**). In theory, the titanium-coordinated propargyl ligand can isomerize from a η^3 - to a η^1 -hapticity. This change in hapticity would open up a free coordination site on the titanium(III) center of the (η^1 -propargyl)titanocene(III) species **146**, which can then abstract a bromine radical from *i*-propyl bromide, this forms the (η^1 -propargyl)titanium(IV) species **147**. The resulting *i*-propyl radical which would then combine with another equivalent of (η^3 -propargyl)titanocene(III) (**132**) and afford the titanacyclobutene **133**. In the presence of activated manganese powder, the (η^1 -propargyl)titanium(IV) intermediate **147** would be recycled back to the starting (η^3 -propargyl)titanocene(III) complex **132**; this cycle presumably continues until the remaining (η^3 -propargyl)titanocene complex **132** has been converted to the desired titanacyclobutene **133**.

Scheme 2.8



The identity of the alkyl radical-generating species was deduced by performing a control experiment where *i*-propyl bromide was added to the (η^3 -propargyl) titanocene(III) complex **132** in the absence of activated manganese metal. Theoretically, if the radical generating species is the activated manganese powder, no reaction would be observed. When a THF solution containing *i*-propyl bromide was added to a THF solution containing independently prepared and purified (η^3 -propargyl)titanocene(III) complex **132**, we obtained titanacyclobutene complex **133** 30 % yield (Equation 2.5). This result establishes that (η^3 -propargyl)titanocene(III) intermediates are the principal alkyl radical generator in the second step in the reaction. Also, considering that one equivalent of **132** is consumed in generating the *i*-propyl radical, this result also demonstrates that (η^3 -propargyl)titanocene(III) is an effective radical generator, as the “low” yield of **133** is actually half of what the hypothetical yield should be when using a stoichiometric reductant. Presumably, the activated manganese is instead responsible for obtaining higher yields of **133**, as rapid reduction of the (η^1 -propargyl)titanium(IV) intermediate **147** prevents its decomposition.

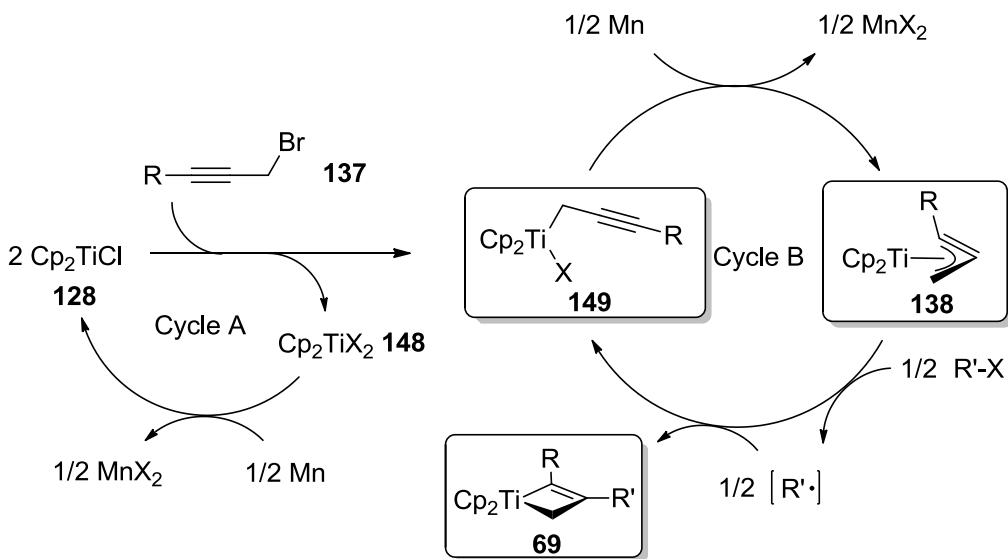
Equation 2.5



In summary, the experimental evidence suggests the overall mechanism for the preparation of titanacyclobutene complexes involves two cycles (Scheme 2.9). In cycle A, (η^3 -propargyl)titanocene(III) complex **133** is prepared from two equivalents of titanocene(III) monochloride and one equivalent of a propargyl halide. The two intermediate titanium(IV) complexes **149** and **148** are subsequently reduced by activated manganese powder to their corresponding titanium(III) complexes **138** and **128**. This cycle continues until the remaining titanocene(III) monochloride is depleted.

In cycle B, organic free-radicals are generated by combining two equivalents of (η^3 -propargyl)titanocene(III) intermediate **138** with an alkyl halide. The two products in this cycle are a transient organic radical, which is trapped by a second equivalent of (η^3 -propargyl)titanocene(III) **138**, forming the titanacyclobutene product **69**, and one equivalent of the (η^1 -propargyl)titanium(IV) intermediate **149** which is reduced back to **138** by activated manganese powder. This cycle subsequently continues until the remaining (η^3 -propargyl)titanocene(III) species **138** is depleted.

Scheme 2.9

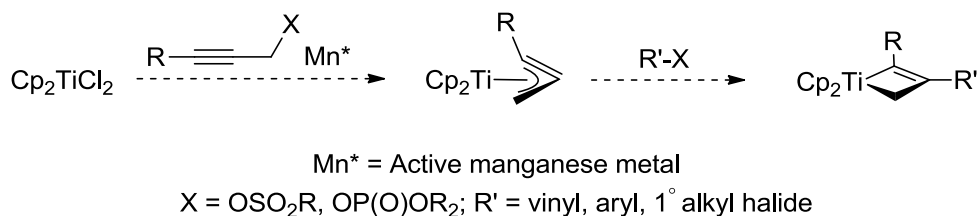


2.2.4 Conclusions

A procedure for preparing titanacyclobutene complexes using activated manganese powder in place of samarium(II) iodide, has been developed. The advantages of using manganese over samarium(II) iodide are its relative inexpensiveness (\$0.4/g) and robustness under atmospheric conditions. Furthermore, manganese(II) salts produced during the reaction are significantly less Lewis-acidic than samarium(II) and samarium(III) halides.¹⁰¹ We expect that this modification will extend the scope and utility of this particular titanacyclobutene synthesis.

Further investigations should include a more in-depth exploration into the use of other electron-rich manganese species that may possess greater activity. This modification could expand the substrate scope of titanacyclobutene complexes to include aryl, vinyl or primary alkyl halides (Scheme 2.10), all of which are more difficult to generate with samarium(II) iodide. Rieke has also reported that activated manganese metal inserts into benzylic and allylic sulfonates, and phosphates.¹⁰² The corresponding reactions with propargylic sulfonates and phosphates, in the presence of titanium precursors, would also extend the substrate classes amenable to preparing titanacyclobutene complexes.

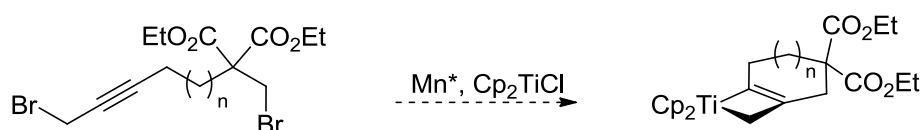
Scheme 2.10



Among other applications that should be re-investigated with these new manganese(0) conditions, is the use of malonate-containing bifunctional substrates for preparing bicyclic titanacyclobutene complexes, as initially investigated by Quesnel

(Scheme 2.11).⁴⁹ In his work, samarium(II) and samarium(III) halides appeared to interfere with the cyclization by selectively coordinating to the malonate unit.

Scheme 2.11

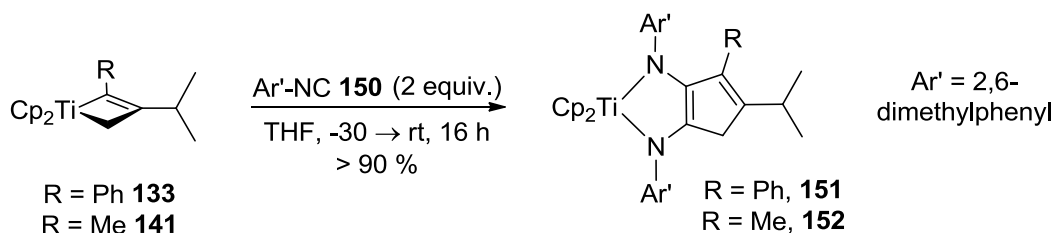


2.3 Preparation of five-membered carbocycles from titanacyclobutene complexes

2.3.1 Introduction

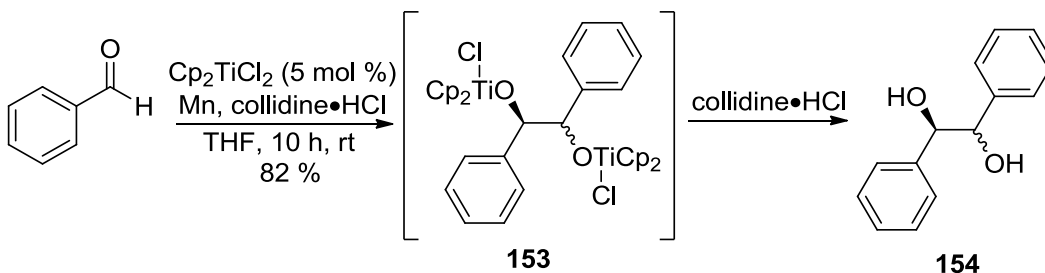
Titanium-alkyl complexes have been demonstrated to undergo insertion reactions with one or two equivalents of organic isonitrile compounds (see Schemes 1.21-1.23);^{6,55,62,63} these reactions afford (η^1 -iminoacyl)titanium complexes, or titanium enediamidate complexes respectively. We have recently explored the addition of organic isonitriles to titanacyclobutenes (Equation 2.6) and found that two equivalents of 2,6-dimethylphenyl isonitrile **150** combines with titanacyclobutene complexes **133** and **141** and furnishes carbocyclic titanium-enediamidate complexes **151** and **152** in good yields.⁶ These complexes are interesting as functionalized five-membered carbocycles can be obtained by successful removal of the titanocene unit. However, effective conditions for demetallating the carbocyclic enediamidate moiety were not identified in that work, as protonolysis using HCl resulted in complex product mixtures.⁶ The development of ideal demetallating conditions was thus targeted, completing the conversion of titanacyclobutene complexes into functionalized organic compounds.

Equation 2.6



One class of reagents that were investigated were substituted pyridinium salts, which have been reported by Gansäuer to demetallate the titanium alkoxide products that are formed from his titanium-mediated Pinacol coupling reactions (Scheme 2.12).¹⁰³ Substituted pyridinium salts such as 2,4,6-collidine were selected for these reactions because of the relative acidity of the pyridinium proton ($\text{pK}_a = 5\text{-}7$), the formation of a hindered pyridine preventing deactivation of the unsaturated titanium catalyst by coordination, and the inertness towards the titanium-alkoxyalkyl radical, titanocene(III) chloride and manganese metal. As a result, the pyridinium salts allowed for clean conversion of the titanium alkoxide complex to the corresponding diol, and titanocene(IV) dichloride, which is recycled by one-electron reduction from manganese metal to regenerate the catalyst.¹⁰³

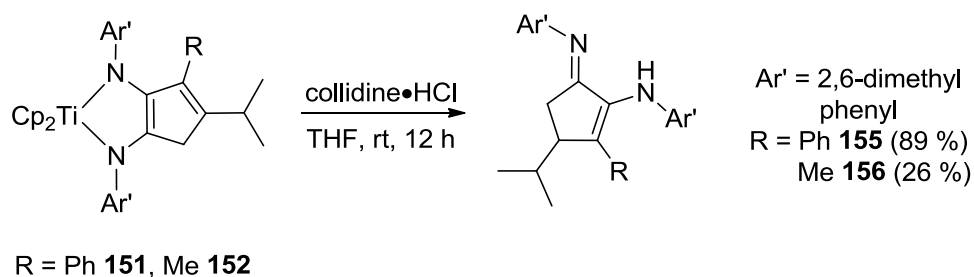
Scheme 2.12



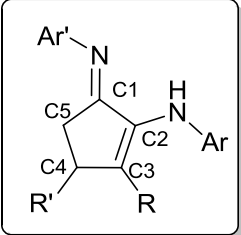
2.3.2 Results

Considering Gansäuer's successes, protonated collidine salts were highly considered as potential demetallating reagents for carbocyclic-titanium(IV) enediamidate complexes (Equation 2.7). By independently treating two known titanium(IV) enediamidate complexes **151** and **152** in THF with two equivalents of collidine•HCl, we obtained the corresponding 3,4-disubstituted carbocyclic α -iminoenamines **155** and **156**, albeit in highly variable yields.

Equation 2.7



Compounds **155** and **156** were fully characterized by 1D and 2D NMR and IR spectroscopies, mass spectrometry and elemental analysis; selected ^1H and ^{13}C NMR data is presented in Figure 2.2. IR data supports the presence of the conjugated enamine functionality as a C=N stretch was observed at 1658 cm^{-1} along with corresponding C=C stretches at 1632 cm^{-1} . The low frequency C=N stretch is attributed to hydrogen bonding between the imine nitrogen and the hydrogen of the neighboring enamine; this was observed by IR spectroscopy as a broad N-H stretch around 3354 cm^{-1} .



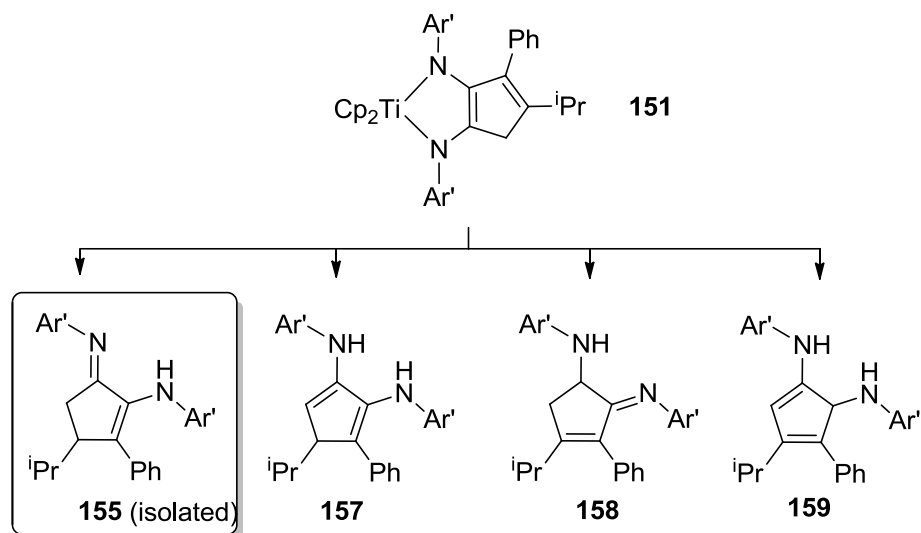
Entry	R	R'	$\delta(\text{C4})$	$\delta(\text{C5})$	$\delta(\text{CH})$	$\delta(\text{CH}_2)$
155	Ph	ⁱ Pr	47.2	27.6	3.06	2.10, 2.00
156	Me	ⁱ Pr	49.0	27.8	2.60	2.03, 1.85

Figure 2.2: Selected ^1H and ^{13}C NMR chemical shifts of **155** and **156**.

Considering the connectivity of the atoms in the ring, there is the possibility of forming two tautomeric α -iminoenamine carbocycles. However, HMBC correlations between the methylene protons on the C5-carbon and the imine carbon establish that the α -iminoenamine compound drawn in these examples (Figure 2.2) is the correct structure. Other 2D NMR techniques such as COSY and HMQC, were important in determining the structure of the α -iminoenamine compounds, as they reveal the connectivity between the carbon and hydrogen atoms of the C5- and C4- positions, as well as that of the R' substituents. A spectroscopic anomaly was also observed in the ^1H NMR spectrum of α -iminoenamine compounds **155** and **156**, where the C3-substituents and the methyl groups of the 2,6-dimethylphenylamine moiety appear as broad singlets. This same spectroscopic oddity was observed in the ^1H NMR spectrum of the carbocyclic titanium-enedi amidate precursors **151** and **152**; we deduced that the origin of this anomaly is due to restricted rotation about the two C-C bonds and will be commented on later in the discussion.

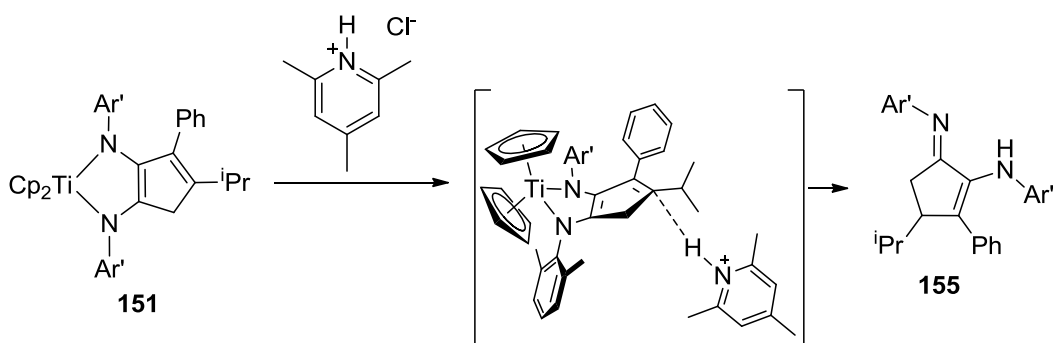
It should be noted that various products that can be formed by protonating carbocyclic-titanium(IV) enedi amidate complexes (Scheme 2.13); these include bis(imino)cyclopentadiene compounds **157** and **159**, as well as α -iminoenamine compounds **155** and **158**. The multitude of potential products may explain why multiple spots were observed when using non-buffered HCl containing ether solutions in our initial investigation.⁶ However, when using the collidine buffered conditions, only the α -iminoenamine compound **155** is isolated from the crude reaction mixture, as determined by NMR spectroscopy.

Scheme 2.13



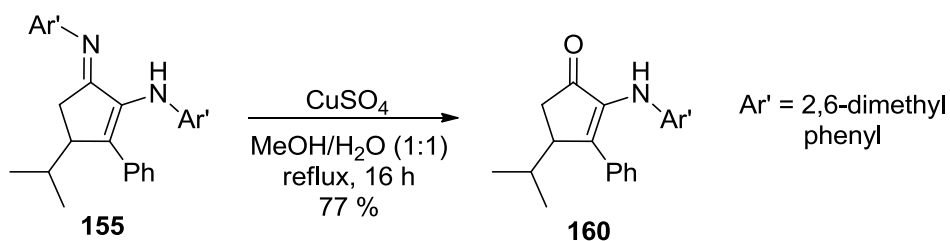
This can be attributed to a few reasons. The first is that the initially formed products undergo rapid base mediated tautomerizations and 1,5-sigmatropic shifts to the more thermodynamically favoured product **155**. This reasoning is flawed however, as none of the above structures appears to be more stable than another. Alternatively, **155** could be the kinetic product formed because the bulky 2,4,6-collidine salt prevents interactions with other basic sites on the titanium enediamide (Scheme **2.14**). This also explains the varying reactivity with other HCl sources, as other potential products may arise from access to other, more basic sites on the titanium diamide which would then follow other reaction pathways.

Scheme 2.14



By subjecting the α -iminoenamine carbocycle **155** to hydrolysis, we obtained the semi-hydrolyzed 3,4- α -ketoenol **160** in high selectivity and good yield (Equation 2.8). Optimal conditions for the hydrolysis involve the use of a copper(II) salt, whereas no imine hydrolysis was observed when the copper (II) salt was omitted. A suitable explanation for the requirement of a copper(II) salt in this reaction, is that the hydrated copper(II) salt is a Bronstead acid and aids in the protonation of the imine. Similar examples involving the semi-hydrolyzed acyclic α -ketoenamine compounds have been reported using buffered conditions (AcOH/KOAc);¹⁰⁴ fully hydrolyzed α -ketoenol compounds can be obtained by addition of aqueous hydroxide, although this avenue was not pursued.¹⁰⁴ Upon attempting to hydrolyze the methyl substituted α -iminoenamine compound **156**, we were not able to isolate the corresponding 3,4- α -ketoenol compound, or any tractable products.

Equation 2.8



The α -ketoenamine carbocycle **160** was fully characterized by 1D and 2D NMR and infrared spectroscopies, as well as mass spectrometry. HMBC correlations between the C5-methylene protons and the newly formed carbonyl carbon were observed; this implies that the imine at the C1-position was indeed the nitrogen-containing functionality that was hydrolyzed. Other 2D NMR techniques were utilized in order to confirm the connectivity between the atoms at the C5-, and C4- positions, as well as the C4-alkyl side chain. The ¹³C chemical shifts of the C4- and C5- carbons are also similar to that of the parent α -iminoenamine (Figure 2.3). The carbonyl stretching frequency was observed at 1701 cm^{-1} , which is lower than normal conjugated enone compounds. Similar to α -iminoenamine compounds, this low carbonyl stretching frequency is

attributed to hydrogen bonding that exists between the carbonyl and the enamine hydrogen.

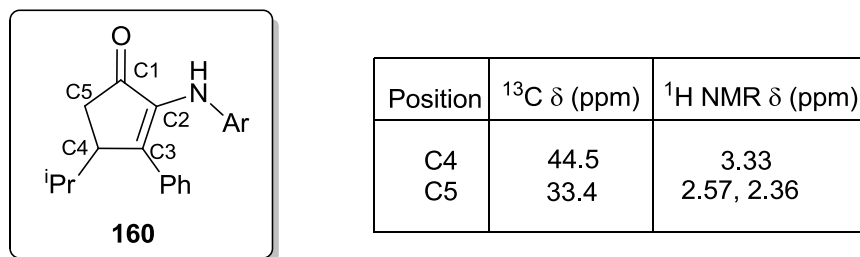


Figure 2.3: Selected ^1H and ^{13}C NMR chemical shifts of **160**.

Similar broad signals which correspond to the C3-substituents, and the methyl groups of the 2,6-dimethylphenyl moiety, were observed in the ^1H NMR spectrum of **160**. Since this was observed in both titanium diamidate, and α -iminoenamine carbocycles, we decided to investigate this anomaly by attempting to resolve the broad signals into sharp separate signals at low temperature. An NMR tube containing α -ketoenamine **160** in CDCl_3 was cooled by increments of 20°C , where complete resolution of the two proton signals shown in Figure **2.4** was observed at -60°C . This result implies that a substantial rotational barrier exists from unfavourable steric interactions between the adjacent groups (Figure **2.4**). However, at higher temperatures the internal energy is sufficient to overcome the rotational barrier, resulting in a coalescence of the signals.

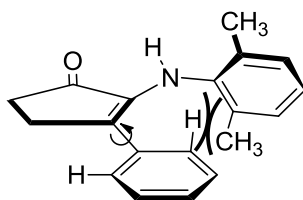


Figure 2.4: Representation of the steric interactions between *o*-phenyl and *o*-methyl substituents of **160** that result in broadening of the corresponding ^1H NMR signals by restricting rotation.

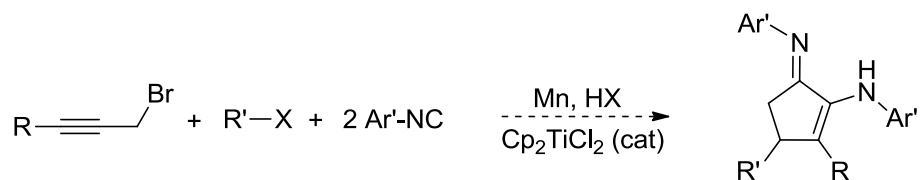
2.3.3 Conclusions

From this work, we report an improved method for demetallating carbocyclic-titanium(IV) enediamidate compounds, which affords five-membered α -iminoenamine carbocycles. We were also able to demonstrate that these α -iminoenamine compounds can be hydrolyzed to their corresponding α -ketoenamine analogues. These results complete one of our original project goals, which had been finding a suitable method for converting titanacyclobutene complexes into functionalized organic compounds.

One future exploration in this area is to continue to find optimal demetallation conditions in order to achieve higher yields of α -iminoenamine carbocycles. As mentioned earlier, more sterically encumbered pyridinium salts should be investigated; as their increased steric bulk would allow greater selectivity towards protonation at the C4- carbon of the titanium diamidate complex and thus, reducing the amount of by-products.

Another avenue to explore is the development of reaction conditions for preparing carbocyclic α -iminoenamine complexes by using a catalytic amount of titanocene(IV) dichloride (Scheme 2.15). This would require careful control over the choice of acid salt and isonitrile, as not to interfere during the formation of the titanacyclobutene intermediate.

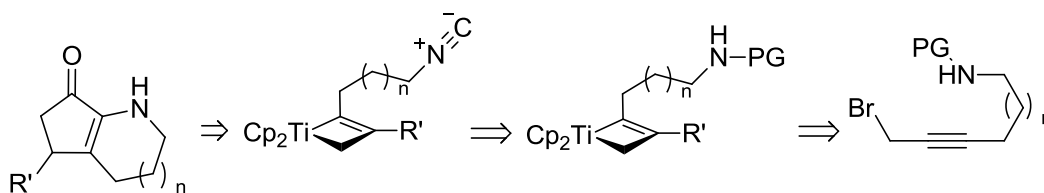
Scheme 2.15



A more challenging project would involve preparing bicyclic α -ketoenamine compounds from a titanacyclobutene bearing a masked isonitrile (Scheme 2.16). However, to prepare these types of complexes, a number of obstacles would have to be

overcome. The first is the development of ideal reaction conditions for synthesizing titanacyclobutene complexes with “masked” isonitrile containing tethers. The second major challenge is developing conditions for “unmasking” the isonitrile functionality in the presence of the titanacyclobutene moiety.

Scheme 2.16



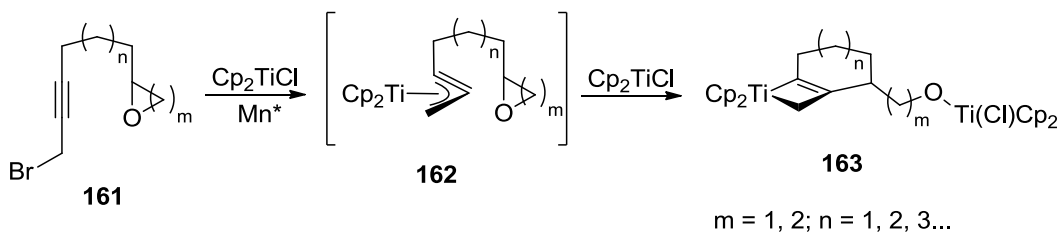
2.4 Investigations into the preparation of bicyclic titanacyclobutene complexes using bi-functional substrates containing cyclic ethers as alkyl radical precursors

2.4.1 Introduction

This final section discusses the preparation of bicyclic titanacyclobutene complexes **163** from new bifunctional substrates **161** which do not contain a combination of two propargyl halides that are linked by a linear alkyl chain, or a propargyl halide which is tethered to a terminal halo-alkane.^{3,4,49,105} The goal was to explore alternative radical precursors which, when tethered to a (η^3 -propargyl)titanocene(III) intermediate **162** will undergo intramolecular radical coupling to afford bicyclic titanacyclobutene complexes **163** with a higher degree of functionality. Although this has not been fully investigated, we hypothesize that the overall formation of bicyclic titanacyclobutene complexes is highly dependent on the relatively faster rate of generating the (η^3 -propargyl)titanocene(III) intermediate, than the transient alkyl radical from the tethered alkyl halide in order to prevent possible side reactions. The potential bifunctional substrates we investigated were propargyl halides that are tethered by a saturated hydrocarbon chain to a strained cyclic-ether (Scheme **2.17**). The

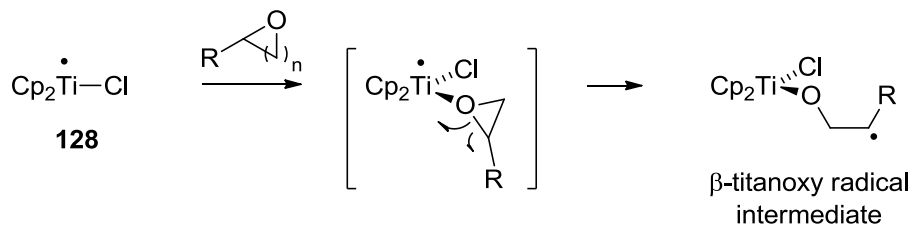
significance of the bicyclic titanacyclobutene complexes formed from these substrates is that they would contain a protected terminal alcohol. This can be subsequently “unmasked” following further conversion of the titanacyclobutene moiety.

Scheme 2.17



Carbon-based organic radicals have been generated from the reaction of titanocene(III) monochloride with epoxides (Scheme **2.18**).^{84,105-110} The reaction proceeds by initial coordination of the Lewis basic oxygen lone pair to a vacant site on the titanium, followed by radical ring opening to give the more stabilized substituted alkyl radical.¹¹¹

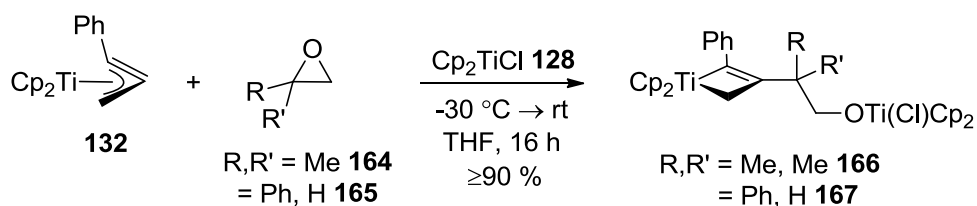
Scheme 2.18



Previously in the Stryker group, these transient alkyl radicals have been trapped effectively by the (η^3 -propargyl)titanocene(III) species **132** affording bimetallic titanacyclobutene complexes **166** and **167** containing a tethered titanium alkoxide

(Equation 2.9).^{45,49} Similar reactivity was also reported between epoxides and titanacyclobutanes, but will not be discussed.

Equation 2.9

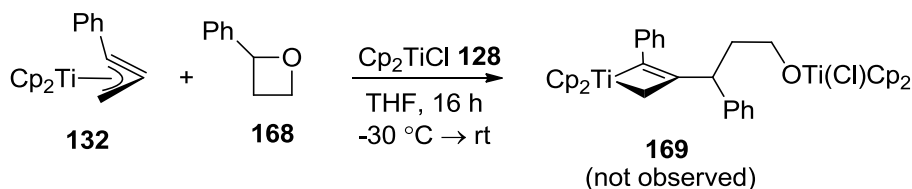


Similar to epoxides, Gansäuer demonstrated that oxetanes exhibit similar reactivity with titanocene(III) monochloride **128**, which generates a similar titanium alkoxyalkyl radical. Based on recent DFT calculations, oxetanes undergo slower radical ring openings by titanocene(III) monochloride than epoxides; this is attributed to increased steric interactions existing between the C2-substituents on the oxetane ring, and the Cp rings of titanocene(III) monochloride, which hinders the coordination of the oxygen atom of the oxetane to the titanium center.¹¹² Based on Gansäuer's results, we envision that oxetane-containing bifunctional substrates have a higher probability of success than epoxide-containing bifunctional substrates. Larger cyclic ethers such as furans and pyrans were also considered as tethers, but these were not selected for this investigation as radical ring closing to form these oxygen-containing heterocycles is highly favoured thermodynamically. The development of samarium(II) iodide-free conditions, as discussed earlier, was also a significant factor in favour of this investigation, as samarium(II) iodide also activates epoxides towards radical polymerization, even at low temperature.⁷⁸

2.4.2 Intermolecular radical coupling of oxetanes with (η^3 -propargyl)titanocene

Before efforts were contributed to preparing suitable bifunctional substrates, we wanted to determine if the tentative alkyl radicals generated from oxetanes and titanocene(III) monochloride, are capable of coupling with (η^3 -propargyl)titanocene(III) complexes. Prior to this investigation, no such trapping products have been isolated. When a dark green THF solution containing (η^3 -phenylpropargyl)titanocene(III) (**132**) and 2-phenyloxetane **168** was treated with titanocene(III) monochloride (**128**) at $-30\text{ }^\circ\text{C}$ a reddish-purple product was formed instantaneously (Equation **2.10**). The ^1H NMR spectrum of the isolated product mixture contained paramagnetic products which were not easy to remove by simple filtration. Subsequent attempts to obtain crystals suitable for x-ray diffraction, or analysis by mass spectrometry were also unsuccessful. The sources of paramagnetism in the product are presumably titanium(III) residues, therefore, isolating and identifying the demetallated organic product would be useful.

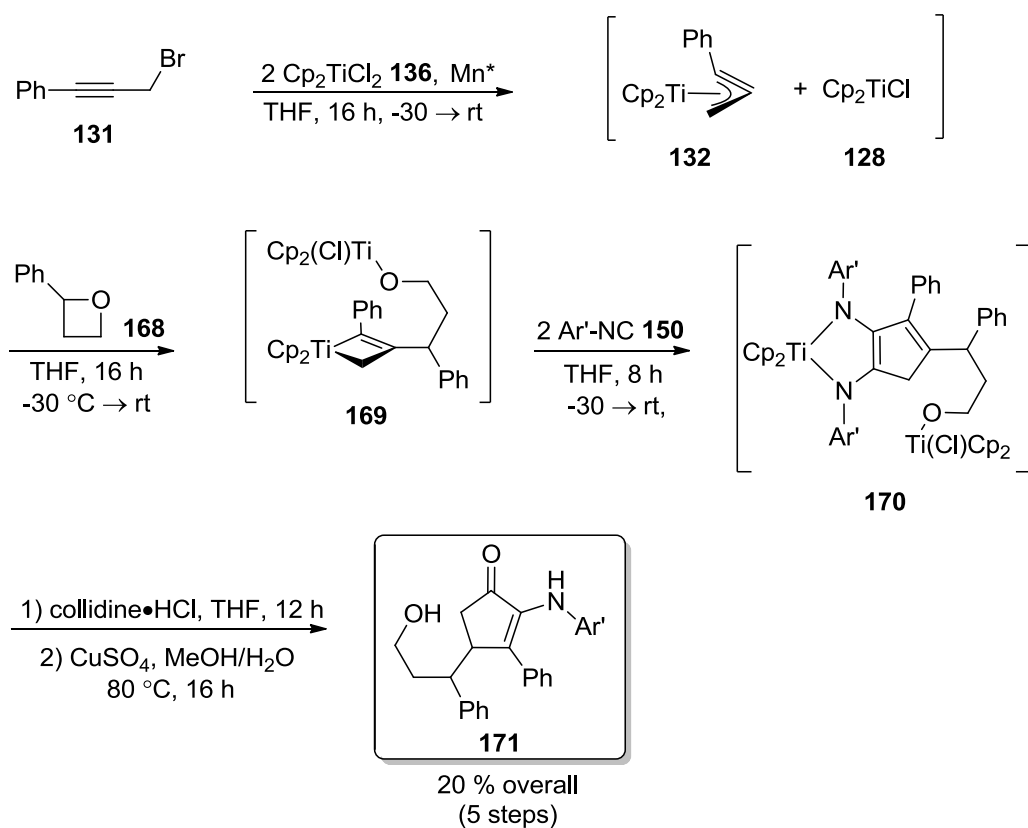
Equation 2.10



This example presented a perfect opportunity to validate our newly completed demetallating procedure discussed in section **2.2**, where we can confirm the formation of **169** by isolating the corresponding α -ketoenamine. Starting from titanocene(IV) dichloride (**136**); the overall conversion required five steps, four of which were performed in a single flask without switching solvents (Scheme **2.19**). This procedure started by treating a THF solution containing two equivalents of titanocene(IV) dichloride **136** and activated manganese powder, with propargyl bromide **137** at $-30\text{ }^\circ\text{C}$. The resulting product mixture was then treated with a THF solution of 2-phenyloxetane **169** and allowed to warm to room temperature, whereupon a similar reddish-purple

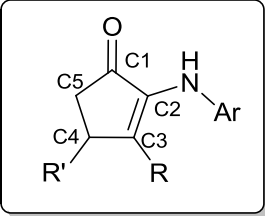
solution was obtained. Cooling the resultant mixture to -30 °C and subsequently adding two equivalents of 2,6-dimethylphenylisonitrile (**150**) furnished a light brown product mixture. The tentative titanium(IV) enediamidate **170** was treated with an excess of collidine•HCl, giving the crude α -iminoenamine; this was immediately hydrolyzed to afford the targeted α -ketoenamine **171** in an overall isolated yield of 20 % over five combined steps after purification.

Scheme 2.19



The α -ketoenamine **171** was fully characterized by 1D and 2D and infrared spectroscopies, as well as mass spectrometry (Figure 2.5). A comparison of key ^1H and ^{13}C NMR signals of α -ketoenamine **171** is consistent with the previously obtained α -ketoenamine **160**. Proton-proton (COSY) and proton-carbon (HMQC) correlations were

crucial in determining the connectivity through the terminal alkoxyalkyl chain at the C4-position, as well as the atoms at the C4- and C-5 positions.



Entry	R	R'	$\delta(\text{C4})$	$\delta(\text{C5})$	$\delta(\text{CH})$	$\delta(\text{CH}_2)$
160	Ph	ⁱ Pr	44.5	33.4	3.33	2.57, 2.36
171	Ph	CH(Ph) (CH ₂) ₂ OH	43.9	35.1	3.70	2.66, 2.57

Figure 2.5: Comparison of the selected ¹H and ¹³C NMR chemical shifts of **160** and **171**.

This result was promising, as it establishes that alkyl radicals obtained from oxetanes and titanocene(III) monochloride, will couple with (η^3 -propargyl)titanocene(III) intermediates. This provided us enough precedent to investigate bifunctional precursors containing saturated alkyl chain tethered-oxetanes, as well as epoxides. Bifunctional substrates **172**, **173** and **174** (Figure 2.6) were chosen as the synthetic targets for this investigation, as five- and seven-carbon alkyl tether lengths would result in the formation of both small and medium sized B-rings. Epoxide substrates **172** and **173** were also chosen to evaluate whether the formation of bicyclic titanacyclobutene complexes is favoured over intramolecular 5-*exo* radical cyclization reactions,^{109,110} which have been reported from the treatment of epoxide-containing bifunctional substrates with titanocene(III) monochloride.

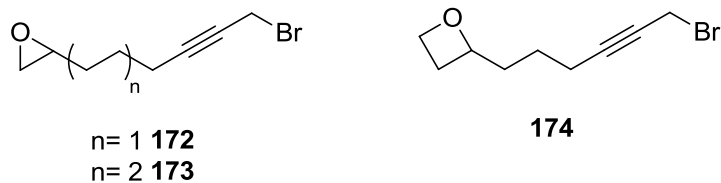
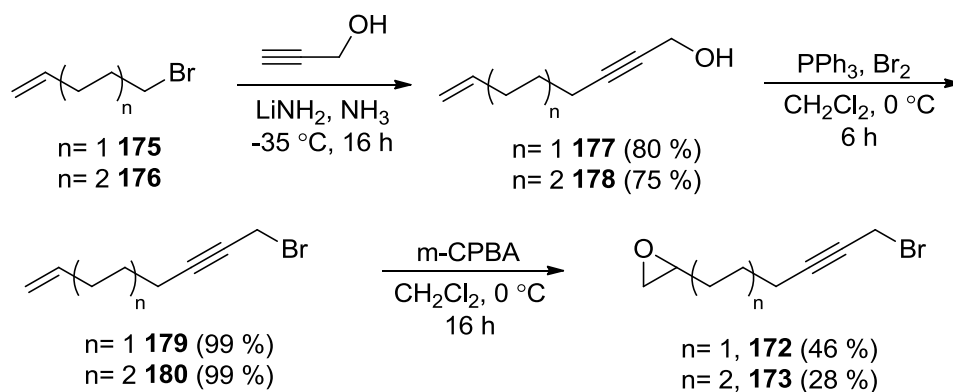


Figure 2.6: Synthetic targets.

2.4.3 Construction of the epoxide-containing substrates

The synthetic strategy for preparing bifunctional epoxide-containing substrates **172** and **173** consisted of three steps (Scheme 2.20) when starting from commercially available α,ω -haloalkenes **175** and **176**.¹¹³ Conversion of **175** and **176** into propargyl alcohols **177** and **178** was accomplished via bromide displacement by the dilithium salt of propargyl alcohol in liquid ammonia.¹¹⁴ Subsequent addition of $[\text{Ph}_3\text{PBr}]\text{Br}$ to **177** and **178** afforded the propargyl halides **179** and **180** quantitatively.¹¹⁵ Conversion of the terminal olefins into the corresponding terminal epoxides was then accomplished using *m*-CPBA, which furnished the desired bifunctional epoxide-containing substrates **172** and **173**. The order in which the second and third steps were conducted was important, as $[\text{Ph}_3\text{PBr}]\text{Br}$ has been reported to react with epoxide-containing substrates.¹¹⁶ The low yields associated with the final step of these syntheses were attributed to the reactivity of the propargyl bromide with residual *m*-CPBA or benzoic acid, the by-product of this reaction. The displacement of the propargyl bromides by carboxylate anions have been studied, in which alkynoate ester products have been obtained.¹¹⁷ Although not investigated, higher yields could have been obtained by employing dimethyldioxirane (DMDO),¹¹⁸ where the by-product from the oxidation is acetone, which will not displace the propargyl bromide.

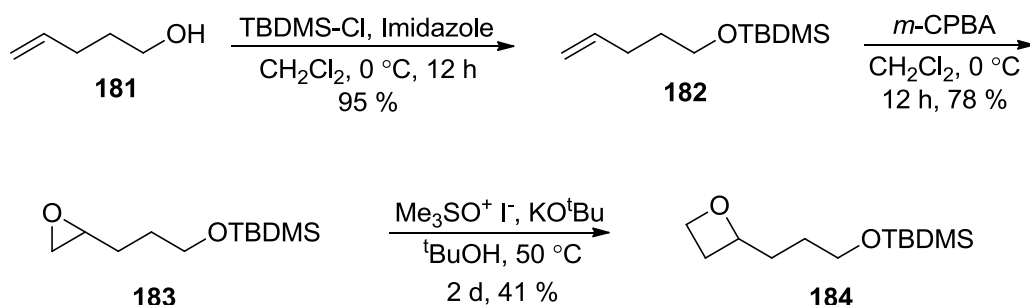
Scheme 2.20



2.4.4 Construction of the oxetane-containing bi-functional substrate

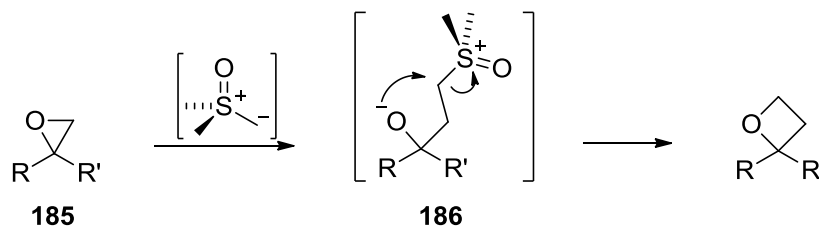
The synthesis of the oxetane containing bifunctional substrate **174** was accomplished using a more extended synthetic pathway involving the formation of the oxetane prior to installing the propargyl bromide. Siloxy-oxetane **184** was prepared according to a procedure reported by Kwon,¹¹⁹ which involves a one-carbon ring expansion of epoxy-silyl ether **183** by addition of dimethylsulfoxinium methylide, which is generated *in situ* by the deprotonation of trimethylsulfoxonium iodide with potassium *t*-butoxide (Scheme 2.21).

Scheme 2.21



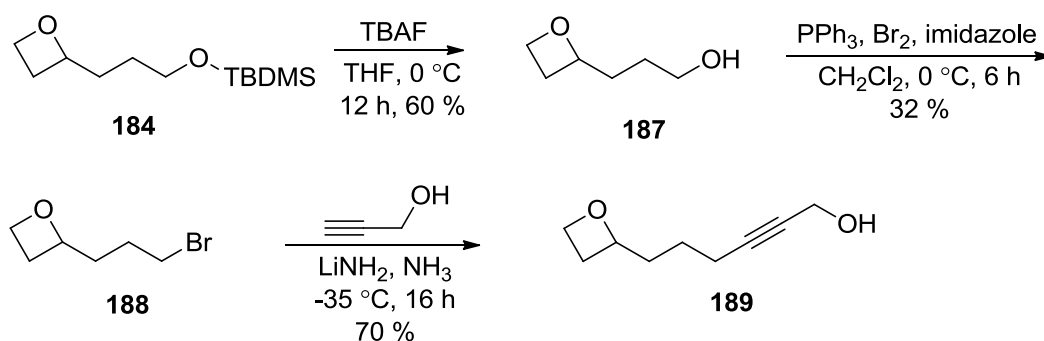
The use of dimethylsulfoxinium methylide to prepare oxetanes from epoxides (Scheme 2.22) is a modification of the Johnston-Corey-Chaykovsky reaction.¹²⁰ This was discovered by Okuma and co-workers, who isolated oxetanes as by-products from the addition of excess dimethylsulfoxinium methylide to simple carbonyl groups.¹²¹ The reaction proceeds by nucleophilic attack of dimethylsulfoxinium methylide on the epoxide. This affords an alkoxide intermediate **186** which then undergoes an intramolecular displacement of dimethyl sulfoxide (Scheme 2.22).

Scheme 2.22



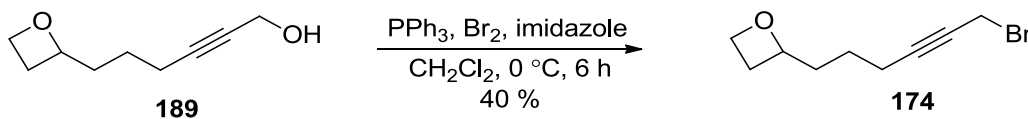
To prepare the oxetanyl-propargyl alcohol derivative **189**, the siloxyoxetane **184** was converted to the bromide **188** by removal of the silyl-ether (TBAF), then treated without purification with $[\text{Ph}_3\text{PBr}]\text{Br}$ and an equivalent of imidazole.⁶ Propargyl alcohol **189** was prepared similarly to compounds **177** and **178** (see Scheme 2.20) by addition of the dilithium salt of propargyl alcohol to **188** (Scheme 2.23). The chemoselectivity of the propargyl dianion towards the bromide functionality in **188** is worth noting, as an excess of the dilithium salt of propargyl alcohol was used without affecting the integrity of the oxetane. Prior reports have commented on the robustness of oxetanes towards nucleophilic attack by organolithium reagents, at least in the absence of Lewis-acids.¹²²

Scheme 2.23



The final substrate, bifunctional bromide **174**, was prepared using precisely one equivalent of both $[\text{Ph}_3\text{PBr}]\text{Br}$ and imidazole (Equation 2.11). Precise stoichiometry of triphenylphosphine, bromine and imidazole are crucial in this process because by-products are readily formed when any of the reagents is in excess.¹²³ The order of addition is also important as the dichloromethane solution containing $[\text{Ph}_3\text{PBr}]\text{Br}$, must be added dropwise to the cooled solution of **189** and imidazole; deviation from this procedure afforded intractable product mixtures.

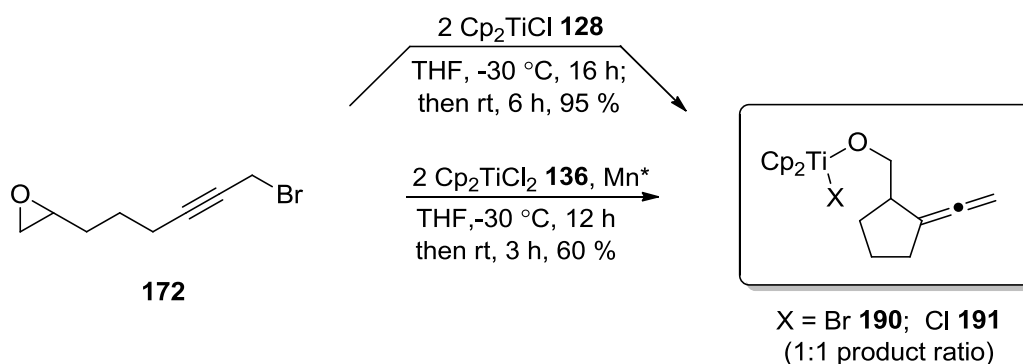
Equation 2.11



2.4.5 Attempted preparation of bicyclic titanacyclobutene complexes by intramolecular cyclizations involving oxirane and oxetane containing bi-functional substrates

To evaluate our bicyclization strategy, a THF solution of the epoxide-containing substrate **172** was treated with two equivalents of titanocene(IV) dichloride (**136**) and excess activated manganese powder at $-30\text{ }^{\circ}\text{C}$, followed by warming to ambient temperature (Equation **2.12**). The desired bicyclic titanacyclobutene complex was not observed; instead, a mixture containing titanium alkoxide complexes **190** and **191** was isolated in 95 % combined yield. The reaction afforded the same product mixture in higher yield when two equivalents of titanocene(III) monochloride (**128**) was used in place of activated manganese powder and titanocene(IV) dichloride (**136**).

Equation **2.12**



The products are formed in an almost 1:1 ratio, which was determined by comparing the integrations of the nicely separated alkoxide (C1) protons; no attempts, however, were made to assign either bromide or chloride complexes to the two sets of characterization data. The mixture of titanium alkoxide complexes **190** and **191** were characterized by 1D and 2D NMR techniques as well as by infrared spectroscopy (Figure **2.7**).

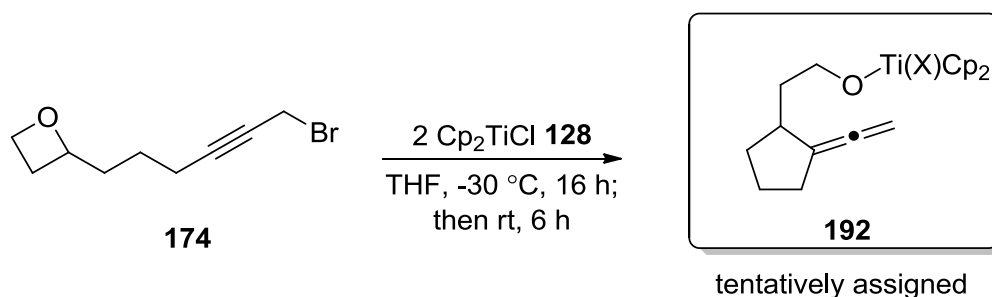
Atom label	¹³ C NMR (ppm)		¹ H NMR (ppm)	
	product		product	
	A	B	A	B
1	85.8	86.2	4.49, 4.29	4.43, 4.23
2	46.9	46.8	2.75	2.75
3	105.1	105.0	-	-
4	32.4	32.4	2.35	2.35
5	26.3	26.3	1.63	1.63
6	31.5	31.5	1.75	1.75
7	203.5	203.5	-	-
8	77.1	77.1	4.75	4.75

Figure 2.7: ¹H and ¹³C NMR chemical shifts of compounds **190** and **191**.

The exocyclic allenes were identified by the downfield ¹³C NMR chemical shift of the central carbons which were both observed at 203.5 ppm, and the ¹H chemical shifts of the vinylic protons at 4.75 ppm. A strong stretch at 1900 cm⁻¹ in the IR spectrum was observed which is characteristic of the allenyl moiety. Other assignments regarding the structural connectivity of **190** and **191** were done using 2D NMR techniques (COSY, HMQC, HMBC).

Treatment of the oxetane-containing substrate **174** using titanocene(IV) dichloride (**136**) and activated manganese powder, or two equivalents of titanocene(III) monochloride (**128**), afforded paramagnetic product mixtures (Equation 2.14). An attempt to produce the corresponding carbocyclic α -ketoenamine by *in situ* conversion was also unsuccessful, suggesting that the bicyclic titanacyclobutene complex was not formed. An infrared spectrum obtained from the crude product mixture however, displayed a stretch at 1900 cm⁻¹ which infers that the allenyl-containing product **192** is present.

Equation 2.14

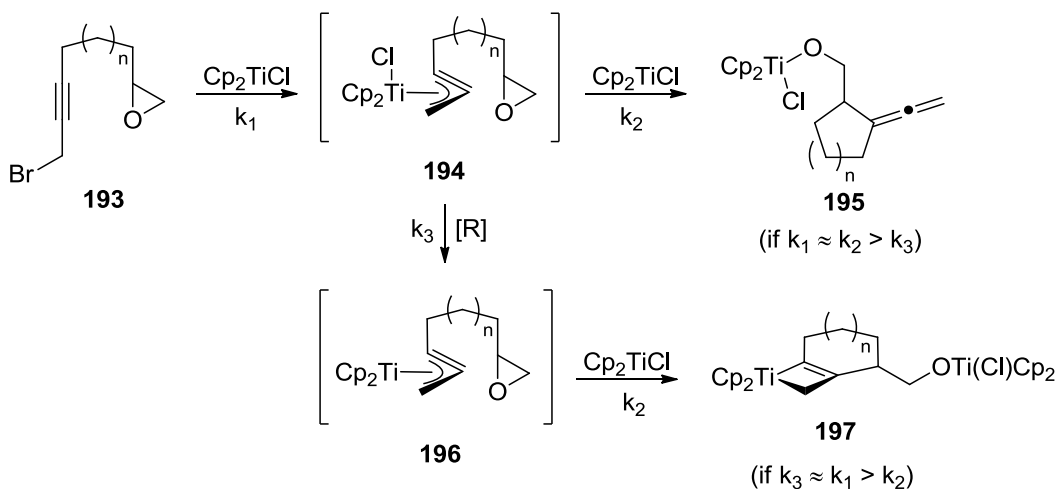


To limit the amount of paramagnetic contaminants in the product mixture, Gansäuer's catalytic conditions were employed using oxetane-containing substrate **174**; activated manganese powder, two equivalents of collidine•HCl, and a catalytic amount of titanocene(IV) dichloride (**136**). Three organic products were isolated from the crude reaction mixture using silica flash chromatography in a single spot; efforts to further resolve these compounds were unsuccessful. The identification of these compounds was also unsuccessful because of conflicting IR and NMR spectroscopic data; mass spectrometry was also utilized but molecular ion peaks were not observed. The product mixture, however, contains a downfield ¹³C NMR chemical shift (208 ppm), as well as a stretching frequency in the infrared spectrum of 1900 cm⁻¹, indicative of an allenyl moiety. These spectroscopic observations imply that a demetallated titanium alkoxide product may be present. The compound mixture was relatively stable when left dilute in NMR solvents; more concentrated solutions, however, quantitatively converted into three new compounds, as observed by the gas chromatograph of a GC-MS analysis. These compounds were not identified, but the differences between the mass spectrographs of the initial three compounds obtained, and the three "decomposition" products, was a loss of a bromine atom. These results suggest that alternative bromine-containing cyclization products are being formed under the reaction conditions and should be investigated in further studies.

2.4.6 Discussion

It is apparent that bifunctional substrates involving cyclic ethers are not suitable for preparing bicyclic titanacyclobutene complexes, at least under the present conditions. The isolation of the tentatively assigned titanium(IV) alkoxide products **190** and **191** establishes that the rate of radical epoxide opening is significantly greater than the rate of formation of the (η^3 -propargyl)titanocene(III) intermediate **196** (Scheme **2.24**). The same can be assumed for oxetane-containing substrates, however no assignment of the product can be offered at the moment.

Scheme 2.24



A variety of modifications to the existing reaction conditions were also explored to favour formation of bicyclic titanacyclobutene **197**. Titanocene(III) monobromide and decamethyltitanocene(III) monochloride were investigated in place of titanocene(III) monochloride in the reactions. These “modified” titanium(III) reagents were chosen because they are known to display slower rates of radical ring-opening of epoxides.¹²⁴ In these experiments, a THF solution containing epoxide bifunctional precursor **172** was added to a THF solution containing two equivalents of either “modified” titanium(III) reagent, along with activated manganese powder, and resulted only in paramagnetic product mixtures. A third experiment involved adding a THF solution of the epoxide bifunctional substrate **172** to a THF solution containing two equivalents of titanocene(III) monochloride (**128**) and three equivalents of samarium(II) iodide. The samarium(II) iodide used in this reaction was to replace the activated manganese powder, but afforded intractable solids also. A final experiment was conducted in which titanocene(IV) dichloride (**136**) was added slowly over 3 hours at low temperature to a THF solution containing the epoxide substrate **172** and activated manganese powder. This experiment was conducted under the presumption that the rate of titanocene(III) monochloride reduction of the propargyl halide, and subsequent reduction of the (η^3 -propargyl)titanium(IV) to the (η^3 -propargyl)titanocene moiety by activated manganese powder, is faster than the titanocene(III) monochloride mediated ring opening of the

epoxide. The product mixture obtained from the reaction, however, contained the same mixture of 5-*exo* cyclization products **190** and **191** which were identified earlier (see Equation **2.14**). These modifications were also employed for the oxetane-containing substrate **174**, which afforded similar results when compared to the epoxide substrate **172**.

2.1.7 Conclusions

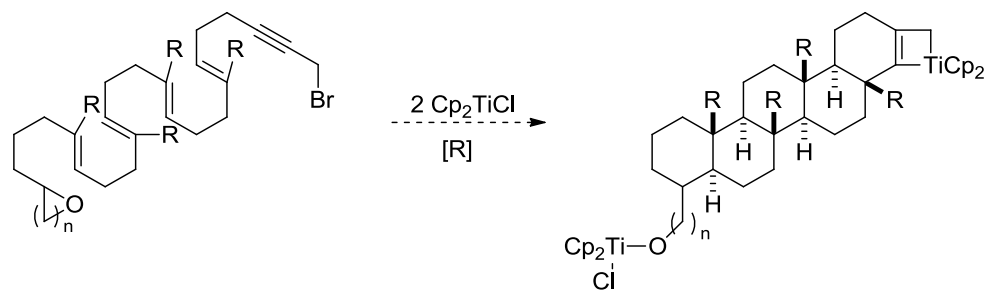
The results of this investigation establish that cyclic ethers are not compatible functional triggers for preparing bicyclic titanacyclobutene complexes. One future research avenue is the development of a reaction protocol that would increase the rate of formation of the (η^3 -propargyl)titanocene(III) moiety, decrease the rate of radical epoxide opening, or a combination of the two ideally.

One modification to the bifunctional substrates is incorporating other small heterocyclic rings containing nitrogen and sulfur. However, recent computational studies suggest that the rate of radical initiation of these heterocycles by titanocene(III) monochloride may be faster rather than slower.¹²⁵

The utility of intramolecular radical cyclizations between cyclic ethers and propargyl halides should be further investigated and may prove useful in preparing polycyclic or polyether frameworks through activation of epoxides or oxetanes by titanocene(III) monochloride. Radical cyclizations have been used as a valuable tool for preparing polycyclic frameworks, which can be observed in selected works of Macmillan,¹²⁶ Gansäuer,¹²⁷ and others. This methodology can be useful for two potential reasons, the first being the ability to assemble polycyclic arrays from epoxides or oxetanes, which are tethered by polyene chains (Equation **2.15**). Secondly, these substrates are interesting because the time required for the radical cascade to reach the final olefin in polyene chain may be sufficient for the (η^3 -propargyl)titanocene moiety to be generated. If successful, this would be an entry into assembling polycyclic titanacyclobutene complexes. The synthetic utility of these compounds is the

titanacyclobutene unit, as well as the titanium alkoxide, which can be further transformed into other functional groups.

Equation 2.15

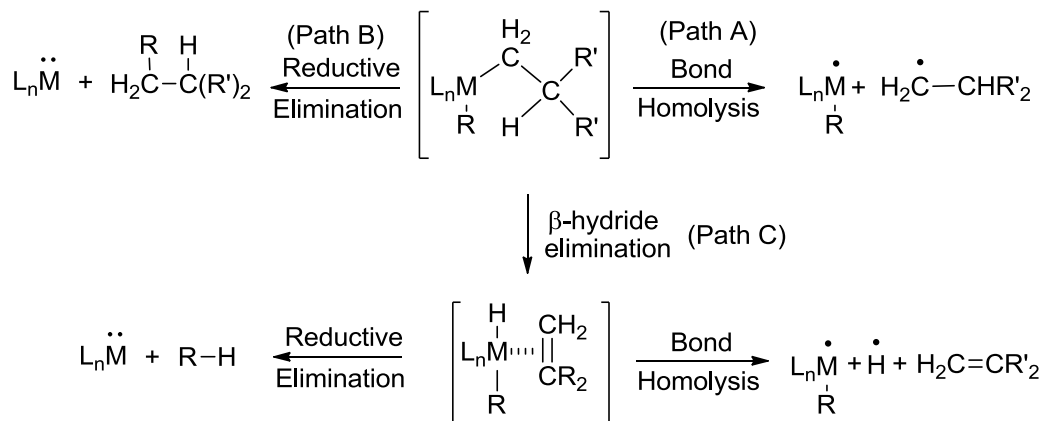


Chapter 3: A Review of Phosphinimide Containing Transition Metal Complexes

3.1 Introduction. The stabilizing capability of electron-rich transition metal ligands

The choice of transition metal auxiliary ligands can sometimes have a profound influence on the outcome of transition metal organometallic reactions; this statement applies to any scenario that requires catalytic or stoichiometric amounts of a metal complex. In an extreme case, the incorrect choice of ligand system can lead to intractable product mixtures caused by the decomposition of unstable reactive organometallic intermediates (Scheme 3.1). There are a few common pathways in which organometallic compounds are known to decompose. In the homolytic pathway (Path A), the scission of the metal-carbon bond results in a one-electron reduction of the metal center, as well as the generation of a carbon-based radical. In the reductive elimination pathway (Path B), the two metal-bound organic fragments are reductively coupled, this process restores two electrons to the metal. The third pathway involving β -hydride elimination (Path C) does not result in a change in oxidation state of the metal. However, the resulting metal-hydride product is generally less stable than the initial metal-alkyl complexes, and is more prone to decomposition by bond homolysis, or reductive elimination.

Scheme 3.1



Auxiliary ligands inhibit such decomposition pathways from occurring by providing additional electron density to fill empty metal orbitals. Chelating ligands are the first type of stabilizing ligand, which provide electron density from multiple σ -donors such as lone pairs on heteroatoms. Conjugated aromatic ring systems such as neutral η^6 -arene ligands or anionic η^5 -cyclopentadienyl ligands are the second type of stabilizing ligand, which donate electron density to metal centers from filled σ - and π -orbitals (Figure 3.1).¹²⁸ In order for this type of donation to occur, empty metal orbitals must be available with σ - and π - symmetry; an example of this interaction is depicted for the computed molecular orbitals of CpTiCl₃ (**198**).

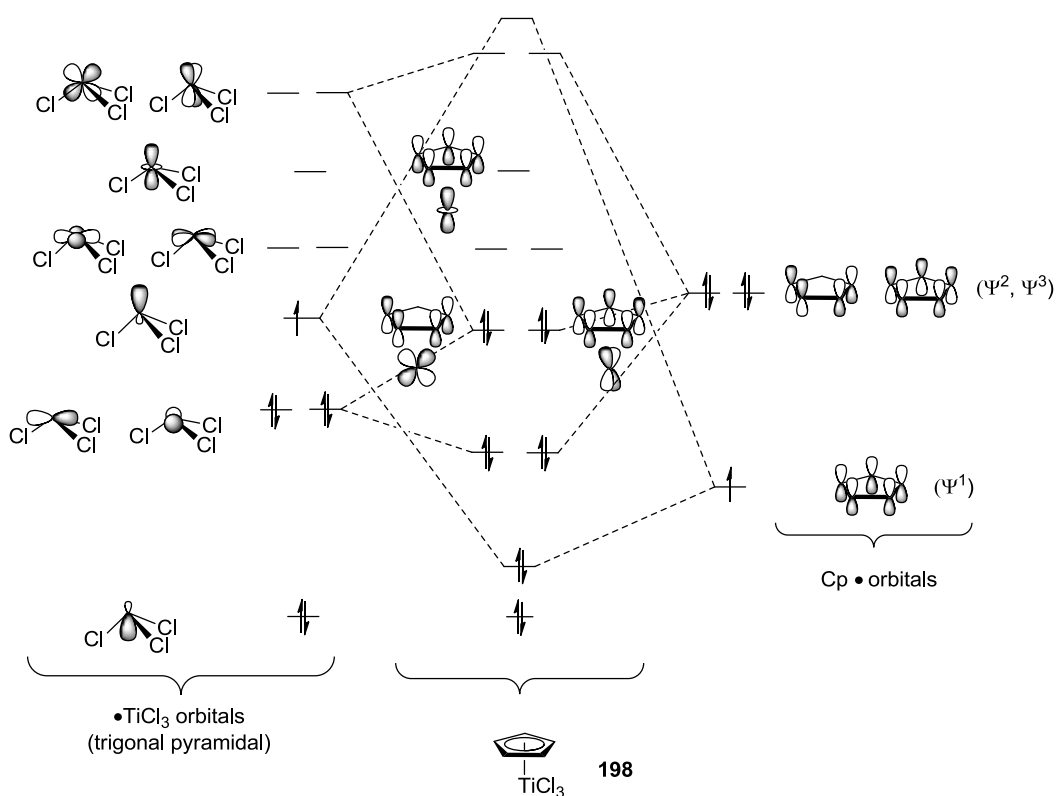


Figure 3.1: Calculated molecular orbitals of CpTiCl₃ (**198**).

Anionic heteroatom-derived ligands, such as the examples in Figure 3.2, also provide electronic stability to transition metal centers through filled σ - and π -type orbitals.¹²⁹⁻¹³² The symmetry of the bonding orbitals of these heteroatom ligands is similar to Cp ligands; this type of relationship is defined as an isolobal relationship.^{133,134}

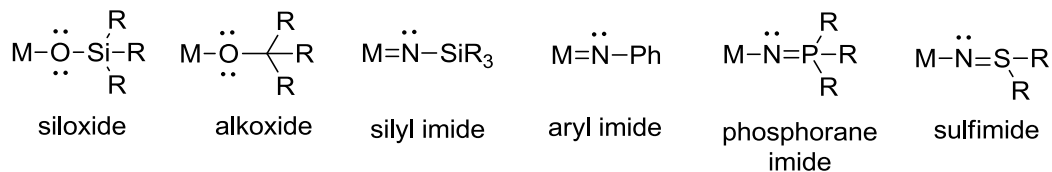


Figure 3.2: Alternative ligand systems investigated as isolobal analogues for Cp ligands.

From this list, the number of main group-, rare earth-, and transition metal phosphorane imide (commonly referred to as phosphinimide) complexes has been growing significantly over the past decade.¹³⁵⁻¹³⁹ This chapter discusses the physical and electronic properties of phosphinimide ligands and why these properties are so desirable in transition metal complexes. Also included is a brief overview regarding the various methods used to prepare transition metal phosphinimide complexes.

3.2 Physical characteristics of phosphinimide ligands

3.2.1 Electronic properties of phosphinimide ligands

Phosphinimide ligands can donate up to six electrons to a transition-metal center; two via σ -donation, and two or four via π -donation, as depicted by the resonance structures in Figure 3.3. DFT calculations by Schoeller and co-workers, indicate that the nitrogen-phosphorous double bond of phosphinimide compounds is highly polarized, favouring the zwitterionic resonance structure B, which has significant electron density on the nitrogen atom (Figure 3.3).¹⁴⁰ One of the nitrogen lone-pairs is located in a sp type orbital ($1e$), which provides σ -donation to the metal, leaving the remaining two lone-pairs in p orbitals ($3a^1$) which provide π -donation.

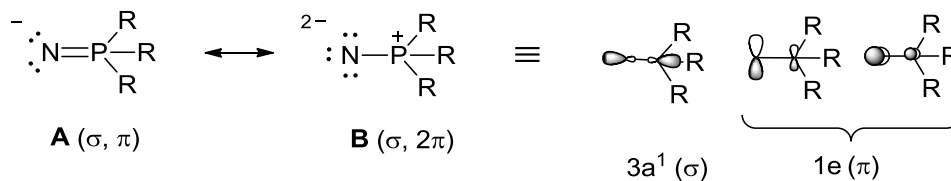


Figure 3.3: Highest occupied molecular orbitals associated with dipolar resonance of phosphinimide ligands.

The electronic interactions between phosphinimide ligands and transition metals have also been explored computationally, from which, the isolobal relationship with cyclopentadienyl ligands is further supported (Figure 3.4). One such example is the calculated molecular orbitals of $\text{Cl}_3\text{Ti-N}=\text{PH}_3$ (**199**), and the similarity with the molecular orbitals of CpTiCl_3 (**198**) (see Figure 3.1). In these examples, one can observe the significant σ -overlap occurring between the ligands ($1e$, and ψ^1) and the titanium d_{z^2} orbital, and also significant π -overlap between both ligands ($3a^1$ and ψ^2 , ψ^3) and the titanium d_{xz} and d_{yz} orbitals.¹⁴¹

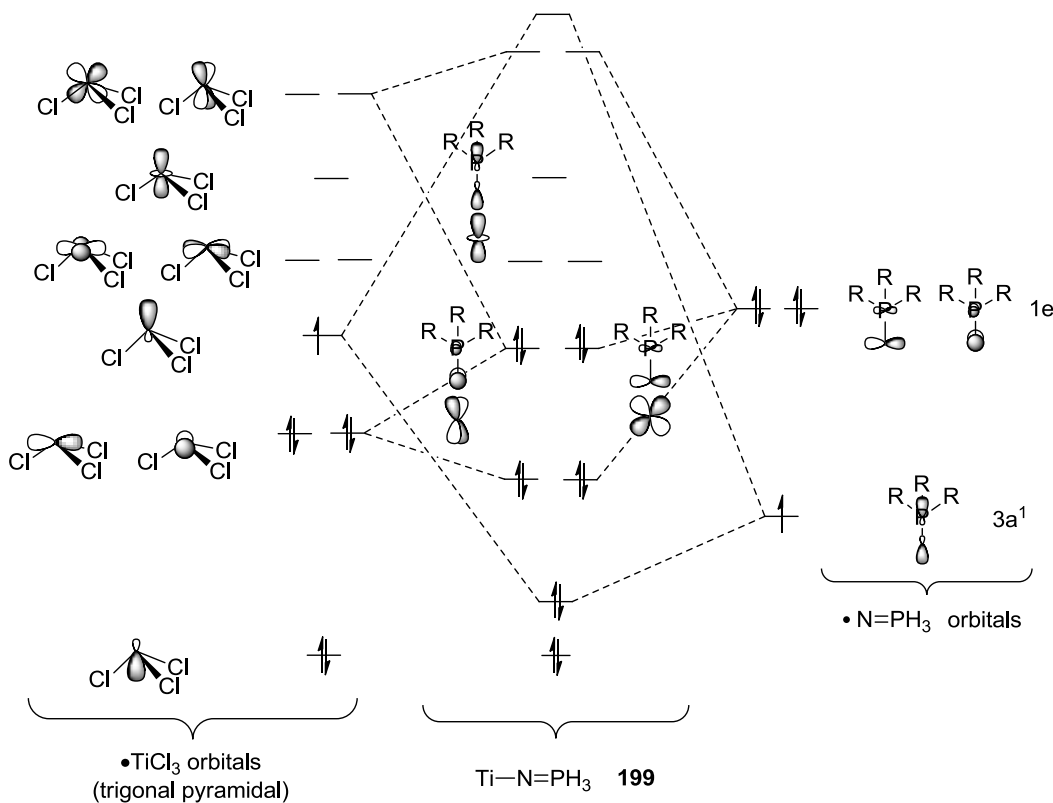


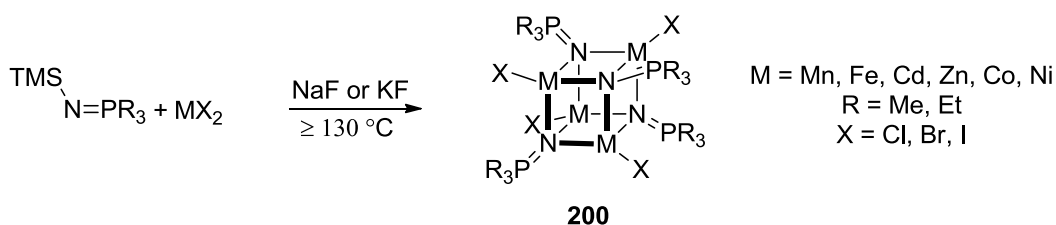
Figure 3.4: Calculated molecular orbital diagram of $\text{H}_3\text{P}=\text{N-TiCl}_3$ (**199**).

Due to significant orbital overlap, the resulting nitrogen-titanium bond of **199** has triple-bond character; this is consistent with other transition metal phosphinimide complexes where the metals center is in a lower electron configuration (d^0 to d^3).

Consequentially, the M-N-P bond angles of monomeric transition-metal phosphinimide complexes such as the above examples are typically observed between 150°-180°. The difference in energy associated with adjusting the M-N-P bond angles within this range is relatively small (~2 kcal/mol), as determined by Bickelhaupt and co-workers in a computational investigation of the effects of varying the Re-N-P bond angles (150°-180°) in the hypothetical oxo-rhenium phosphinimide complex O₃Re(N=PH₃).¹⁴¹

Phosphinimide ligands can also bridge between multiple metal centers; but this motif is commonly observed with more electron-rich metals and metals in higher electron configurations (d⁴ to d¹⁰) (Equation 3.1). One such example is a series of first-row transition metal phosphinimide complexes with the generic formula [R₃P=N-M-X] (M= Mn, Fe, Co, Ni, Zn)¹³⁵ that were prepared by Dehnicke and co-workers; all are tetrameric heterocubane clusters with the general formula **200** with triply-bridging (or μ³-) phosphinimide ligands.

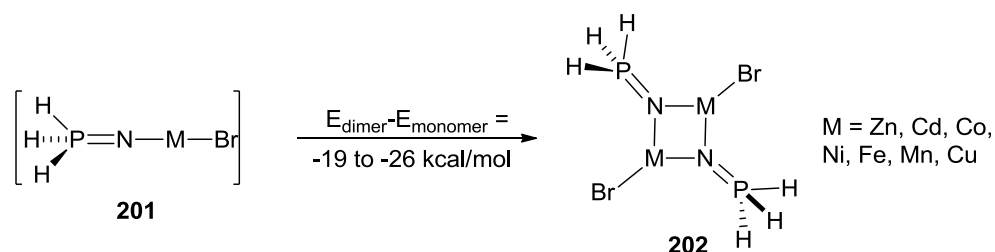
Equation 3.1



The electronic and structural properties of hypothetical monomeric first-row transition metal phosphinimide complexes with the formula [H₃P=N-M-Br] (M= Mn, Fe, Co, Ni, Cu, Zn) (**201**) have also been modelled by Schoeller and co-workers (Equation 3.2).¹²⁹ The results from the computations revealed short metal-nitrogen bond distances and M-N-P bond angles close to 180°; unfortunately the monomeric species have only been described from computations. In this series, two anomalies were encountered in terms of the computed M-N-P bond angles for the Cu(II) and Zn(II) phosphinimide complexes, which were closer to 130°. This was attributed to the greater occupancy of higher energy metal d-orbitals which decreases the overall π-accepting

character of the metal centers. Experimentally, these monomeric units are not stable and only tetrameric heterocubane clusters are observed. Schoeller and co-workers have explored the energetics pertaining to the formation of higher order clusters from the hypothetical [Br-M-N=PH₃] monomeric unit **201**. Their calculations demonstrated that the net stabilization energy gained from the dimerization of the monomeric unit is between 19 and 26 kcal/mol. In further calculations, Schoeller determined that the formation of heterocubane clusters from the monomeric units is more thermodynamically favourable, with typical stabilization energies in the range of 23 to 38 kcal/mol.^{129,140}

Equation 3.2



Due to the delocalization of the electron density of the nitrogen atom among two or more metal centers, longer metal-nitrogen bond distances and more acute metal-phosphinimide bond angles (120°-140°) are typically observed. Three types of bridging transition metal-phosphinimide complexes have been reported (Figure 3.5). Bridging modes A and C represent complete delocalization of electron density of the nitrogen of the phosphinimide ligand among two or three metals. Bridging mode B has been observed typically in bimetallic transition-metal phosphinimide complexes where the metal centers vary in electron density.

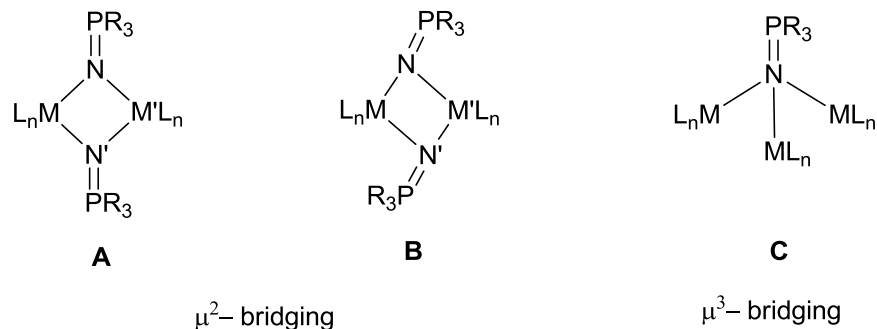


Figure 3.5: Different bridging modes of phosphinimide ligands in bi- and tri-molecular complexes.

3.2.2 Steric and electronic properties of phosphinimide ligands

Simple alteration of the phosphorus substituents on phosphinimide ligands allows for the steric environment about the metal center to be readily adjusted. In cases such as the large tri(*t*-butyl)phosphinimide ligands, Stephan and co-workers have demonstrated that the shielding provided to the titanium center in (^tBu₃P=N)TiCl₃ (**203**) is greater than that of the unsubstituted cyclopentadienyl ligand in CpTiCl₃ (Figure 3.6).¹⁴² Although both ligands provide similar shielding, the steric bulk of the phosphinimide ligand is situated farther away from the titanium center, with the nitrogen-phosphorous bond acting as a molecular “spacer”. Such steric differences can be important when considering the coordination of small molecules to the metal center.

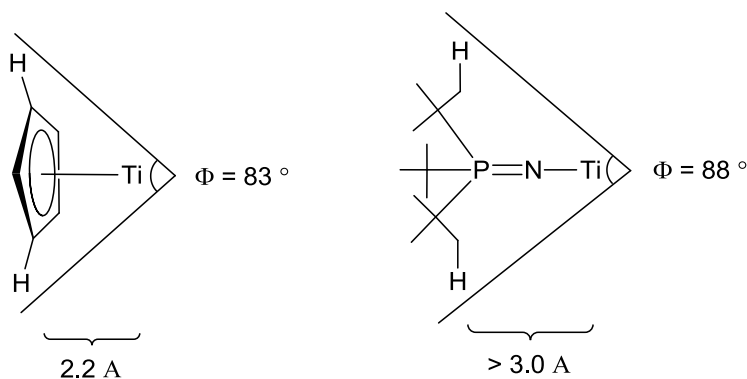
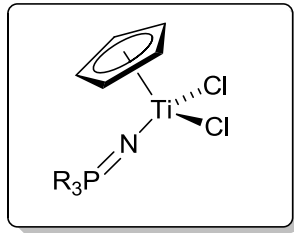


Figure 3.6: A comparison between the Tolman's cone angles^{143,144} plus the measured distances between the titanium atom and the steric bulk of tri(*t*-butyl)phosphinimide ligands, and the unsubstituted Cp ligand.

The nature of the phosphorous substituents also has an effect on the N-P bond lengths of phosphinimide ligands. Through computational experiments on various unsubstituted phosphinimine compounds, Lu and co-workers reported the following trend in terms of increasing N-P bond lengths: halide \ll H $<$ methyl $<$ aryl $<$ 1° alkyl $<$ 3° alkyl.¹⁴⁵ This result implies that the shorter N-P bond lengths are the result of additional donation of electron density from the nitrogen lone pair to the empty phosphorus π -type orbital; electron withdrawing substituents are incapable of providing such stability to an electrophilic phosphorous center. Alkyl substituents, in contrast, are capable of providing such stabilization to the phosphorous center, which decreases the amount of donation from the nitrogen lone pair. A similar trend is observed in transition metal complexes, where longer N-P bonds are observed in phosphinimide ligands bearing more substituted alkyl substituents in the Cp(R₃PN)TiCl₂ series (Figure 3.7).^{142,146,147}



Entry	R	Ti-N (pm)	N-P (pm)	Ti-N-P (°)
204	Ph	178	156	174
205	Me	174	159	170
206	ⁱ Pr	175	161	170
207	Cy	176	161	172
208	^t Bu	178	162	176
209	N(Me) ₂	176	159	164
210	N(Me ⁱ Pr)	176	159	174

Figure 3.7: Selected bond lengths and angles of half-sandwich titanium phosphinimide complexes **204** to **210**.

3.2.3 Physical methods for characterizing transition metal phosphinimide complexes

Various analytical techniques have been used to characterize transition-metal phosphinimide complexes.¹³⁶ NMR spectroscopy is a good qualitative tool for determining the various ¹⁵N, ³¹P, ¹H nuclei in each complex. The asymmetric and symmetric IR stretching modes of the nitrogen-phosphorous double bond typically occur at $\sim 1100\text{ cm}^{-1}$ and $\sim 600\text{ cm}^{-1}$ respectively. The difference between the two frequencies has been used to differentiate between terminal ($\Delta\nu_{\text{NP}} \sim 550\text{ cm}^{-1}$) and bridging ($\Delta\nu_{\text{NP}} \leq$

500 cm^{-1}) phosphinimide ligands. The higher frequency difference for terminal phosphinimide ligands is the result of greater mechanical overlap between the two stretching vibrations, causing a greater coupling, or splitting, of the signals. Very few techniques however, are capable of quantifying the degree of donation between the phosphinimide ligand and transition metal.¹³⁶ Presently, X-ray crystallography is the only technique that can determine the degree of donation between phosphinimide ligands and transition metal by determining the critical bond distances (M-N, N-P) and angles (M-N-P) within transition metal phosphinimide complexes.

3.3 Synthetic methodologies towards preparing transition metal phosphinimide complexes

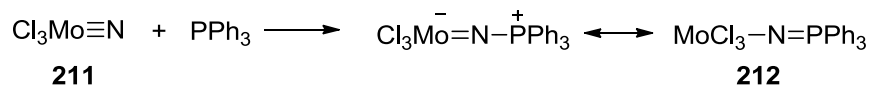
The remaining sections in this chapter will focus on the various methods used to prepare transition metal phosphinimide complexes. This rather broad area can be divided into three general methods: the addition of phosphines to metal precursors containing nitrogen-based ligands; the addition of neutral phosphinimine compounds to metal halides, oxides, or nitrides, as well as the addition of anionic phosphinimide precursors to metal halides; and finally, the oxidative addition of low valent metals into nitrogen-halogen bonds of N-halophosphinimine compounds. It should be noted that this chapter is not a comprehensive review, as greater detail is available in various reviews.¹³⁵⁻¹³⁹ The aim of this chapter is to instead provide an introduction to the general methods used for preparing transition metal phosphinimide complexes, while focusing on more recent highlights in the field.

3.3.1 Phosphinimide complexes from phosphine addition to metal-nitrogen multiple bonds

Transition metal phosphinimide complexes have been prepared from rhenium, osmium, ruthenium, molybdenum, tungsten, and vanadium nitride complexes ($\text{M}\equiv\text{N}$) by the addition of trialkyl-, or triarylphosphines.^{135,136} The overall reaction involves a two-electron reduction of the metal center and a two electron oxidation of the phosphine.

To illustrate, Dehnicke and co-workers has prepared complexes such as trichloromolybdenum(IV) triphenylphosphinimide (**212**) by adding one equivalent of triphenylphosphine to a solution of trichloromolybdenum(IV) nitride (**211**) (Scheme 3.2).

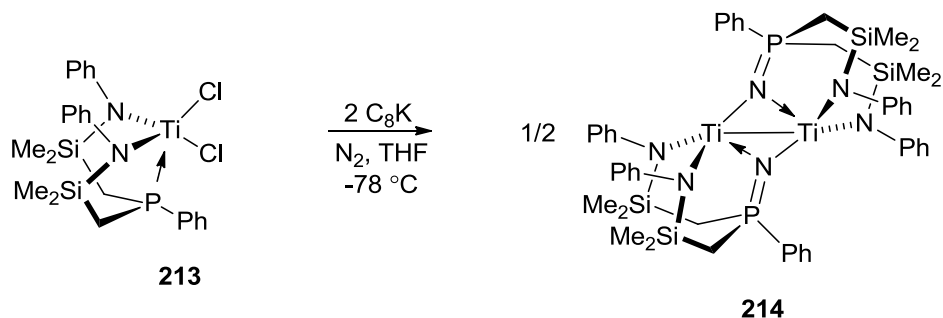
Scheme 3.2



Recent developments involve the use of metal nitride precursors bearing a range of alternative ligands. Some osmium phosphinimide complexes have been prepared that contain either *ter*-pyridylpyridine (tpy),¹⁴⁸ trispyrazolymethide (tpm),¹⁴⁹ trispyrazolborate (Tp)¹⁵⁰ and di(*t*-butyl)catechol (DBCat)¹⁵¹ ligands. Ruthenium phosphinimide complexes have also been recently prepared; these complexes were prepared using Klaui's phosphorous-derived half-sandwich cobalt tripodal ligand,¹⁵² or Keggin's tungsten-derived polyoxometallate ligand (PW₁₁O₃₉⁷⁻).¹⁵³

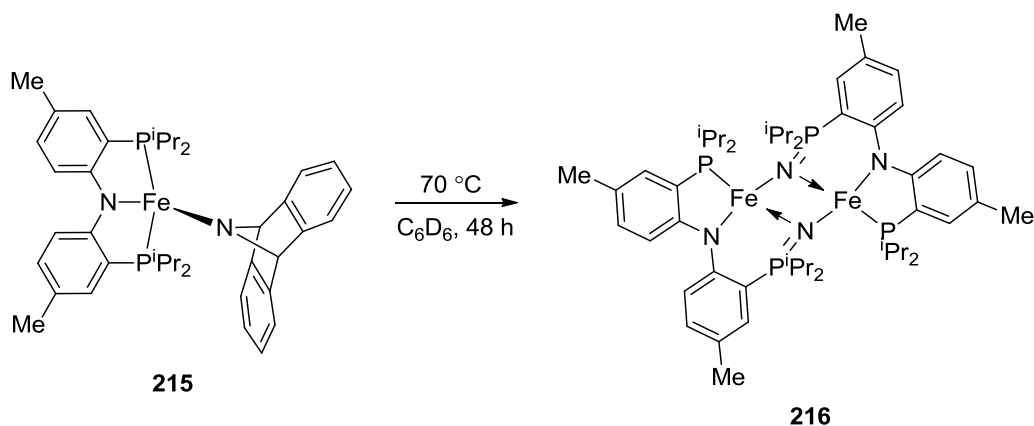
The most significant advance has been the preparation of first-row transition metal phosphinimide complexes by *in situ* trapping of highly reactive terminal first-row metal nitrides. This has been accomplished by using metal precursors with ancillary ligands bearing a chelating phosphine (Equations 3.3-3.5). Fryzuk recently prepared the titanium(III) phosphinimide dimer (**214**) by reduction of the starting [NPN]TiCl₂ complex **213** with C₈K under nitrogen (Equation 3.3).¹⁵⁴ In this reaction, the proposed titanium nitride intermediate is proposed to form by the oxidative cleavage of molecular dinitrogen which is coordinated to the initially reduced [NPN]Ti(II) species.¹⁵⁴

Equation 3.3



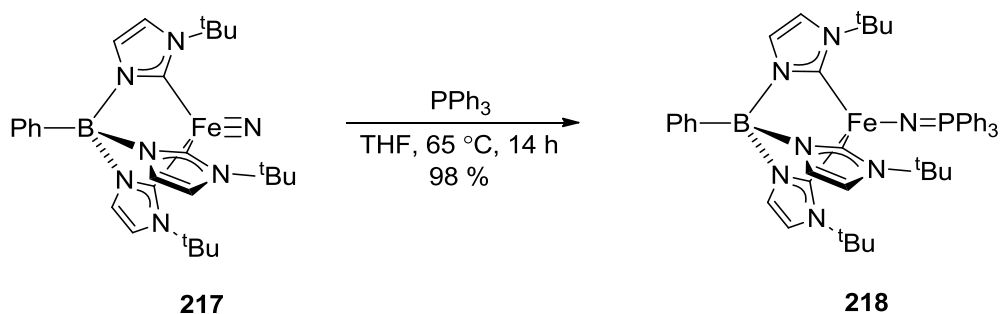
In a similar example, Mindiola and co-workers isolated an iron(II) phosphinimide dimer (**216**) by heating a solution of the iron(II) amide **215**; compounds of this nature are known to generate iron nitride species by the thermal expulsion of anthracene (Equation 3.4).¹⁵⁵

Equation 3.4



Most recently, the iron(II) phosphinimide complex **218** was prepared by Smith, *et al.*. This complex was prepared by adding one equivalent of triphenylphosphine to phenyltris(1-*tert*butylimidazol-2-ylidene)borate-supported iron(IV) nitride (**217**) (Equation 3.5).¹⁵⁶ This result was significant because the Smith group was the first to directly observe the addition of a phosphine to first-row transition metal nitride; presumably due to the lack of isolable first-row nitride complexes.

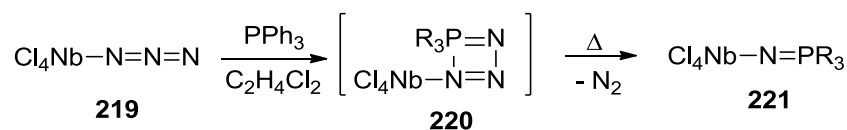
Equation 3.5



3.3.2 Transition metal phosphinimide complexes by phosphine induced rearrangement of nitrogen containing ligands

Alkyl- and arylphosphines are capable of converting transition-metal azides (M-N₃) into transition-metal phosphinimide complexes; this proceeds with the expulsion of nitrogen gas (Scheme 3.3). Strähle and co-workers demonstrated that heating a solution containing tetrachloroniobium(V) azide (**119**) and triphenylphosphine results in the niobium(V) triphenylphosphinimide complex **221**.¹⁵⁷ This reaction is accepted to proceed by a Staudinger-type mechanism which involves a metallo-phosphazide intermediate (**220**) which collapses via a thermal [2+2] cycloreversion at elevated temperatures and extruding dinitrogen.

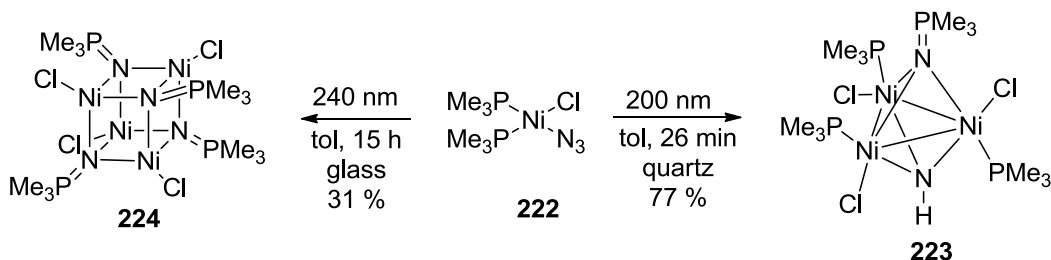
Scheme 3.3



Klein and co-workers prepared two different nickel(II) phosphinimide complexes **223** and **224**; these were obtained from independent solutions of chlorobis(trimethylphosphine) nickel(II) azide (**222**) which were subjected to differing photolytic conditions (Scheme 3.4).¹⁵⁸ The mechanism explaining the formation of either nickel(II) phosphinimide complexes was not provided, although speculation can be made. The bridging nickel imide observed in compound **223** suggests that a transient nickel nitride is formed during the reaction. This reactive nickel nitride species can then be either converted into the corresponding nickel phosphinimide products by nucleophilic addition of trimethylphosphine (see Scheme 3.2), or will undergo hydrogen atom abstraction from readily available sources including the solvent generating a nickel imide as is observed in compound **224**. Another plausible pathway is the displacement of dinitrogen by an intramolecular 1,2-phosphine shift from the nickel(II) center onto the azide ligand. Such reactivity has been observed by Eberhardt and co-workers during

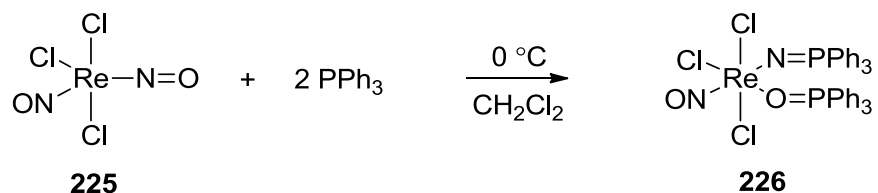
their study on the photolysis of alkyl azide compounds; in this case the reactions proceed in a similar fashion by a 1,2-alkyl of an alkyl substituent from the *ipso*-carbon onto the azide nitrogen which displaces dinitrogen and produces a substituted imine.¹⁵⁹ Photolytic conditions were also employed by Caulton and co-workers who recently prepared an iron(II) phosphinimide dimer from a PNP supported iron(II) azide precursor (PNP = (^tBu₂PCH₂SiMe₂)N-).¹⁶⁰

Scheme 3.4



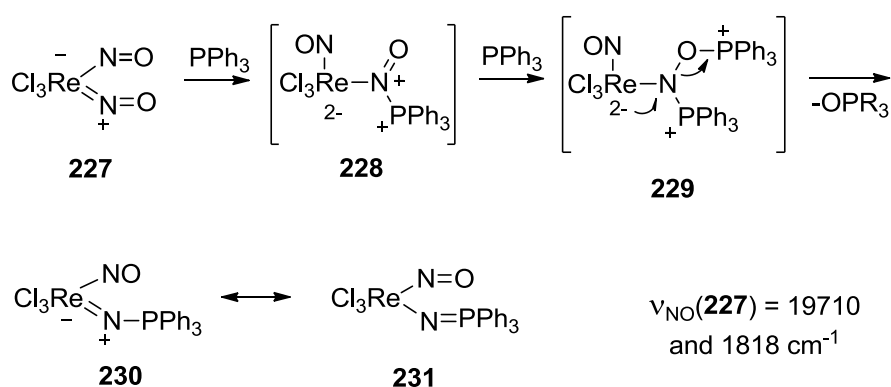
A less atom-economical “extraction” process is required in order to convert transition metal nitrosyl precursors into phosphinimide complexes through the addition of phosphines (Equation 3.6). In these reactions, a second equivalent of phosphine is important in the process, as it aids in the digestion of the nitrosyl ligand by sequestering the oxygen atom as one equivalent of triphenylphosphine oxide. Dehnicke and co-workers obtained a rhenium(III) phosphinimide complex **225** using this methodology by treating a solution containing the rhenium(I) dinitrosyl complex **226** with two equivalents of triphenylphosphine.¹⁶¹

Equation 3.6



Dehnicke proposed that the reaction proceeds through the intermediate **229**, which incorporates both the metal precursor plus both equivalents of phosphine.¹⁶¹ The intermediate **229** is formed by sequential addition of both phosphines to the nitrosyl ligand, first at the nitrogen atom, then at the oxygen atom (Scheme 3.5). The collapse of this intermediate results in the displacement of one equivalent of the phosphine oxide and affords transition metal phosphinimide complex **231**.

Scheme 3.5

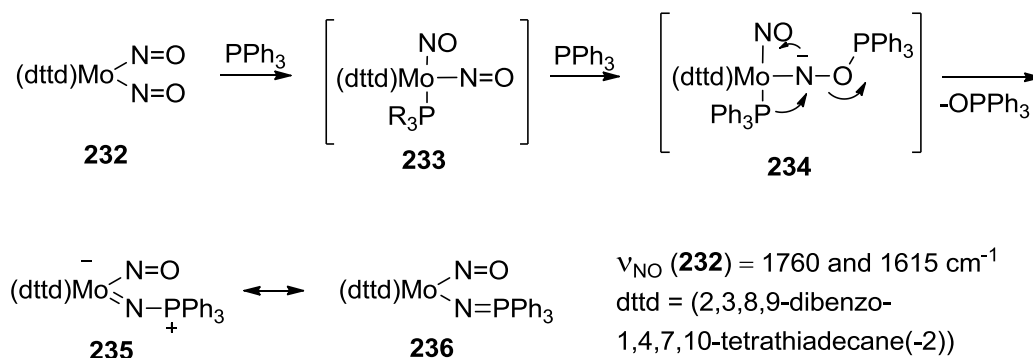


Dehnicke's proposed mechanism occurs in metal nitrosyl compounds which show a high energy N-O stretching frequency ($\nu \geq 1870 \text{ cm}^{-1}$); these complexes are described by Bottomley and co-workers as electrophilic at the nitrosyl ligand. Similar complexes will also react with other neutral nucleophiles including H_2O and NH_3 .¹⁶² It should be noted that the mechanism that appears in this chapter is an adaptation of the mechanism proposed by Dehnicke, which shows the initial intermediate bearing a negatively charged phosphine. This species is an odd depiction, considering the nitrosyl ligand is the active electrophile in the reaction.

Sellmann and co-workers proposed an alternate mechanism for preparing metal phosphinimide complexes from metal nitrosyl complexes which have less electrophilic nitrosyl ligands ($\nu \geq 1760 \text{ cm}^{-1}$).¹⁶³ This was deduced while studying the addition of excess triphenylphosphine to $\text{Mo}(\text{NO})_2(\text{dttd})$ (**232**). In the generic mechanism, a nitrosyl

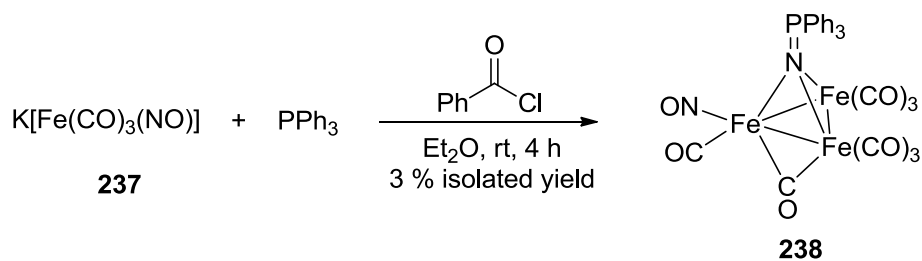
intermediate **234** similar to **229** (see Scheme 3.6) is formed except that the second phosphine is coordinated to the metal center instead of the nitrosyl nitrogen.¹⁶³ The intermediate **234** then collapses in a concerted fashion by extruding phosphine oxide and forming the phosphinimide ligand. This mechanism will not be discussed in detail however, as it is covered in depth in a comprehensive review.

Scheme 3.6



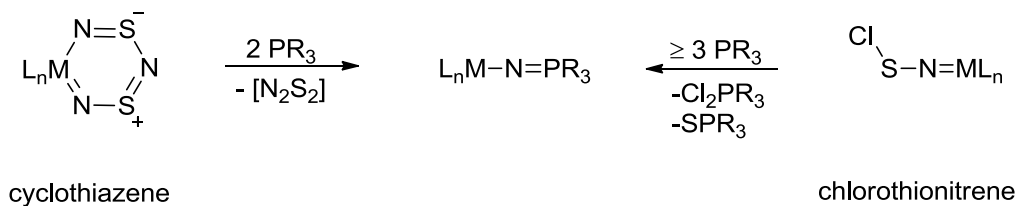
One final example not discussed in the reviews is Eberhardt's preparation of an tri-iron phosphinimide cluster **238** which was obtained as the minor product from the addition of triphenylphosphine and benzoyl chloride to an ether solution containing the anionic iron nitrosyl complex **237** (Scheme 3.7).¹⁶⁴ Although a mechanistic pathway was not discussed in the publication, one can speculate that this product is formed by the capturing of $[\text{Fe}(\text{CO})_2(\text{NO})_2]$ with two equivalents of triphenylphosphine, and incorporation of two equivalents of $\text{Fe}(\text{CO})_5$. Each of these intermediates were obtained from the addition of methyl iodide to the anionic iron nitrosyl complex **237**, suggesting the proposed disproportionation is reasonable.¹⁶⁵

Scheme 3.7



Similar to transition-metal nitrosyl complexes, metal cyclothiazene ($\text{M-N}_3\text{S}_2$) and chlorothionitrene complexes (M-NSCl) have also been converted into the corresponding phosphinimide complexes by adding two or more equivalents of phosphine (Scheme 3.8).¹³⁶ The by-products that are typically formed in these reactions from metal-cyclothiazene complexes are ' N_2S_2 ' units, which form oligomers with other ' N_2S_2 ' units or with additional equivalents of phosphine molecules. The by-products typically formed from the metal chlorothionitrene precursors are oxidized phosphine sulphide and dichlorophosphorane compounds. This topic will not be further discussed, as it is well covered in the comprehensive reviews.

Scheme 3.8

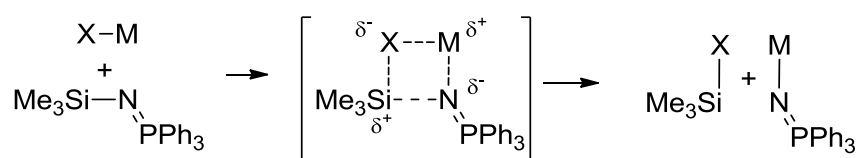


3.3.3 Transition metal phosphinimide complexes by neutral σ -bond metathesis

N-(trimethylsilyl)phosphinimide compounds are common reagents for the preparation of transition metal phosphinimide complexes starting from metal halide precursors. One distinct advantage to using silylphosphinimide compounds is that they are easily prepared in one step, and in high yields using Staudinger's oxidation of

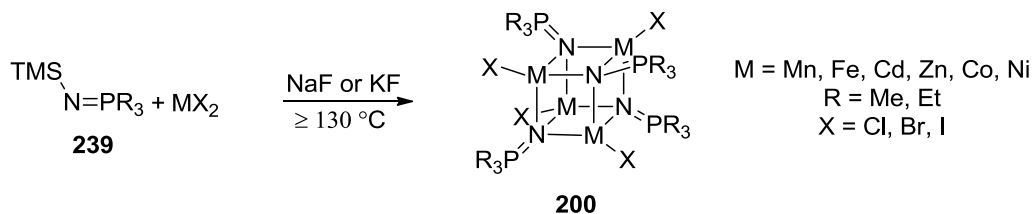
phosphines with trimethylsilyl-azide.^{166,167} This installation of phosphinimide ligands proceeds by a polarized neutral σ -bond metathesis between the nitrogen-silicon bond of the coordinated silylphosphinimide and the metal-chloride bond of a Lewis-acidic metal (Scheme 3.9). The products obtained from this reaction are the desired transition metal phosphinimide complex and an equivalent of the chlorosilane. Trimethylsilyl groups have also been used to install Cp ligands onto transition-metals through a similar σ -bond metathesis pathway.¹⁶⁸

Scheme 3.9



Dehnicke and co-workers prepared a series of first-row transition metal phosphinimide complexes by heating a 1:1 mixture of a metal(II) salt and silyl-(trialkyl)phosphinimide compounds (**239**) compound to 130 °C; in some cases inorganic fluoride salts such as NaF or KF were added to aid in the desilylation (Equation 3.7).¹⁶⁹⁻¹⁷⁶ Under these conditions, transition metal phosphinimide heterocubane complexes (**200**) of many metals were produced. These tetrameric phosphinimide clusters are not generally formed from other preparative methods.

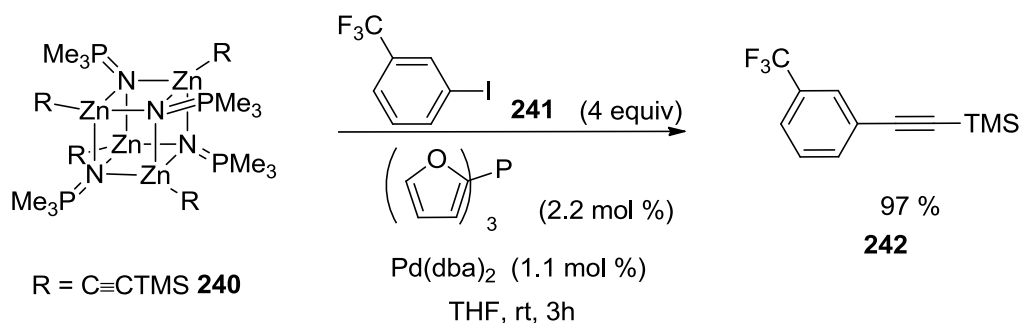
Equation 3.7



The displacement of the halide ligands in some heterocubane complexes by addition of various carbanionic and hydridic reagents have afforded stabilized metal

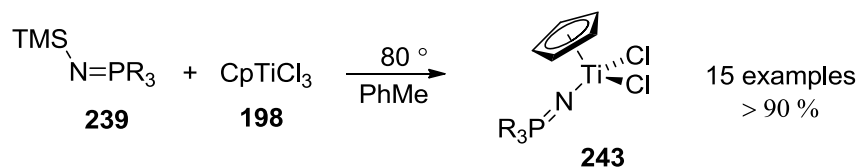
hydride, alkyl, alkenyl or alkynyl complexes (Equation 3.8).¹⁷⁶⁻¹⁸² These functionalized heterocubane complexes have been used for coupling terminal acetylides with sp^2 and sp^3 hybridized carbon centers.¹⁸³ When subjected to Negishi-type cross-coupling reaction conditions, Dehnicke *et al.*, demonstrated that the acetylated zinc(II) heterocubane complex **240** will transfer all four acetylide groups to the active palladium(II) catalyst, coupling 3-trifluoromethyl-iodobenzene (**241**) quantitatively. Dehnicke and co-workers also demonstrated that similar alkynyl cobalt(II) heterocubane complexes will quantitatively transfer acetylide groups to allylic bromides.¹⁷⁴

Equation 3.8



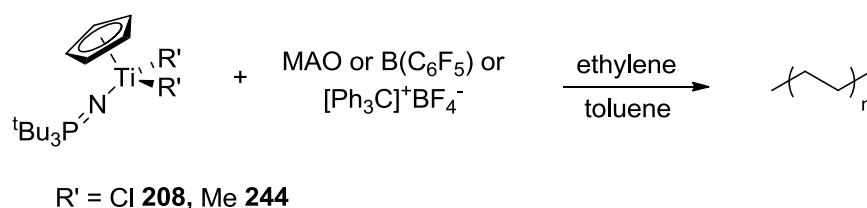
Early-metal half-sandwich titanium(IV) phosphinimide complexes were similarly prepared by Dilworth and co-workers through the combination of cyclopentadienyl titanium trichloride (**198**) and silylphosphinimide compounds (**239**) (Equation 3.9).^{142,184,185} More recently, Stephan and co-workers have dramatically expanded this series to include a wider range of phosphinimide ligands for half-sandwich and bis(phosphinimide)titanium(IV) complexes (**243**) and a series of half-sandwich and bis(phosphinimide)zirconium(IV) complexes.^{142,185}

Equation 3.9



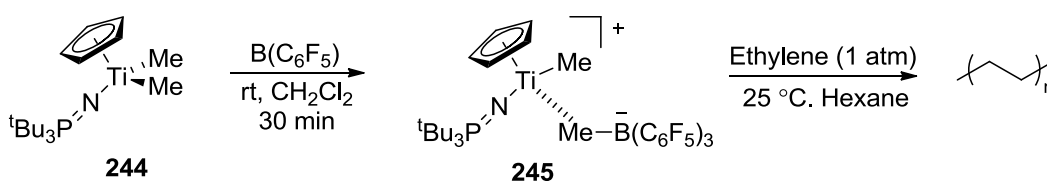
These half-sandwich titanium(IV) phosphinimide complexes, as well as their dimethyl derivatives, are highly active single-site precatalysts for olefin polymerization (Equation 3.10).^{137,142,186} Up to this point, group IV metallocene and half-metallocene derivatives are known to be highly effective precatalysts for the production of polyethylene.^{187,188} In comparison, the titanium(IV) phosphinimide-based catalysts have exhibited up to eight times the activity of olefin polymerization than the majority of most active metallocene derived catalysts.

Equation 3.10



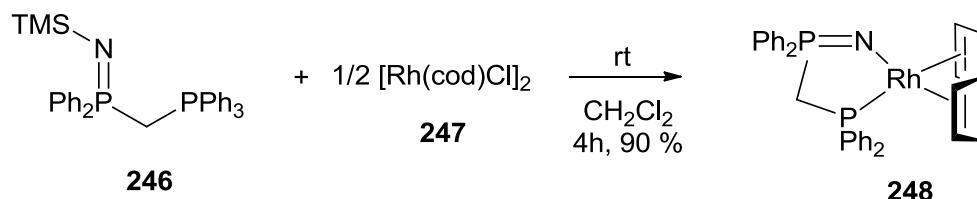
The high activity of the phosphinimide precatalysts **208** and **244** is attributed to the thermal stability of the highly reactive cationic titanium(IV) alkyl intermediates (Scheme 3.10). Stephan and co-workers were able to isolate a rare example of a cationic titanium(IV) monomethyl complex **245**, by abstraction of a methyl group from the methylated complex **244** using tris(pentafluorophenyl)borane.¹⁸⁵ When exposed to one atmosphere of ethylene under inert conditions, this cationic species produced polyethylene without prior activation, albeit in lower activities than other titanium phosphinimide precatalyst systems.¹⁸⁹

Scheme 3.10



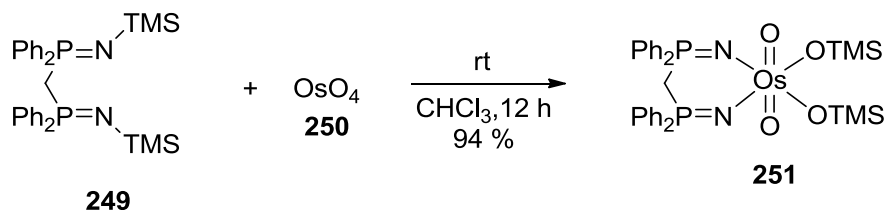
A limited number of second row late-transition metal phosphinimide complexes have been prepared from silylphosphinimide reagents (Equation 3.11). One of these examples was reported by Cavell and co-workers in which dimeric (1,5-cyclooctadiene)rhodium(I) chloride (**247**) undergoes σ -bond metathesis with the silylphosphinimide-containing heterobifunctional ligand **246** affording the corresponding rhodium(I) phosphinimide complex **248**.¹⁹⁰ Similar reactivity is also observed between the bifunctional ligand **248** and dimeric (1,5-cyclooctadiene)iridium(I) chloride.^{190,191}

Equation 3.11



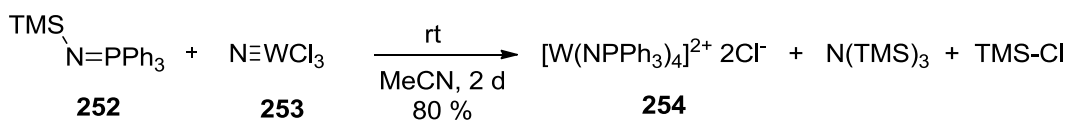
Silylphosphinimide compounds will also undergo σ -bond metathesis between the nitrogen-silicon and metal-oxygen bonds of high oxidation state metal oxides. The products obtained from the reaction are a transition-metal phosphinimide complex, plus one equivalent of a siloxane¹⁹² or free disiloxane.¹⁹³ Roesky and co-workers recently reported that the combination of the methylene bridged bis(silylphosphinimide) ligand **249** with osmium tetroxide (**250**) affords the cyclic osmium(VIII) bis(phosphinimide) complex **251**, with two siloxy ligands (Equation 3.12).¹⁹²

Equation 3.12



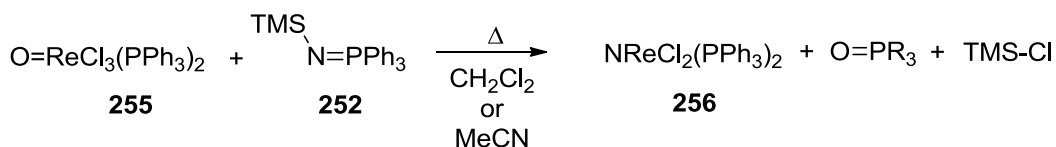
Similar reactivity is observed between the silicon-nitrogen bond of silylphosphinimide compounds and the metal-nitrogen bonds of transition-metal nitride complexes (Equation 3.13). Dehnicke and co-workers reported that the addition of four equivalents of silyltriphenylphosphinimine **252** to an acetonitrile solution containing trichlorotungsten(VI) nitride (**253**), produces the tetrakis(triphenylphosphinimide) tungsten(VI) dication **254**, along with one equivalent of chlorotrimethylsilane and tris(trimethylsilyl)amine.¹⁹⁴ In this example, the reaction occurs between silylphosphinimide **252** and both the metal halide and nitride functionalities, suggesting that the reactivity of silylphosphinimide compounds is not selective.

Equation 3.13



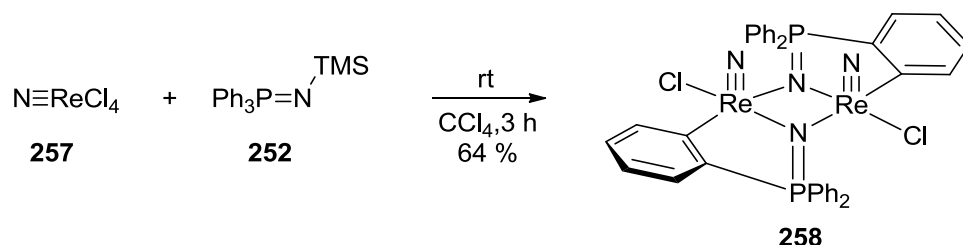
Silylphosphinimide compounds, however, will not react predictably with most metal oxides or metal nitrides (Equation 3.14). Abram and co-workers reported that treating a solution of bis(triphenylphosphine)trichlororhenium(V) oxide (**255**) with silylphosphinimide **252** did not afford the expected rhenium phosphinimide, but gave instead triphenylphosphine oxide, chlorotrimethylsilane, and the rhenium nitride **256**.¹⁹⁵ Since chlorotrimethylsilane is one product isolated from the reaction, one can postulate that a rhenium(V) phosphinimide complex is initially generated by σ -bond metathesis with the rhenium-chloride bond. The presence of triphenylphosphine oxide in the reaction mixture implies that this intermediary species undergoes heteroatom exchange between the nitrogen-phosphorus bond of the phosphinimide ligand and the rhenium-oxygen bond of the oxide.

Equation 3.14



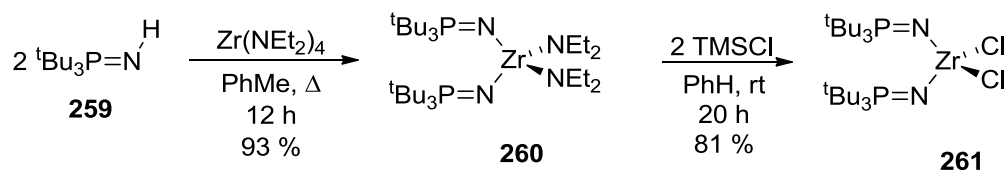
In another example, Dehnicke and co-workers reported that the addition of silylphosphinimide **252** to a solution containing tetrachlororhenium(VII) nitride (**257**) afforded the dimeric rhenium phosphinimide(VII) complex **258** (Equation 3.15).¹⁹⁶ The rhenium nitride functionality in the starting complex **257** is unreactive under these conditions, as even C-H activation is observed at the *ortho*-carbons of the phosphinimide, resulting in the formation of rhenium-aryl bonds.

Equation 3.15



Unsubstituted phosphinimine compounds have also been used to prepare transition metal phosphinimide complexes by neutral σ -bond metathesis. In this case, the hydrogen atom on the phosphinimide nitrogen is acidic, and can be deprotonated by metal precursors containing basic, dialkyl amide ligands. Stephan and co-workers demonstrated that treating solutions of zirconium(IV) diethylamide with two equivalents of tri(*t*-butyl)phosphinimine (**259**) affords the corresponding bis(phosphinimide)zirconium(IV) complex **260** in excellent yield (Scheme 3.11).¹⁹⁷ The extraneous diethylamide ligands in the bis(phosphinimide)zirconium complex **260** are effectively converted to chloride ligands by the addition of two equivalents of chlorotrimethylsilane.¹⁹⁷

Scheme 3.11



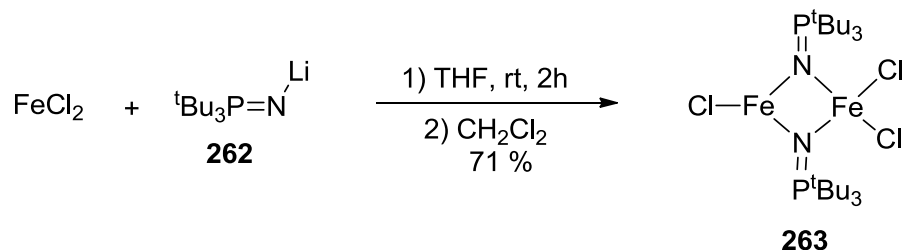
Unsubstituted phosphinimine compounds are generally prepared by one of two methods: desilylation of silylphosphinimide compounds using alcohol solvents¹⁹⁸ and deprotonation of phosphiniminium compounds by alkali amide salts.¹⁹⁹⁻²⁰¹ The first method is less time intensive as phosphinimine compounds are prepared in two steps from the parent phosphine. This method, however, is limited to silylphosphinimide compounds that contain bulky, electron donating substituents such as cyclohexyl or *t*-butyl groups. Silylphosphinimides composed of smaller, less electron donating phosphorus substituents will react under these conditions, however the transient phosphinimine intermediates are rapidly hydrolyzed to the corresponding phosphine oxide by residual water in the solvent. The second method, involving the use of alkali amide, can be used to prepare a broader range of phosphinimines, this same method can also be used to prepare anionic phosphinimide compounds directly. These metallated compounds have been used to prepare transition metal phosphinimide complexes, some of which will be discussed in the following section.

3.2.4 Transition metal phosphinimide complexes by anionic σ -bond metathesis

Alkali or alkali earth (Na, K, Li) phosphinimide salts have been used to prepare transition metal phosphinimide complexes via anionic displacement of metal chloride, bromide, iodide, sulfonate, and azide ligands.

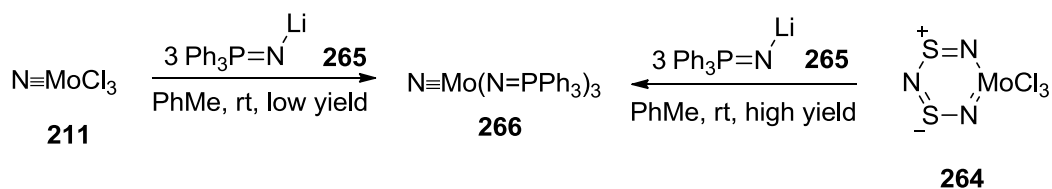
Stephan and co-workers reported that the addition of lithium tri(*t*-butyl)phosphinimide (**262**) to a solution of iron(II) chloride in THF affords the mixed iron(II)/iron(III) bis(phosphinimide) complex **263** (Equation **3.16**) with bridging phosphinimide ligands.²⁰² Based on electrochemical results, the authors' suggest that **263** is formed by an irreversible one electron oxidation of an iron(II)/iron(II) bis(phosphinimide) intermediate by dichloromethane during the work-up of the reaction. The mixed oxidation state bis(phosphinimide) complex **263** was subsequently oxidized to an iron(III)/iron(III) bis(phosphinimide) complex by the addition of ferrocenium hexafluorophosphate.

Equation 3.16



Dehnicke and co-workers demonstrated that three equivalents of lithium triphenylphosphinimide **265** can displace the three chloride ions of either trichloromolybdenum(IV) nitride (**211**), or trichloromolybdenum(IV) cyclothiazene (**264**), affording tris(triphenylphosphinimide)molybdenum(VI) nitride (**266**) in variable yields (Equation 3.17).²⁰³ What is interesting about this reaction is that the molybdenum nitride functionality is retained in these reactions. However, this is not the case when three equivalents of silylphosphinimide **252** was added to trichloromolybdenum(VI) nitride (**211**), which affords the tetrakis(triphenylphosphinimide)molybdenum(VI) diadduct (similar to the products in Equation 3.13). These examples imply that alkali-phosphinimide compounds can be potentially useful in scenarios where more sensitive functionalities are present.

Equation 3.17

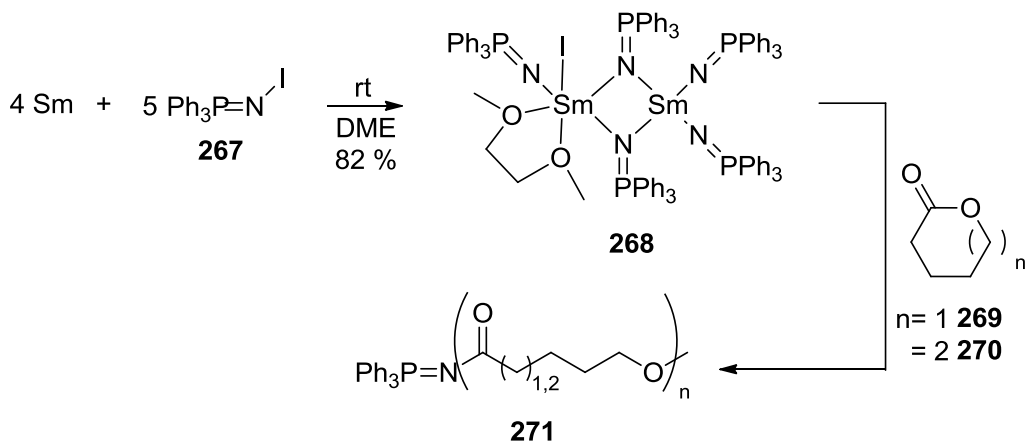


3.2.5 Phosphinimide complexes from low-valent metals

Very few transition metal phosphinimide complexes have been prepared by the oxidative insertion of low-valent transition metals into the N-X bond of phosphinimide precursors. In fact, the majority of examples arise from the oxidative addition of low-valent heavy-metal powders into N-halophosphinimide precursors (Scheme 3.12). A

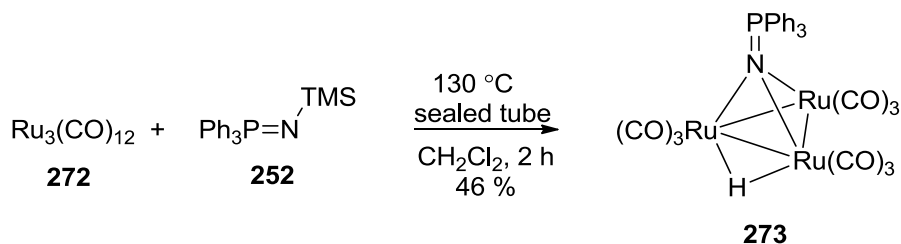
bimetallic samarium(III) phosphinimide complex **268** was prepared by Dehnicke and co-workers through the addition of five equivalents of N-(iodo)triphenylphosphinimide (**267**) to a suspension of finely divided samarium powder (Scheme 3.9).¹³⁹ The samarium(III) phosphinimide complex **268** is an efficient catalyst for “living” ring opening polymerizations (ROP) of cyclic lactones such as δ -valerolactone (**269**) and ϵ -caprolactone (**270**).²⁰⁴

Scheme 3.12



Only one, and rather odd example was reported where low-valent transition metal precursors will oxidatively insert into the N-X bond of phosphinimine precursors (Equation 3.18). This was a triruthenium phosphinimide cluster **273**, which was prepared by heating (130 °C) a sealed vessel containing a 1:1 mixture of triruthenium dodecacarbonyl (**272**) and silylphosphinimide **252** in dichloromethane.²⁰⁵

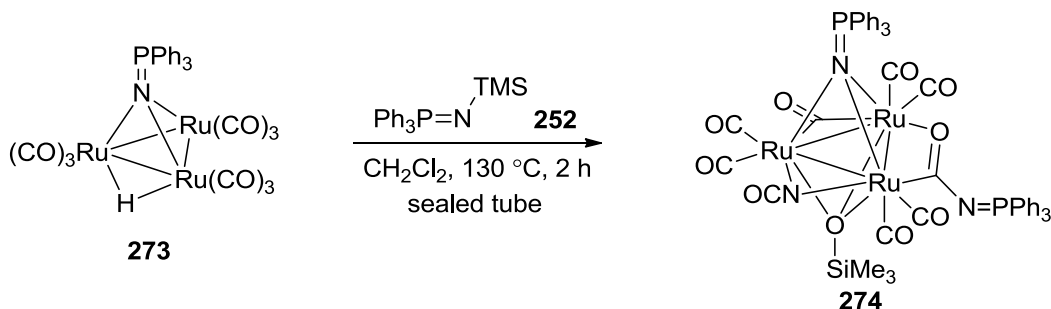
Equation 3.18



Although no mechanistic rationale was discussed to explain the formation of the tri-ruthenium phosphinimide cluster **273**, one plausible pathway involves the oxidative addition of triruthenium dodecacarbonyl (**272**) into the N-H bond of triphenylphosphinimine; which could be formed by desilylation of **252** with dichloromethane. Previous communications from Süss-Fink and co-workers demonstrated the capability of ruthenium dodecacarbonyl to insert into N-H bonds of substituted urea compounds; these reactions afford similar triruthenium clusters which feature μ_2 -bridging hydride ligands.^{206,207}

In a subsequent experiment, Tiripicchio and co-workers isolated a second triruthenium cluster **274** by heating (130 °C) a sealed tube which containing a 1:1 mixture of the cluster **273** and silylphosphinimide **252** in dichloromethane (Equation **3.19**).²⁰⁸ The newly formed ruthenium cluster **274** contains the intact μ^3 -phosphinimide ligand, plus a new μ^3 -siloxane ligand, a phosphinimide-incorporated η^2 -acyl ligand, and a μ^2 -isocyanide ligand.

Equation 3.19



The formation of the μ^2 -coordinated isocyanate ligand in this cluster was investigated computationally, where the reaction likely proceeds by a pseudo-Hoffmann rearrangement of the coordinated η^2 -acyl ligand (Figure **3.8**). One can imagine that instead of the classic 1,2-alkyl shift of the Hoffmann rearrangement, a 1,2-ruthenium shift occurs from the acyl position of the η^2 -acyl ligand to the acyl nitrogen atom, which displaces triphenylphosphine and affords the bridging isocyanate.

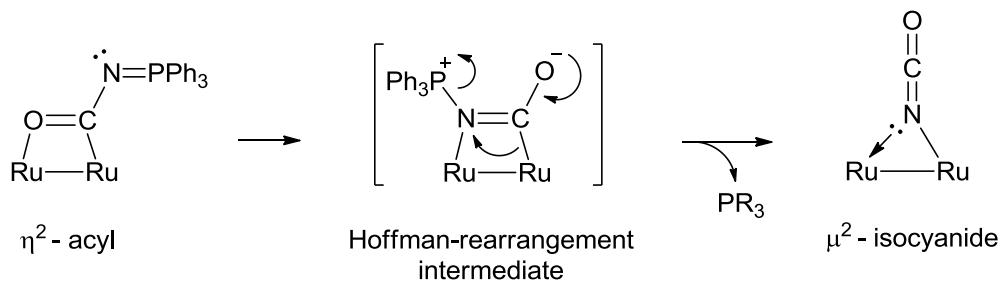
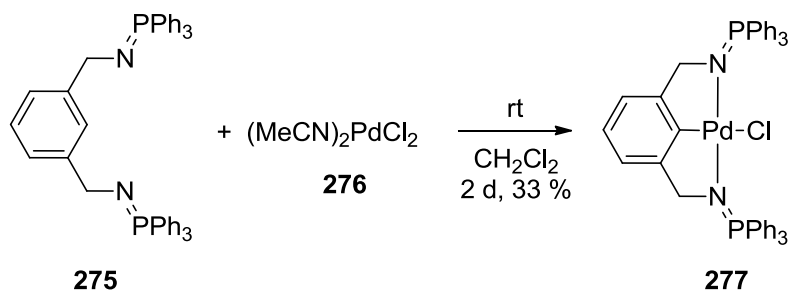


Figure 3.8: Proposed Mechanism of Pseudo-Hoffmann rearrangement.

The absence of transition metal phosphinimide complexes prepared from low-valent transition metals and N-halophosphinimide compounds suggests an area of research that is ripe for exploration. Further investigation into underdeveloped areas such as this, could result in the discovery of new transition metal phosphinimide catalysts which may exhibit desirable reactivity patterns useful for industrial or laboratory processes.

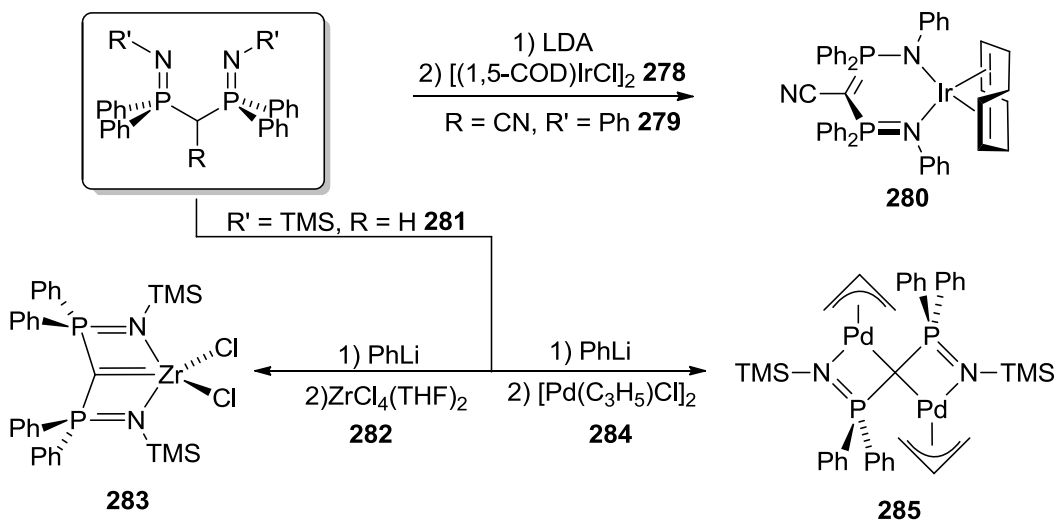
3.3 Chelating bis(phosphinimide) complexes

Closely related complexes to transition-metal phosphinimide compounds are dative coordination complexes of metal salts and neutral phosphinimine ligands (Equation 3.20). Simple bis(silylphosphinimide)cobalt(II) salts have been prepared by Dehnicke and co-workers through the combination of two equivalents of silylphosphinimide and one equivalent of the cobalt(II) salt.²⁰⁹ A more recent example was a palladium(II) pincer complex **277** prepared by Stephan, *et al.*; during the formation of **277**, oxidative C-H bond activation of the proximal *ortho*-hydrogen of the phenyl ring also occurs.²¹⁰

Equation 3.20

Most remaining examples of dative phosphinimine complexes are prepared by the addition of the single- or double-metallated methylene bridged N,N-disubstituted bis(phosphinimine) ligands to metal salts (Scheme **3.13**). With one nitrile located in the methylene bridge, deprotonation of the bridged bis(silylphosphinimide) precursor **279**, followed by addition to (1,5-COD)iridium(I) chloride (**278**) affords **280**. The metallated bis(phosphinimine) ligands in the product are similar to acetylacetonate (acac), or 1,3-diketimide (nacnac) ligands.²¹¹ With no “blocking” group, the bridged bis(phosphinimine) compound **281** has been doubly deprotonated at the methylene bridge. The addition of the carbon based dianion to metal halides has resulted in monomeric complexes such as the zirconium complex **283**. Bimetallic complexes have also been prepared where the methylene unit is distributed between two metals, such as the dipalladium complex **285**.^{212,213}

Scheme 3.13

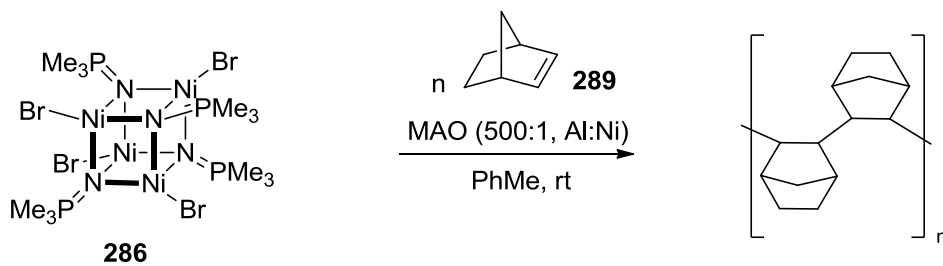


3.4 Conclusions

The chemistry of transition-metal phosphinimide complexes is an area of science that is continually growing. This includes both the discovery of new phosphinimide linked polymetallic scaffolds and investigations into the reactivity patterns of these complexes towards small molecules. Further computational and experimental investigations would also allow chemists to continue the discussion regarding the isolobal analogy with cyclopentadienyl ligands.

A relatively unexplored area is the use of transition metal phosphinimide complexes for catalysis (Equation 3.18). Such advances were made by Stephan in the field of olefin polymerization catalysis, primarily involving group IV (Zr, Ti) transition metal phosphinimide complexes. Stephan and co-workers also examined the possibility of using other early metal (V, Ta) and late metal (Fe) phosphinimide complexes as olefin polymerization precatalysts; but exhibited low catalytic activities in the presence of olefins.¹³⁷ Dehnicke has also contributed to this field of catalysis, demonstrating that the heterocubane nickel(II) phosphinimide cluster **286** is a highly active precatalyst in the vinyl-type polymerization of norbornene.²¹⁴

Equation 3.18



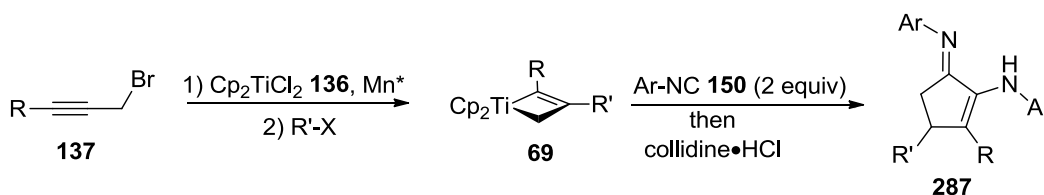
Apart from these examples, the state of late-metal phosphinimide mediated transformations is still in its nascent stage. One way to expand this field is to continue replacing metallocene complexes with transition metal phosphinimide complexes in known stoichiometric, or catalytic metallocene-mediated transformations. Considering the significant amount of metallocene mediated reactions, it is safe to say that the number of opportunities to use phosphinimide complexes will not diminish quickly.

Chapter 4: Alternatives to Cyclopentadienyl Ligands: Preparation of Titanium Phosphinimide and Sulfimide Compounds

4.1 Introduction to the use of titanium phosphinimide precursors to titanacyclobutene complexes

Recently, a one-pot four-step reaction sequence was developed for constructing carbocyclic- α -iminoenamine compounds from Cp_2TiCl_2 , propargyl halides, alkyl halides and organic isocyanides. The general scheme is provided below (Scheme 4.1) and greater detail can be found in Chapter 2 (see Sections 2.2.2 and 2.4.2). This methodology is significant as it highlights the potential synthetic usefulness of titanacyclobutene complexes which are intermediates in this process. These complexes have been a focus of our research for quite some time.^{4-6,38,48,49,55,215}

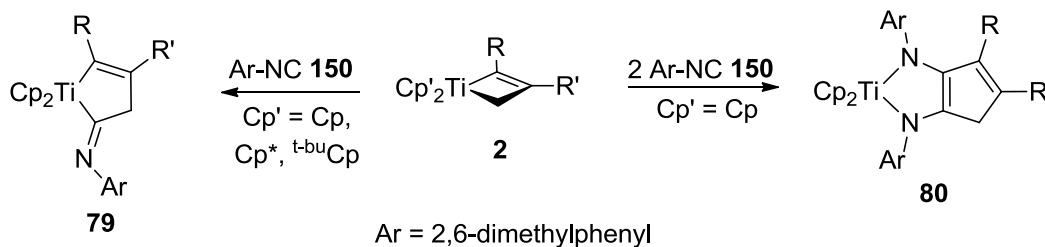
Scheme 4.1



We encountered a problem with using Cp_2TiCl_2 (136) or $[\text{Cp}_2\text{TiCl}]_2$ (128) (Nugent's reagent), as only a narrow range of propargyl- and alkyl halides can be coupled to it to prepare titanacyclobutene intermediates.^{4,6} When using $\text{Cp}'_2\text{TiCl}$ precursors ($\text{Cp}' = \text{Cp}^*$ or $^t\text{-BuCp}$) with more substituted cyclopentadienyl ligands, however, we established that these titanium(III) reagents couple with a larger variety of propargyl- and alkyl halides and generate titanacyclobutenes in near quantitative yield.^{3,5,48,49,55} The success of highly substituted Cp ligands in this methodology is attributed to an increase in donation from the semi-filled $3a^1$ " Cp_2Ti " orbital to the empty ψ^3 propargyl orbital (See Figure 1.5). The increased orbital density on the central

carbon of the propargyl ligand therefore enhances its reactivity with organic radicals, thus allowing for a larger substrate scope. In our hands however, the resulting Cp'-templated titanacyclobutene complexes could not be converted into carbocyclic- α -iminoenamine compounds (Scheme 4.2) by addition of excess isonitrile **150**; only (η^2 -iminoacyl)titanacyclopentene complexes (**79**) were obtained.⁵⁵

Scheme 4.2

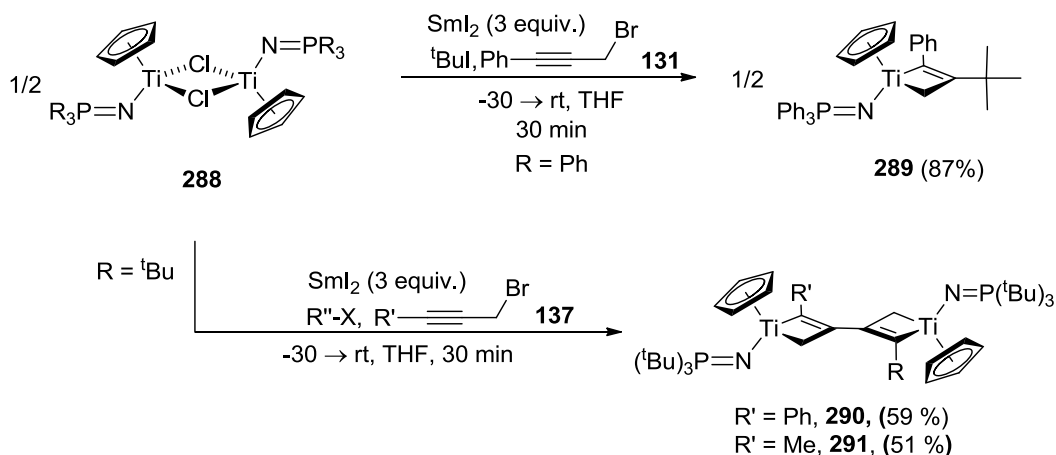


The problems encountered in using Cp₂TiCl and Cp'₂TiCl imply that this reaction sequence is limited with regard to step-wise efficiency. These limitations were addressed in two ways. First, we investigated modified reaction conditions to afford titanacyclobutenes (**69**) from Cp₂TiCl₂ in higher yields (see Chapter 2, Section 2.2.2). In this chapter we investigated titanium(III) halide precursors with ancillary ligands that are not Cp or Cp'. One class of ligands chosen for this study were tri-alkylphosphinimides (or phosphoranimides), which are regarded as Cp analogues in early-transition metal complexes due to their ability to donate six electrons to a metal center.^{135,136,142,186,189,216} Evidence supporting this hypothesis was discussed in chapter 3 (See Section 3.2.1), where Stephan discovered that titanium(IV) phosphinimide complexes are highly reactive single-site olefin polymerization catalysts. This is intriguing because previous olefin-polymerization catalysts were also generated from Cp'₂TiX₂ complexes.^{142,186,189,216} Given the parallels between cyclopentadienyl and phosphinimide ligands, as well as the usefulness of titanium(IV) phosphinimide complexes in olefin polymerization, we chose to pursue titanium(IV) phosphinimide complexes as precursors to titanacyclobutenes.

In conjunction with this study, a second class of ancillary ligands was investigated and will be discussed later in this chapter.

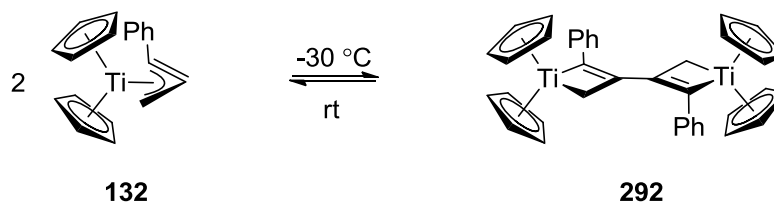
Previous to the work presented in this chapter, the Stryker group investigated the use of half-sandwich titanium phosphinimide complexes as the dimeric titanium(III) halide **288** (Scheme 4.3).³⁸ Using existing samarium(II)-mediated reaction conditions, a series of new titanacyclobutene complexes such as **289** were successfully prepared from half-sandwich titanium(III) phosphinimide precursors in good yields.³⁸ However, most of these titanacyclobutene products were 3,3'-bi(titanacyclobutene) complexes (**290**, **291**), which are formed by the competitive dimerization of two (η^3 -propargyl)titanium(III) intermediates which is irreversible at low temperature. This is obviously unfavourable for preparing titanacyclobutenes, because the dimerization of (η^3 -propargyl)titanium(III) intermediates is now competitive with the intermolecular radical trapping reaction between (η^3 -propargyl)titanium(III) intermediates and alkyl radicals. In order to prevent the dimerization of (η^3 -propargyl)titanium(III) intermediates, half-sandwich titanium(III) phosphinimide precursors with less electron-rich phosphinimide ligands had to be used in combination with alkyl radicals that are generated easily at low temperature.³⁸

Scheme 4.3



Two other instances of (η^3 -propargyl)titanium(III) intermediate dimerization have been observed in titanocene-based templates.^{5,48,49} The first 3,3'-bi(titanacyclobutene) complex was isolated from the samarium(II)-mediated coupling between one equivalent of propargyl bromide and one equivalent of decamethyltitanocene(III) chloride.^{5,48} The second instance was the dimerization of (η^3 -phenylpropargyl)titanocene (**132**) at -30 °C (Equation 4.1). We found this reaction to be reversible, however, as the 3,3'-bi(titanacyclobutene) **292** quantitatively converts back to **132** at room temperature.⁴⁹ These results demonstrate that phosphinimide ligands are strongly electron-donating to titanium(III) centers, as are Cp* ligands. More importantly, these results imply that titanium(IV) phosphinimide complexes could be useful for preparing titanacyclobutenes in high yields. The problem with these reagents, however, is that the dimerization of (η^3 -propargyl)titanium(III) intermediates hinders the formation of titanacyclobutenes through the intermolecular trapping of carbon-based radicals. Because of this, we abandoned the exploration of half-sandwich titanium(IV) phosphinimide and instead pursued titanium(IV) bis(phosphinimide) complexes,²¹⁷ the focus of the first half of this chapter.

Equation 4.1



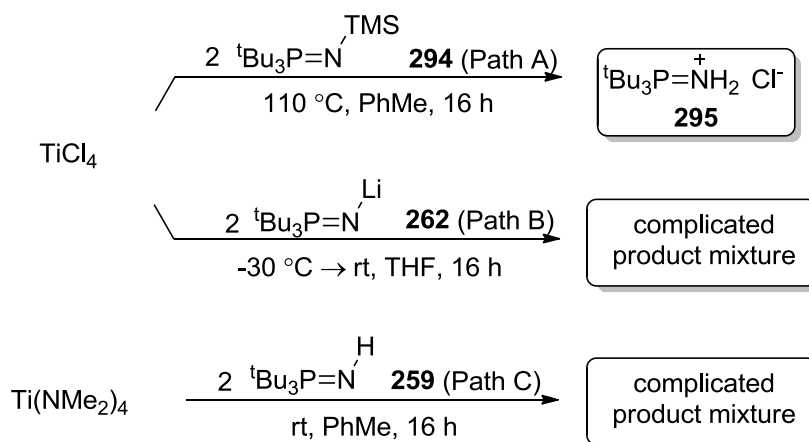
4.2 The chemistry of Bis(tri(*tert*-butyl)phosphinimide)titanium(IV) dichloride

4.2.1 Preparation of bis(tri(*tert*-butyl)phosphinimide)titanium(IV) dichloride (**293**)

Our survey of the literature revealed three methods for preparing bis(tri(*tert*-butyl)phosphinimide)titanium(IV) dichloride (**293**), all of which involve combining neutral or anionic phosphinimide ligands with simple titanium(IV) starting materials

(Scheme 4.4).^{131,186,217} Two of these methods were reported by Stephan *et al.*, who prepared **293** by treating titanium(IV) tetrachloride with two equivalents of silylphosphinimide **294** (Path A), or two equivalents of lithium phosphinimide **262** (Path B).^{186,217} The third method was reported by Sundermeyer, who treated titanium(IV) tetrakis(trimethylamide) with two equivalents of tri(*t*-butyl)phosphinimine (**259**) (Path C).¹³¹ This third method also requires a second step to convert residual dimethylamide ligands to chlorides using BCl₃.¹³¹ Although attempts were made to reproduce all three procedures, we either obtained a complex product mixture containing low yields of **293**, or the phosphiniminium chloride salt **295**.

Scheme 4.4



Of the three methods, we chose to investigate Sundermeyer's method (Path C) more thoroughly.¹³¹ Through multiple recrystallizations in cold toluene, single crystals of bis(tri(*t*-butyl)phosphinimide)titanium(IV) bis(dimethylamide) (**296**) were isolated from the complex product mixture, albeit in low isolated yield (~11 %). The single crystals of **296** were suitable for X-ray diffraction, but the bulk solid was not analytically pure. The crystallographic analysis of **296** reveals near-linear Ti-N-P bond angles and short Ti-N bond distances between the phosphinimide ligands and the titanium center (Figures 4.1 and 4.2). Such observations indicate strong bonding interactions between the two phosphinimide ligands and the titanium(IV) center. Another interesting aspect of the solid state structure of **296** is that the nitrogen atoms of the two dimethylamide

ligands are of trigonal planar geometry, with short Ti-N bond distances. These observations imply that the dimethylamide ligands are also forming strong bonding interactions with the titanium(IV) center. Due to the low isolated yield of **296** from the initial step, we did not attempt to convert this intermediate to **296** using BCl_3 , as reported by Sundermeyer.¹³¹ Instead, we explored alternative reaction conditions to Sundermeyer's that would inhibit the formation of multiple products.

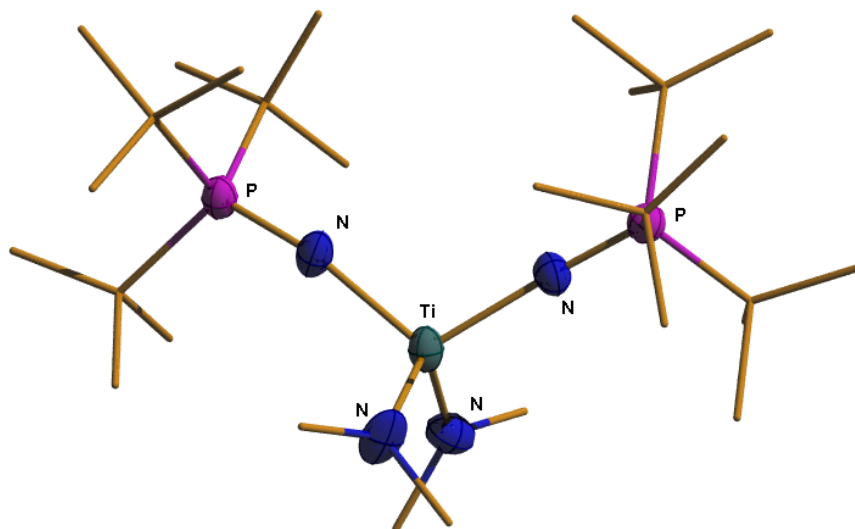


Figure 4.1: Perspective view of **296** showing selected atom labelling scheme. Non-hydrogen atoms are represented by either Gaussian ellipsoids at the 20% probability level, or as “wire and stick” representations. $R_1 = 0.0373$, $R(w) = 0.0946$.

Bond	Distance (pm)	Bond	Angle (°)
Ti-N ₁	190(3)	Ti-N ₁ -P ₁	159.9(9)
Ti-N ₂	191(2)	Ti-N ₁ -P ₁	166.8(15)
Ti-N ₃	189(3)	Ti-N ₄ -Me	124.9(13)
Ti-N ₄	197(4)	Ti-N ₄ -Me'	122.0(14)
N ₁ -P ₁	155.8(19)		
N ₂ -P ₂	149(3)		

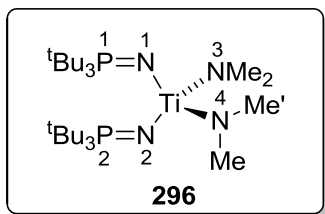
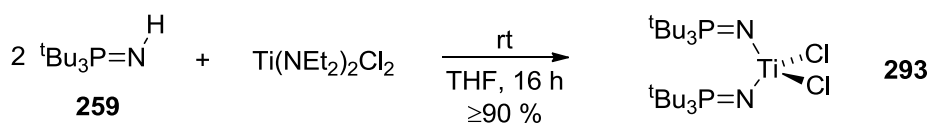


Figure 4.2: Selected bond distances and angles of **296**.

A successful modification to Sundermeyer's reaction conditions replaced the titanium(IV) tetrakis(dialkylamide) precursors with bis(dialkylamido)titanium(IV) dichloride reagents (Equation 4.2).²¹⁸ Through combination of two equivalents of tri(*t*-butyl)phosphinimine and one equivalent of bis(diethylamido)titanium(IV) dichloride in toluene, we obtained a simpler product mixture containing only bis(tri(*t*-butyl)phosphinimide)titanium(IV) dichloride (**293**) and tri(*t*-butyl)phosphininium chloride (**295**). By repeating the reaction in THF instead of toluene, **293** was obtained in almost quantitative yield. These results suggest that the complex product mixture obtained from Sundermeyer's conditions¹³¹ was likely due to the uncontrolled deprotonation of the two equivalents of tri(*t*-butyl)phosphinimine by the four dialkylamide ligands of titanium(IV) tetrakis(dialkylamide). In our modified conditions, mixed titanium reagents are advantageous over titanium tetrakis(dialkylamide) complexes as only two basic amide ligands are present; this modification eliminates the possibility of more than two equivalents of tri(*t*-butyl)phosphinimine being added to each atom of titanium. We repeated the modified procedure on multi-gram scale (~2 g), from which **293** was obtained without significant diminishment in yield. **293** could now be prepared in excellent yield and on large scale. With copious amounts of **293** in hand, we proceeded with investigating its conversion into titanacyclobutenes.

To confirm its identity, **293** was analyzed by ¹H and ³¹P NMR spectroscopy. The spectral data match those previously reported by Stephan (Equation 4.2).²¹⁷ Single crystals of **293** suitable for X-ray diffraction were grown from low temperature solutions of toluene, and the resulting solid state structure of **293** matches the solid state structure previously obtained by Stephan.²¹⁷

Equation 4.2



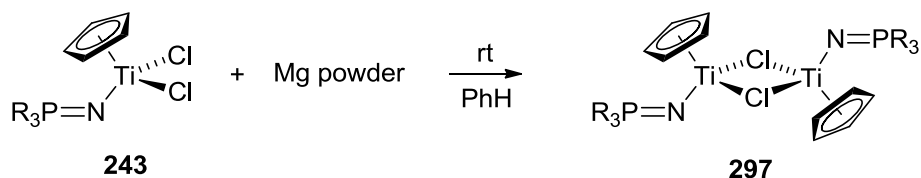
¹H NMR(C₆D₆) δ 1.32 (13.2 Hz)
³¹P NMR(C₆D₆) δ 36.1

4.3 Reactivity of bis(tri(*t*-butyl)phosphinimide)titanium(IV) dichloride

4.3.1 Attempted reduction of bis(tri(*t*-butyl)phosphinimide)titanium(IV) dichloride

Our initial goal was to reduce bis(tri(*t*-butyl)phosphinimide)titanium(IV) dichloride **293** to bis(tri(*t*-butyl)phosphinimide)titanium(III) chloride using metal powders. This approach has been demonstrated in Cp'₂TiCl₂ systems,^{88,219,220} as well as by Stephan (Equation 4.3), who prepared similar half-sandwich titanium(III) phosphinimide complexes such as **297** by stirring benzene solutions of titanium(IV) phosphinimide precursors such as **243** over magnesium powder.^{189,221} Strangely, although Stephan *et al.*, prepared a series of bis(phosphinimide)titanium(IV) dihalide complexes,^{186,217} they failed to comment on any subsequent reduction studies. This indicates that reduction studies were either unsuccessful or were not attempted.

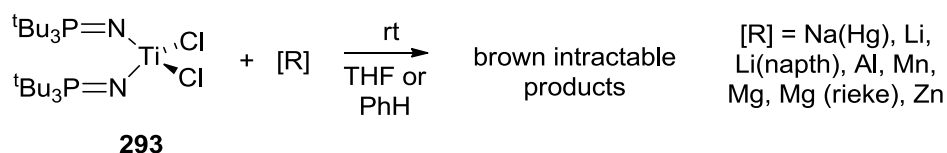
Equation 4.3



Given the successful reduction of half-sandwich titanium(IV) phosphinimide complexes with metal powders, the reduction of bis(tri(*t*-butyl)phosphinimide)titanium(IV) dichloride (**293**) was explored under similar reducing conditions. By stirring either benzene or THF solutions of **293** over aluminum, zinc, manganese, or magnesium powders, or upon addition of one equivalent samarium(II) diiodide in THF, we unfortunately obtained only the titanium starting material. These results indicate that **293** is more robust toward reduction than titanocene(IV) and half-sandwich titanium(IV) phosphinimide dichloride complexes, and therefore, stronger reducing conditions must be employed. When THF or toluene solutions of **293** were stirred over more powerful reducing agents such as Na, Li or Rieke Mg (Equation 4.4),

we obtained brown intractable product mixtures, which indicated that the titanium starting material had decomposed. These results unfortunately establish that bis(tri(*t*-butyl)phosphinimide)titanium(IV) dichloride (**293**) is not conducive to one-electron reduction by metal powders. More importantly, the failure to obtain bis(phosphinimide) titanium(III) halide complexes implies that stable (η^3 -propargyl)titanium(III) intermediates are also unobtainable, which is an impediment to our goal of preparing titanacyclobutenes.

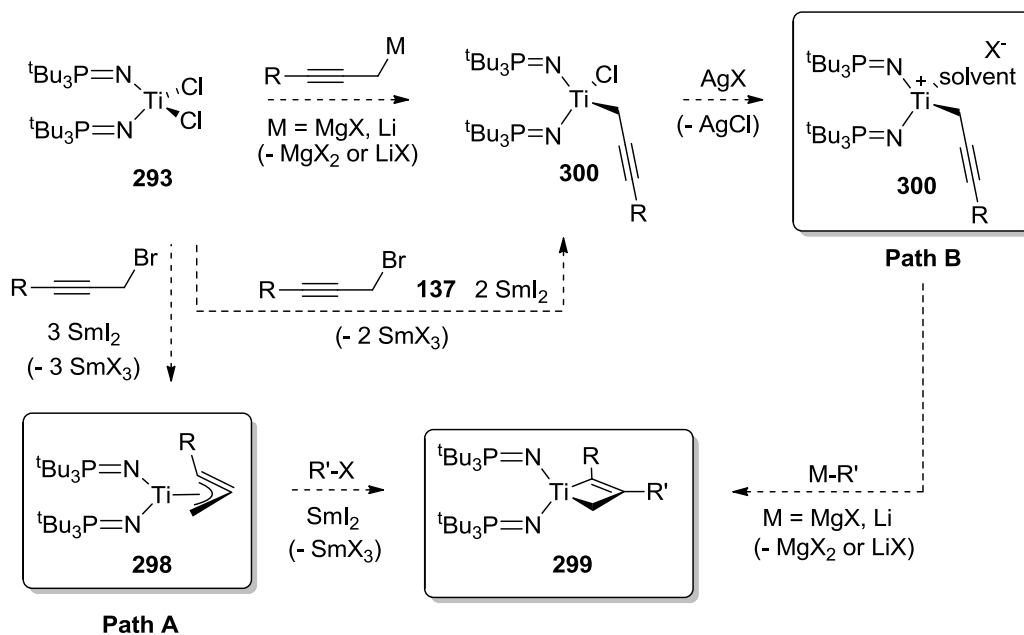
Equation 4.4



4.3.2 Attempted preparation of titanacyclobutene complexes

Although the preparation of bis(tri(*t*-butyl)phosphinimide)titanium(III) monochloride was unsuccessful, we persisted in our attempts to convert bis(tri(*t*-butyl)phosphinimide)titanium(IV) dichloride (**293**) into titanacyclobutene complexes. Two methods that were developed recently in the Stryker group to prepare titanacyclobutene complexes from half-sandwich titanium phosphinimide precursors were investigated for preparing titanacyclobutenes (Equation 4.5).³⁸ The first method requires the samarium(II)-mediated coupling between **293**, a propargyl halide and an alkyl halide (Path A). The second method furnishes titanacyclobutenes through the addition of hindered carbon-based nucleophiles to cationic titanium(IV) propargyl precursors (**301**) (Path B).

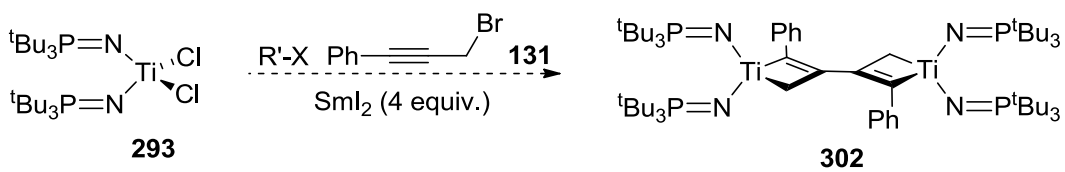
Scheme 4.5



4.3.3 Attempted preparation of titanacyclobutenes using samarium(II)-mediated coupling conditions

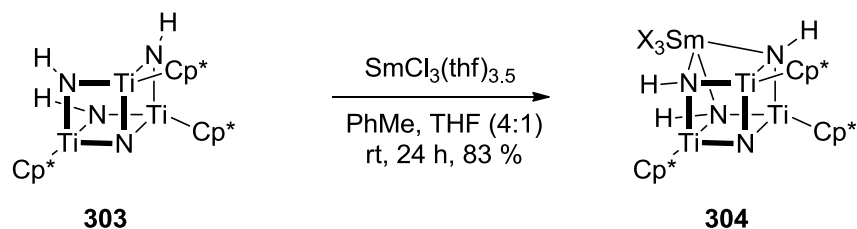
Based on previous experiments with half-sandwich titaniumphosphinimide complexes,³⁸ we expected that bis(tri(*t*-butyl)phosphinimide)titanium(IV) dichloride (**293**) would combine with 1-bromo-3-phenyl-prop-2-yne **131** in the presence of three equivalents of samarium(II) diiodide to give 3,3'-bi(titanacyclobutene) complex **302** (Equation 4.5). This dimerization was expected to occur in the presence of an alkyl radical ($\text{R}-\text{X}'$ and one equivalent of SmI_2).

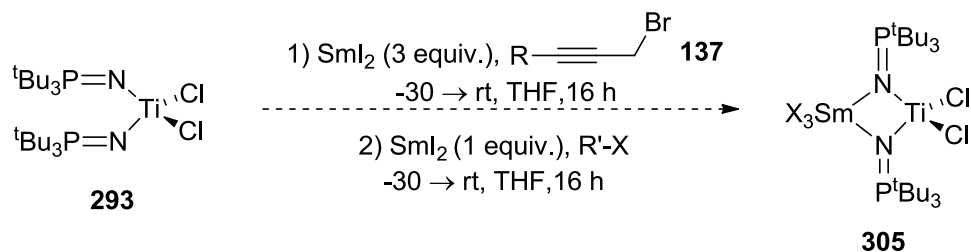
Equation 4.5



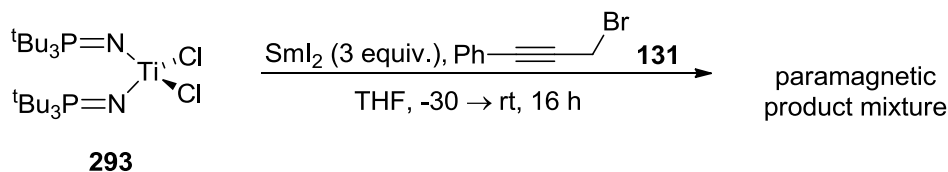
To test this hypothesis, a THF solution containing **293** and four equivalents of samarium(II) iodide was treated with one equivalent each of 1-bromo-3-phenyl-prop-2-yne (**131**) and *i*-propyl bromide at -30 °C, leading to a blue product mixture. The reaction mixture was extracted with benzene and then filtered through Celite, furnishing a paramagnetic reddish-purple solid. We also tested a modified procedure in which propargyl bromide **131** was added to the THF mixture containing **293** and samarium(II) iodide four hours prior to the addition of *i*-propyl bromide. These modified reaction conditions also afforded a reddish-purple paramagnetic product after work-up. No serious attempts were made to isolate or characterize the unknown products, but the lack of insoluble samarium(III) halide salts in the reaction products suggests the incorporation of “SmX₃” into the titanium products. Since samarium(II) diiodide does not reduce **293** and is insoluble in benzene, this could explain the paramagnetic nature of the product. Similar reactivity was recently reported by Yélamos and co-workers²²² who isolated a mixed samarium-titanium cluster from the combination of SmCl₃ and the titanium-nitride cluster **304** (Equation 4.6). Analogous to this example, a bimetallic titanium-samarium phosphinimide complex with bridging phosphinimide ligands might be formed by the combination of samarium(III) trihalide and the bi-metallic species **305** (Equation 4.7).^{131,139,223} Unfortunately, these results indicate that titanacyclobutenes cannot be prepared using samarium(II)-mediated coupling conditions due to the reactivity between phosphinimide ligands and Lewis-acidic samarium compounds.

Equation 4.6



Equation 4.7**4.3.4 Attempted preparation of cationic titanium(IV) propargyl complexes**

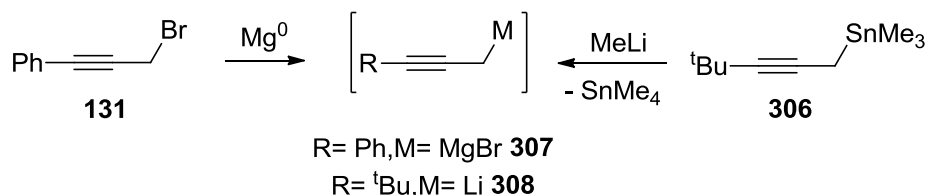
Our second attempt to prepare titanacyclobutenes from titanium(IV) phosphinimide complexes was the addition of carbon-based anions to cationic (propargyl)titanium(IV) complexes.³⁸ This methodology was previously investigated in our group by Morita for preparing titanacyclobutene complexes from half-sandwich titanium(IV) phosphinimide precursors. This presented a few new challenges, however, as his approach uses two equivalents of samarium(II) diiodide for installing the propargyl ligands onto half-sandwich titanium(IV) phosphinimide complexes. Due to the apparent reactivity between phosphinimide ligands and samarium salts (see Equation **4.7**) we did not expect success, but this method was still investigated for scientific interest (Equation **4.8**). Upon addition of propargyl bromide **131** to a THF solution containing bis(tri(*t*-butyl)phosphinimide)titanium(IV) dichloride (**293**) and three equivalents of samarium(II) iodide, not surprisingly we obtained a reddish-purple paramagnetic product after work-up.

Equation 4.8

To circumvent the use of samarium(II) diiodide, pre-formed anionic propargyl transfer reagents were investigated as a route to install propargyl ligands onto bis(tri(*t*-butyl)phosphinimide)titanium(IV) dichloride (**293**).²²⁴ The reactivity between **293** and various carbanionic reagents has been well documented and in most cases the reactions afford stable alkyl- and di(alkyl)titanium(IV) bis(phosphinimide) complexes.^{142,217} Although this method has not been reported for anionic propargyl reagents, we thought that this would furnish the corresponding neutral (propargyl)titanium(IV) bis(phosphinimide) complex.

Two propargyl transfer agents were selected for this experiment, 3-phenyl-2-propynylmagnesium bromide (**307**)²²⁵ and 3-(*t*-butyl)-2-propynyl lithium (**308**) (Scheme 4.6)²²⁶ as both phenyl and *t*-butyl groups are common substituents at the 2-position of titanacyclobutenes.^{3-5,38,48} These reagents were also selected because they are readily prepared from either propargyl halide **131** or from 3-(*t*-butyl)-2-propynylstannane (**306**), respectively (Scheme 4.6).^{225,226}

Scheme 4.6



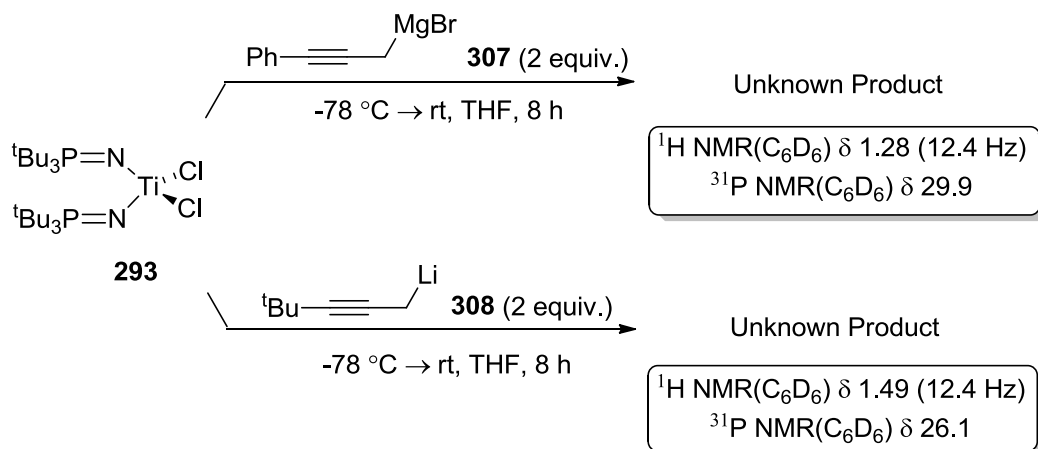
When a THF solution of bis(tri(*t*-butyl)phosphinimide)titanium(IV) dichloride (**293**) was treated with one equivalent of propargylmagnesium bromide reagent **307**,²²⁵ a colorless oil was obtained. This product mixture was analyzed by ¹H NMR spectroscopy and showed two broad doublets between 1.4 and 1.3 ppm (⁴J_{PH} = 12.8 Hz and 13.2); these signals correspond to the *t*-butyl substituents on the phosphinimide ligand. The same product mixture was analyzed by ³¹P NMR spectroscopy; the presence of multiple phosphorous signals in the ³¹P spectrum reveals that the two “broad doublets” observed by ¹H NMR spectroscopy are actually a series of overlapping

doublets, and that multiple *t*-butyl-phosphinimide-containing products are present in the product mixture.

In a second experiment, excess propargylmagnesium bromide reagent **307** was added to bis(tri(*t*-butyl)phosphinimide)titanium(IV) dichloride (**293**), affording a white solid after work-up (Scheme **4.7**). The solid was analyzed by ^1H and ^{31}P NMR spectroscopy, which revealed one doublet in the ^1H NMR spectrum at 1.28 ppm ($^4J_{\text{PH}} = 12.4$ Hz), and one signal in the ^{31}P NMR spectrum at 29.3 ppm. The spectroscopic data imply that one product was obtained from the reaction, but we did not observe signals in the ^1H NMR spectrum that would correspond to the aryl- or propargylic protons of a titanium-coordinated propargyl ligand. Therefore, we conclude that propargylmagnesium halide reagents will react with **293**, but not in the manner that we desired; thus are not suitable for adding propargyl ligands to **293**.

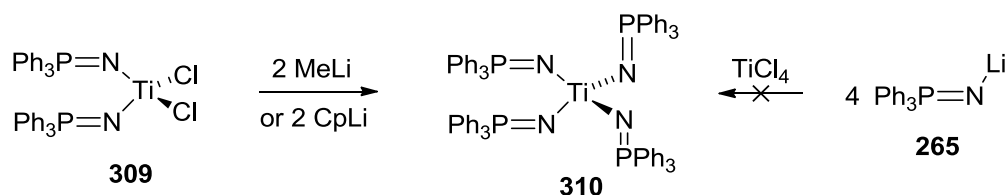
We then switched our focus to 3-(*t*-butyl)-2-propynyl lithium (**308**)²²⁶ as the propargyl transfer reagent; this gave different results than 3-phenyl-2-propynylmagnesium bromide (**307**). When one equivalent of the propargyl lithium reagent **308** was added to bis(tri(*t*-butyl)phosphinimide)titanium(IV) dichloride (**293**) at -78 °C, a light brown product mixture was obtained (Scheme **4.7**). We determined through ^1H and ^{31}P NMR spectroscopic analysis that two compounds were present in the product mixture, one of which was the **293**. The spectroscopic data for the second product contained only a doublet at 1.49 ppm ($^4J_{\text{PH}} = 12.4$ Hz) in the ^1H NMR spectrum, and one phosphorous signal at 26.1 ppm in the ^{31}P NMR spectrum. As observed in the addition of propargylmagnesium bromide reagent **307** to **293**, both propargylic and *t*-butyl proton signals were absent from the ^1H NMR spectrum, which implies that the propargyl ligand was not added to the titanium(IV) center. Repeating the experiment in the presence of excess propargyl lithium **308** (Scheme **4.7**), the starting complex **293** was completely converted into a product with the same spectroscopic characteristics as the same product obtained with adding one equivalent of **308**, as determined by ^1H and ^{31}P NMR spectroscopy.

Scheme 4.7



Brief attempts were made to identify this second phosphinimide-containing product, in which the propargyl ligand is absent. The reactivity between bis(phosphinimide)titanium(IV) dichloride complexes has been documented by Dehnicke *et al.* (Scheme 4.8), who obtained titanium(IV) tetrakis(triphenyl phosphinimide) (**310**) from the addition of two equivalents of methyl- or cyclopentadienyl lithium to bis(triphenylphosphinimide)titanium(IV) dichloride (**309**).²²⁷ Dehnicke's observations of disproportionation by ligand exchange is consistent with the results from our experiments, where complete conversion of our titanium(IV) starting material **293** was obtained upon addition of two equivalents of 3-(*t*-butyl)-2-propynyl lithium **308**. The product formed from the combination of bis(phosphinimide)titanium(IV) dichloride (**293**) and propargyl lithium **308** is thus likely to be titanium(IV) tetrakis(*t*-butyl)phosphinimide, along with a titanium(IV) tetrakis(*t*-butyl)propargyl species which decomposes upon forming.

Scheme 4.8



4.3.5 Conclusions

The results from these experiments establish that bis(tri(*t*-butyl)phosphinimide) titanium(IV) dichloride (**293**) is not a suitable precursor for preparing titanacyclobutene complexes. More importantly, this study demonstrates that phosphinimide ligands should not be considered to be Cp' analogues, despite opinions in the literature.^{135,136,186,228} Evidence supporting this conclusion was first obtained in the reduction of **293**, where no reaction or quantitative decomposition was observed. These results indicate that phosphinimide ligands, by themselves, are incapable of supporting lower oxidation state titanium complexes. However, by replacing one of the phosphinimide ligands with a Cp' ligand, both Stephan^{189,221} and our group³⁸ were able to isolate titanium complexes in which the titanium atoms are in the +2 or +3 oxidation state.

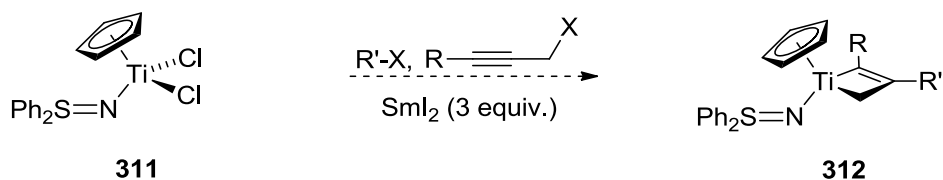
An addition reaction between bis(phosphinimide)titanium(IV) dichloride and samarium(II) diiodide was indicated from our attempts to prepare titanacyclobutene complexes, since insoluble SmX₃ salts were not found in the reaction mixture. This adduct formation was not observed when Cp'(R₃PN)TiCl precursors were used to prepare titanacyclobutenes, as insoluble SmX₃ salts were present in that reaction mixture. In light of these experiments, we still hold that phosphinimide ligands maintain strong bonding interactions with titanium(IV) atoms. However, our results emphasize that titanium(IV) phosphinimide complexes remain Lewis basic at one or more R₃PN-ligands and are not tolerant of changing electronic conditions as titanocene-based complexes, and therefore should not be considered as exact replacements for cyclopentadienyl ligands.

4.4 Sulfimide ligands as Cp mimics

4.4.1 Introduction to sulfimide ligands

The preparation and reactivity of transition metal phosphinimide complexes are well studied, whereas little is known about transition metal sulfimide complexes.²²⁹⁻²³³ Based on the isoelectronic relationship between phosphinimide and sulfimide ligands, we next investigated titanium(IV) sulfimide complexes as precursors to titanacyclobutenes (Equation 4.9).

Equation 4.9



Sulfimide ligands contain a highly polarized sulfur-nitrogen double bond, which is similar to the nitrogen-phosphorous bond in phosphinimide ligands.²³⁴⁻²³⁶ Although no computational studies have been conducted on the bonding orbitals of the “naked” sulfimide, one can assume that three similar nitrogen-based σ - and π - bonding orbitals are available to interact with empty metal d-orbitals (Figure 4.3).²³⁴ Strong bonding interactions between sulfimide ligands and transition metal centers have been inferred from crystallographic analysis of transition metal sulfimide complexes. The range of M-N-S bond angles in transition metal sulfimide complexes (135° to 171°) is similar to the M-N-P bond angles found in transition metal phosphinimide complexes.^{231,232} The near-linear geometrical alignment between the N-S bonds of sulfimides with some transition metal centers emphasizes that sulfimide ligands are capable of being six-electron donors. With such similarities between phosphinimide and sulfimide ligands, we propose that sulfimides be considered isolobal analogues of Cp ligands.

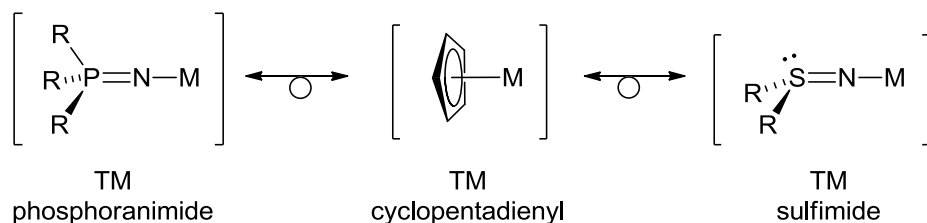


Figure 4.3: Phosphinimide and sulfimide ligands as isolobal analogues to Cp ligands.

4.4.2 Preparation of transition metal sulfimide complexes

Given the ubiquity of Group IV complexes bearing Cp and phosphinimide ligands, the lack of reports on the corresponding sulfimide complexes seemed surprising to us. This unexplored area of research was intriguing; we decided target the half-sandwich titanium(IV) sulfimide complexes **313** and **314**, as well as the titanium(III) analogues **315** and **316** (Figure 4.4) as possible routes to titanacyclobutene complexes. If these preparations were successful, these complexes could also be used in other ways, such as precatalysts for olefin polymerization.

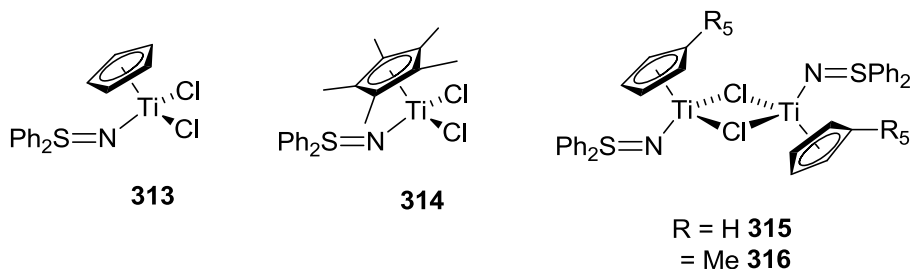
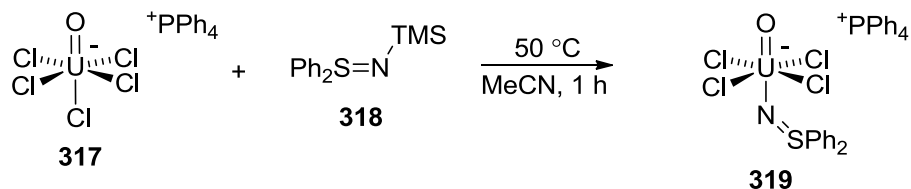


Figure 4.4: Synthetic targets **313**, **314**, **315** and **316**.

The methods for preparing transition metal sulfimide complexes are the same as those used to prepare transition metal phosphinimide complexes. Roesky and co-workers prepared a series of transition metal sulfimide complexes through the combination of N-(trimethylsilyl)-S,S-diphenylsulfimide (**318**) and various Lewis-acidic transition metal halides (WF_6 ²³¹, NbCl_4 , $\text{V}(\text{O})\text{Cl}_3$, $\text{V}(\text{O})\text{F}_3$, MoCl_5 and FeCl_3 ²³²); Green and

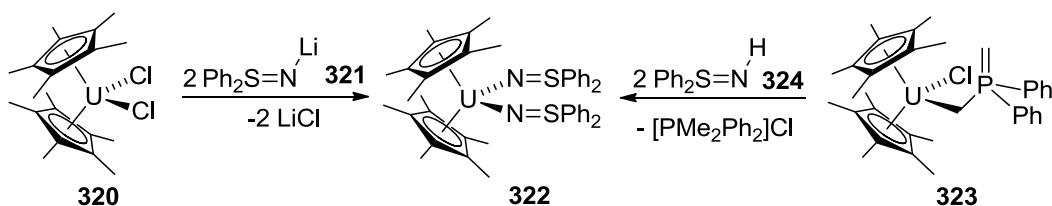
co-workers reported similar reactivity between **318** and $[\text{Ph}_4\text{P}]^+[\text{U}(\text{O})\text{Cl}_5]^-$ (**317**) (Equation 4.10).²³³

Equation 4.10



Metal sulfimide complexes have also been prepared from the combination of lithium sulfimide salts and metal halides. Gilje *et al.*, prepared bis(pentamethyl)uranyl sulfimide derivatives by treating $\text{Cp}^*_2\text{UCl}_2$ (**320**) with one or two equivalents of lithium *S,S*-diphenylsulfimide (**321**). These bis(pentamethyl)uranyl sulfimide complexes were also prepared by the addition of two equivalents of *S,S*-diphenylsulfimine (**324**) to $\text{Cp}^*\text{UCl}(\text{CH}_2\text{P}(\text{CH}_2)\text{Ph}_2)$ (**323**) (Scheme 4.9).²³⁰ This second method takes advantage of the basicity of phosphoylide ligands; both sulfimide equivalents were deprotonated and the doubly-protonated phosphoylide ligand was removed as dimethyldiphenylphosphonium chloride.

Scheme 4.9

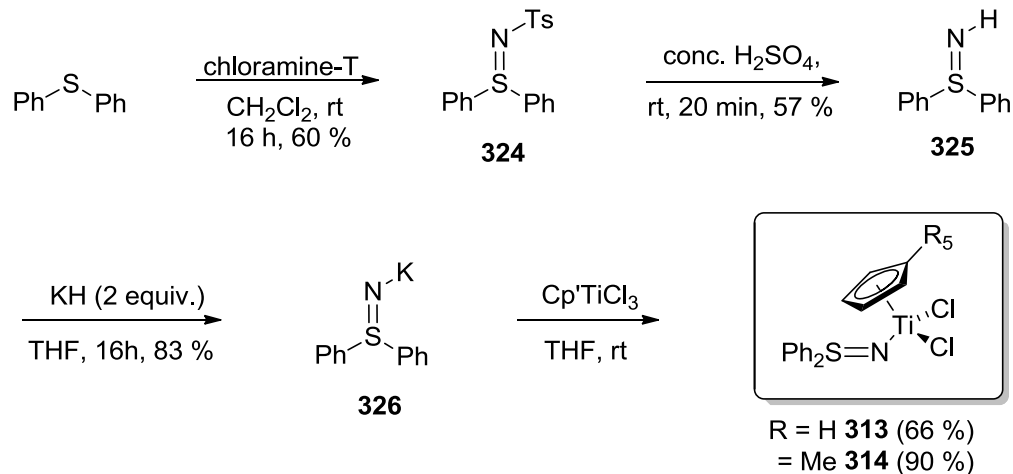


4.4.3 Preparation of half-sandwich titanium(IV) sulfimide complexes

We hypothesized that half-sandwich titanium(IV) sulfimide complexes could be prepared from CpTiCl_3 or Cp^*TiCl_3 by anionic salt metathesis. Lithium *S,S*-diphenylsulfimide (**321**) has been readily prepared by deprotonating *S,S*-

diphenylsulfimide (**324**) with one equivalent of *n*-BuLi.²³⁷ However, we chose to prepare the potassium sulfimide analogue **326** under the assumption that KCl could be more readily separated from the crude product than LiCl, which is typically more soluble in organic solvents. The precursor *S,S*-diphenylsulfimine (**324**) was prepared in two steps from reported procedures by Mann and Pope, and Oae (Scheme 4.10). In the first step, diphenylsulfide was oxidized to *N*-(*p*-toluenesulfonyl)-*S,S*-diphenylsulfimine (**325**) using chloramine-T.²³⁸ In the second step, **325** was converted into *S,S*-diphenylsulfimine (**324**) through protolytic cleavage of the sulfonate group.²³⁹ The potassium sulfimide reagent **326** was then obtained by adding 2 equivalents of potassium hydride to a THF solution containing **324** and stirring overnight. Due to its unexpected solubility in aromatic hydrocarbon solvents, the potassium sulfimide salt **326** was readily separated from the product mixture by extraction with toluene and filtration of the extracts through Celite to remove the insoluble KCl salts. Upon removal of toluene from the filtered extracts, a yellow powder was obtained that was carried on to subsequent steps without further purification. The desired half-sandwich titanium(IV) sulfimide complexes **313** and **314** were obtained in appreciable yields by the addition of one equivalent of the yellow potassium sulfimide salt to THF solutions containing either CpTiCl₃ or Cp*TiCl₃ respectively (Scheme 4.10). These results were exciting, as **313** and **314** are the first group IV transition metal sulfimide complexes to be reported.

Scheme 4.10



Both half-sandwich titanium(IV) sulfimide complexes **313** and **314** were characterized by ^1H and ^{13}C NMR spectroscopy, IR spectroscopy, single crystal X-ray crystallography (Figure 4.5) and elemental analysis. The single crystals of **313** and **314** used for X-ray diffraction were grown from concentrated toluene solutions at $-30\text{ }^\circ\text{C}$ (Figures 4.5 and 4.6). Since titanium(IV) sulfimide complexes had not been prepared prior to this study, crystallographic analysis was crucial to establish the bonding interactions between sulfimide ligands and the titanium(IV) center. The crystallographic data (Figure 4.7) reveal that the Ti-N bond distances of **313** and **314** are comparable to the Ti-N bond distances in the analogous half-sandwich titanium(IV) triphenylphosphinimide complex **204**.¹⁸⁴ This is consistent with the hypothesis that sulfimide ligands contribute additional electron density from at least one of the filled nitrogen p-orbitals. However, the N-S bonds of the sulfimide ligands in **313** and **314** are shorter than the average N-S distance in non-coordinated sulfimine compounds (163.6 pm).²³⁴ This observation implies that sulfimide ligands are likely contributing four of six nitrogen-based bonding electrons,¹⁴⁷ and that the remaining two potential bonding electrons remain in the N=S bond.

The Ti-N-S and Ti-N-P distances are also similar in the titanium sulfimide complexes **313** and **314** compared to the analogous phosphinimide complex **204**. These values indicate that sulfimide ligands provide an “open” coordination environment around the titanium center, similar to phosphinimide ligands. The Ti-N-S bond angles of **313** and **314** lie within the normal range of reported transition metal sulfimide complexes (135° to 171°).^{229,231-233} However, the two Ti-N-S bond angles differ by 21° ; we suggest that the geometrical distortion is induced by the sulfimide ligands relieving an unfavourable steric interaction between the proximal substituents of the Cp* ligand and the sulfur lone pair (Figures 4.5 and 4.6). This implies that the difference in Ti-N-S bond angles is unlikely to be the result of significant energy differences in the titanium-sulfimide bonds.

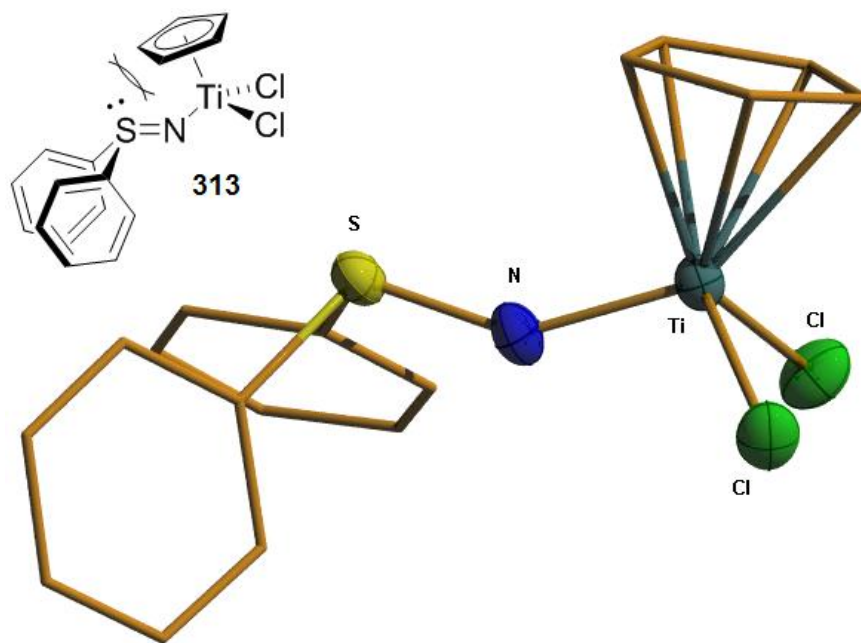


Figure 4.5: Perspective view of **313** showing selected atom labelling scheme. Non-hydrogen atoms are represented by either Gaussian ellipsoids at the 20% probability level or as “wire and stick” representations. $R_1 = 0.0263$, $R(w) = 0.0742$.

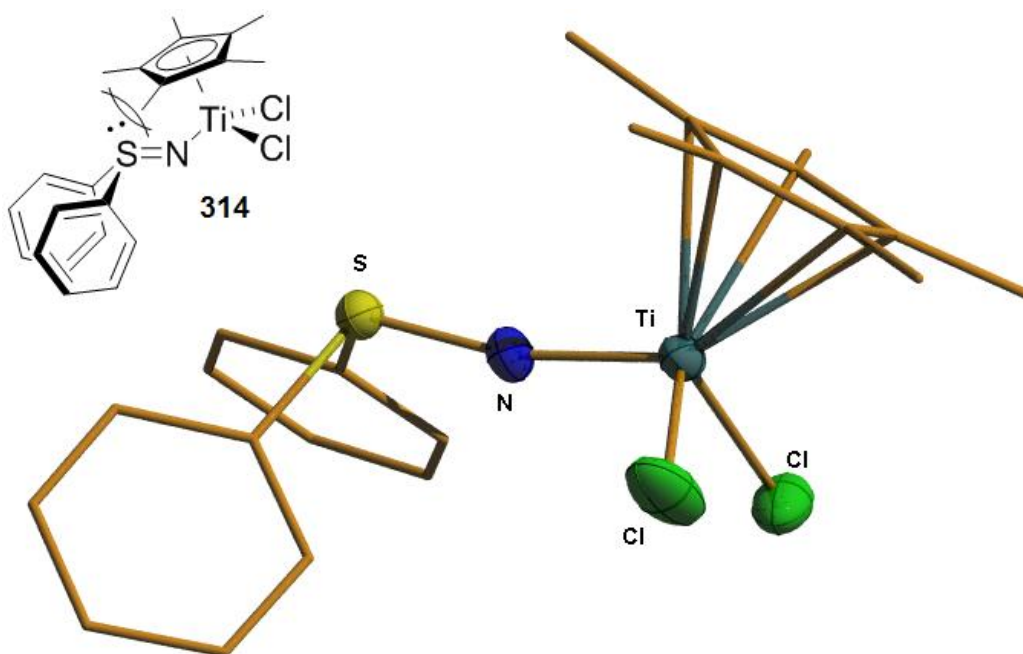


Figure 4.6: Perspective view of **314** showing selected atom labelling scheme. Non-hydrogen atoms are represented by either Gaussian ellipsoids at the 20% probability level or as “wire and stick” representations. $R_1 = 0.0381$, $R(w) = 0.0987$.

Entry	Ti-N (pm)	N-(S,P) (pm)	Ti-(S,P) (pm)	Ti-N-(S,P) (°)
313	178.82(14)	159.46(13)	323	145.43(8)
314	178.68(16)	158.10(17)	334	166.28(12)
204	178(1)	156(1)	333	174.7(9)

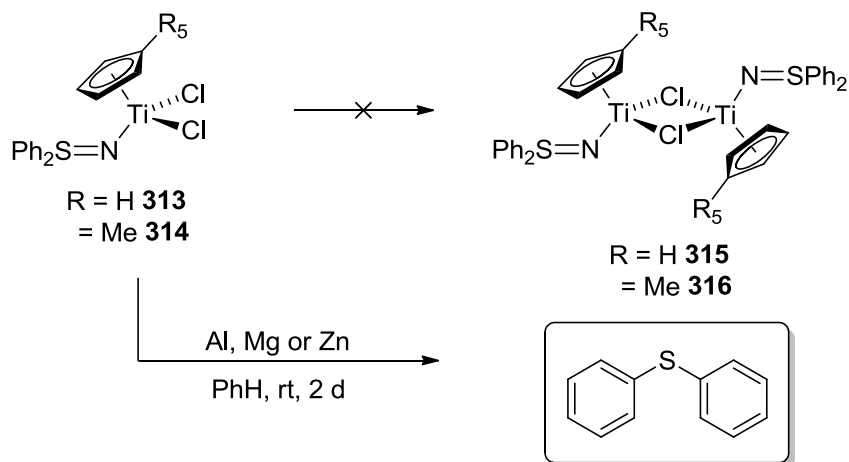
Figure 4.7: Selected bond distances of **313**, **314**, and **204**.

4.5 Reactivity of half-sandwich titanium(IV) sulfimide complexes **313** and **314**

4.5.1 Reduction of **313** and **314**

With two half-sandwich titanium(IV) sulfimide complexes in hand, our first step was to study one-electron reduction using metal powders.^{88,219-221} This study was crucial in determining whether **313** and **314** could be used to prepare titanacyclobutenes, as the isolation of titanium(III) sulfimide complexes would indicate that sulfimide ligands are capable of stabilizing (η^3 -propargyl)titanium(III) intermediates. Benzene solutions of **313** or **314** were stirred over magnesium, aluminum, manganese or zinc powders; unfortunately only brown product mixtures were obtained. The product mixtures were extracted with benzene and filtered through Celite, affording colourless oils after the removal of volatile solvents (Scheme 4.11). Based on ^1H NMR spiking experiments, we deduced that the colourless oils were composed only of diphenylsulfide. These results indicate that sulfimide ligands are less stable under reducing conditions than phosphinimide ligands, and therefore are likely not good candidates for preparing titanacyclobutenes. The fate of the remaining pieces of the titanium sulfimide complexes in these reduction reactions was also puzzling, as Cp' signals were absent in the ^1H NMR spectra; these observations imply that the Cp' ligands remain coordinated to the titanium(IV) centers after the decomposition of the sulfimide ligand. This issue will be addressed further in the chapter.

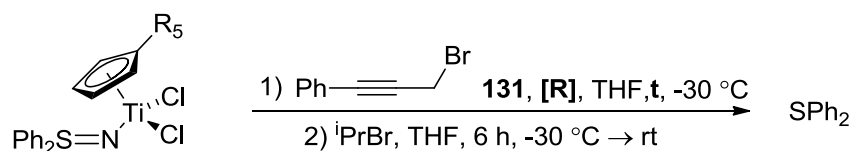
Scheme 4.11



4.5.2 Attempted preparation of titanacyclobutene complexes

Despite the apparent sensitivity of sulfimide ligands towards reducing conditions, we nonetheless attempted to prepare titanacyclobutenes from half-sandwich titanium(IV) sulfimide complexes **313** and **314**. To probe this transformation, we used both samarium(II)- and manganese(0)-reductants to prepare 2-phenyl-3-(*i*-propyl)titanacyclobutene complexes from the half-sandwich titanium(IV) sulfimide complexes **313** and **314** (Equation 4.12).^{3-6,38,48,49} Unfortunately, the addition of 1-bromo-3-phenyl-prop-2-yne (**131**) and *i*-propyl bromide to a cooled THF solution of titanium(IV) sulfimide complex **313** and activated manganese powder resulted in a similarly brown product mixture. The brown residue was extracted with benzene and filtered through Celite affording a colorless oil which was identified by ¹H NMR spectroscopic analysis as diphenylsulfide. In subsequent experiments, we investigated the effects of changing the reducing agent, the time of addition between propargyl halide **131** and *i*-propyl bromide, and the starting half-sandwich titanium(IV) sulfimide complex **314**. In all cases, we obtained diphenylsulfide as the only isolable product.

Scheme 4.12



conditions used for **313**: [R] = activated Mn powder (2 equiv) or Sml₂ (4 equiv)
t = 0 or 16 h

314: [R] = activated Mn powder (2 equiv) or Sml₂ (4 equiv)
t = 0 or 16 h

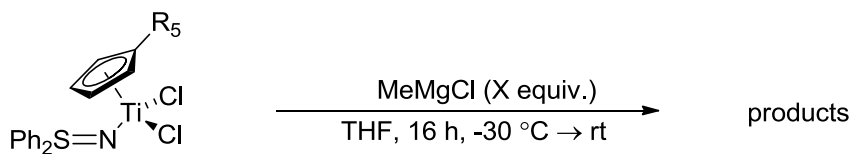
4.5.3 Alkylation of half-sandwich titanium(IV) sulfimide complexes

Due to the sensitivity of sulfimide ligands to reductive conditions, we abandoned our initial goal of preparing titanacyclobutene complexes from half-sandwich titanium(IV) sulfimide precursors **313** and **314**. Since titanium(IV) sulfimide complexes had not been reported previously, however, we examined other areas of reactivity to compare titanium(IV) phosphinimide and titanium(IV) sulfimide complexes. Stephan *et al.*, demonstrated that half-sandwich titanium(IV) phosphinimide complexes are readily alkylated by the addition of an organomagnesium reagent, which afforded thermally stable dialkyltitanium complexes.^{142,217} Based on that report, we explored the addition of organomagnesium reagents to **313** and **314**.

4.5.4 Addition of MeMgCl to **313** and **314**

We initially attempted to prepare the mono(methyl)- and di(methyl)titanium complexes by addition of methylmagnesium chloride to titanium sulfimide complexes **313** and **314** (Scheme 4.13).^{142,217} The products were analyzed by ¹H NMR spectroscopy, demonstrating that the addition of one equivalent of methylmagnesium chloride to either precursor at -30 °C furnished a 1:1 product ratio containing the starting complex and diphenylsulfide. These results imply that the double addition of methylmagnesium chloride is favoured over mono-addition to **313** or **314**. However, the proposed methylated products are only metastable and decompose at low temperature.

Scheme 4.13

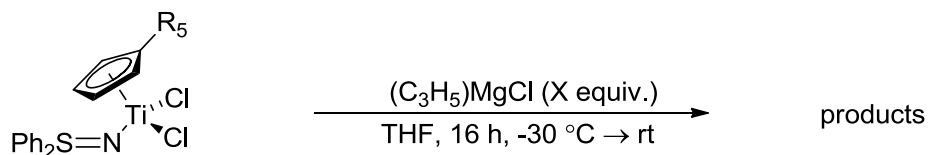


starting material	equivalents (X)	isolated products	product ratio (NMR)
313	1	313 , SPh ₂	1:1
314	2	SPh ₂	only product
313	1	314 , SPh ₂	1:1
314	2	SPh ₂	only product

4.5.5 Addition of (allyl)magnesium chloride to **313** and **314**

Similar metastable products were obtained upon addition of (allyl)magnesium chloride, as diphenylsulfide was identified as the only product (Scheme **4.14**).^{142,217} Surprisingly, however, we were able to obtain the bis(η^3 -allyl)titanium(IV) sulfimide complex **327** by conducting the reaction at low temperature. This modification was applied to additions of methyl- and (allyl)magnesium chloride to **313** and **314** in an effort to observe alkylated products spectroscopically. Unfortunately, we found this modification was only successful for the preparation of the bis(allyl)titanium(IV) sulfimide complex **327**.

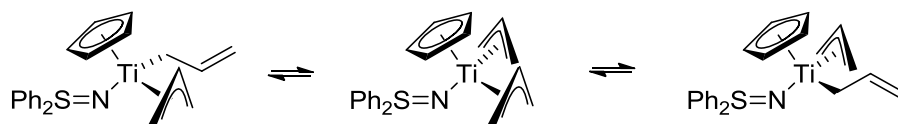
Scheme 4.14



starting material	equivalents (X)	isolated products
313	1	313 , SPh ₂ (1:1)
313	2	SPh ₂
313	2 (-78 °C)	Cp(Ph ₂ S=N)Ti(C ₃ H ₅) ₂ 327
314	1	314 , SPh ₂ (1:1)
314	2	SPh ₂

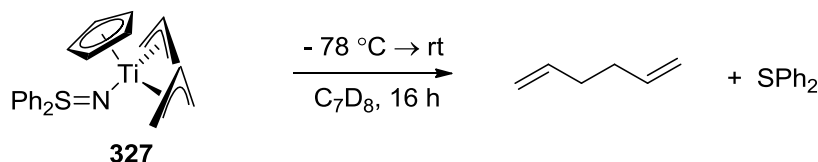
The bis(η^3 -allyl)titanium complex **327** was characterized by ^1H NMR spectroscopy at $-10\text{ }^\circ\text{C}$, as no decomposition was observed in solution at or below this temperature. Characteristic splitting patterns for fluxional η^3 -coordinated allyl ligands were observed; this included a quintet at 6.18 ppm corresponding to the central olefinic proton, and an upfield doublet at 3.61 ppm corresponding to the four terminal olefinic protons. An attempt was made to observe distinct η^1 and η^3 -allyl signals by cooling the NMR sample to $-80\text{ }^\circ\text{C}$, but we did not observe any separation of the two allylic proton signals. The combined ^1H NMR data suggests that both allyl groups are fluxional. Martin and co-workers observed similar allylic splitting patterns in the NMR spectra of bis(allyl)zirconocene complexes, but the IR spectroscopic data of these complexes contained two different allyl C=C stretching frequencies at 1533 cm^{-1} (π) and $\sim 1590\text{ cm}^{-1}$ (σ). These data are therefore consistent with the allyl ligands rapidly interconverting between η^3 - and η^1 -hapticities (Equation 4.11).²⁴⁰ We attempted to collect an IR spectrum of our bis(allyl)titanium(IV) sulfimide complex **327**, but decomposition to a brown sludge occurred rapidly at room temperature.

Equation 4.11



The thermal decomposition products from bis(allyl)titanium complex **327** were determined by ^1H NMR spectroscopy to be diphenylsulfide and 1,5-hexadiene (Equation 4.12). Based on previous reports of bis(allyl)titanocene(IV) complexes, the decomposition of **327** likely proceeds through homolytic cleavage of one Ti-C bond. The generated allyl radical can then combine at the terminal carbon of the titanium(III) allyl species generating 1,5-hexadiene.

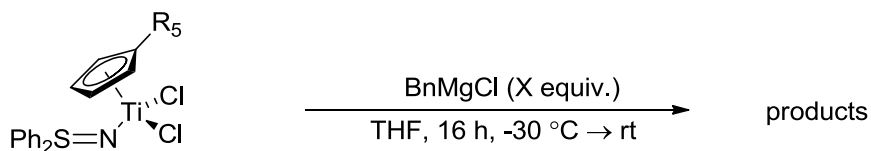
Equation 4.12



4.5.6 Addition of benzylmagnesium chloride

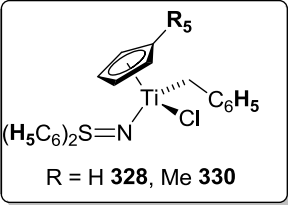
The addition of (benzyl)magnesium chloride solutions to **313** and **314** afforded isolable (benzyl)titanium sulfimide complexes **328**, **329** and **330** (Scheme 4.15).^{142,217} Oddly, in order to fully convert (pentamethylcyclopentadienyl)titanium(IV) (S,S-diphenyl)sulfimide dichloride (**313**) into the mono(benzyl)titanium product **330**, an additional equivalent of (benzyl)magnesium chloride was required. This was odd because the same (benzyl)magnesium chloride solution was used to prepare both mono- and dialkylated Cp analogues **328** and **329** without complications. Addition of three equivalents of (benzyl)magnesium chloride to **314** produced mostly diphenylsulfide and bibenzyl. The formation of bibenzyl was evidence of the same reductive degradation process that produced 1,5-hexadiene from the allyl complex (see Equation 4.12).

Scheme 4.15

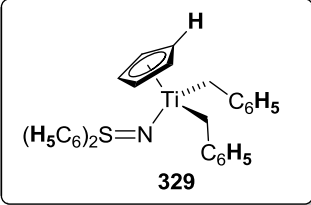


starting material	equivalents (X)	isolated products
313	1	Cp(Ph ₂ S=N)Ti(Bn)Cl 328 (product mixture)
313	2	Cp(Ph ₂ S=N)Ti(Bn) ₂ 329 (60 % isolated yield)
314	2	Cp*(Ph ₂ S=N)Ti(Bn)Cl 330 (> 90 % crude yield)
314	3	bibenzyl, SPh ₂ (1:1)

All three (benzyl)titanium(IV) sulfimide products were stable in solution at room temperature and were characterized by ^1H NMR spectroscopy (Figure 4.8). In all cases the benzylic protons were evidenced as two first-order doublets between 3.40 ppm and 2.38 ppm. The chemical nonequivalence of the benzylic protons in the mono(benzyl)titanium complexes **328** and **330** arises from the stereogenic tetrahedral titanium(IV) center. In the bis(benzyl)titanium product, however, the diastereotopicity of the two benzylic protons is due to the differing chemical environments of the benzylic hydrogen atoms of the benzylic groups.



R = H **328**, Me **330**



329

Entry	δ Ar-H (ppm)	δ C ₅ H ₅ (ppm)	δ C ₅ Me ₅ (ppm)	δ CH ₂ Ph (ppm)
328	7.68 (<i>mult.</i>), 6.88 (<i>mult.</i>) 6.79(<i>mult.</i>)	5.76 (<i>singlet</i>) 5.78 (<i>singlet</i>)	-	3.40, 3.21 (2 doublets, J = 9.4 Hz)
329	7.80-7.13 (<i>mult.</i>), 7.08 (<i>mult.</i>) 6.98-6.84 (<i>mult.</i>)	-	-	3.00, 2.68 (2 doublets, J = 9.4 Hz)
330	7.47-7.36 (<i>mult.</i>), 7.10 (<i>mult.</i>) 6.96-6.72 (<i>mult.</i>)	-	1.94 (<i>singlet</i>)	2.53, 2.38 (2 doublets, J = 10.8 Hz)

Figure 4.8: Selected ^1H NMR data from **328**, **329** and **330**.

Two of the benzylated titanium compounds were also characterized by X-ray crystallography (Figures 4.9, 4.10 and 4.11); suitable single crystals of **329** and **330** were grown from diethylether solutions at -30 °C. When compared to data for the parent dichloride complexes **313** and **314**, crystallographic analyses of **328** and **330** reveal no significant changes in the Ti-N, or N-S bond lengths, or the Ti-N-S angles (See Figure 4.5). This implies that the benzyl substituents do not have a dramatic effect on the bonding between the titanium and the sulfimide ligand. However, the Ti-C bonds associated with the benzyl ligands are surprisingly long in comparison to typical Ti-C bond distances of around 210 pm.²⁴¹ These data indicate that the Ti-C bonds are weak, consistent with the observed facility of homolytic bond cleavage.

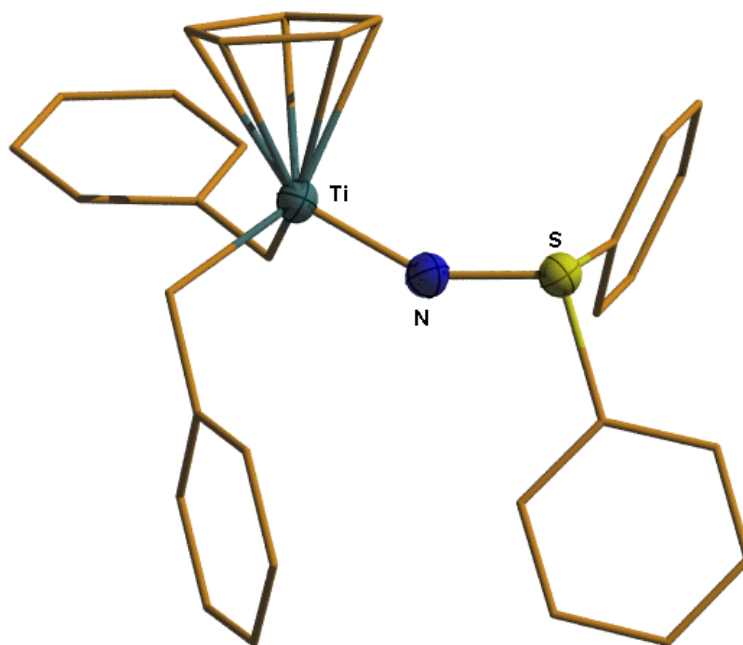


Figure 4.9: Perspective view of **328** showing selected atom labelling scheme. Non-hydrogen atoms are represented by either Gaussian ellipsoids at the 20% probability level, or as “wire and stick” representations. $R_1 = 0.0463$, $R(w) = 0.1180$.

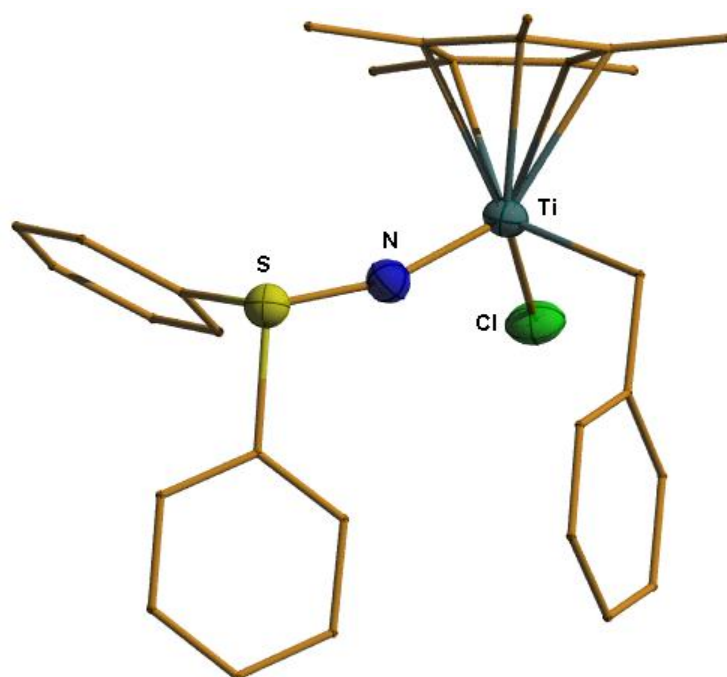


Figure 4.10: Perspective view of **330** showing selected atom labelling scheme. Non-hydrogen atoms are represented by either Gaussian ellipsoids at the 20% probability level, or as “wire and stick” representations. $R_1 = 0.326$, $R(w) = 0.0908$.

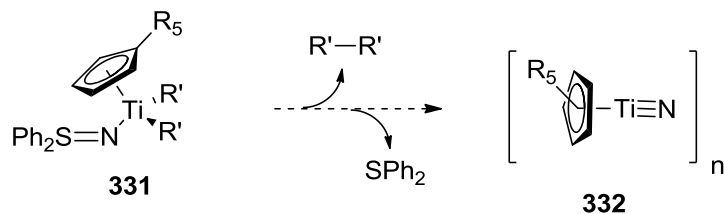
Entry	Distance (pm)			Angle (°)
	Ti-N	N-S	Ti-C	Ti-N-S
329	180.6(2)	157.6(2)	234.9(3) 238.5(3)	149.60(15)
330	180.47(13)	157.28(13)	231.62(5)	161.91(9)

Figure 4.11: Selected interatomic distances and angles of **329** and **330**.

4.5.7 Conclusions

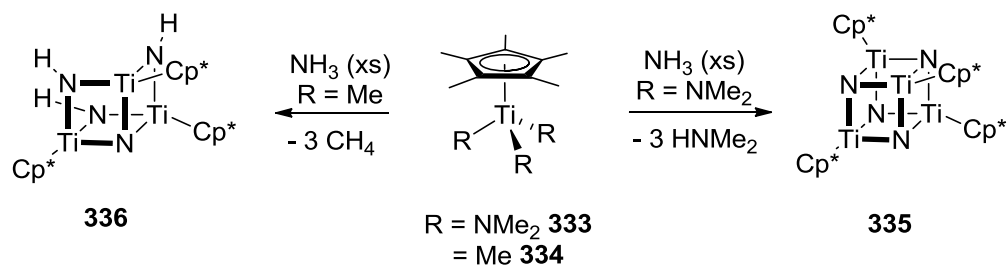
We have assessed the sulfimide ligand as a potential replacement for Cp' ligands in titanium(III) complexes. However, our results establish that sulfimide ligands do not tolerate changing electronic environments around the titanium(III) center and readily decompose by expelling diphenylsulfide. In comparison, we determined that di(alkyl)titanium(IV) sulfimide complexes decompose by expelling diphenylsulfide and the reductively coupled product from the two alkyl substituents (Equation **4.13**). The loss of both alkyl ligands and diphenylsulfide from half-sandwich di(alkyl)titanium(IV) sulfimide complexes implicates to concomitant formation of a cyclopentadienyl-supported titanium nitride complex (**333**), which is presumably oligomeric.

Equation 4.13



To our knowledge, Mena and Roesky have prepared the only isolable titanium(IV) nitride complexes **335** and **336** through high temperature aminolysis of Cp*TiR₃ complexes **333** and **334** respectively (Scheme 4.16).²⁴²⁻²⁴⁴ The isolation of a titanium-nitride species from the decomposition of titanium(IV) sulfimide complexes is significant, as it constitutes a novel method for preparing titanium-nitride complexes at lower temperature. Our preparation of the Cp-supported titanium(IV) nitride is still speculative at this point, as we have as yet been unable to purify and characterize the titanium-containing products from any of the “decomposition studies”.

Scheme 4.16



4.6 Conclusions and Insights

Throughout the experiments described in this chapter, we focused on finding replacements for the “titanocene” template in titanium-mediated transformations. Instead, we gained an added respect for cyclopentadienyl ligands. Although cyclopentadienyl, phosphinimide and sulfimide ligand systems have similar electronic interactions with early transition metal centers, the previously unsuspected reactivity patterns of titanium(IV) phosphinimide and titanium(IV) sulfimide complexes became apparent during our investigations. Such reactivity patterns included the decomposition of both titanium(IV) phosphinimide and sulfimide complexes upon reduction, the decomposition of titanium(IV) sulfimide complexes upon alkylation, and the inherent reactivity between titanium(IV) phosphinimide complexes and samarium halide salts. We conclude that phosphinimide ligands may be the closest replacements for Cp ligands

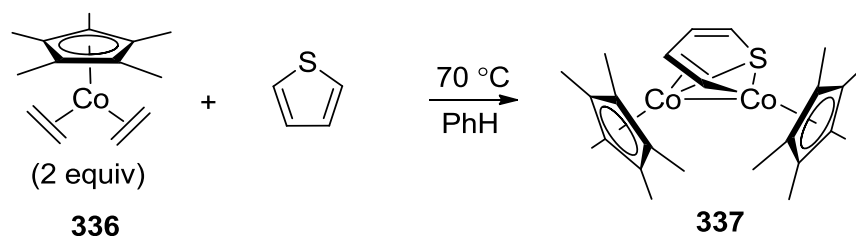
when considering the preparation of titanacyclobutene complexes, but advances in the discovery of new anionic ancillary ligands must be made before cyclopentadienyl ligands can be dethroned as the “work-horse” of titanium-mediated transformations.

Chapter 5: Preparation of Cobalt (II) Phosphinimide Compounds: Dehydrohalogenation of Cobalt (II) Phosphinimine Complexes

5.1 Introduction to selected uses of cobalt(I) cyclopentadienyl complexes

Hydrodesulfurization is extremely important to the oil and gas sector, as environmental restrictions require very low amounts of sulfur in consumable fuels.^{245,246} These restrictions have compelled researchers to investigate methods for removing sterically “embedded” sulfur from polycyclic aromatic compounds containing aromatic carbon-sulfur bonds such as those found in thiophene and dibenzothiophene. Of particular interest are half-sandwich cobaltocene(I) complexes, which are known to oxidatively insert into the C-C or C-X bonds of small molecules (Equation 4.1). One such example was reported by Jones who demonstrated that Cp*Co(ethylene)₂ (**336**) will insert into the C-S bonds of thiophene²⁴⁷ and dibenzothiophene.²⁴⁸ In the case of benzothiophene, the resulting dicobalt(III) sulfide complex **337** was obtained. Precursors such as **336** cannot be used in industrial settings, however, and the partially desulfurized product cannot be removed from **337** by adding reducing gases such as H₂, or CO.

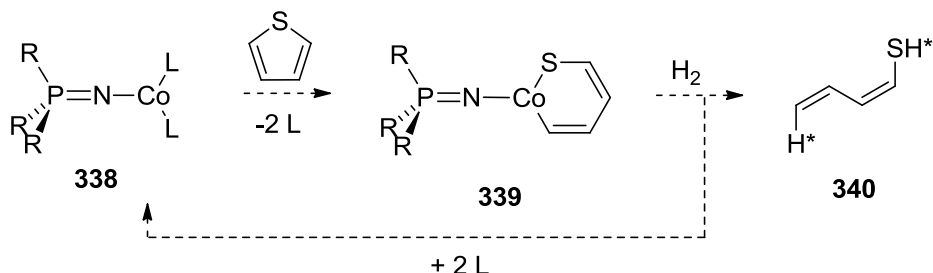
Equation 5.1



Early transition-metal phosphinimide complexes display comparable reactivity to early transition-metal metallocene and half-metallocene complexes. However, similar comparisons have not been made between late-metal phosphinimide and late-

metal cyclopentadienyl complexes.^{137,142,186,189,216} The advantage to using phosphinimide ligands is that they create a more sterically relaxed environment around the cobalt center. This is accomplished through the presence of the N-P bond, which shifts the steric bulk created by the ligand substituents further from the cobalt center. The additional freedom created around the cobalt center may allow the development of catalytic versions of currently known (cyclopentadienyl)cobalt(I) mediated reactions (Scheme 5.1). A specific example would be development of a cobalt(I) phosphinimide hydrodesulfurization catalyst **338**. In this example, however, the analogous cobalt(I) phosphinimide “catalyst” could be recycled under an atmosphere of hydrogen by reducing off the sulfide product **340**.

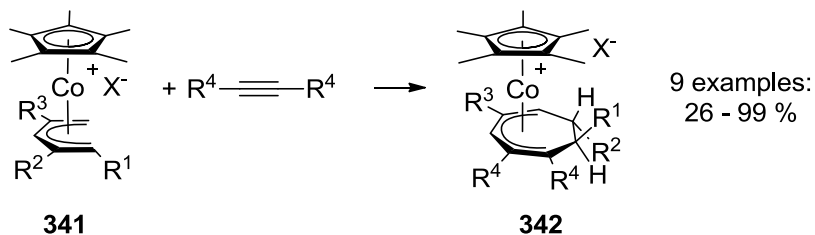
Scheme 5.1



Cobalt(I) cyclopentadienyl complexes have also been demonstrated by the Stryker group to be suitable starting materials for preparing a variety of substituted cationic acyclic-(pentamethylcyclopentadienyl)cobalt(III) pentadienyl complexes (**341**) (Equation 5.2).²⁴⁹ This communication describes the potential synthetic utility of these cobalt(III) complexes, as the acyclic-pentadienyl ligands undergo regioselective [5+2] cycloadditions with substituted alkynes, affording η^5 -coordinated seven-membered rings (**342**).^{249,250} Although a novel method for preparing seven-membered rings, this reaction is extremely dependent on the presence of R^1 substituents, and mostly intolerant of substitution at other positions. The limitations to this chemistry were investigated computationally. It was determined that unfavourable steric interactions

exist between the acyclic-pentadienyl substituents and the Cp* ligand which prevent the formation of the required η^3 -coordinated allyl intermediate.

Equation 5.2



We propose that the reactivity between such organic fragments and cobalt(I) phosphinimide precursors would afford similar cobalt(III) pentadienyl products such as **341**. Since additional freedom around the cobalt center is created by the phosphinimide ligands, we anticipated observing a greater variety of acyclic pentadienyl substrates that undergo [5+2] cycloadditions with alkynes. In addition, the greater freedom about the cobalt(III) center might also expand the usable range of di-substituted alkynes to include bulkier substituents, as well as substituted alkenes which have not been reported to undergo [5+2] cycloadditions with acyclic cobalt(III) pentadienyl complexes.

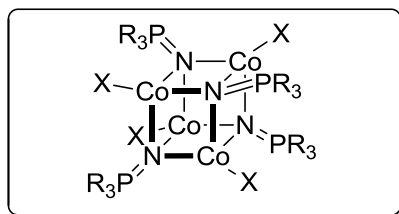
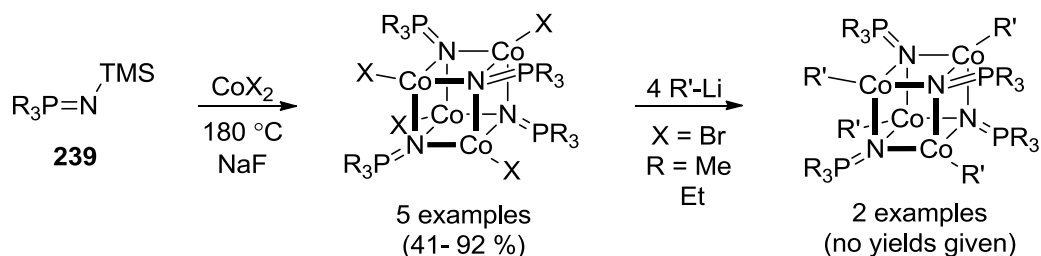
5.2 Introduction to cobalt(II) phosphinimide complexes

The specific goals of this project were to prepare lower coordinate bis(phosphinimide)cobalt(II) and mono(phosphinimide)cobalt(II) complexes. We postulated that these complexes would be suitable precursors to cobalt(I) phosphinimide complexes through alkali metal reduction using sodium or potassium. Such conditions have been used to prepare cyclopentadienylcobalt(I) complexes from cobalt(II) cyclopentadienyl precursors.^{251,252}

Up to this point, cobalt(II) phosphinimide complexes had been primarily isolated as heterocubane clusters, each containing μ^3 -phosphinimide ligands (Scheme 5.2).^{169,170,174,175,180,253} These complexes had been prepared by heating to high

temperatures a mixture containing one equivalent of a cobalt(II) salt and one equivalent of a silylphosphinimide compound.

Scheme 5.2



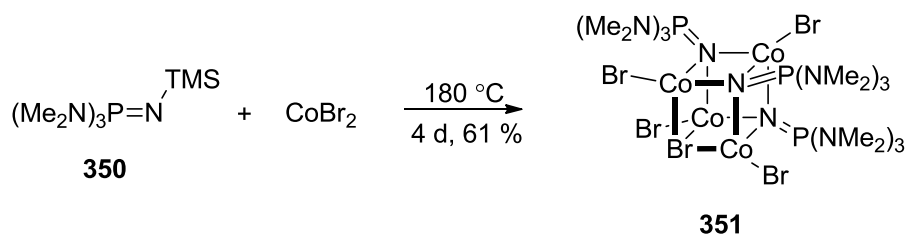
Entry	R	X	Bond Distances (pm)		Bond angles (°)		
			P=N	Co-N	Co-N-P	Co-N-Co	N-Co-N
343	Me	I	158.3(7)	202.5(7)	127.8(3)	86.8(2)	93.3(2)
344	Me	Br	158.8(4)	203.7(4)	127.2(2)	87.2(2)	92.8(2)
345	Me	C≡C ^t Bu	157.4(3)	204.1(3)	126.6(2)	88.1(1)	91.8(1)
346	Et	Cl	159.6(6)	204.8(5)	-	86.5(2)	93.4(2)
347	Et	Br	159.2(6)	204.4(6)	122.4(2)	86.0(2)	93.9(2)
348	Et	OAc	158.3(4)	203.4(4)	131.5(2)	85.5(2)	90.0(2)
349	Et	C≡CTMS	159.7(4)	204.4(4)	123.1(2)	87.0(2)	92.9(2)

Figure 5.1: Selected interatomic distances and angles of complete cobalt(II) phosphinimide heterocubane clusters **343** to **349**.

Our hypothesis was that the formation of higher order clusters depends on the bulkiness of the alkyl phosphinimide substituents, as trimethyl- or triethylphosphinimide ligands are generally observed in the heterocubane complexes **343-349** (Scheme 5.3).^{169,170,174,175,180,253} The influence of steric effects on the self-assembly of lower order cobalt(II) phosphinimide complexes was demonstrated by Dehnicke and co-workers who isolated an incomplete heterocubane cluster **351** by heating a mixture containing

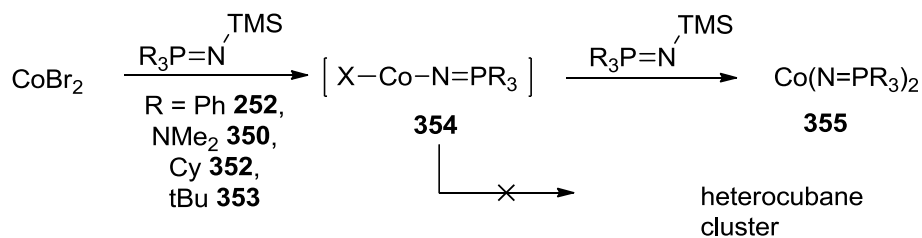
cobalt(II) bromide and N-(trimethylsilyl)tris(dimethylamido)phosphinimide (**350**) (Equation 5.3).¹⁷⁵ This result suggested that the increasingly crowded steric environment around the forming heterocubane cluster favours the incorporation of a [CoBr₂] unit instead of the fourth equivalent of [(Me₂N)₃P=N]-CoBr].

Equation 5.3



Concurrent attempts were also made by the Stryker group to prepare low-coordinate cobalt(II) phosphinimide complexes (Scheme 5.3). We envisioned that lower-coordinate cobalt(II) clusters (**355**) could react with a second equivalent of silylphosphinimide to afford bis(phosphinimide)cobalt(II) complexes.^{170,174,175,180,253-257}

Scheme 5.3



Our initial investigation involved repeating Dehnicke's melt procedure with silylphosphinimide precursors which contained bulkier aryl-, cyclohexyl-, or *t*-butyl phosphorous substituents. However, in our hands this method was unsuccessful, as

heating cobalt(II) bromide to 180°C in the presence of excess silylphosphinimide **252** or **353** led only to intractable product mixtures. The absence of heterocubane products from these reactions, however, implies that bulky phosphinimide ligands do have an effect on the outcome of the reaction, an idea that we decided should be pursued further. A new preparative method was required in order to make any significant advances, however. This method is described in the following sections.

5.3 Preparation of bis(phosphinimine)- and mono(phosphinimide)cobalt(II) halide complexes

5.3.1 Cobalt(II) phosphinimine complexes from cobalt(II) halides and cobalt(II) acetate

We proposed that bis(phosphinimide)cobalt(II) complexes could be prepared by base-mediated dehydrohalogenation of bis(phosphinimine)cobalt(II) halide complexes. Since only one other bis(phosphinimine)cobalt(II) complex had been reported,²⁵⁶ we wanted to develop a general strategy for preparing a broad range of similar complexes (Equation **5.4**). Our overall strategy involved first forming the bis(phosphinimine)cobalt(II) coordination complex, then adding an appropriate base which would deprotonate the phosphinimine ligand. Our first attempts involved stirring two equivalents of a neutral phosphinimine compound with one equivalent of a cobalt(II) salt. We initially used tri(*t*-butyl)phosphinimine (**257**) because it is readily prepared from N-(trimethylsilyl)tri(*t*-butyl)phosphinimide (**353**) upon treatment with wet methanol.¹⁹⁸ By stirring two equivalents of tri(*t*-butyl)phosphinimine (**259**) and one equivalent of cobalt(II) bromide in THF, we obtained our first coordination complex, bis[tri(*t*-butyl)phosphinimine]cobalt(II) bromide (**356**) in high yield. Analytically pure dark blue crystals of **356** were grown from layering a saturated benzene solution containing **356** with hexanes. The details regarding its characterization will be discussed later.

Equation 5.4

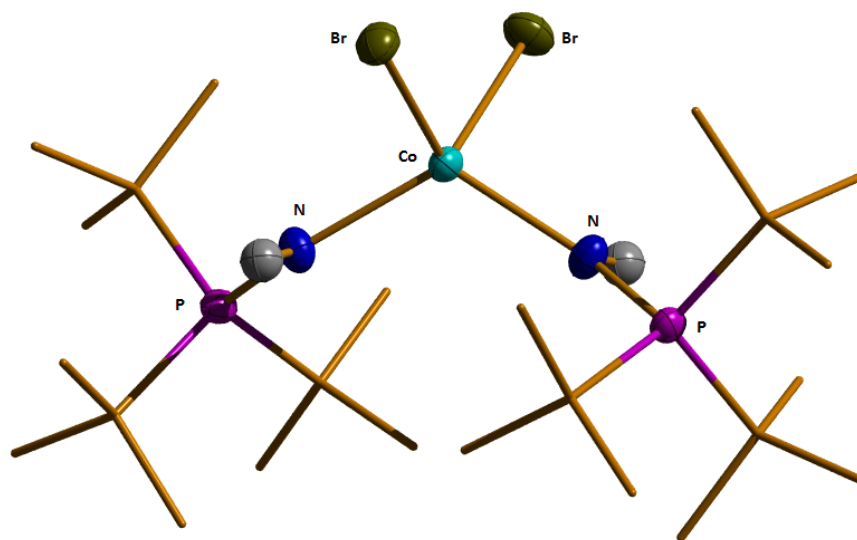
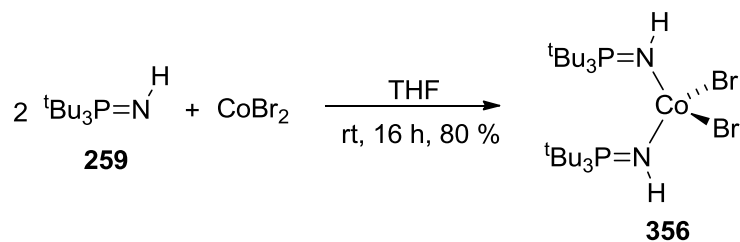


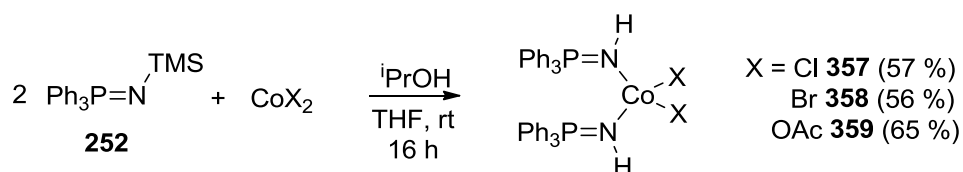
Figure 5.2: Perspective view of **356** with key atoms labelled. Non-hydrogen atoms are represented by either Gaussian ellipsoids at the 20% probability level, or as “wire and stick” representations. The displayed thermal ellipsoids of phosphinimine hydrogen atoms are predicted at the 20% level. $R_1 = 0.0281$, $R(w) = 0.0657$.

We planned to use this procedure to also prepare bis(triphenylphosphinimine) cobalt(II) complexes, but unexpected problems were encountered. Initially, when a THF solution of cobalt(II) bromide was treated with two equivalents of “triphenylphosphinimine” (prepared from the silylphosphinimide **252** in hot methanol), an impure product mixture was obtained. We analyzed the “triphenylphosphinimine” using ^1H NMR spectroscopy, and found that only triphenylphosphine oxide was present. This suggested that triphenylphosphinimine was completely hydrolyzed in hot methanol

and that alternate conditions were needed to reduce the amount of water present in the reaction mixture. Unfortunately, we found that using “dried” methanol or *i*-propanol, in combination with water sequestering agents such as calcium hydride and activated 4 Å molecular sieves, did not suppress the hydrolysis of triphenylphosphinimine.

A subtle yet successful modification to the reaction conditions was developed. This procedure requires forming the bis(silylphosphinimine)cobalt(II) complex first, then removing the silyl group by adding hot *i*-propanol. We performed this reaction by combining two equivalents of silylphosphinimide **252** and cobalt(II) chloride in THF, 1 hour prior to the addition of excess “dry” *i*-propanol (Equation 5.5). This reaction mixture was then heated to reflux overnight and afforded bis(triphenylphosphinimine)cobalt(II) chloride (**357**) as the major product. This procedure was also repeated using two equivalents of silylphosphinimide **252** in combination with either one equivalent of cobalt(II) bromide, which afforded **358**, or one equivalent of cobalt(II) acetate, which afforded **359**; both were isolated as major products. These paramagnetic bis(phosphinimine)cobalt(II) complexes **356-359** were each characterized by X-ray crystallography, IR spectroscopy and elemental analysis (Figure 5.6).

Equation 5.5



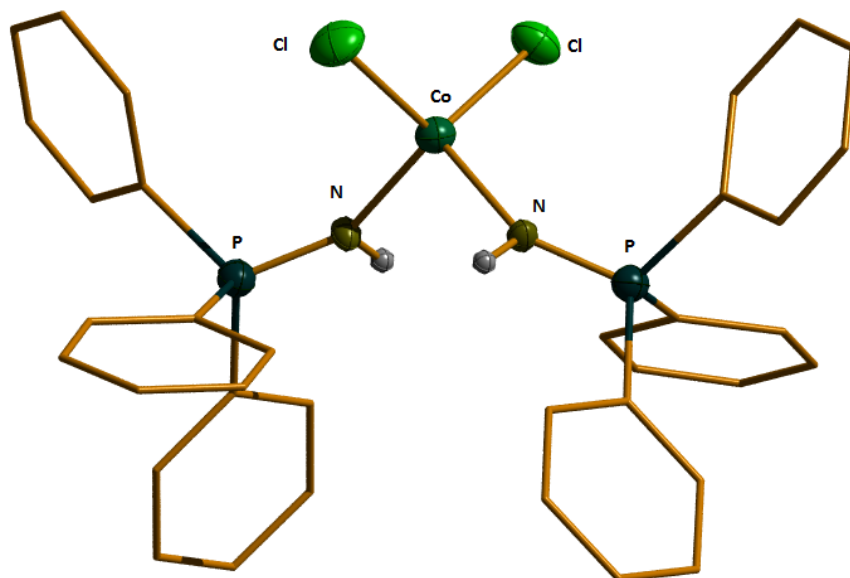


Figure 5.3: Perspective view of **357** with key atoms labelled. Non-hydrogen atoms are represented by either Gaussian ellipsoids at the 20% probability level, or as “wire and stick” representations. The displayed thermal ellipsoids of phosphinimine hydrogen atoms are predicted at the 20% level. $R_1 = 0.0492$, $R(w) = 0.1515$.

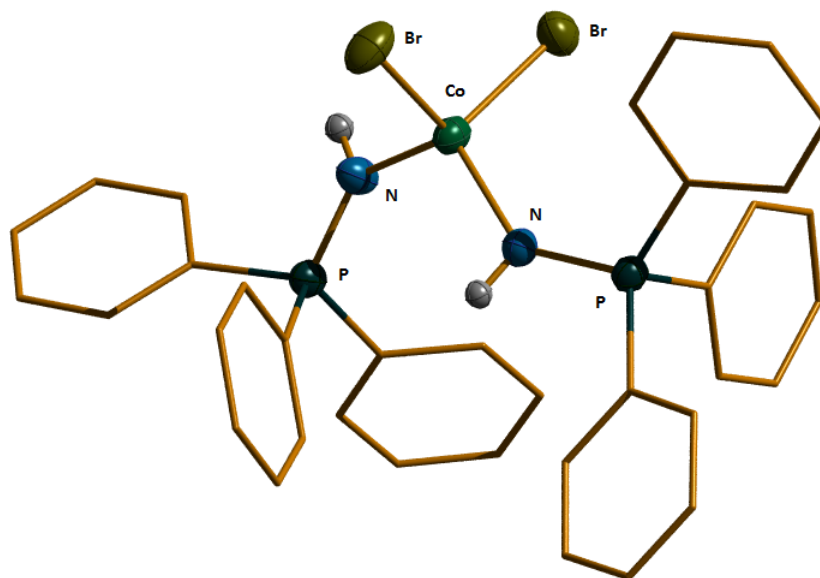


Figure 5.4: Perspective view of **358** with key atoms labelled. Non-hydrogen atoms are represented by either Gaussian ellipsoids at the 20% probability level, or as “wire and stick” representations. The displayed thermal ellipsoids of phosphinimine hydrogen atoms are predicted at the 20% level. $R_1 = 0.0251$, $R(w) = 0.0577$.

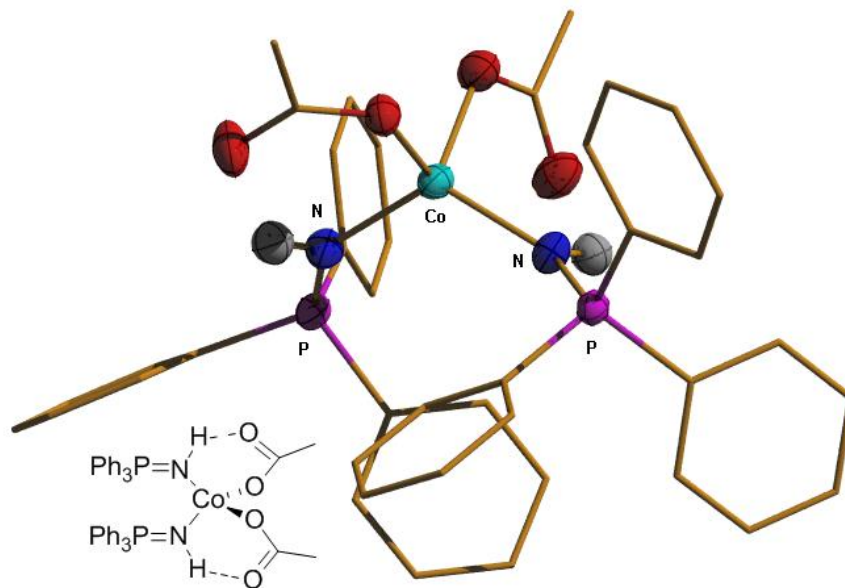


Figure 5.5: Perspective view of **359** with key atoms labelled. Non-hydrogen atoms are represented by either Gaussian ellipsoids at the 20% probability level, or as “wire and stick” representations. The displayed thermal ellipsoids of phosphinimine hydrogen atoms are predicted at the 20% level. $R_1 = 0.0328$, $R(w) = 0.0912$.

Entry	Interatomic bond distances (pm)			angles (°)
	P-N	Co-N	NH...O	Co-N-P
357	150.45(15)	198.62(14)		140.51(9)
	150.50(15)	197.57(14)		142.36(9)
358	159.44(19)	198.72(18)		131.75(11)
	159.95(18)	200.26(18)		136.22(11)
359	159.20(12)	198.65(12)	217	131.13(8)
	158.62(12)	199.94(12)	244	139.79(7)
356	161.1(2)	198.6(2)		148.14(16)
	161.3(2)	200.0(2)		142.31(14)

Entry	R	P=N (pm)
360	Ph	152.4(3)
259	^t Bu	165.2(11)

Figure 5.6: Selected interatomic distances and angles of cobalt(II) phosphinimine complexes **356-359** and “free” phosphinimine ligands, with standard deviations in parentheses.

The difference between these two hydrolysis procedures in the formation of triphenylphosphine oxide or triphenylphosphinimine is interesting. From our results, we propose that a strong dative bond is formed between the silylphosphinimide and the Lewis-acidic cobalt(II) salt.¹³⁵ Upon protolytic desilylation, this binding interaction presumably inhibits the nitrogen lone pair from further interactions with other acidic species such as adventitious water, which can catalyze the hydrolysis of the N=P bond.

Compounds **356-359** are the first bis(triphenyl)- and bis(tri(*t*-butyl)phosphinimine) cobalt(II) complexes to be characterized crystallographically. Some interesting observations can be made. Our first observation was that relatively short Co-N bond distances exist between the cobalt(II) atoms and the phosphinimide nitrogens. Similar Co-N distances were also observed by Dehnicke from the crystallographic analysis of bis(trimethylphosphinimine)cobalt(II) chloride (200.1(9) pm and 198.6(8) pm).²⁰⁹ The Co-N distances are shorter in the coordination complexes **356-359** than are the Co-N lengths of the anionic phosphinimide ligands in Dehnicke's heterocubane clusters (see Figure 5.6).^{169,170,174,175,180,253} This is peculiar, as we expected anionic phosphinimide ligands to have shorter Co-N bonds because of stronger interactions with the cobalt(II) metals. We also compared the N-P bond distances of "free" phosphinimine compounds to the coordinated phosphinimines in **356-359** (see Figure 5.6). In some cases, the N-P distances we observed in compounds **356-359** were drastically increased through coordination; this suggests that the electron density from the polar N-P double bond is contributed to some extent to empty d orbitals on the the cobalt(II) center.^{258,259} We also observed in two cases that the N-P bond was shorter than in the "free" phosphinimines, which would suggest that electron density is being contributed back into the polarized N-P double bond. These conflicting observations prevent us making any conclusions regarding the strength of the dative Co-N bonds in these complexes.

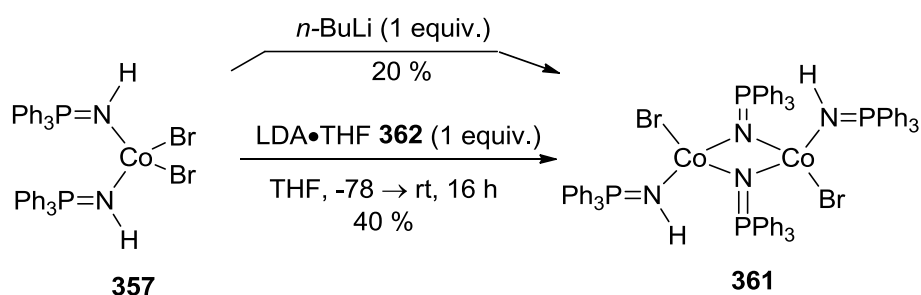
The observed Co-N-P bond angles range between 130° and 150°. Based on the congestion around the cobalt(II) center, we propose that the differences in the Co-N-P bond angles are likely due to induced distortions of the phosphinimide ligand. This distortion would relieve steric conflicts between the adjacent phosphorous substituents in the solid state. We also observed intramolecular hydrogen-bonding interactions

occurring in the solid state structure of **359** (see Figure 5.5). In this case, the hydrogen-bonding interactions exist between the imine hydrogen of the phosphinimine and the oxygen of the acetate ligands. This observation was supported by IR spectroscopy, where we observed a broad N-H stretching frequency between 3400-2800 cm^{-1} . Hydrogen-bonding was not detected in the solid-state structures of **356**, **357** and **358**; this lack was also reflected in the IR spectra of these complexes, where sharp N-H stretching frequencies were observed.

5.3.2 Deprotonation of bis(phosphinimine)cobalt(II) halide and acetate complexes

Following our determination of an adequate method for preparing various cobalt(II) phosphinimine complexes, we pursued deprotonation conditions which would convert the coordinated phosphinimines into anionic phosphinimide ligands (Scheme 5.4). We found that optimal results were obtained when lithium di-*i*-propylamide (LDA) was used as the base. By adding one equivalent of LDA to one equivalent of bis(triphenylphosphinimine)cobalt(II) bromide **357**, we obtained the mono-deprotonated product **361**, albeit in low isolated yield. This, however, was the most effective base tested, as adding other strong bases such as *n*-butyl lithium resulted in lower isolated yields of **361** (20 %), while addition of tertiary amine bases only returned the starting material. More importantly, we were able to use solid lithium di-*i*-propylamide (**362**) (LDA•THF); this proved advantageous over other available organic bases as it is stable under an inert atmosphere and exact amounts can be consistently measured on a balance.²⁶⁰ As a result, LDA•THF (**362**) was used throughout this study.

Scheme 5.4



The solid state structure of the mono-deprotonated product **361** was determined by X-ray crystallography; this product was interesting because of its close structural relationship to heterocubane clusters.^{169,170,174,175,180,253} One of the most important observations was that the mono-deprotonated cobalt(II) phosphinimide complex **361** exists as a simple dimer with bridging μ^2 -phosphinimide ligands. This was significant in itself, because cobalt(II) phosphinimide complexes with μ^2 -phosphinimide ligands had not been observed prior to this work (see Figure 5.1).^{169,170,174,175,180,253} Even more importantly, the mono-deprotonated complex **361** constitutes exactly one-half of a heterocubane cluster in the absence of triphenylphosphinimine ligands; this suggests that bulky substituents on μ^2 -phosphinimide ligands inhibit aggregation of smaller clusters. In the absence of the bridging μ^3 -phosphinimide ligands found in heterocubane clusters, the vacant coordination site on the cobalt(II) centers are occupied by a triphenylphosphinimine ligands. This observation demonstrates that mono(phosphinimide)cobalt(II) bromide species do not favor low-coordination around the cobalt(II) centers.

We also explored the structural differences between the μ^2 -phosphinimide ligands in our complex, and the μ^3 -phosphinimide ligands in the heterocubane clusters.^{169,170,174,175,180,253} We found that the interatomic Co-N and P-N distances associated with μ^2 -phosphinimide ligands in **361** are generally shorter than in the μ^3 -phosphinimide ligands of Dehnicke's heterocubane clusters (see Figure 5.1). We also observed that the geometry about the nitrogen atom in the μ^2 -phosphinimide ligands was closer to trigonal planar (see Figure 5.8), while the geometry about the nitrogen in the μ^3 -phosphinimide ligand is closer to tetrahedral geometry. These observations imply that only two of the three potential bonding orbitals from the nitrogen atom (one σ and one π) are participating in the bonding between the two cobalt(II) centers. The third nitrogen-based π bonding orbital is therefore participating in the P=N bond of the phosphinimide ligand.

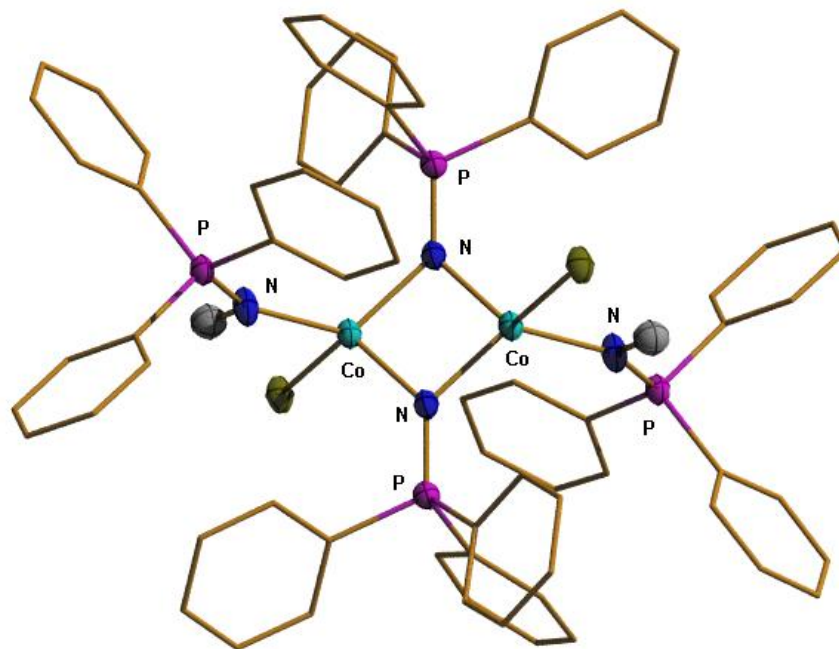


Figure 5.7: Perspective view of **361** with key atoms labelled. Non-hydrogen atoms are represented by either Gaussian ellipsoids at the 20% probability level, or as “wire and stick” representations. The displayed thermal ellipsoids of phosphinimine hydrogen atoms are predicted at the 20% level. $R_1 = 0.0287$, $R(w) = 0.0795$.

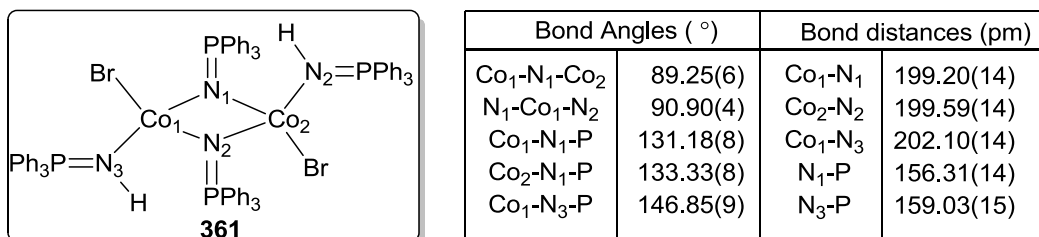
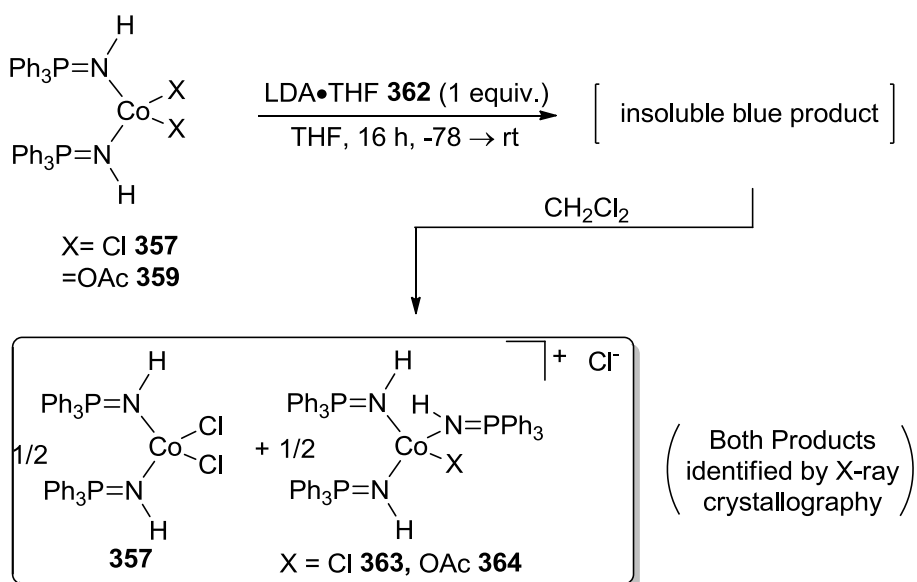


Figure 5.8: Selected interatomic distances and angles of **361**.

With our new mono-deprotonated product **361** in hand, we attempted to obtain the mono-deprotonation products from bis(triphenylphosphinimine)cobalt(II) chloride (**357**) and bis(triphenylphosphinimine)cobalt(II) acetate (**359**); these reactions, however, furnished surprising results (Scheme 5.5). We treated THF solutions of **357** and **359** with one equivalent of LDA•THF (**362**), which afforded light blue solids. Unlike

compound **361**, these solids were insoluble in all organic solvents we tested except dichloromethane. By layering the dichloromethane solutions with hexanes, we obtained product mixtures consisting of light and dark blue crystals. Two products were identified from each reaction. In both cases, bis(triphenylphosphinimine)cobalt(II) chloride (**357**) was isolated; the second products that were isolated in each case was chlorotris(triphenylphosphinimine)cobalt(II) chloride (**363**) and acetatotris(triphenylphosphinimine)cobalt(II) chloride (**364**) respectively.

Scheme 5.5



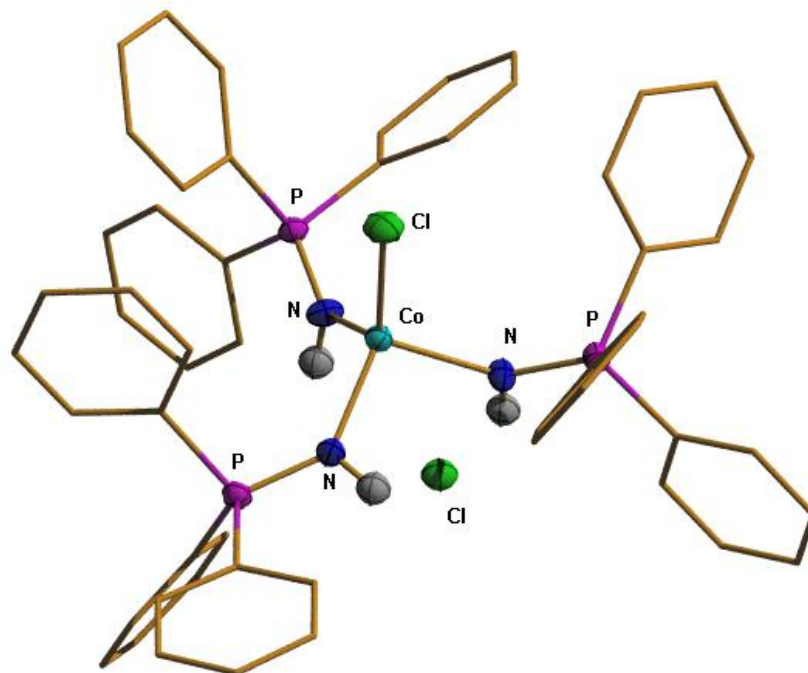
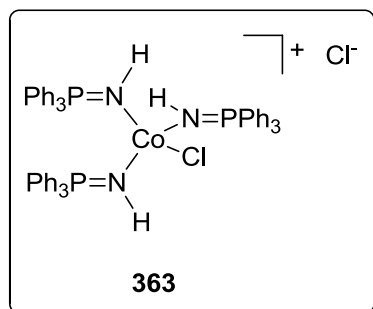


Figure 5.9: Perspective view of **363** with key atoms labelled. Non-hydrogen atoms are represented by either Gaussian ellipsoids at the 20% probability level, or as “wire and stick” representations. The displayed thermal ellipsoids of phosphinimine hydrogen atoms are predicted at the 20% level. $R_1 = 0.0292$, $R(w) = 0.0808$.



Interatomic bond distances		angles
P-N (pm)	Co-N (pm)	Co-N-P (°)
158.77(12)	201.47(13)	135.25(7)

Figure 5.10: Selected interatomic distances and angles of **363**.

The formation of the tris(phosphinimine)cobalt(II) chloride salts **363** and **364** was surprising, as we expected to isolate cobalt(II) phosphinimide complexes from the reaction conditions, which are similar to **361**. The structures of both cationic complexes **363** and **364**, however, led us to believe that both cobalt(II) precursors **357** and **359**

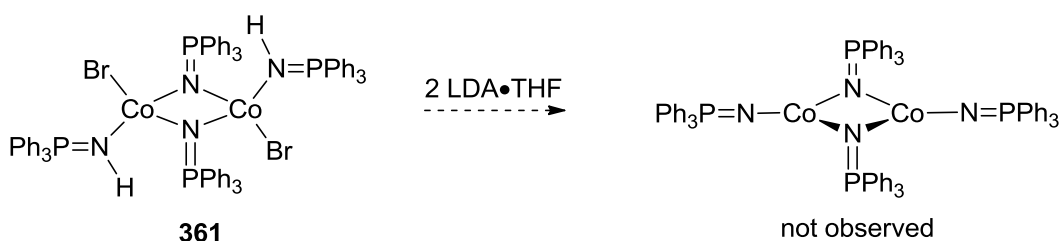
were initially deprotonated by LDA•THF, but “protonated” during the work-up with dichloromethane. The primary evidence supporting the initial formation of cobalt(II) phosphinimide complexes was the multiple chloride-containing products obtained from deprotonating the initial cobalt(II) acetate complex **359**. Because no other chloride sources were present in the starting materials, we assume that an intermediary cobalt(II) phosphinimide complex extracted an equivalent of “HCl” from dichloromethane. Secondly, outer-sphere chloride ions are incorporated into both cationic products. This suggests that the protonated phosphinimide ligands do not dissociate from our assumed cobalt(II) phosphinimide complex, thus preventing the chloride ions from entering the cobalt(II) atom’s coordination sphere. Since an inner-sphere acetate ion is also observed in **364**, we proposed that the unidentified cobalt(II) phosphinimide complex may have a solid state structure similar to the mono(phosphinimide)cobalt(II) bromide complex **361**. These results also revealed for the first time that cobalt(II) phosphinimide complexes can act as strongly basic species; this reactivity was further studied and will be discussed later.

5.3.3 Double deprotonation of bis(phosphinimine)cobalt(II) bromide complexes

With evidence that LDA•THF (**362**) can deprotonate one of the phosphinimine ligands, we wanted to determine if a second equivalent of LDA•THF would deprotonate the second phosphinimine ligand. This would afford the desired bis(phosphinimide) cobalt(II) complexes (Equation 5.6). We first treated the mono(triphenylphosphinimide) cobalt(II) bromide dimer **361** with one equivalent of LDA•THF (**362**) at low temperature. From this, we observed an immediate change in solution color from dark blue to dark green. We also obtained a similar dark green solution by treating a THF solution of bis(triphenylphosphinimine)cobalt(II) bromide (**358**) with two equivalents of LDA•THF (**362**). Unfortunately we can only speculate as to the identity of the green product, because exhaustive efforts to identify the products from either reaction were unsuccessful. Based on these results, we obtained evidence that LDA•THF (**362**) will deprotonate both triphenylphosphinimine ligands in complexes **358** and **361**, but

crystallographic data needs to be gathered on both complexes before any concrete conclusions can be made.

Equation 5.6



We also attempted to doubly-deprotonate bis(tri(*t*-butyl)phosphinimine) cobalt(II) bromide (**356**), with similar results. By slowly adding two equivalents of LDA•THF (**362**) to a THF solution containing **356**, similar color changes were noted from dark blue (1 equivalent of base) to dark green (2 equivalents of base). These results again appeared promising, but we were unable to identify the products from the reaction mixture.

5.3.4 Conclusions

This study was at least partly successful as we confirmed that our dehydrohalogenation strategy is an effective method for preparing cobalt(II) phosphinimide complexes. We also demonstrated that bulky phosphorous substituents on phosphinimide ligands affect the assembly of [(R₃P=N)-CoX] units, which form dimeric cobalt(II) phosphinimide complexes with μ²-phosphinimide ligands. Unfortunately, we were unable to identify the majority of the deprotonated products due to apparent problems with crystallization. In the process of preparing some of these substrates, we demonstrated that cobalt(II) phosphinimide complexes exhibit reactivity towards acidic compounds; this will be discussed later. We decided to

abandon cobalt(II) precursors with halide and acetate ligands at this point and use our newly developed dehydrohalogenation strategy to prepare cobalt(II) phosphinimide complexes from alternative cobalt(II) salts.

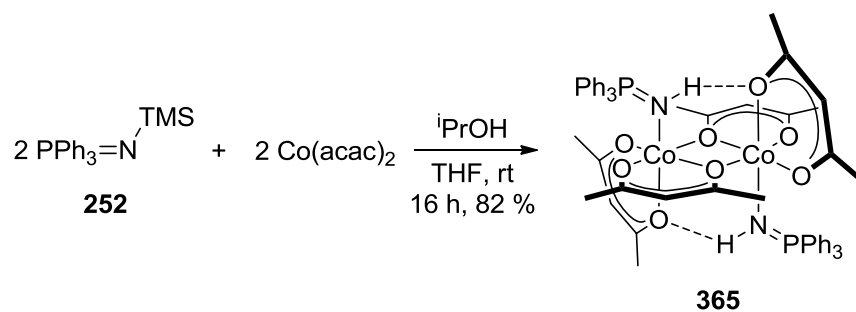
5.4 Preparation of mono(phosphinimine)cobalt(II) acetylacetonate complexes

5.4.1 Preparation of mono(phosphinimine)cobalt(II) acetylacetonate precursors

We next targeted the preparation of cobalt(II) phosphinimide complexes such as **361** (see Equation 5.4) but devoid of neutral phosphinimine ligands. We reasoned that the extraneous phosphinimine ligands might have interfered with the selective single-deprotonation of bis(phosphinimine)cobalt(II) complexes, and this was the reason why the deprotonated complexes were obtained in low yields. To address this problem, we chose to investigate the use of cobalt(II) salts with anionic ligands that have chelating heteroatoms. In theory, the chelating heteroatom should occupy the fourth coordination site on the cobalt(II) center and inhibit coordination of phosphinimine ligands. We decided to investigate cobalt(II) acetylacetonate (“acac”) as a precursor to mono(phosphinimide) cobalt(II) complexes, because acac ligands are well known to form chelating interactions with metals.²⁶¹

We found that by using the same protolytic desilylation conditions as before, we were able to successfully convert silylphosphinimide **252** and Co(acac)₂ into the corresponding phosphinimine-coordination complex **365** (Equation 5.7). This was accomplished by first mixing Co(acac)₂ and two equivalents of silylphosphinimide **252** in THF for one hour; then *i*-propanol was added and the mixture was heated to reflux overnight. We found that these reaction conditions afforded the desired cobalt(II) phosphinimine complex **365** in excellent isolated yield. We also found that the resulting complex contained only one triphenylphosphinimine ligand, even in the presence of excess silylphosphinimide **252**.

Equation 5.7



The cobalt(II) phosphinimine complex **365** was characterized by X-ray crystallography, by which we determined that the acac ligands have a profound effect on the coordination environment about the cobalt(II) center. Complex **365** unsurprisingly exists as a dimer in the solid state, but surprisingly with acac ligands bridging between the two cobalt(II) centers (Figure 5.11). Bridging hydrogen-bonding interactions exist between the imine hydrogen of the neutral triphenylphosphinimines and the oxygen atom of a non-bridging acac ligand on the opposing cobalt(II) center. The existence of these hydrogen-bonding interactions is supported by IR spectroscopy, as we observed a broad N-H stretching frequency between 3300 and 3100 cm^{-1} . The cobalt(II) centers are of pseudo-octahedral geometry with acac ligands occupying 5 of the 6 sites. This explains why only one triphenylphosphinimine ligand is coordinated to the cobalt(II) center. This result indicated to us that we could control the number of coordinated phosphinimine ligands to cobalt(II) salts by varying the anionic ligands.

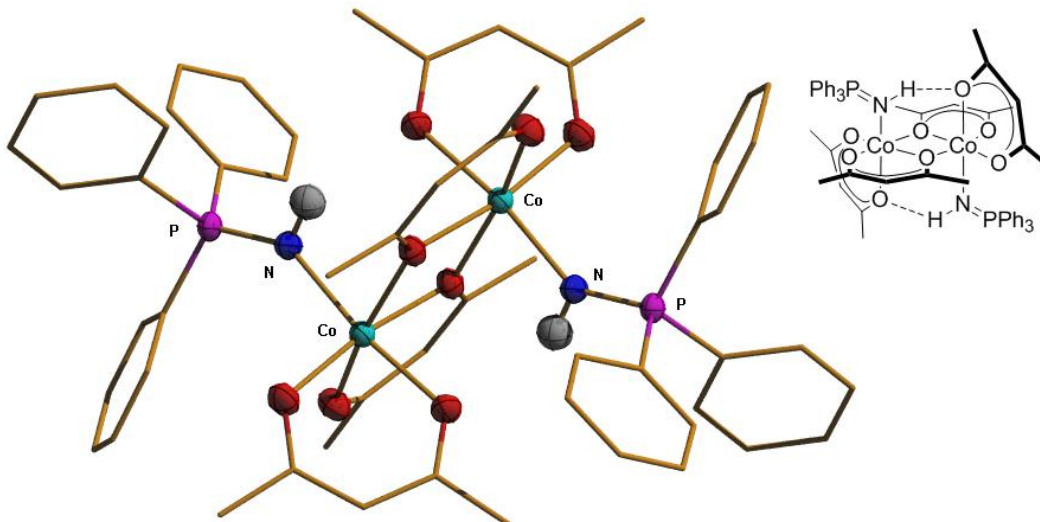
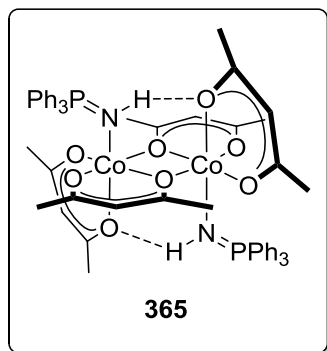


Figure 5.11: Perspective view of **365** with key atoms labelled. Non-hydrogen atoms are represented by either Gaussian ellipsoids at the 20% probability level, or as “wire and stick” representations. The displayed thermal ellipsoids of phosphinimine hydrogen atoms are predicted at the 20% level. $R_1 = 0.0313$, $R(w) = 0.0892$.



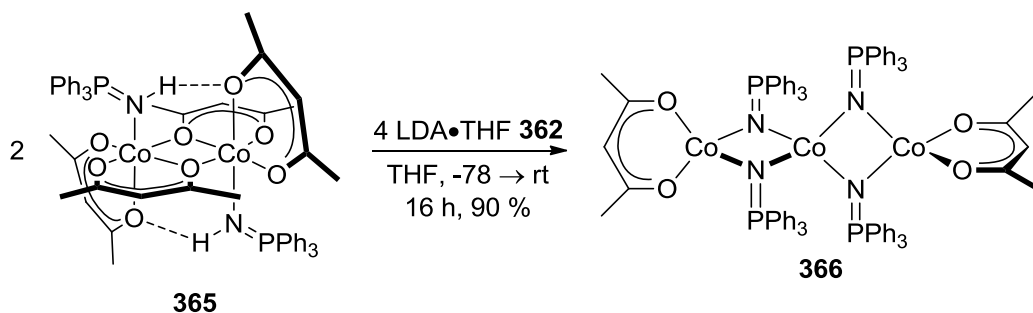
Interatomic bond distances			angle
P-N (pm)	Co-N (pm)	H-bond (pm)	Co-N-F
157.70(13)	206.24(13)	231	143.36

Figure 5.12: Selected Interatomic distances and angles of **365**.

5.4.2 Deprotonation of (triphenylphosphinimine)cobalt(II) acetylacetonate

We proceeded with the deprotonation of the (triphenylphosphinimine)cobalt(II) acetylacetonate dimer **365**, from which we hoped to obtain a cobalt(II) phosphinimide complex in better yield (Equation 5.8). We found that the reaction proceeds smoothly as adding two equivalents of LDA•THF (**362**) to **365**, furnished the surprising dark blue linear tri-cobalt phosphinimide complex **366** in high yield. The resulting cobalt(II) phosphinimide complex is exceptionally soluble in aromatic hydrocarbon solvents, unlike our previous products. This allowed us to extract analytically pure material from the crude reaction mixture and subsequently remove any unwanted metal salts by filtering toluene extracts through a plug of celite. This procedure was reproduced on larger scales (~ 5 g) where we observed no diminution in yield of **366**. Crystals suitable for X-ray diffraction were grown from saturated solutions of **366** in toluene that were layered with hexanes.

Equation 5.8



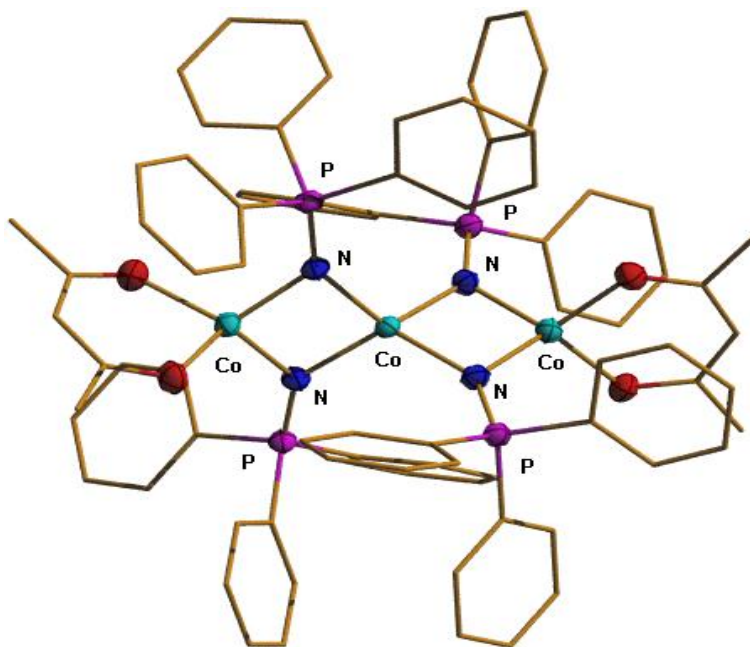
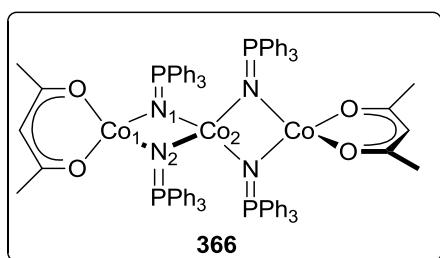


Figure 5.13: Perspective view of **366** with key atoms labelled. Non-hydrogen atoms are represented by either Gaussian ellipsoids at the 20% probability level, or as “wire and stick” representations. $R_1 = 0.0392$, $R(w) = 0.1167$.



Bond angles (°)		Bond distances (pm)	
N ₁ -Co ₁ -N ₂	91.87(7)	Co ₁ -N ₁	197.62(16)
Co ₁ -N ₁ -Co ₂	89.74(6)	Co ₁ -N ₂	195.85(16)
N ₁ -Co ₂ -N ₂	89.31(6)	Co ₂ -N ₁	201.69(16)
Co ₁ -N ₁ -P	126.09(10)	Co ₂ -N ₂	200.55(16)
Co ₂ -N ₁ -P	144.11(10)	N ₁ -P	155.32(16)
Co ₁ -N ₂ -P	133.60(10)	N ₂ -P	155.58(16)

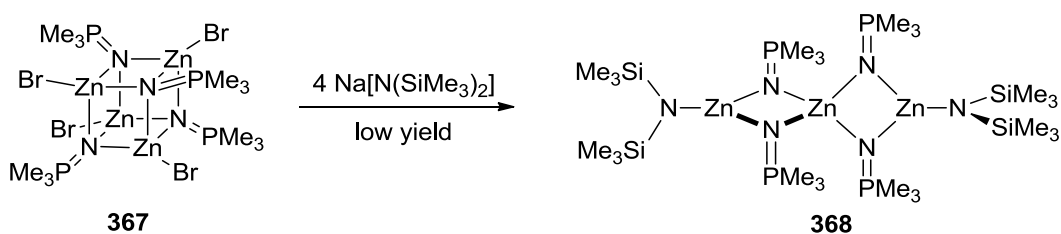
Figure 5.14: Selected interatomic distances and angles of **366**.

The structure of **366** was extremely interesting to us because of its unique linear tri-metallic assembly. We found that this cluster has structural components similar to Dehnicke’s heterocubane complexes, and also to the mono-deprotonated phosphinimide complex **361** (see Figures 5.1 and 5.14).^{169,170,174,175,180,253} The major similarity between all three structures is the recurring [Co₂N₂] unit. We note that the [Co₂N₂] unit is found in its simplest form in the mono-deprotonated cobalt(II)

phosphinimide complex **361**. A larger set of interlocking $[\text{Co}_2\text{N}_2]$ units can be seen in each face of Dehnicke's heterocubane clusters (see Figure 5.1). In our present example, we observe that two $[\text{Co}_2\text{N}_2]$ units make up the linear $[\text{Co}_3\text{N}_4]$ framework of **366**, but are connected through the central cobalt(II) atom. In all three types of molecules, the $[\text{Co}_2\text{N}_2]$ units are square planar, with Co-N-Co and N-Co-N bond angles of around 90° . The primary differences between the $[\text{Co}_2\text{N}_2]$ units of these three molecules, is that the interatomic Co-N and P-N distances corresponding to the μ^2 -phosphinimide ligands are shorter than μ^3 -phosphinimide ligands. The best feature of **366**, however, is that it contains both cobalt(II) bis(phosphinimide) and acetoacetato cobalt(II) phosphinimide complexes, which we were initially targeting.

Although it is a common structural motif in cobalt(II) coordination complexes, transition metal phosphinimide complexes with the linear $[\text{M}_3\text{N}_4]$ framework are rarely observed.²⁶²⁻²⁶⁷ To our knowledge, Dehnicke isolated the only other tri-metallic phosphinimide complex **368** from a reaction mixture containing the zinc(II) phosphinimide heterocubane cluster **367** and four equivalents of sodium hexamethyldisilazide (NaHMDS); this product was, however, only isolated in trace quantities.¹⁸³ Even more interesting to us is that **368** also contains a central bis(triphenylphosphinimide)cobalt(II) unit which had never before been observed.

Equation 5.9



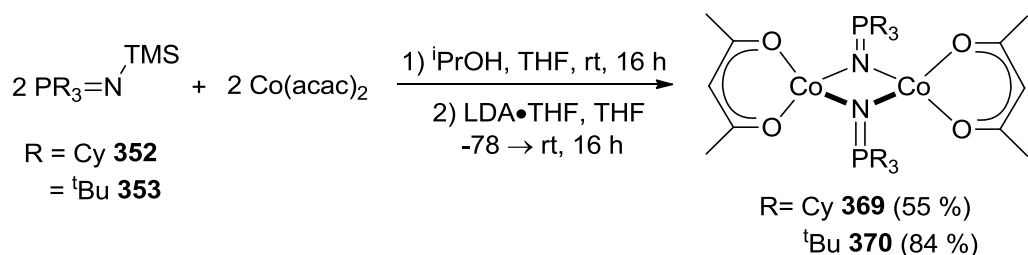
We were able to take away two valuable conclusions from this experiment. First, our previous double-deprotonation experiment was undoubtedly successful and a bis(phosphinimide)cobalt(II) complex was likely formed. Second, obtaining monomeric

bis(phosphinimide)cobalt(II) complexes is highly unlikely because of the tendency of phosphinimide ligands to bridge at least two cobalt(II) atoms.

5.4.3 Preparation of mono(tricyclohexylphosphinimide)- and mono(tri(*t*-butyl)phosphinimide)cobalt(II) complexes

Since we were successful in preparing the linear tri-cobalt phosphinimide complex **366**, we wanted to expand the number of acetoacetatocobalt(II) phosphinimide complexes that could be obtained. We prepared two other (phosphinimide)cobalt(II) acetylacetonate complexes, **369** and **370**, using the same protodesilylation/deprotonation sequence as before. However, we found that each of the resulting cobalt(II) phosphinimide complexes was a simple dimer instead of adopting the linear tri-cobalt framework we observed with **366**. The dimeric structures of these complexes were established by crystallographic analysis, but the high disorder in the single crystals of **369** and **370** prevented us from determining accurate interatomic parameters. We were able to confirm the atomic composition of both **369** and **370** by elemental analysis. These results are important to us, as at the time we did not know the factors governing the preferential formation of dimers vs. linear tri-metallic frameworks or heterocubane structures. Through briefly studying the reactivity of the acetoacetatocobalt(II) phosphinimide complexes, we were able to gain sufficient insight as to these governing factors, as will be discussed in a later section. Since we were able to obtain large quantities of **370** and the linear tri-cobalt(II) phosphinimide complex **366**, we began to investigate the reactivity of these molecules.

Equation 5.10



5.5 Reactivity of mono(phosphinimide)cobalt(II) acetylacetonate complexes

Our explorations next led us to investigate the reactivities of acetoacetatocobalt(II) phosphinimide complexes. This discussion specifically focuses on experiments in which we were able to identify the products through crystallographic analysis. Due to the complex and paramagnetic nature of these products, X-ray crystallography was crucial to this effort.

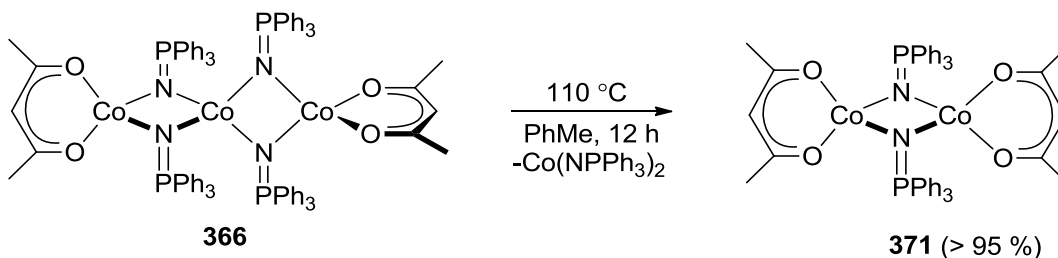
5.5.1 Reduction using various low-valent metals

We first investigated the reduction of cobalt(II) phosphinimide complexes **361**, **366** and **370**, by which we planned to prepare our initially targeted cobalt(I) phosphinimide complexes. Based on existing methodology with cobalt(II) cyclopentadienyl compounds, we envisioned that these cobalt(II) compounds could be reduced by solid metal reducing agents, possibly in the presence of stabilizing ligands such as olefins or phosphines.^{251,252} Under similar reaction conditions used to prepare cobalt(I) cyclopentadienyl complexes, THF solutions of **361**, **366**, or **370**, were stirred over a variety of strong reducing agents, including Rieke magnesium,²⁶⁸ lithium naphthalenide,²⁶⁹ and 1% mercury amalgams (Na or K). These reactions unfortunately all afforded black intractable product mixtures. The reactions were repeated in the presence of either excess trimethylphosphine, carbon monoxide, or ethylene; all resulted in similar black intractable product mixtures. Weaker metal reducing agents such as manganese, zinc, and aluminum metals were also investigated, but the reactions returned only the cobalt starting materials. These results were unfortunate, but they indicated that acetoacetatocobalt(II) phosphinimide complexes are not appropriate precursors for preparing cobalt(I) phosphinimide complexes. In order to isolate the reduced cobalt(I) species, alternative precursors or alternative reducing agents had to be explored.

5.5.2 Thermal decomposition of the linear tri-cobalt(II) phosphinimide complex **366**

One of our more interesting discoveries was the thermal decomposition of the linear tri-cobalt(II) phosphinimide complex **366** (Equation 5.11). We discovered this reactivity serendipitously, when unsuccessfully trying to activate the C-S bonds of dibenzothiophene. In our initial experiment, heating a toluene solution containing **366** and dibenzothiophene to 110°C returned a dark blue product mixture. The product, to our surprise, was the mono(triphenylphosphinimide)cobalt(II) acetylacetonate dimer **371**, which was identified by crystallographic analysis (Figure 5.14). We repeated the reaction in the absence of dibenzothiophene and obtained the same product in high yield.

Equation 5.11



This complex is significant to us for two reasons. First, we were able to obtain crystallographic data on a simple dimeric mono(phosphinimide)cobalt(II) acetylacetonate complex. The interatomic Co-N-P angles and Co-N lengths in this complex fall within the expected range of values for [Co₂N₂] units bound by μ²-phosphinimide ligands (Figure 5.15). This complex also closely resembles our initial mono-deprotonated complex **361**; the only observable difference is that the acetate ligand is occupying the fourth coordination site on the cobalt(II) atom instead of a triphenylphosphinimine ligand. By comparing the compositions of these two complexes, we have demonstrated that chelating ligands indeed prevented

phosphinimine ligands from forming dative bonds to the fourth coordination site on cobalt(II) centers.

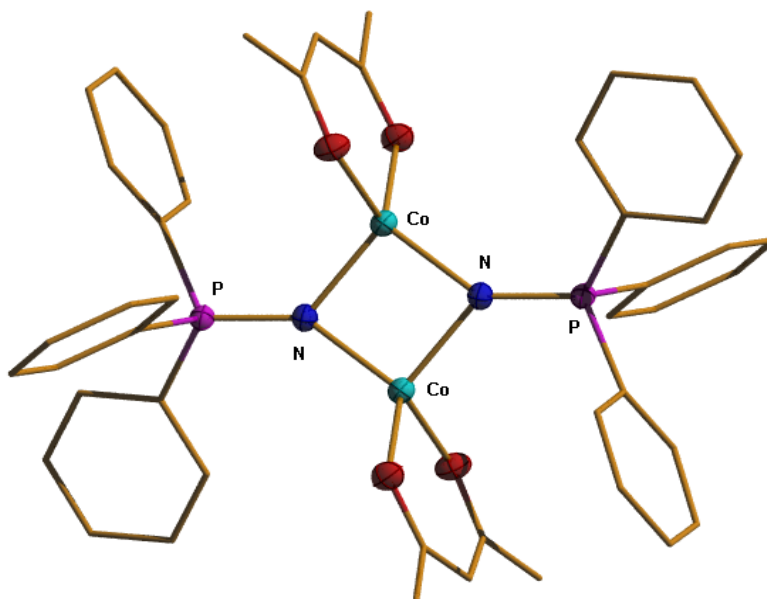
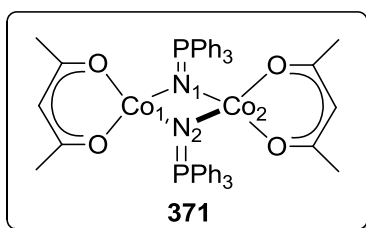


Figure 5.15: Perspective view of **371** with key atoms labelled. Non-hydrogen atoms are represented by either Gaussian ellipsoids at the 20% probability level, or as “wire and stick” representations. $R_1 = 0.0265$, $R(w) = 0.0736$.



Bond angles (°)		Bond distances (pm)	
N ₁ -Co ₁ -N ₂	92.33(5)	Co ₁ -N ₁	197.70(13)
Co ₁ -N ₁ -Co ₂	87.67(5)	Co ₁ -N ₂	195.48(12)
Co ₁ -N ₁ -P	128.39(7)	N ₁ -P	155.57(13)
Co ₂ -N ₁ -P	140.25(8)		

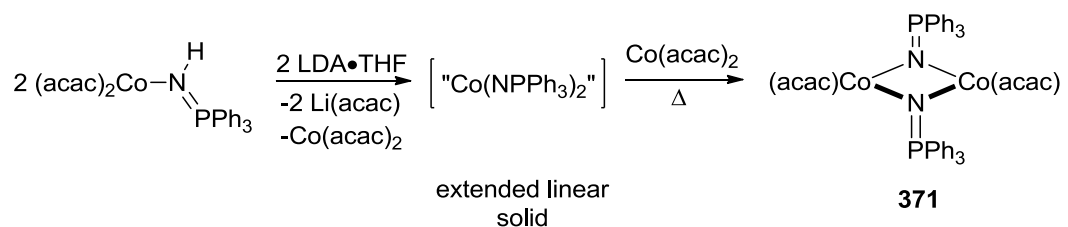
Figure 5.16: Selected interatomic distances and angles of **371**.

This result is also significant because structural reorganization of cobalt(II) phosphinimide complexes is unprecedented. This demonstrates that larger linear cobalt(II) phosphinimide clusters are thermodynamically less stable than dimeric cobalt(II) phosphinimide complexes. This reactivity presumably arises to minimize unfavorable steric interactions between adjacent phosphorous substituents. This is

observed in the tri-cobalt(II) phosphinimide complex **366** and is driven by the highly congested cobalt(II) center surrounded by four triphenylphosphinimide ligands. This result also explains why the tricyclohexyl- and tri(*t*-butyl)phosphinimide complexes **369** and **370** only exist as dimers, as the steric interactions between the phosphorous substituents are likely too great to sustain the linear tri-cobalt framework.

The linear tri-cobalt(II) phosphinimide complex **366** is converted into **371** by expelling one equivalent of bis(triphenylphosphinimide)cobalt(II) (Scheme 5.6). This result is significant because it implies that the double deprotonation of cobalt(II) phosphinimine complexes with LDA•THF (**362**) does not proceed through a simple deprotonation/displacement pathway. From these observations, we propose an alternative mechanistic pathway in which higher order bis(phosphinimide)cobalt(II) complexes are initially formed at low temperature. These higher order clusters then extrude bis(phosphinimide) cobalt(II) units at higher temperatures and combine with an equivalent of CoX₂ to furnish the observed products.

Scheme 5.6

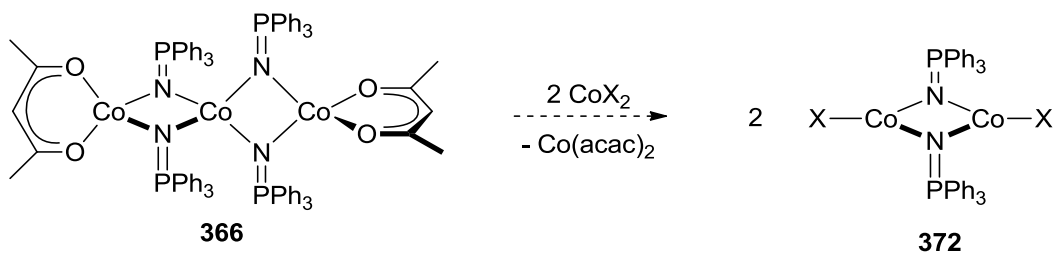


5.5.3 Addition of electrophilic compounds to the linear tri-cobalt phosphinimide complex

Up to this point we had been unable to isolate a low-coordinate mono(phosphinimide)cobalt(II) halide complex. The closest we came to obtaining these complexes was by a route that involved the mono-deprotonation of bis(phosphinimine)cobalt(II) bromide (**358**); this afforded an analogous complex **361**, which also incorporated unwanted coordinated phosphinimine ligands (see Schemes 5.4

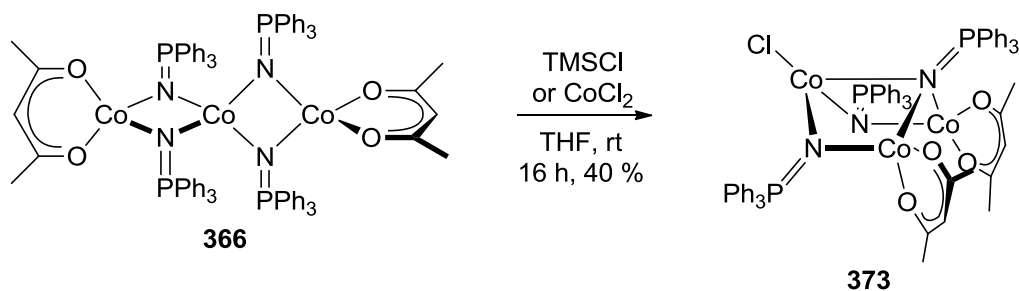
and **5.5**). We hoped that terminal acac ligands in complexes such as **366** could be converted into the desired halide ligands through the addition of cobalt(II) halides (Equation **5.12**). In this case, the cobalt(II) halides would not only provide the four desired chloride ligands, but would also contribute the one additional cobalt(II) atom required to form only the tetrameric heterocubane cluster.

Equation 5.12



We initially decided to use CoCl_2 in these reactions, hoping to generate one equivalent of Co(acac)_2 and two equivalents of mono(phosphinimide)cobalt(II) chloride (see Equation **5.13**). However, we found that by combining two equivalents of CoCl_2 and one equivalent of **366**, we unexpectedly obtained a new tri-cobalt(II) phosphinimide cluster **373**. By treating **366** with CoBr_2 , on the other hand, we obtained only an intractable product mixture. We also found that the same product **373** could be prepared more directly by combining **366** with two equivalents of chlorotrimethylsilane. These results establish that adding electrophilic reagents to **366** is not a viable route for preparing mono(phosphinimide)cobalt(II) halide complexes, as the reactivity of the phosphinimide ligands is clearly greater than the reactivity of the acac ligands. This result also demonstrates that the central bis(phosphinimide)cobalt(II) unit is the most reactive part of the starting cluster **366**.

Equation 5.13



Although we obtained this new cluster **373** serendipitously, it was probably one of the more significant products in this study. The solid-state structure of **373** is interesting because it contains both μ^2 - and μ^3 -phosphinimide ligands in a single crystal; to this point, no other cobalt(II) phosphinimide complexes of this type have been isolated. The bonding interactions directly vary between the μ^2 - and μ^3 -phosphinimide ligands when they are attached to one cobalt(II) atom. From the crystallographic analysis, the interatomic Co-N distances for each phosphinimide ligand in this cluster are consistent with normally observed values (Figures 5.17 and 5.18).^{169,170,174,175,180,253} However, the Co-N distance between the μ^3 -phosphinimide and the cobalt(II) atom with a chloride ligand is significantly longer. This observation implies that the bulk of the electron density from the μ^3 -phosphinimide ligand is located on the two cobalt atoms bearing acac ligands, whereas minimal donor contribution is made to the third cobalt atom. Another observation is that the interatomic P-N distance of the μ^3 -phosphinimide ligand is shorter than other reported values.^{169,170,174,175,180,253} This implies that the bonding of the μ^3 -phosphinimide ligand to the metals is composed primarily of the σ - and one of the π -orbitals from the nitrogen atom, with only a slight contribution from the second π -orbital. To the best of our knowledge, this is the only example where μ^3 -phosphinimide ligand forms apparently stronger interactions between two metal atoms than among three.

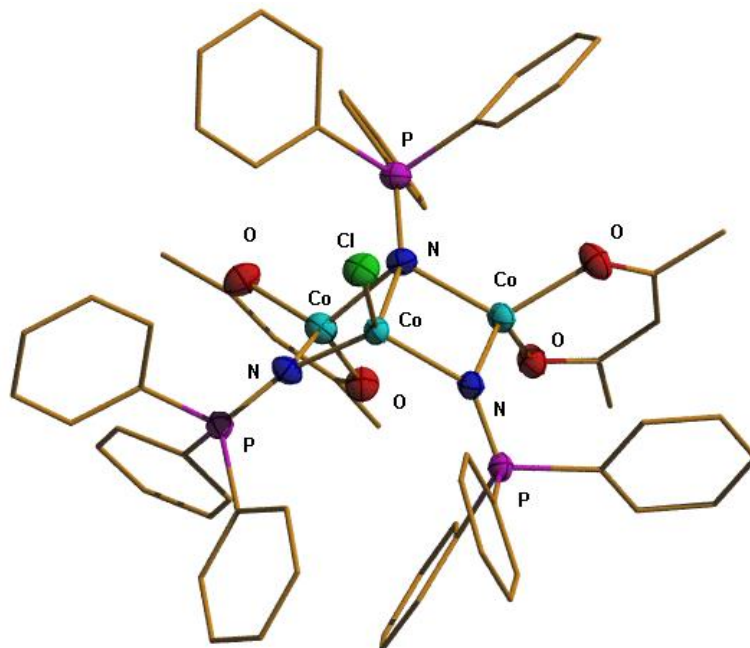


Figure 5.17: Perspective view of **373** with key atoms labelled. Non-hydrogen atoms are represented by either Gaussian ellipsoids at the 20% probability level, or as “wire and stick” representations. $R_1 = 0.0419$, $R(w) = 0.1136$.

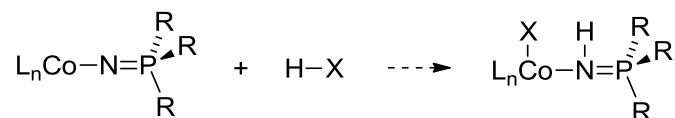
Bond angles (°)		Bond distances (pm)	
Co ₁ -N ₁ -Co ₂	84.69(9)	Co ₁ -N ₁	215.4(2)
Co ₁ -N ₂ -Co ₂	90.86(10)	Co ₂ -N ₁	202.1(2)
N ₁ -Co ₁ -N ₂	89.83(9)	Co ₁ -N ₂	198.2(2)
N ₁ -Co ₂ -N ₂	94.19(10)	Co ₂ -N ₂	196.9(2)
Co ₁ -N ₁ -P	134.07(14)	N ₁ -P	157.1(3)
Co ₂ -N ₁ -P	122.93(14)	N ₂ -P	155.9(2)
Co ₁ -N ₂ -P	134.40(15)		
Co ₂ -N ₂ -P	127.19(14)		

Figure 5.18: Selected interatomic distances and angles of **373**.

5.5.4 Reactivity between acetoacetatocobalt(II) phosphinimide complexes and H-X bonds

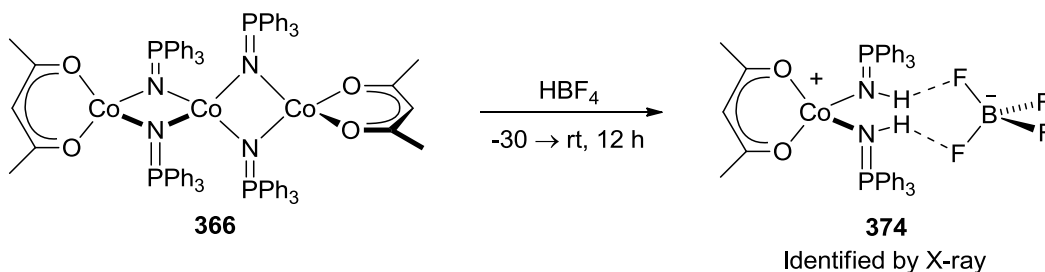
Previously, we obtained evidence that cobalt(II) phosphinimide ligands are capable of deprotonating dichloromethane (see Scheme 5.5). We therefore decided to investigate the reactivity of cobalt(II) phosphinimide complexes **366** and **370** with other protic compounds, hoping to observe similar results using other weak acids (Equation 5.14).

Equation 5.14



In these events, tri-cobalt(II) phosphinimide complex **366** reacts with a variety of protic compounds, including dichloromethane, thiophenol, methanol, and *i*-propanol; unfortunately we could not unambiguously identify any of the reaction products. We did, however, manage to isolate crystals of the bis(triphenylphosphinimine)cobalt(II) acetylacetonate cation **374** from the addition of two equivalents of $\text{HBF}_4 \cdot \text{OEt}_2$ to the linear tri-cobalt(II) phosphinimide complex **366** (Equation 5.15 and Figure 5.19). This product is very similar to the tris(triphenylphosphinimine)cobalt(II) cations **363** and **364** that we obtained earlier. In this new complex, the acetylacetonate anion occupies the coordination site previously held by the third triphenylphosphinimine ligand (see Scheme 5.5).

Equation 5.15



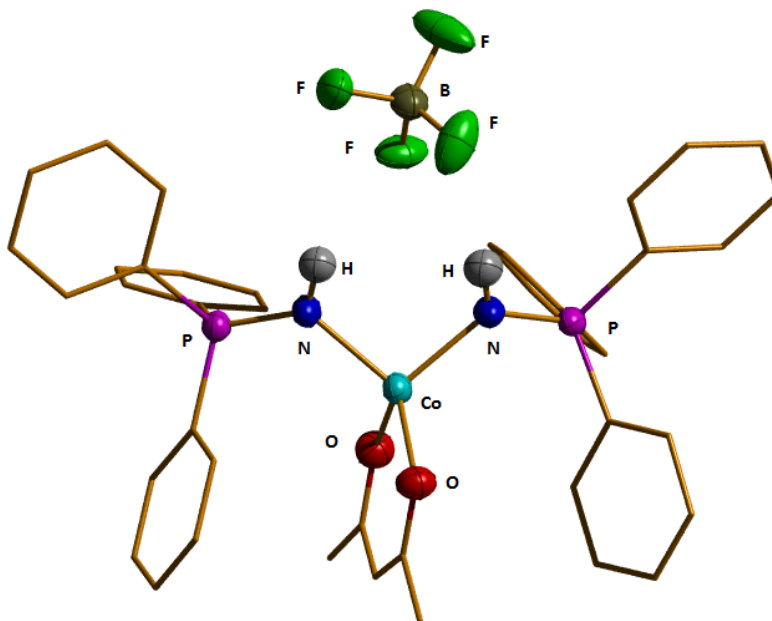
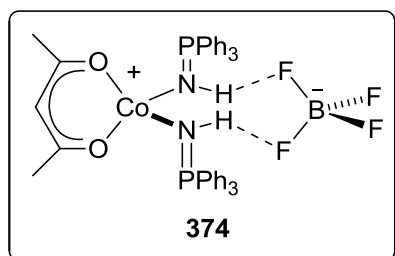


Figure 5.19: Perspective view of **374** with key atoms labelled. Non-hydrogen atoms are represented by either Gaussian ellipsoids at the 20% probability level, or as “wire and stick” representations. The displayed thermal ellipsoids of phosphinimine hydrogen atoms are predicted at the 20% level. $R_1 = 0.0418$, $R(w) = 0.1177$.

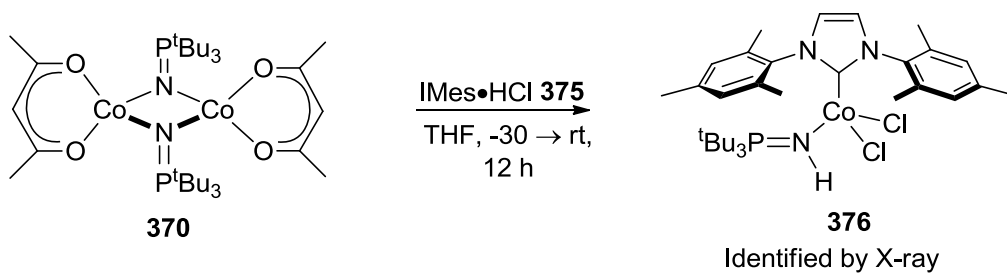


Interatomic bond distances		angles
P-N (pm)	Co-N (pm)	Co-N-P (°)
159.22(2)	198.6(2)	126.46(12)

Figure 5.20: Selected interatomic distances and angles of **374**.

The [tri(*t*-butyl)phosphinimide]cobalt(II) acetylacetonate dimer **370** also reacts with a variety of protic compounds, but none of these products could be isolated. We found, however, that adding one equivalent of a protonated N-heterocyclic carbene (NHC) precursor **375** to **370** afforded the NHC-complexed (tri(*t*-butyl)phosphinimine)cobalt(II) chloride complex **376** (Equation 5.16); this product was characterized by X-ray crystallography (Figure 5.21).

Equation 5.16



IMes = N,N'-bis(2,4,6-trimethylphenyl)imidazole

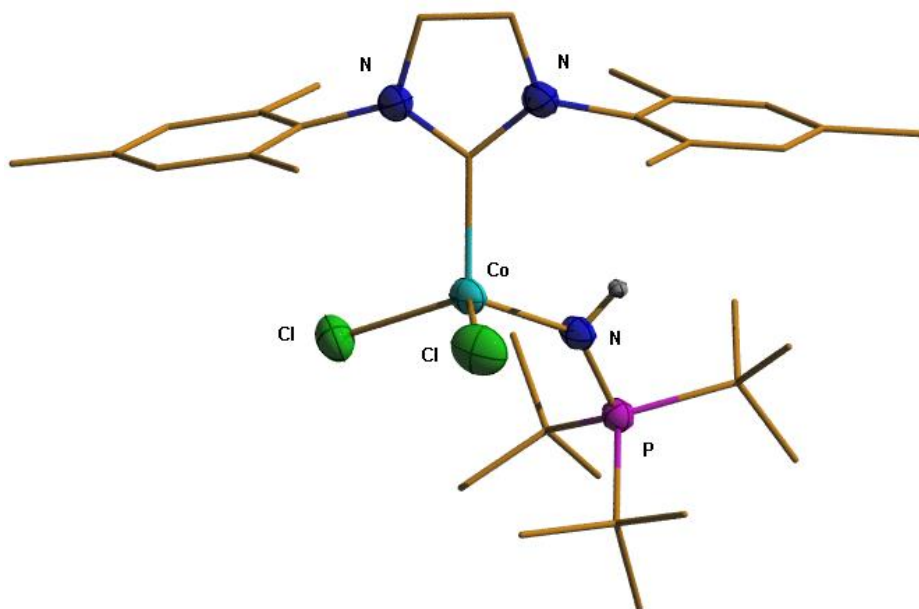


Figure 5.22: Perspective view of **376** with key atoms labelled. Non-hydrogen atoms are represented by either Gaussian ellipsoids at the 20% probability level, or as “wire and stick” representations. The displayed thermal ellipsoids of phosphinimine hydrogen atoms are predicted at the 20% level. $R_1 = 0.0564$, $R(w) = 0.1660$.

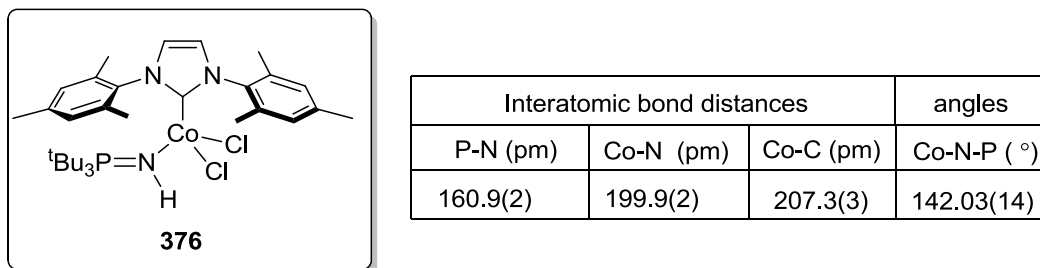
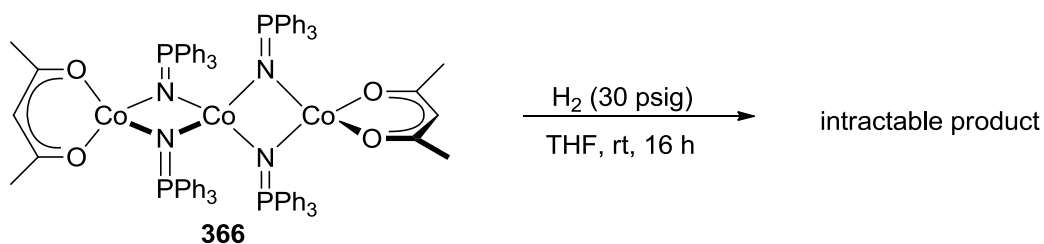


Figure 5.23: Selected interatomic distances and angles of **376**.

A final and even more interesting discovery is the reactions between cobalt(II) phosphinimide complexes and molecular dihydrogen (Equation 5.17). We initially conducted these experiments by bubbling hydrogen gas via syringe through a blue THF solution containing the linear tri-cobalt complex **366**. To our surprise, the color of the solution drastically evolved from dark blue to light brown over four hours. A control experiment was performed with a THF solution containing the tri-cobalt phosphinimide complex **366** stirred overnight in the absence of hydrogen gas; no apparent discoloration was noticed in the solution over the 16 hours. Conducting the reactions under higher pressures of hydrogen gas dramatically increases the rate of de-coloration. We suspect that one of the products from the reaction was a phosphinimine-coordinated cobalt(II) hydride species derived from heterolytic activation of hydrogen.²⁷⁰⁻²⁷⁴ Unfortunately we could not find any evidence of cobalt hydride species when the brown mixtures were analyzed by ¹H NMR and IR spectroscopies or by mass spectrometry.²⁷³

Equation 5.17



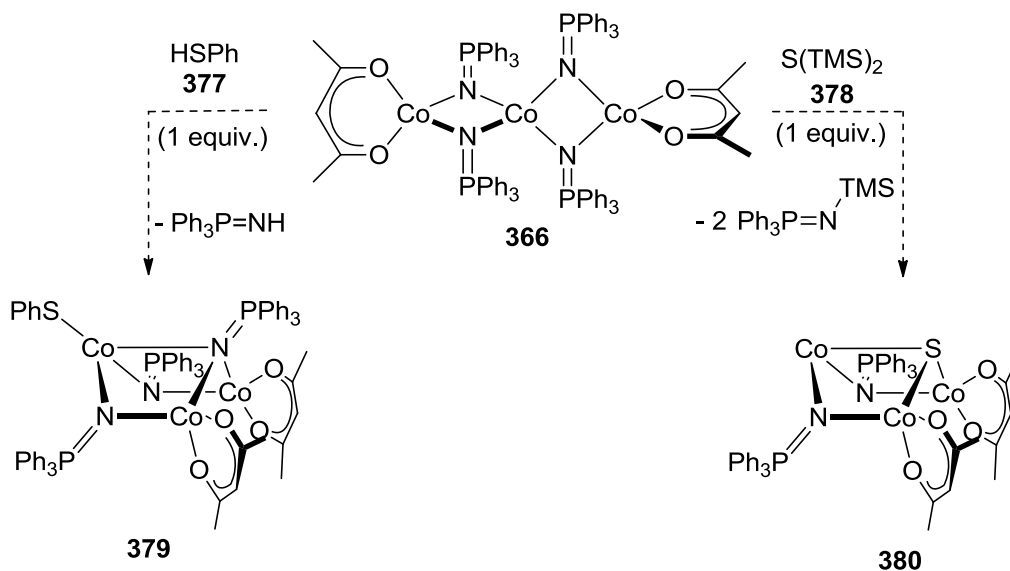
We reasoned that if a metastable cobalt-hydride species was being formed *in situ*, observing the reduction of alkenes, alkynes, and carbonyl bonds would provide indirect evidence of a cobalt hydride catalyst present in the reaction mixture (Equation 5.18).²⁷⁰⁻²⁷⁴ We performed these reactions by first combining equimolar amounts of the cobalt(II) phosphinimide complex **366** with one of the organic substrates which are suitable hydride acceptors in THF; this mixture was then placed under an atmosphere of hydrogen gas. The addition of hydrogen to these reaction mixtures resulted in an instantaneous change in solution color from dark blue to light brown, which indicated that an “active” cobalt species is generated in the presence of the organic substrates. Upon workup, only the unreacted substrates were observed by ¹H NMR spectroscopy. If a cobalt hydride is generated from **366** and hydrogen, it is unreactive with these traps. Similar reactions were repeated except that the dimeric (tri(*t*-butyl)phosphinimide) cobalt(II) acetylacetonate complex **370** was used; unfortunately, similar results were obtained. These experiments suggest that the reactions between cobalt(II) phosphinimide complexes **364** and **365**, and dihydrogen either furnish a highly unstable cobalt(II) hydride species or a completely unrelated product. Even if these conditions do generate a cobalt-hydride species, alternative cobalt phosphinimide precursors would be required to provide additional stability to the hydrogenolysis.

5.6 Preparation of (phosphinimine)- and (phosphinimide)cobalt(II) thiolate complexes

The final class of cobalt(II) phosphinimide and cobalt(II) phosphinimine complexes we pursued involved thiolate ligands. We were interested in thiolate ligands because they are monodentate, similar to halide ligands, but tend to form bridging interactions between multiple cobalt(II) centers.²⁷⁵ In our project, the thiolate ligands would be useful to prevent extraneous phosphinimine ligands from coordinating to the empty coordination site in mono-deprotonated cobalt phosphinimide complexes.

Initial attempts to prepare phosphininime-coordinated cobalt(II) thiolate complexes were unsuccessful. Two of our more notable attempts involved the addition of electrophilic or acidic thiol compounds to the linear tri-cobalt(II) phosphinimide complex **366** (Scheme 5.7). Based on our previous experience (see Equation 5.13), we envisioned that the careful addition of thiophenol (**377**) or $S(TMS)_2$ (**378**) would furnish similar boat-shaped tri-cobalt(II) phosphinimide clusters **379** and **380** respectively; these would incorporate either an equivalent of $[S^{2-}]$ or $[Co-SPh]$ in place of the $[Co-Cl]$ unit in **373** (see Equation 5.13).

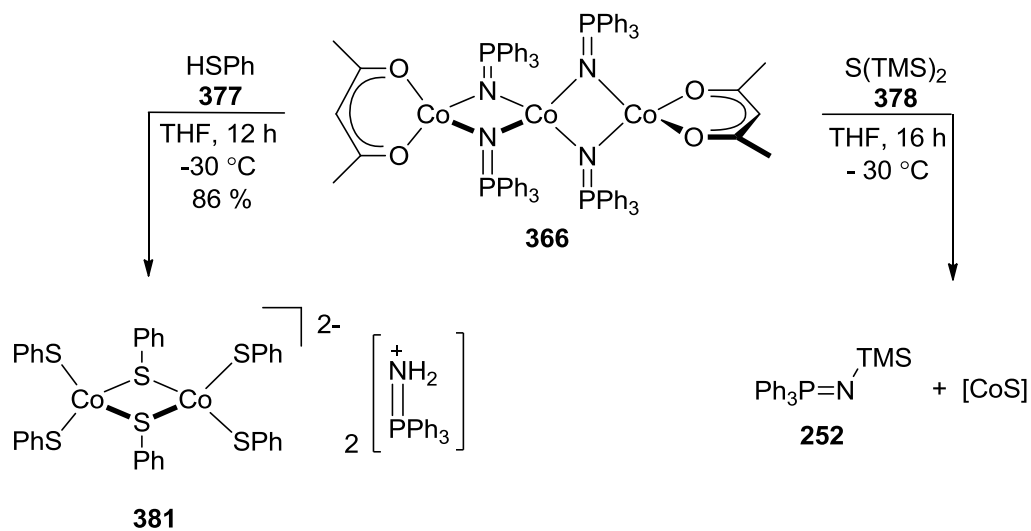
Scheme 5.7



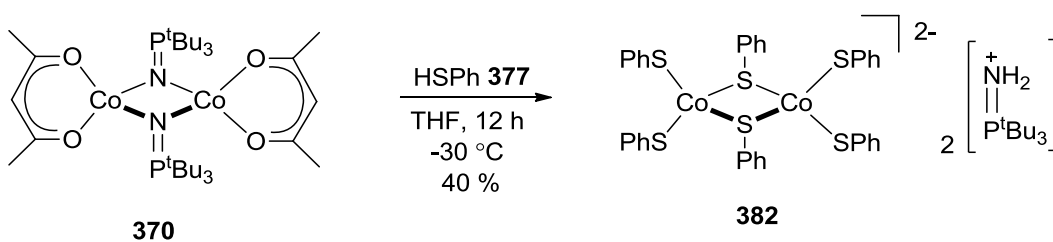
We found, however, that upon addition of one equivalent of $S(TMS)_2$ to **366** we obtained an insoluble black residue which we assume is cobalt(II) sulfide (Scheme 5.8). The addition of one equivalent of thiophenol to **366** also failed to afford any desirable products; instead the tris(phenylthiolato)cobaltate dimer **381** was isolated in good yield. As it turns out, the phosphinimide ligands were converted into triphenylphosphininium cations which hydrogen bonds to the terminal thiophenolate ligands as determined by X-ray crystallography. Purified products were obtained by

evaporating volatiles from the benzene solutions containing the crude product mixture. We also tried to add one equivalent of thiophenol to the tri(*t*-butyl)phosphinimidocobalt(II) acetylacetonate dimer **370** (Equation 5.18); this also afforded the tris(thiophenolato)cobaltate dimer **382** but with tri(*t*-butyl)phosphiniminium counter-cations. These results imply that the difficulty in preparing phosphinimine- or phosphinimidocobalt(II) thiolate complexes arises because dative cobalt-sulfur bonds are vastly more thermodynamically favoured over cobalt-nitrogen bonds.

Scheme 5.8

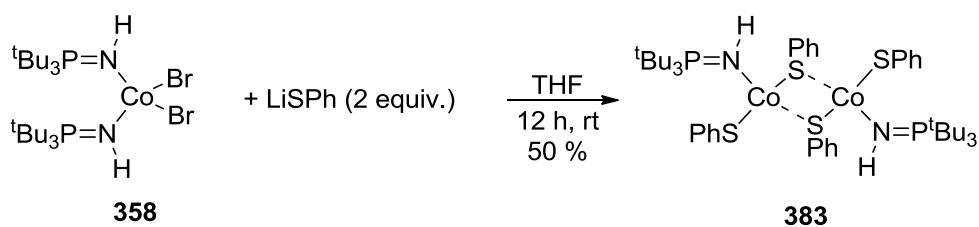


Equation 5.18



Our only successful approach to preparing cobalt(II) phosphinimine complexes with thiolate ligands was by simply displacing halide ligands on the bis(phosphinimine)cobalt(II) halide complexes with thiolate anions. More specifically, we found that the addition of two equivalents of lithium thiophenolate to bis(tri(*t*-butyl)phosphinimine)cobalt(II) bromide **358** furnished the corresponding mono(phosphinimine)cobalt(II) dithiophenolate complex **383**, albeit in only 50% yield (Equation 5.19).

Equation 5.19



As predicted, the phosphinimine-coordinated cobalt(II) dithiophenolate complex **383** exists in the solid state as a dimer with bridging μ^2 -thiophenolate ligands. The problem with this procedure is that one equivalent of tri(*t*-butyl)phosphinimine was wasted in the process, as only one phosphinimine ligand is retained in the product. By addition of one equivalent of CoBr_2 to compound **358** in THF, followed by four equivalents of lithium thiophenolate, the dithiolate complex **383** was obtained in excellent yield (Scheme 5.9). We also attempted to prepare the analogous (triphenylphosphinimine)cobalt(II) thiophenolate complex by adding two equivalents of lithium thiophenolate to bis(triphenylphosphinimine)cobalt(II) acetate (**359**), -chloride (**357**), and -acetylacetonate (**365**) precursors; these reactions unfortunately afforded intractable dark brown product mixtures.

Scheme 5.9

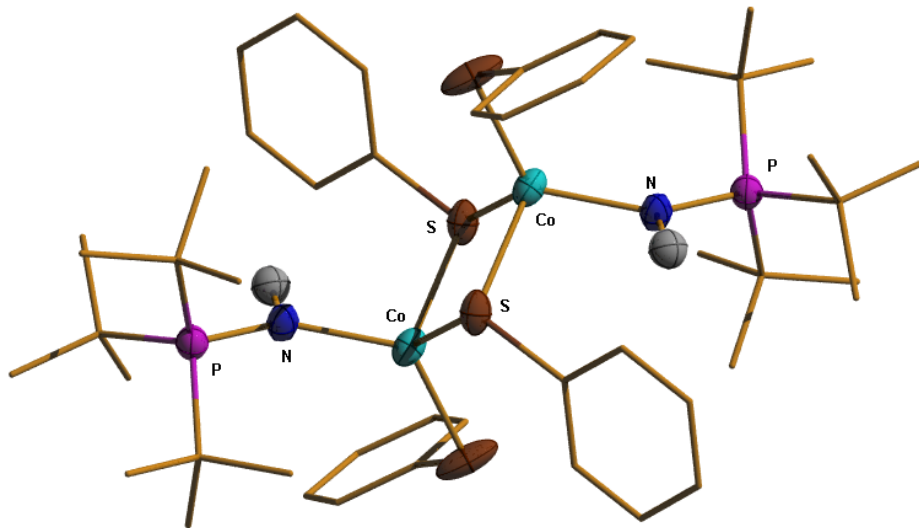
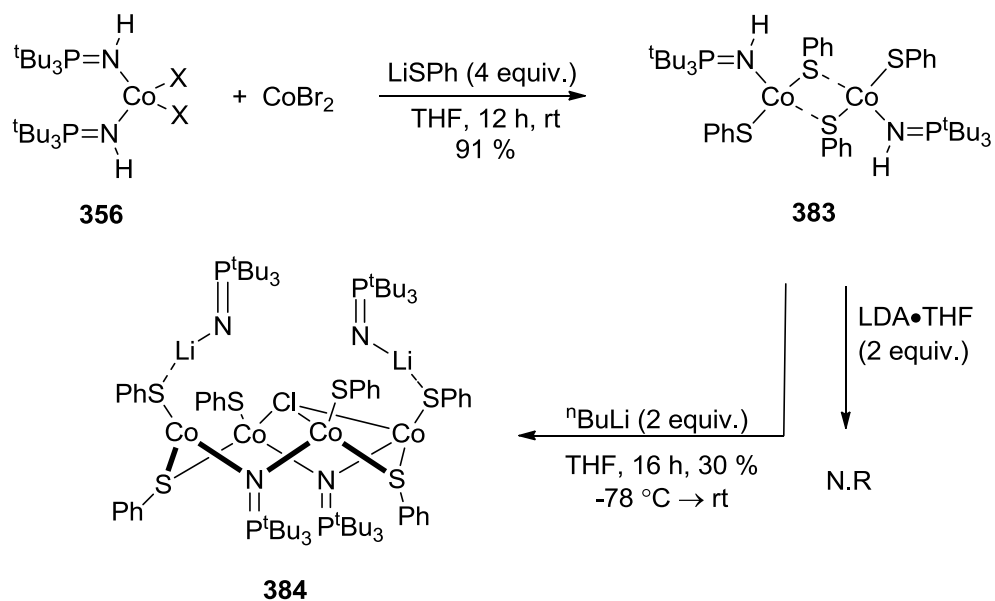


Figure 5.24: Perspective view of **384** with key atoms labelled. Non-hydrogen atoms are represented by either Gaussian ellipsoids at the 20% probability level, or as “wire and stick” representations. The displayed thermal ellipsoids of phosphinimine hydrogen atoms are predicted at the 20% level. $R_1 = 0.0320$, $R(w) = 0.0825$.

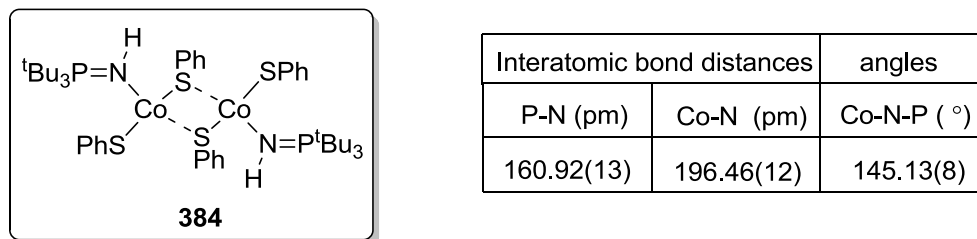


Figure 5.25: Selected interatomic distances and angles of **384**.

The deprotonation of the mono(tri(*t*-butyl)phosphinimine)cobalt(II) thiophenolate complex **383** required a very strong base, as the addition of two equivalents of LDA•THF (**362**) resulted in quantitative recovery of the cobalt starting material (see Scheme 5.9). By treating a THF solution containing **383** with two equivalents of *n*-BuLi at -78 °C, however, we observed an immediate change in color from emerald green to dark brown. From this reaction, we could isolate crystals suitable for X-ray crystallography by allowing pentane extracts from the reaction mixture to slowly evaporate. To our surprise, this reaction afforded an unusual new thiolatocobalt phosphinimide cluster **384**.

The structure of this cobalt phosphinimide cluster **384** is extremely interesting, containing features that have not been observed in cobalt(II) phosphinimide complexes.^{169,170,174,175,180,253} First, the cobalt(II) thiophenolate cluster consists of an eight-membered ring with four cobalt atoms occupying the top half of the ring and alternating μ^2 -tri(*t*-butyl)phosphinimide and μ^2 -thiophenolate ligands occupying the bottom half of the ring. The pseudo-axial positions on the top half of this macrocycle coordinate four thiophenolate ligands, two of which are also coordinated to an equivalent of lithium tri(*t*-butyl)phosphinimide each. The presence of these extruded lithium phosphinimides emphasizes that the correct amount of *n*-BuLi was used in the reaction. This also implies that the displacement of the thiophenolate ions from the two remaining Co(SPh)₂ units by the lithium phosphinimides is not favorable. More specifically, we believe that lithium thiophenolate readily displaces phosphinimide ligands to form more stable cobalt-sulfur bonds.

The crystallographic structure for **384** also reveals the presence of a μ_3 -chloride ligand within its framework. Since none of the starting materials contained chloride ions, we presumed that its origin is the solution of *n*-BuLi where lithium chloride is often present. Most significant about the μ_3 -chloride ligand in this cluster is that one of the cobalt atoms is consequently in the +3 oxidation state. This, therefore constitutes the first cobalt(III) phosphinimide complex to be reported. Unfortunately, due to high disorder in the single crystal of **384**, accurate Co-N, N-P and Co-N-P bonding parameters of the cobalt(III) phosphinimide unit could not be obtained, so that no comparisons may be made. This, however, re-establishes that multiple oxidation state cobalt phosphinimide complexes can be prepared, and that our goal of preparing cobalt(I) phosphinimide complexes should not be discarded.

5.7 Conclusions and future work

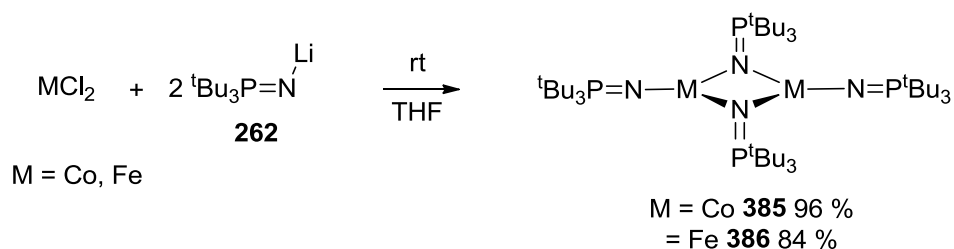
Overall, this study was successful, as we have developed a new method for preparing cobalt(II) phosphinimine and cobalt(II) phosphinimide complexes. Our dehydrohalogenation protocol resulted in the characterization of new cobalt(II) phosphinimide complexes, which allowed us to study the physical properties of μ^2 -phosphinimide ligands with cobalt(II) centers, as well as the differences between μ^2 - and μ^3 -phosphinimide ligands. We also discovered that cobalt(II) phosphinimide complexes are reactive towards weakly acidic and electrophilic compounds. Our attempts to obtain reduced cobalt(I) phosphinimide complexes were unsuccessful, but we were able to serendipitously obtain one example of a cobalt(III) phosphinimide complex, embedded in a mixed-valent cluster.

One of the successful aspects of this project is that it opened a variety of doors for future development. Since the termination of this specific work, the Stryker lab has expanded the investigation of transition metal phosphinimide chemistry from one person to at least half a dozen. By including more researchers in one specific area, we have been able to rapidly develop our command over transition metal-phosphinimide complexes. New methods for preparing first-row transition metal phosphinimide

complexes have been demonstrated and new catalysts for a range of reactions including hydrodesulfurization have been developed.

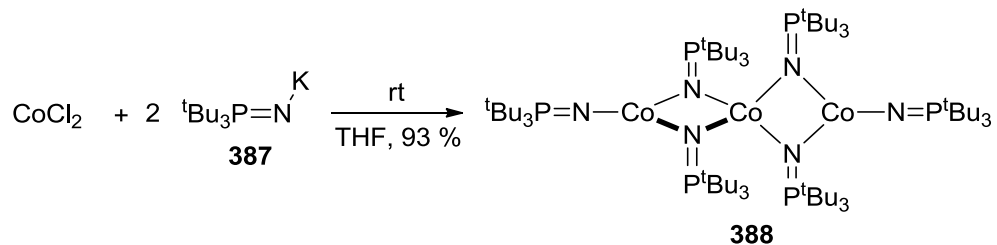
In subsequent projects, we were also able to successfully isolate and characterize both cobalt(II) and iron(II) bis(tri(*t*-butyl)phosphinimide) complexes **385** and **386** (Equation 5.20). Through crystallographic analysis, we discovered that these complexes exist as dimers in the solid state, which contain two μ_2 -bridging and two terminal phosphinimide ligands.

Equation 5.20



The bis(triphenylphosphinimide)cobalt(II) complex **388** was recently obtained by salt metathesis between two equivalents of potassium triphenylphosphinimide **389** and cobalt(II) chloride (Equation 5.20). This complex exists in the same linear tri-cobalt geometrical arrangement that we observed previously (see Equation 5.8). We have also developed suitable procedures for obtaining cobalt(I) monophosphinimide and cobalt(III) tris(phosphinimide) complexes.

Equation 5.20



Most importantly, we have recently made significant contributions regarding the reactivity of cobalt phosphinimide complexes with molecular dihydrogen. Presently, we have demonstrated that two cobalt phosphinimide complexes are active hydrodesulfurization, hydrodeoxygenation, and alkene hydrogenation precatalysts when placed under hydrogen gas. However, these projects will be discussed in greater detail by other researchers.

To conclude, the results discussed in this chapter were essential because they opened a variety of doors to catalysis, all of which are being actively pursued. This type of exploratory work, although frustrating at times, is absolutely crucial in developing new methodologies.

Chapter 6: Experimental Section

6.1 General Procedures

All procedures were performed using standard Schlenk techniques using a double manifold vacuum/N₂ line or in an MBraun labmaster 100 inert atmosphere dry glovebox, any modifications will be mentioned. All solvents were dried and purified under a N₂ atmosphere using sodium (toluene), sodium/benzophenone ketyl (tetrahydrofuran, diethyl ether, benzene), potassium/benzophenone ketyl (hexane, pentane) or calcium hydride (acetonitrile, dichloromethane). Any purified liquids were stored either in Schlenk flasks or in cylindrical medium walled glass vessels which are referred to as reaction or storage bombs. Reactions that required elevated temperatures were performed either by using sand filled heating mantles, whereas reactions that required a more controlled temperature were performed using a heavy mineral oil bath using IKA stir plates. All glassware was dried either over a flame or in an oven at 130 °C for at least 2 hours prior to use and cooled either under vacuum or under nitrogen or argon. Products that required additional vacuum ($< 10^{-5}$ torr) for removal of solvents were done on a high vacuum line equipped with a diffusion pump. Purification of organic products using flash column chromatography was performed using flash silica gel (40-63 μm) from Silicycle. The storage of temperature sensitive compounds or low temperature recrystallizations was performed in a - 30 °C freezer located in the nitrogen glovebox. NMR spectroscopic analysis was performed in standard NMR tubes with plastic caps. Elemental analysis of all samples were prepared by instrumentation staff; when air sensitive samples were involved, the samples are prepared in the glove box using two weigh boats and transported under an atmosphere of nitrogen in a one dram vial that is capped and wrapped in parafilm. Samples for IR spectroscopy were prepared on KBr plates and where air sensitive samples are involved, the sample was prepared in the dry glovebox using two KBr plates, the sample was deposited in the middle of one plate and an atmosphere of nitrogen is kept above the sample by placing a greased o-ring on the outside of the plate and a second KBr plate is placed on top. Samples requiring air sensitive mass spectrometry were prepared by making a solution in a one dram vial with an appropriate solvent, capped and wrapped with parafilm.

6.2 Instruments Used

^1H , ^{31}P and ^{13}C NMR analyses were performed at 27 °C using either a Varian Inova 300 MHz spectrometer, Varian Inova or Varian Mercury 400 MHz spectrometers or two Varian Inova 500MHz spectrometer, one of which is equipped with a $^{13}\text{C}/^1\text{H}$ dual cold probe. ^1H NMR and ^{13}C NMR chemical shifts are reported in ppm which is measured using either tetramethylsilane or the protonated NMR solvent peaks that occur as impurities. Variable temperature NMR studies were performed by the staff at the University of Alberta NMR spectroscopy laboratory. All X-ray crystallographic analyses were performed on either a Bruker DB diffractometer with a SMART APEX II CCD area detector or a Bruker PLATFORM diffractometer with a SMART APEX II CCD detector. All solutions to diffraction pattern obtained using these instruments were accomplished by the Dr. Robert McDonald or by Dr. Michael Ferguson of the University of Alberta X-ray crystallography laboratory. All elemental analysis and infrared spectroscopic analyses were performed by the University of Alberta analytical and instrumentation Laboratory. Samples analyzed for CHNS elemental analysis were performed on a Carlo Erba EA1108 Elemental Analyzer. Samples analyzed for IR spectroscopy are performed using a Nicolet Magna 750 FTIR Spectrometer and a Nic-Plan FTIR Microscope. All mass spectrometric analyses were performed by the staff at the University of Alberta Mass Spectrometry Facility. Samples requiring high resolution electron impact (EI) mass spectrometry are performed using an Kratos Analytical MS-50, samples requiring GC-MS was performed on an Agilent Technologies 5975C MSD, samples requiring electrospray ionization (ESI) or atmospheric pressure photoionization (APPI) are performed on an Agilent Technologies 6220 aoTOF mass spectrometer.

6.3 Materials Used

All reagents were purchased from the Sigma-Aldrich, VWR or Strem chemical supply companies and used as received. Necessary purifications of any reagents were done according to "The Purification of Laboratory Chemicals, fifth edition" by Armarego and Chai; any changes to the purification of specific chemicals will be listed in the experimental section. Any materials that were prepared by published methods will be

referenced accordingly. Celite is dried for 16 h in a vacuum oven ranging from 80 °C to 100 °C prior to use. $[\text{Cp}_2\text{TiCl}]_2$,⁸⁶ 1-bromo-3-phenyl-2-propyne,^{6,276} 1-bromo-2-butyne,⁶ N-(trimethylsilyl)triphenylphosphinimine,^{166,167} N-tricyclohexylphosphinimine,^{166,167} N-(trimethylsilyl)tri(*tert*-butyl)phosphinimine,^{166,167} tri(*tert*-butyl)phosphinimine,¹⁹⁸ S,S-diphenylsulfimine,^{238,277} (η^5 -pentamethylcyclopentadienyl)titanium(IV) trichloride,²⁷⁸ titanium tetrakis(dimethylamide),²⁷⁹ titanium(IV) tetrakis(diethylamide),²⁷⁹ bis(dimethylamido) titanium(IV) dichloride²¹⁸ and bis(diethylamido)titanium(IV) dichloride²¹⁸ were prepared using literature procedures.

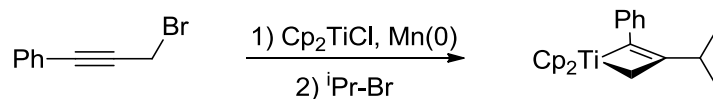
6.4 Annotation of Acyclic and Cyclic Assignments

The method of assigning the carbon and hydrogen atoms to the corresponding resonances is denoted by highlighting the atom in an alkyl chain by both *italic and underline*. For terminal acyclic fragments, the beginning of the chain is denoted by using a dash such as “-CH₂CH₂CH₃”. For cyclic systems, the atoms that are connected are denoted with colons; for example in titanacyclobutenes “:CH₂TiC=C:” denotes that a four-membered ring is present, and is connected between the aliphatic and olefinic carbons.

6.5 Procedures

6.5.1 Chapter 2 Experimental Section

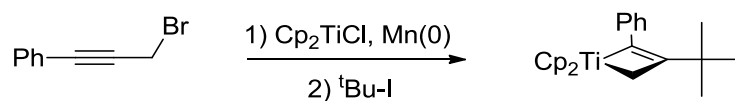
1,1-Bis(cyclopentadienyl)-3-isopropyl-2-phenyltitanacyclobutene (133)



80 mg of Mn powder (1.46 mmol), 5 mg of PbCl₂ (0.02 mmol), 5 mg of TMS-Cl (0.05 mmol) and 2 mL of THF were combined in a flame-dried 5 dram glass vial. The mixture was then stirred at 40 °C for 1 hour, or until a grey aggregate was formed. 38 mg of solid $[\text{Cp}_2\text{TiCl}]$ (0.17 mmol) was then added *via* spatula to the 5 dram vial

containing the grey heterogeneous mixture; the vial was then placed in the drybox freezer (-30 °C) for 1 hour. The cooled vial was removed from the freezer and quickly treated with a solution of 35 mg of 1-bromo-3-phenyl-2-propyne^{6,276} (0.18 mmol) in 1 mL THF *via* glass pipette, then placed back in the drybox freezer (-30 °C) where it remained for 16 hours. After 16 hours, the color of the reaction mixture was reddish-purple. The vial containing the reddish-purple mixture was then removed from the freezer and warmed to room temperature over 4 hours; over this time the color of the solution changed from reddish-purple to brown, and then to emerald green. The vial containing the green solution was placed back in the drybox freezer (-30 °C) for 1 hour. Once removed from the freezer, the mixture was treated with a solution of 22 mg of 2-bromo-propane (0.18 mmol) in 1 mL of THF *via* glass pipette. The resulting mixture was warmed to room temperature over 1 hour, and stirred for an additional 7 hours, which affords a brownish-red colored solution. The volatile compounds were removed *in vacuo* and the resulting red residue was extracted with pentane and filtered through celite until the extracts were colorless. The volatile compounds in the filtrate were then removed *in vacuo*; this results in 54 mg (87 %) of the desired product. The ¹H NMR spectrum of the product exactly matches that of the ¹H NMR spectrum of **133** from previous characterization data.⁶

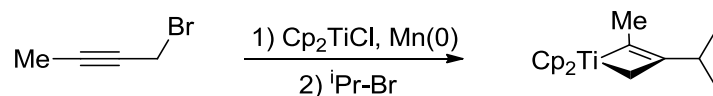
1,1-Bis(cyclopentadienyl)-3-(*tert*-butyl)-2-phenyltitanacyclobutene (**139**)



80 mg of Mn powder (1.46 mmol), 5 mg of PbCl₂ (0.02 mmol) and 5 mg of TMS-Cl (0.05 mmol), and 2 mL of THF were combined in a flame-dried 5 dram glass vial. The mixture was then stirred at 40 °C for 1 hour, or until a grey aggregate was formed. 38 mg of solid [Cp₂TiCl] (0.17 mmol) was then added *via* spatula to the 5 dram vial containing the grey heterogeneous mixture; the vial was then placed in the drybox freezer (-30 °C) for 1 hour. The vial was removed from the freezer and quickly treated with a solution containing 35 mg of 1-bromo-3-phenyl-2-propyne^{6,276} (0.18 mmol) in 1

mL THF *via* glass pipette, then the vial was placed back in the freezer (-30 °C) for 16 hours. After 16 hours, the color of the reaction mixture became reddish-purple. The vial containing the reddish-purple mixture was removed from the freezer and warmed to room temperature over 4 hours; during this time the color of the solution became emerald green. The resulting green solution was then placed in the drybox freezer (-30 °C) for 1 hour, removed, and treated with a solution containing 34 mg of *tert*-butyl iodide (0.18 mmol) in 1 mL THF *via* glass pipette. The resulting solution was warmed to room temperature over 1 hour and stirred for an additional 8 hours; during this time the color of the solution evolved from green to brownish-red. The volatile solvents were removed *in vacuo* giving a red residue, which was extracted with pentane and filtered through celite until the extracts were colorless. The volatile solvents were removed from the filtrate *in vacuo* affording 53 mg (82 %) of the desired product. The ¹H NMR spectrum of the product exactly matches that of the ¹H NMR spectrum of **139** from previous characterization data.⁶

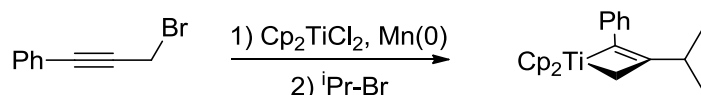
1,1-Bis(cyclopentadienyl)-3-isopropyl-2-methyltitanacyclobutene (141)



80 mg of Mn powder (1.46 mmol), 5 mg of PbCl₂ (0.02 mmol), 5 mg of TMS-Cl (0.05 mmol), and 2 mL of THF were combined in a flame-dried 5 dram glass vial. The mixture was then stirred at 40 °C for 1 hour, or until a grey aggregate was formed. 38 mg of solid [Cp₂TiCl] (0.17 mmol) was added *via* spatula to the vial containing the grey heterogeneous mixture and the vial was placed in the drybox freezer (-30 °C) for 1 hour. This vial was removed from the freezer, then quickly treated with a solution containing 24 mg of 1-bromo-2-butyne⁶ (0.18 mmol) in 1 mL THF *via* glass pipette, then placed back in the drybox freezer (-30 °C) for 16 hours; during this time the color of the reaction mixture became reddish-purple. The vial was removed from the freezer and warmed to room temperature over 4 hours; during this time the color of the mixture changed from reddish-purple to emerald green. The vial was then placed in the drybox freezer (-30 °C)

for 1 hour, then removed and treated with a solution containing 22 mg of 2-bromopropane (0.18 mmol) in 1 mL THF *via* glass pipette. The resulting solution was allowed to warm to room temperature over 1 hour and stirred for an additional 7 hours; during this time the color of the solution changed from green to brownish-red. The volatile compounds were then removed *in vacuo* and the resulting red residue was extracted with pentane and the extracts were filtered through celite until the extracts were colorless. The volatile compounds were removed from the filtrate *in vacuo*, which affords 40 mg (87 %) of the desired product. The ^1H NMR spectrum of the product exactly matches that of the ^1H NMR spectrum of **141** from previous characterization data.⁶

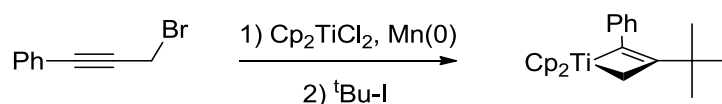
1,1-Bis(cyclopentadienyl)-3-isopropyl-2-phenyltitanacyclobutene (**133**)



80 mg of Mn powder (1.46 mmol), 5 mg of PbCl_2 (0.02 mmol) and 5 mg of TMS-Cl (0.05 mmol) and 2 mL of THF were combined in a flame-dried 5 dram glass vial. This mixture was stirred at 40 °C for 1 hour, or until a grey aggregate was formed. 44 mg of solid Cp_2TiCl_2 (0.18 mmol) was then added *via* spatula to the vial containing the grey heterogeneous mixture; the vial was then placed in the drybox freezer (-30 °C) for 1 hour. The vial was then removed from the freezer and quickly treated with a solution containing 35 mg of 1-bromo-3-phenyl-2-propyne^{6,276} (0.18 mmol) in 1 mL THF *via* glass pipette, then placed back in the drybox freezer (-30 °C) for 16 hours. During this time the reaction mixture became reddish-purple in color. The vial was removed from the freezer and warmed to room temperature over 4 hours; during this time the color of the solution changed from reddish-purple to emerald green. The vial was then placed back into the drybox freezer (-30 °C) for 1 hour. The vial was then removed from the drybox freezer, and then treated with a solution containing 22 mg of 2-bromopropane (0.18 mmol) in 1 mL THF *via* glass pipette. The mixture was warmed to room temperature over 1 hour and then stirred for an additional 7 hours; a brownish-red solution was

obtained. The volatile compounds were then removed *in vacuo*. The red residue was extracted with pentane and the extracts were filtered through celite until the extracted fractions were colorless. The volatile compounds were removed from the filtrate *in vacuo* and afforded 53 mg (93 %) of the desired product. The ^1H NMR spectrum of the product exactly matches that of the ^1H NMR spectrum of **133** from previous characterization data.⁶

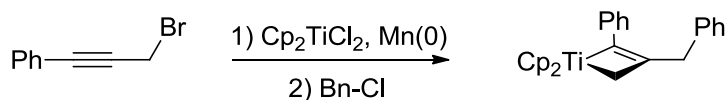
1,1-Bis(cyclopentadienyl)-3-(tert-butyl)-2-phenyltitanacyclobutene (139)



80 mg of Mn powder (1.46 mmol), 5 mg of PbCl_2 (0.02 mmol), 5 mg of TMS-Cl (0.05 mmol), and 2 mL of THF were added to a flame-dried 5 dram vial. The resulting mixture was stirred at 40 °C for 1 hour, or until a grey aggregate was formed. 44 mg of solid Cp_2TiCl_2 (0.18 mmol) was added *via* spatula to the vial containing the grey heterogeneous mixture and then the vial was placed in the drybox freezer (-30 °C) for 1 hour. The cooled vial was removed from the freezer, and a solution containing 35 mg of 1-bromo-3-phenyl-2-propyne^{6,276} (0.18 mmol) in 1 mL THF was quickly added *via* glass pipette, then the vial was placed back in the drybox freezer (-30 °C) for 16 hours; after 16 hours this time a reddish-purple solution formed. The vial containing the reddish-purple mixture was removed from the freezer and warmed to room temperature over 4 hours; during this time the color of the solution changed from reddish-purple to emerald green. The vial was placed back into the drybox freezer (-30 °C) for 1 hour, then removed, and quickly treated with a solution containing 34 mg of *tert*-butyl iodide (0.18 mmol) in 1 mL THF *via* glass pipette, then placed back in the drybox freezer for 3 hours. The vial was then removed from the drybox freezer and was warmed to room temperature over 1 hour and stirred for an additional 7 hours; during this time the color of the reaction mixture changed from green to purple. The volatile compounds were then removed *in vacuo* and the resulting red residue was extracted with pentane; the extracts were filtered through celite and continued until the color of the extracts were

colorless. The volatiles were removed from the filtrate *in vacuo*, which resulted in 50 mg (77 %) of the desired product. The ^1H NMR spectrum of the product exactly matches that of the ^1H NMR spectrum of **139** from previous characterization data.⁶

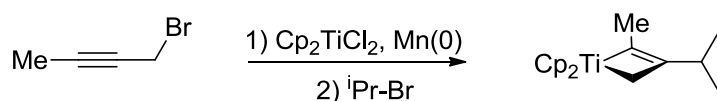
1,1-Bis(cyclopentadienyl)-3-benzyl-2-phenyltitanacyclobutene (140)



80 mg of Mn powder (1.46 mmol), 5 mg of PbCl_2 (0.02 mmol), 5 mg of TMS-Cl (0.05 mmol) and 2 mL of THF were added to a flame-dried 5 dram vial. The resulting mixture was then stirred at 40 °C for 1 hour, or until a grey aggregate was formed. 44 mg of Cp_2TiCl_2 (0.18 mmol) was then added to the vial containing the grey heterogeneous mixture *via* spatula, then the vial was placed in the drybox freezer (-30 °C) for 1 hour. The cooled vial was removed from the freezer and quickly treated with a solution containing 35 mg of 1-bromo-3-phenyl-2-propyne^{6,276} (0.18 mmol) in 1 mL of THF *via* glass syringe, then the vial was placed back in the drybox freezer for 16 hours; during this time the color of the reaction mixture became reddish-purple. The vial was then removed from the freezer, and warmed to room temperature over 4 hours; during this time the color of the solution changed from reddish-purple to emerald green. The vial was placed back into the drybox freezer (-30 °C) for 1 hour, then removed, and quickly treated with a solution containing of 23 mg of benzyl chloride (0.18 mmol) in 1 mL THF *via* glass pipette; this resulted in an immediate change in solution color from green to dark purple. The vial was quickly placed back into the drybox freezer for 3 hours. The vial was removed from the freezer and warmed to room temperature over 1 hour and then stirred for an additional 7 hours. The volatile compounds were then removed *in vacuo* and the resulting red residue was extracted with pentane, and the extracts were filtered through celite until the color of the extracted solvents was colorless. The volatile compounds were removed from the filtrate *in vacuo* which resulted in 50 mg (73 %) of the desired product. The ^1H NMR spectrum of the product

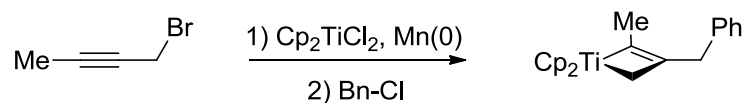
exactly matches that of the ^1H NMR spectrum of **140** from previous characterization data.⁶

1,1-Bis(cyclopentadienyl)-3-isopropyl-2-methyltitanacyclobutene (**141**)



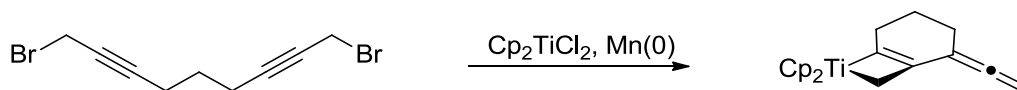
80 mg of Mn powder (1.46 mmol), 5 mg of PbCl₂ (0.02 mmol), 5 mg of TMS-Cl (0.05 mmol), and 2 mL of THF were added to a flame-dried 5 dram vial. The resulting mixture was then stirred at 40 °C for 1 hour, or until a grey aggregate was formed. 4 mg of solid Cp₂TiCl₂ (0.18 mmol) was added *via* spatula to the vial containing the grey heterogeneous mixture; then the vial was placed in the drybox freezer (-30 °C) for 1 hour. The cooled vial was then removed from the freezer and quickly treated with a solution containing 24 mg of 1-bromo-2-butyne⁶ (0.18 mmol) in 1 mL of THF *via* glass pipette, and placed back in the drybox freezer for 16 hours; during this time the color of the reaction mixture became reddish-purple. The vial containing the reddish-purple mixture was removed from the freezer and warmed to room temperature over 4 hours; during this time the color of the mixture changed from reddish-purple to emerald green. The vial containing the green solution was then placed back into the drybox freezer for 1 hour, then removed, and treated with a solution containing 22 mg of 2-bromo-propane (0.18 mmol) in 1 mL THF *via* glass pipette. The resulting mixture was warmed to room temperature over 1 hour and stirred for an additional 7 hours; during this time the color of the reaction mixture changed from green to brownish-red. The volatile compounds were removed *in vacuo*. The resulting red residue was extracted with pentane and the extracts were filtered through celite until the color of the extracts was colorless. The volatile compounds were removed from the filtrate *in vacuo*, which resulted in 40 mg (87 %) of the desired product. The ^1H NMR spectrum of the product exactly matches that of the ^1H NMR spectrum of **141** from previous characterization data.⁶

1,1-Bis(cyclopentadienyl)-3-benzyl-2-methyltitanacyclobutene (**142**)



80 mg of Mn powder (1.46 mmol), 5 mg of PbCl_2 (0.02 mmol) and 5 mg of TMS-Cl (0.05 mmol) was stirred in 2 mL of THF for 1 hour at 40 °C, or until a grey aggregate was formed. 44 mg of solid Cp_2TiCl_2 (0.18 mmol) was added to the vial containing the grey heterogeneous mixture *via* spatula, then the vial was placed into the drybox freezer (-30 °C) for 1 hour. The cooled vial was then treated removed from the freezer and quickly treated with a solution containing 24 mg of 1-bromo-2-butyne⁶ (0.18 mmol) in 1 mL of THF *via* glass pipette, then placed back into the drybox freezer for 16 hours; during this time the color of the reaction mixture became reddish-purple. The vial was removed from the freezer and warmed to room temperature over 4 hours; during this time the color of the reaction mixture changed from reddish-purple to emerald green. The vial was then placed back into the drybox freezer (-30 °C) for 1 hour, then removed, and quickly treated with a solution containing 23 mg of benzyl chloride (0.18 mmol) in 1 mL THF *via* glass pipette; upon addition, the color of the reaction changed instantaneously from green to deep purple. The vial was quickly placed back into the drybox freezer (-30 °C) for 3 hours. The vial was then removed from the freezer and warmed to room temperature over 1 hour, then stirred for an additional 7 hours. The volatile compounds were removed *in vacuo* and the resulting red residue was extracted with pentane, and the extracts were filtered through celite until the color of the extracts was colorless. The volatile compounds were removed again *in vacuo*, which resulted in 55 mg (85 %) of the desired product. The ¹H NMR spectrum of the product exactly matches that of the ¹H NMR spectrum of **142** from previous characterization data.⁶

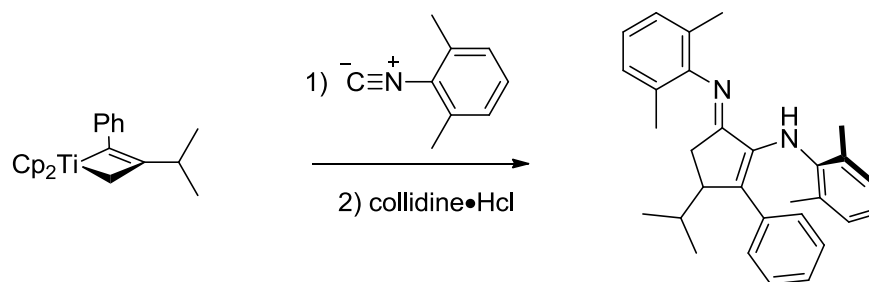
(3-Ethenylidene-2-methanidylcyclohex-1-enyl)titanocene (144)



100 mg of Mn powder (1.83 mmol), 10 mg of PbCl₂ (0.04 mmol), 10 mg of TMS-Cl (0.09 mmol) and 2 mL of THF were added to a flame-dried 5 dram vial. The resulting mixture was stirred at 40 °C for 1 hour, or until a grey aggregate was formed. 121 mg of solid Cp₂TiCl₂ (486 μmol) was added to the vial containing the grey heterogeneous mixture *via* spatula, then the vial was placed in the drybox freezer (-30 °C) for 1 hour. The cooled vial was removed from the freezer and was quickly treated with a solution containing 135 mg of 1,9-dibromo-2,7-nonadiyne⁴ (486 μmol) in 1 mL THF *via* glass pipette, then placed back in the drybox freezer (-30 °C) for 16 hours; during this time the color of the reaction mixture became dark red. The vial was removed from the freezer, and warmed to room temperature over 4 hours; after 4 hours a brownish-red solution was obtained. The volatile compounds were removed *in vacuo* and the resulting red residue was extracted with pentane, and the extracts were filtered through celite until the color of the extracts was colorless. The volatile compounds were removed from the filtrate again *in vacuo*, which resulted in 70 mg (48 %) of the crude product. Purification of this compound was unsuccessful due to the presence of non-separable by-products.

Spectroscopic data for **144**: ¹H NMR (500 MHz, C₆D₆): δ 5.52 (broad s, 10H, Cp-H), δ 4.96 (broad s, 2H, -C=C-CH₂), δ 3.21 (broad s, 2H, :TiCH₂CC:), δ 2.50 (broad s, 2H, -CH₂CH₂CH₂C(allene)), δ 2.38 (broad s, 2H, -CH₂CH₂CH₂C(allene)), δ 1.58 (broad s, 2H, -CH₂CH₂CH₂C(allene)); ¹³C {¹H} NMR (125 MHz, C₆D₆): δ 224.0 (:TiCH₂CC:), 210.1 (-C=C-CH₂), 110.4 (Cp-H), 99.7 (-C=C-CH₂), 88.5 (:TiCH₂CC:), 76.3 (-C=C-CH₂), 70.3 (:TiCH₂CC:), 35.3 (-CH₂CH₂CH₂C(allene)), 28.3 (-CH₂CH₂CH₂C(allene)), 24.3 (-CH₂CH₂CH₂C(allene)); COSY (500 MHz, C₆D₆): δ 4.96 ↔ δ 3.21, 2.38; δ 3.21 ↔ δ 2.50; δ 2.50 ↔ δ 1.58; δ 2.38 ↔ δ 1.58; HMQC (500 MHz, C₆D₆): δ 5.52 ↔ δ 110.4, δ 4.96 ↔ δ 76.3, δ 3.21 ↔ δ 70.3, δ 2.50 ↔ δ 35.3, δ 2.38 ↔ δ 28.3; δ 1.58 ↔ δ 24.3; HMBC (500 MHz, C₆D₆): δ 4.96 ↔ δ 224.0, 210.1, 99.7, 88.5; δ 3.21 ↔ δ 224.0, 99.7, 88.5;

(2,6-Dimethyl-phenyl)-[5-(2,6-dimethyl-phenylimino)-3-isopropyl-2-phenyl-cyclopent-1-enyl]-amine (155)

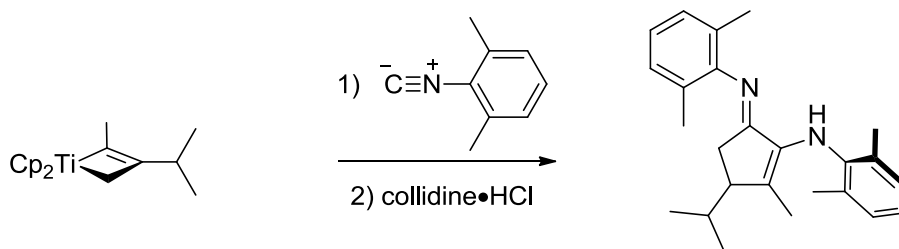


68 mg of 2-phenyl-3-(*i*-propyl)-titanacyclobutene⁶ (0.202 mmol) was dissolved in 2 mL of THF in a flame-dried 5 dram vial; the vial was then placed in the drybox freezer (-30 °C) for 1 hour. The vial was removed from the freezer and was quickly treated with a solution containing 86 mg of 2,6-dimethylphenyl isonitrile (0.657 mmol) in 1 mL THF *via* glas pipette. The resulting mixture was warmed to room temperature over 1 hour and stirred for an additional 16 hours. 81 mg of solid collidine•HCl (0.514 mmol) was then added to the mixture *via* spatula and was stirred at room temperature for 1 day; this afforded a brownish-red solution. ~100 mg of activity III alumina was then added to the vial containing the reaction mixture *via* spatula, and was stirred overnight; the reaction mixture was then filtered through celite and concentrated *in vacuo*. The crude product was purified by flash chromatography (1:1, petroleum ether: benzene) and gave 75 mg (89 %) of the purified product. This workup was repeated without the use of Activity III alumina giving similar yields of **155**.

Spectroscopic data for **155**: IR (cast film, cm⁻¹): 3345 (w, br), 3056 (w), 3020 (w), 2956 (m), 2923 (m), 2869 (w), 2245 (w), 2117 (w), 1658 (s), 1632 (s), 1497 (m), 1468 (m), 1442 (m), 1376 (w), 1279 (w), 1228 (w), 1202 (m), 1094 (w), 1074 (w), 1029 (w), 210 (w), 812 (w), 766 (m), 699 (m); ¹H NMR (400 MHz, C₆D₆): δ 7.16-7.09 (m, 4H, Ar-*H*), δ 7.00 (t, *J*= 7.6 Hz, 1H, Ar-*H*), δ 6.85-6.81 (m, 4H, Ar-*H*), δ 6.80-6.74 (m, 3H, Ar-*H*), δ 6.33 (s, 1H, -N(Ar)*H*), δ 3.06 (ddd, *J*= 7.0, 3.6, 2.4 Hz, 1H, Me₂CHCH₂CH₂), δ 2.30-2.16 (2 overlapping broad s, 8H, 2,6-*Me*₂-Ar), δ 2.10 (dd, *J*= 18.7, 7.0 Hz, 1H, Me₂CHCH₂CH₂), δ 2.00 (dd, *J*= 18.7, 2.3 Hz, 1H, Me₂CHCH₂CH₂), δ 2.00-1.80 (broad s, 4H, 2,6-*Me*₂-Ar), δ 1.73 (dsept, *J*= 3.6, 6.9 Hz, 1H, Me₂CHCH₂CH₂), δ 0.58 (d, *J*=6.9 Hz, 3H, *Me*₂CHCH₂CH₂), δ 0.54 (d, *J*= 6.9

Hz, 3H, $\text{Me}_2\text{CHCHCH}_2$); ^{13}C APT $\{^1\text{H}\}$ NMR (100 MHz, C_6D_6): δ 171.9 ($\text{C}=\text{N}$), 149.7, 138.9, 137.5, 135.5 (Ar or $\text{C}=\text{C}-\text{N}$); 128.7 ($\text{C}=\text{C}-\text{N}$), 128.2 (Ar), 127.6 (Ar), 126.7 (Ar), 125.8 (Ar), 124.9₇ (Ar), 122.9 (Ar), 47.2 ($\text{Me}_2\text{CHCHCH}_2$), 28.1 ($\text{Me}_2\text{CHCHCH}_2$), 27.6 ($\text{Me}_2\text{CHCHCH}_2$), 20.8 ($\text{Me}_2\text{CHCHCH}_2$), 18.3 (2,6- Me_2 -Ar), 17.8 (2,6- Me_2 -Ar), 14.1 ($\text{Me}_2\text{CHCHCH}_2$), signals missing due to incidental overlap; COSY (400 MHz, C_6D_6): δ 3.06 \leftrightarrow δ 2.10, 2.00, 1.73; δ 2.10 \leftrightarrow δ 2.00; δ 1.73 \leftrightarrow δ 0.58, 0.54; HMQC (400 MHz, C_6D_6): δ 7.16-7.09 \leftrightarrow δ 128.2, 127.6; δ 7.00 \leftrightarrow δ 122.9, δ 6.85-6.81 \leftrightarrow δ 125.8, δ 6.80-6.74 \leftrightarrow δ 126.7, 124.9₇; δ 3.06 \leftrightarrow δ 47.2, δ 3.06 \leftrightarrow δ 47.2, δ 3.06 \leftrightarrow δ 47.2, δ 3.06 \leftrightarrow δ 47.2, δ 2.30-2.16 \leftrightarrow δ 18.3, 17.8; δ 2.10, 2.00 \leftrightarrow δ 27.6 δ 1.73 \leftrightarrow δ 28.1, δ 0.58 \leftrightarrow δ 20.8, δ 0.54 \leftrightarrow δ 14.1; HMBC (400 MHz, C_6D_6): δ 7.16-7.09 \leftrightarrow δ 149.7, 128.7, 18.3; δ 7.00 \leftrightarrow δ 125.8, δ 6.85-6.01 \leftrightarrow δ 127.6, 126.7; δ 6.80-6.74 \leftrightarrow δ 135.5, 125.8; δ 6.33 \leftrightarrow δ 171.9, 128.7; δ 3.06 \leftrightarrow δ 137.5, 128.7, 28.1, 14.1; δ 2.30-2.16 \leftrightarrow δ 149.7, 128.2, 125.8; δ 2.10 \leftrightarrow δ 171.9, 137.5, 128.7, 47.2, 17.8; δ 2.00 \leftrightarrow δ 171.9, 137.5, 128.7, 47.2, 17.8; δ 0.58 \leftrightarrow δ 47.1, 28.1, 14.1; δ 0.54 \leftrightarrow δ 47.1, 28.1, 20.8; ESI-MS m/z calculated for $\text{C}_{30}\text{H}_{35}\text{N}_2$ ($\text{M}+\text{H}^+$): 423.27948; found: 423.27902; Elemental Analysis calculated for $\text{C}_{30}\text{H}_{35}\text{N}_2$: C, 85.26 %; H, 8.11 %; Found: C, 85.30 %; H, 8.10 %.

(2,6-Dimethyl-phenyl)-[5-(2,6-dimethyl-phenylimino)-3-isopropyl-2-methyl-cyclopent-1-enyl]-amine (156)

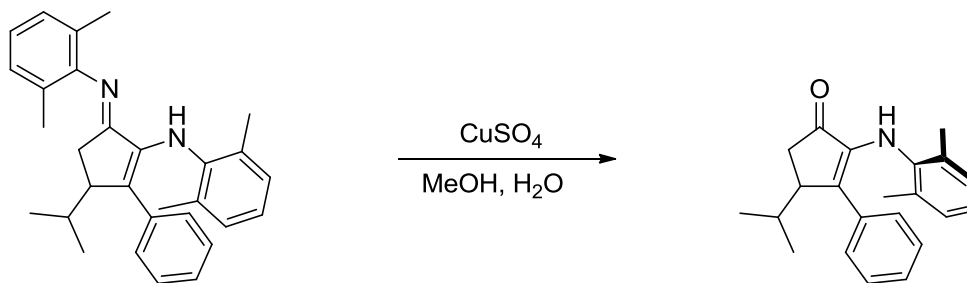


161 mg of the starting titanacyclobutene⁶ (0.588 mmol) and 2 mL of THF were added to a flame-dried 5 dram vial. The vial was then placed in the drybox freezer (-30 °C) for 1 hour. The vial was removed from the freezer and a solution containing 154 mg of 2,6-dimethylphenyl isonitrile (1.17 mol) in 1 mL THF was added *via* glass pipette. The resulting mixture was warmed to room temperature over 1 hour and stirred for an additional 15 hours. 200 mg of collidine•HCl (1.17 mmol) was then added to the

resulting mixture *via* spatula, and was stirred for 1 day at room temperature; this affords a brownish-red solution. The reaction mixture was then filtered through celite and concentrated *in vacuo*. The crude product was purified by flash chromatography (1:1, hexanes: benzene) to give 55 mg (26 %) of the purified product.

Spectroscopic data for **156**: IR (cast film, cm^{-1}): 3339 (w, br), 3012 (w), 2956 (s), 2921 (s), 2869 (m), 1638 (s), 1593 (s), 1469 (s), 1376 (m), 1320 (m), 1264 (m), 1229 (m), 1196 (m), 1162 (w), 1144 (w), 1094 (w), 1034 (w), 985 (w), 928 (w), 899 (w), 832 (w), 766 (s), 738 (w); $^1\text{H NMR}$ (500 MHz, CDCl_3): δ 7.13-7.02 (m, 5H, Ar-H), δ 6.95 (t, J = 7.8 Hz, 1H, Ar-H), δ 5.74 (s, 1H, -N(Ar)H), δ 2.60 (broad s, 1H, $\text{Me}_2\text{CHCHCH}_2$), δ 2.34 (s, 6H, 2,6- Me_2 -Ar), δ 2.16 (s, 3H, 2,6- Me_2 -Ar), δ 2.14 (s, 3H, 2,6- Me_2 -Ar), δ 2.03 (dd, J = 19.0, 7.1 Hz, 1H, $\text{Me}_2\text{CHCHCH}_2$), δ 2.00 (dsept, J = 3.5, 6.9 Hz, 1H, $\text{Me}_2\text{CHCHCH}_2$), δ 1.85 (dd, J = 19.0, 2.1 Hz, 1H, $\text{Me}_2\text{CHCHCH}_2$), δ 1.28 (broad s, 3H, $\text{MeC}=\text{CN}(\text{Ar})\text{H}$), δ 0.58 (d, J = 6.9, 3H, $\text{Me}_2\text{CHCHCH}_2$), δ 0.54 (d, J = 6.9 Hz, 3H, $\text{Me}_2\text{CHCHCH}_2$); $^{13}\text{C APT } \{^1\text{H}\} \text{ NMR}$ (125 MHz, CDCl_3): δ 172.3 ($\text{C}=\text{N}$), 149.6 (Ar), 139.7 (Ar), 137.8 ($\text{C}=\text{C}-\text{N}$), 136.6 (Ar), 128.4 ($\text{C}=\text{C}-\text{N}$), 128.3, 127.9₅, 127.8, 126.4, 126.3, 125.5, 122.6 (Ar); 49.0 ($\text{Me}_2\text{CHCHCH}_2$), 27.8₄ ($\text{Me}_2\text{CHCHCH}_2$), 27.8₁ ($\text{Me}_2\text{CHCHCH}_2$), 21.3 ($\text{Me}_2\text{CHCHCH}_2$), 18.5 (2,6- Me_2 -Ar), 17.9 (2,6- Me_2 -Ar), 14.9₆ ($\text{Me}_2\text{CHCHCH}_2$), 12.2 ($\text{Me}_2\text{CHCHCH}_2$); **COSY** (500 MHz, CDCl_3): δ 2.60 \leftrightarrow δ 2.03, 2.00, 1.85, 1.28; δ 2.03 \leftrightarrow δ 1.85; δ 2.00 \leftrightarrow δ 1.28, 0.58, 0.54; **HMQC** (500 MHz, CDCl_3): δ 6.95 \leftrightarrow δ 122.6, δ 2.60 \leftrightarrow δ 49.0, δ 2.34 \leftrightarrow δ 18.5; δ 2.16, 2.14 \leftrightarrow δ 17.9, δ 2.03, 1.85 \leftrightarrow δ 27.8₄, δ 2.00 \leftrightarrow δ 27.8₁, δ 1.28 \leftrightarrow δ 12.2, δ 0.58 \leftrightarrow δ 21.3, δ 0.54 \leftrightarrow δ 14.9₆, δ 2.30-2.16 \leftrightarrow δ 18.3, 17.8; δ 2.10, 2.00 \leftrightarrow δ 27.6 δ 1.73 \leftrightarrow δ 28.1, δ 0.58 \leftrightarrow δ 20.8, δ 0.54 \leftrightarrow δ 14.1; **HMBC** (500 MHz, CDCl_3): δ 2.34 \leftrightarrow δ 139.7, 136.6; δ 2.16, 2.14 \leftrightarrow δ 172.3, 149.6, 126.4, 126.3; δ 2.03, 1.85 \leftrightarrow δ 172.3, 128.4; δ 1.28 \leftrightarrow δ 172.3, 137.8, 128.4, 49.0; **ESI-MS** m/z calculated for $\text{C}_{25}\text{H}_{32}\text{N}_2$ ($\text{M}+\text{H}^+$): 360.25656; found: 360.25688;

2-(2,6-Dimethyl-phenylamino)-4-isopropyl-3-phenyl-cyclopent-2-enone (160)

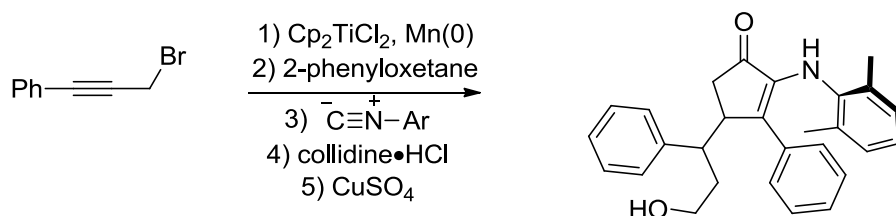


15 mg (0.036 mmol) of the α -imino-enamine, 5 mL of a $\text{MeOH}:\text{H}_2\text{O}$ (1:1) mixture, and a small scoop (~5 mg) of CuSO_4 was added to a 25 mL round bottomed flask. The resulting mixture was then heated at reflux for 16 hours. The mixture was cooled then added to a separatory funnel along with 5 mL diethyl ether. The ether layer was washed with distilled water (2 X 2mL) then the ether layer was separated, and dried over solid MgSO_4 . The mixture was filtered through filter paper and concentrated *in vacuo*. The crude product was then purified using flash chromatography (9:1, Hex , EtOAc) giving 10 mg (88 %) of the purified product.

Spectroscopic data for **160**: **IR** (cast film, cm^{-1}): 3330 (w, br), 3053 (w), 3021 (w), 2956 (m), 2925 (w), 2870 (w), 1701 (s), 1627 (m), 1594 (w), 1499 (m), 1478 (m), 1465 (m), 1442 (w), 1408 (w), 1335 (m), 1277 (m), 1264 (m), 1238 (m), 1227 (m), 1122 (w), 1074 (w), 1028 (w), 1001 (w), 915 (w), 767 (m), 699 (m); **^1H NMR** (500 MHz, CDCl_3): δ 7.00 (m, 1H, Ar-H), δ 6.93 (m, Ar-H), δ 6.80 (broad t, $J = 7.6$ Hz, 1H, Ar-H), δ 6.75 (m, 2H, Ar-H), δ 5.60 (s, 1H, Ar-H), δ 6.80-6.62 (broad s, 1H, -N(Ar)-H), δ 3.33 (ddd, $J = 6.5, 3.4, 2.0$ Hz, 8H, $\text{Me}_2\text{CHCHCH}_2$), δ 2.57 (dd, $J = 19.4, 6.5$ Hz, 1H, $\text{Me}_2\text{CHCHCH}_2$), δ 2.36 (dd, $J = 19.4, 2.0$ Hz, 1H, $\text{Me}_2\text{CHCHCH}_2$), δ 2.20-1.85 (broad s, 5H), δ 1.84 (dsept, $J = 3.4, 7.0$ Hz, 1H, $\text{Me}_2\text{CHCHCH}_2$), δ 0.96 (d, $J = 7.0$, 3H, $\text{Me}_2\text{CHCHCH}_2$), δ 0.56 (d, $J = 7.0$ Hz, 3H, $\text{Me}_2\text{CHCHCH}_2$); **^{13}C APT $\{^1\text{H}\}$ NMR** (125 MHz, CDCl_3): δ 203.7 (C=O), 138.9, 138.1, 137.7, 134.5 (C=C-N, C=C-N or Ar); 127.7, 127.2, 126.8, 126.7, 125.2 (Ar); 44.5 ($\text{Me}_2\text{CHCHCH}_2$), 33.4 ($\text{Me}_2\text{CHCHCH}_2$), 28.2 ($\text{Me}_2\text{CHCHCH}_2$), 21.5 ($\text{Me}_2\text{CHCHCH}_2$), 18.6 (2,6- Me_2 -Ar), 14.2 ($\text{Me}_2\text{CHCHCH}_2$), signals missing due to incidental overlap; **COSY** (500 MHz, CDCl_3): δ 7.00 \leftrightarrow δ 6.93, 6.75; δ 6.93 \leftrightarrow δ 6.75; δ 3.33 \leftrightarrow δ 2.57, 2.36, 1.84; δ 3.33 \leftrightarrow δ 2.57, 2.36, 1.84; δ 2.57 \leftrightarrow δ 2.36; δ 1.84 \leftrightarrow δ 0.96, 0.54; **HMQC** (500 MHz, CDCl_3): δ 7.00 \leftrightarrow δ

126.7; δ 6.93 \leftrightarrow δ 126.8, δ 6.80 \leftrightarrow δ 125.2, δ 6.75 \leftrightarrow δ 127.7; δ 3.33 \leftrightarrow δ 44.5, δ 2.57, 2.36 \leftrightarrow δ 33.4, δ 1.84 \leftrightarrow δ 28.2, δ 0.96 \leftrightarrow δ 21.5, δ 0.56 \leftrightarrow δ 14.2; **EI-MS** m/z calculated for $C_{22}H_{25}NO$ (M^+): 319.19361; found: 319.19360.

**2-(2,6-Dimethyl-phenylamino)-4-(3-hydroxy-1-propyl)-3-phenyl-cyclopent-2-enone
(171)**



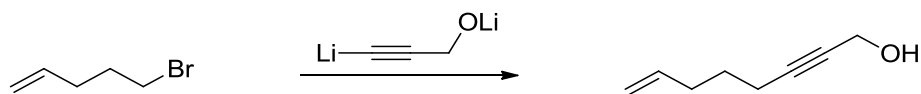
Preparation of titanacyclobutene: 250 mg of Mn powder (4.58 mmol), 10 mg of $PbCl_2$ (0.036 mmol), 10 mg of TMS-Cl (0.093 mmol), and 3 mL of THF was added to a flame-dried 5 dram vial. The mixture was then stirred at 40 °C for one hour, or until a grey aggregate was formed. 460 mg of solid Cp_2TiCl_2 (1.85 mmol) was then added to the vial containing the grey mixture *via*, and the vial was then placed in the drybox freezer (-30 °C) for 1 hour. The vial was removed from the freezer and was quickly treated with a solution containing 180 mg of 1-bromo-3-phenyl-2-propyne^{6,276} (0.983 mmol) in 2 mL THF *via* glass pipette; the vial was then placed back in the drybox freezer (-30 °C) for 16 hours. During this time the color of the solution became a dark purplish-red. The vial was then removed from the freezer and warmed to room temperature over 4 hours; during this time the color of the solution changed from purplish-red to an emerald green. The green reaction mixture was then filtered through celite into another 5 dram vial, and was placed back into the drybox freezer (-30 °C) for 1 hour. The vial was removed, and quickly treated with a solution containing 124 mg of 1-phenyl oxetane (0.924 mmol) in 1 mL THF *via* glass pipette, then placed back in the drybox freezer (-30 °C) for 3 hours; upon addition of the oxetane, the solution color immediately changed from green to purple. The solution was allowed to warm to room temperature over 2 hours, filtered through celite, and then concentrated *in vacuo* which gave a dark red oil.

Insertion of Isonitrile: The dark red crude titanacyclobutene complex was re-dissolved in 2 mL THF in the same 5 dram vial, this vial was then placed in the drybox freezer (-30 °C) for 1 hour. The vial was removed from the freezer and treated with a solution containing 500 mg of 2,6-dimethyl phenyl isonitrile (3.81 mmol) in 1 mL THF *via* glass pipette; the mixture was then warmed to room temperature over 1 hour, then stirred for an additional 15 hours. 1.0 g of solid collidine•HCl (6.35 mmol) was then added the reaction mixture *via* spatula; the mixture was then stirred at room temperature for 1 day. The resulting brown solution was then filtered through celite, and concentrated *in vacuo*, which affords a red oil. The red oil, 5 mL of a MeOH:H₂O (1:1) solution and a pinch of CuSO₄ (~5 mg) was added into a 25 mL round bottomed flask; then the mixture was heated to reflux overnight. The solution was cooled, then 5 mL of both distilled water and 5 mL of diethyl ether was added; the resulting two-layers were transferred to a separatory funnel. The organic layer was separated from the aqueous layer, then the ether layer was washed sequentially with saturated NH₄Cl_(aq) solution (1 X 20 mL) and distilled water (2 X 20 mL). The organic layer was dried over MgSO₄, filtered through filter paper, and concentrated *in vacuo*. The residue was purified by flash chromatography (3:1, Hx:EtOAc) resulting in 63 mg (16.5 %) of the purified product.

Spectroscopic data for **171**: IR (cast film, cm⁻¹): 3365 (w, br), 3059 (w), 3028 (w), 2925 (w), 2271 (w), 1697 (s), 1632 (w), 1594 (w), 1497 (m), 1477 (m), 1442 (w), 1336 (w), 1231 (w), 1046 (w), 911 (w), 766 (m), 732 (m), 701 (m); ¹H NMR (500 MHz, CDCl₃): δ 7.17-7.14 (m, 3H, Ar-H), δ 7.04 (apparent t, *J* = 7.2 Hz, 1H, Ar-H), δ 6.96 (apparent t, *J* = 7.2 Hz, 2H, Ar-H), δ 6.84-6.80 (m, 3H, Ar-H), δ 6.73 (apparent d, *J* = 7.2 Hz, 2H, Ar-H), δ 5.38 (broad s, 1H, N-H), δ 3.70 (m, 1H, -CH₂C(Ph)H-), δ 3.59 (ddd, *J* = 10.9, 6.6, 5.8 Hz, 1H, -C(Ph)HCH₂CH₂OH), δ 3.50 (app dt, *J* = 10.9, 7.0 Hz, 1H, -C(Ph)HCH₂CH₂OH), δ 3.05 (ddd, *J* = 10.9, 5.8, 3.5 Hz, 1H, -C(Ph)HCH₂CH₂OH), δ 2.66 (dd, *J* = 18.9, 6.6 Hz, 1H, -CH₂CH-), δ 2.57 (dd, *J* = 18.9, 1.8 Hz, 1H, -CH₂CH-), δ 2.10-2.02 (m, 1H, -C(Ph)HCH₂CH₂OH), δ 1.96 (dddd, *J* = 13.6, 7.0, 6.6, 5.8 Hz, 1H, -C(Ph)HCH₂CH₂OH), δ 2.20- 1.00 (broad s, 6H, 2,6-Me₂-Ar); ¹³C {¹H} NMR (125 MHz, CDCl₃): δ 202.6 (C=O), 138.9₉, 138.5, 137.6, 136.5, 134.5 (Ar); 128.9 (Ar), 127.8 (Ar), 127.7₅ (Ar), 127.7 (Ar), 126.9₉ (Ar), 126.9, (Ar), 126.8 (Ar), 125.3 (Ar), 61.2 (-C(Ph)HCH₂CH₂OH), 43.9 (-CH₂CH-), 42.7 (-C(Ph)HCH₂CH₂OH), 36.6 (-C(Ph)HCH₂CH₂OH), 35.1 (-CH₂CH-), 18.4 (2,6-Me₂-Ar), signals missing due to incidental

overlap; **COSY** (500 MHz, CHCl₃): δ 3.70 \leftrightarrow δ 3.05, 2.66, 2.57; δ 3.59 \leftrightarrow δ 3.50, 2.06, 1.96; δ 3.50 \leftrightarrow δ 2.06, 1.96; δ 2.66 \leftrightarrow δ 2.57, δ 2.06 \leftrightarrow δ 1.96; **HSQC** (500 MHz, CDCl₃): δ 7.17-7.14 \leftrightarrow δ 127.7₅; δ 7.04 \leftrightarrow δ 127.6. δ 6.96 \leftrightarrow δ 127.7, δ 6.84-6.80 \leftrightarrow δ 128.9; δ 6.73 \leftrightarrow δ 127.8, δ 3.70 \leftrightarrow δ 43.9, δ 3.59, 3.50 \leftrightarrow δ 61.2, δ 3.05 \leftrightarrow δ 42.7, δ 2.66, 2.57 \leftrightarrow δ 35.1; δ 2.06, 1.96 \leftrightarrow δ 36.6, δ 2.20-1.00 \leftrightarrow δ 18.4; **ESI-MS** calculated for C₂₈H₂₉O₂N: 412.2271 (M+H⁺), 434.2091 (M+Na⁺); Found: 412.2269 (M+H⁺), 434.2087 (M+Na⁺).

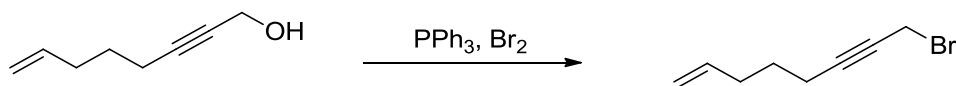
Oct-7-en-2-yn-1-ol¹¹⁴ (177)



150 mL of dry ammonia was condensed into a 500 mL three-neck flask at -78 °C which was equipped with a dry-ice condenser, a glass stopper and a vacuum adapter. A pinch of solid Fe(NO₃)₃ (~0.05 g) was then introduced to the three-neck flask; once the solid Fe(NO₃)₃ had dissolved, 0.763 g of Li wire (0.110 mol) was added in 7 portions over 40 minutes. During each addition of lithium wire, the color of the ammonia solution became initially dark blue then evolved light brown with the expulsion of gas; this indicates that lithium amide was formed. 3.2 mL of propargyl alcohol (0.055 mol) was added dropwise *via* plastic syringe, then the mixture was stirred for 1 hour; during this time a grayish-white solid had formed. 6 mL of 1-bromo-4-pentene (0.051 mol) was added dropwise *via* plastic syringe over 30 minutes, then the mixture was stirred for 16 hours; during this time the mixture was slowly warmed to room temperature, allowing ammonia to be released from the flask. After this time a grey solid remained at the bottom of the flask. 100 mL of saturated NH₄Cl_(aq) was then added to the grey residue and the mixture was stirred for 1 hour. The aqueous solution was then extracted with diethyl ether (3 X 100 mL). The extracts were dried over MgSO₄, filtered through filter paper and the volatiles were removed *in vacuo* which afforded a light yellow oil. The product was purified by flash chromatography (9:1, Hx:EtOAc) which yielded 4.701 g (75

% of the purified product. The ^1H NMR spectrum of the product exactly matches that of the ^1H NMR spectrum of **177** from previous characterization data.¹¹⁴

8-Bromo-oct-1-en-6-yne (179)



4.1 g of solid PPh_3 (0.016 mol) and 30 mL of CH_2Cl_2 were introduced into a 100 mL round bottomed flask; this flask was then cooled 0°C . 0.83 mL of Br_2 (0.016 mol) was then added dropwise *via* plastic syringe to the $\text{PPh}_3/\text{CH}_2\text{Cl}_2$ solution; this solution was then stirred for 15 minutes which affords a white suspension. The resulting heterogeneous solution containing the white suspension was then added dropwise *via* glass pipette to a 200 mL round bottomed flask which contains a cooled (0°C) solution of 2.0 g of oct-7-en-2-yn-1-ol (0.016 mol) in 10 mL CH_2Cl_2 . The mixture was then stirred for 16 hours; during this time the mixture was warmed to room temperature. The volatiles were removed *in vacuo*. 20 mL of diethyl ether was added to create a suspension of triphenylphosphine oxide, which was removed by filtering the heterogeneous mixture through celite. This process was repeated two more times until minimal white solid remained. The resulting residue was purified by flash chromatography (9:1, Hx:EtOAc) in which 2.95 g (99 %) of the desired product was obtained.

Spectroscopic data for **179**: IR (neat film, cm^{-1}): 3076 (w), 2998.1 (w), 2976 (w), 2940 (s), 2862 (w), 2842 (w), 2310 (w), 2233 (w), 1715 (w), 1641 (m), 1454 (w), 1431 (m), 1330 (w), 1209 (s), 992 (m), 915 (s), 862 (w); ^1H NMR (500 MHz, CDCl_3): δ 5.81 (ddt $J=$ 17.1, 10.2, 6.8 Hz, 1H, $-\text{H}_2\text{CCH}=\text{CH}_2$), δ 5.07 (ddt $J=$ 17.1, 1.8, 1.6 Hz, 1H, $-\text{H}_2\text{CCH}=\text{CH}_2$), δ 5.02 (ddt $J=$ 10.2, 1.9, 1.2 Hz, 1H, $-\text{H}_2\text{CCH}=\text{CH}_2$), δ 4.15 (t, $J=$ 2.4 Hz, 2H, $-\text{C}\equiv\text{CCH}_2\text{Br}$), δ 2.28 (tt, $J=$ 7.1, 2.4 Hz, 2H, $-\text{CH}_2\text{C}\equiv\text{C}-$), δ 2.17 (m, 2H, $-\text{H}_2\text{CCH}=\text{CH}_2$), δ 1.64 (pent, $J=$ 7.4 Hz, 2H, $-\text{CH}_2\text{CH}_2\text{CH}_2-$); ^{13}C $\{^1\text{H}\}$ NMR (125 MHz, CDCl_3): δ 137.7 ($\text{H}_2\text{C}=\text{CHCH}_2$), 115.3 ($\text{H}_2\text{C}=\text{CHCH}_2$), 87.9 ($-\text{C}\equiv\text{CCH}_2\text{Br}$), 75.6 ($-\text{C}\equiv\text{CCH}_2\text{Br}$), 32.7 ($-\text{H}_2\text{CCH}=\text{CH}_2$), 27.5 ($-\text{CH}_2\text{CH}_2\text{CH}_2-$), 18.3 ($-\text{CH}_2\text{C}\equiv\text{C}-$), 15.7 ($-\text{C}\equiv\text{CCH}_2\text{Br}$); COSY (500 MHz, CHCl_3): δ 5.81 \leftrightarrow δ 5.07, 5.02, 2.17; δ 5.02 \leftrightarrow δ 2.17; δ 4.15 \leftrightarrow δ 2.28; δ 2.28 \leftrightarrow δ 1.64; δ 2.17 \leftrightarrow δ 1.64; HMQC (500 MHz,

CDCl₃): δ 5.81 \leftrightarrow δ 137.7, δ 5.07, 5.02 \leftrightarrow δ 115.3, δ 4.15 \leftrightarrow δ 15.7, δ 2.28 \leftrightarrow δ 18.3, δ 2.17 \leftrightarrow δ 32.7; δ 1.64 \leftrightarrow δ 27.5; **EI-MS** *m/z* calculated for: C₈H₁₂⁸¹Br(M⁺+H), 189.01019; C₈H₁₂⁷⁹Br(M⁺+H), 187.01224; Found: C₈H₁₂⁸¹Br(M⁺+H), 189.01039; C₈H₁₂⁷⁹Br(M⁺+H), 187.01225; No M⁺ ion found.

2-(6-Bromo-hex-4-ynyl)-oxirane (**172**)

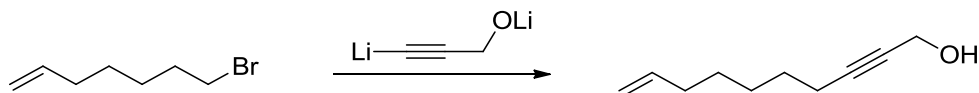


1.96 g of 8-bromo-oct-1-en-6-yne (0.010 mol) and 30 mL of CH₂Cl₂ was introduced into a 100 mL round bottom flask; this flask was then cooled to 0 °C. 3.2 g of *m*-CPBA (75 % by wt., 0.014 mol) was then added *via* spatula in 4 portions over 15 mins; the resulting mixture was then stirred for 18 hours; during this time the reaction was warmed to room temperature. The reaction mixture was then filtered through celite to remove the insoluble benzoic acid that was formed during the reaction. The filtrate was transferred to a separatory funnel and the organic layer was washed in sequence with saturated aqueous solutions of sodium metabisulfite (2 X 30 mL), NaHCO_{3(aq)} (2 X 30 mL) and then brine (1 X 30 mL). The organic layer was then dried over MgSO₄, then filtered through filter paper, and finally concentrated *in vacuo*. The crude product was purified by flash chromatography (9:1, Hx:EtOAc) in which 0.97 g (46 %) of the desired product was obtained.

Spectroscopic data for **172**: **IR** (neat film, cm⁻¹): 3048 (w), 2989 (m), 2943 (s), 2310 (w), 2233 (m), 1482 (w), 1455 (m), 1430 (m), 1411 (m), 1330 (w), 1294 (m), 1217 (s), 1153 (w), 919 (m), 861 (m), 833 (m); **¹H NMR** (400 MHz, CDCl₃): δ 3.90 (apparent t, *J*= 2.4 Hz, 2H, -C≡CCH₂Br), δ 2.85 (m, 1H, -CH₂CH₂CH(O)CH₂), δ 2.74 (dd, *J*= 5.0, 3.8 Hz, 1H, -CH₂CH₂CH(O)CH₂), δ 2.47 (dd, *J*= 5.0, 2.6 Hz, 1H, -CH₂CH₂CH(O)CH₂), δ 2.30 (m, 2H, -CH₂C≡C-), δ 1.80-1.50 (m, 4H, -CH₂CH₂CH(O)CH₂); **¹³C {¹H} NMR** (100 MHz, CDCl₃): δ 86.9 (-C≡CCH₂Br), 75.5 (-C≡CCH₂Br), 51.3 (-CH₂CH₂CH(O)CH₂), 46.5 (-CH₂CH₂CH(O)CH₂), 31.0 (-CH₂CH₂CH(O)CH₂), 24.4 (-CH₂CH₂CH(O)CH₂), 18.3 (-CH₂C≡C-), 15.1 (-C≡CCH₂Br); **COSY** (400 MHz, CHCl₃): δ 3.90 \leftrightarrow δ 2.30; δ 2.85 \leftrightarrow δ 2.74, 2.47, 1.80-1.50; δ 2.74 \leftrightarrow δ 2.47;

δ 2.30 \leftrightarrow δ 1.80-1.50; **HMQC** (400 MHz, CDCl_3): δ 3.90 \leftrightarrow δ 15.1, δ 2.85 \leftrightarrow δ 51.3, δ 2.74, 2.47 \leftrightarrow δ 46.5, δ 2.30 \leftrightarrow δ 18.3, δ 1.80-1.50 \leftrightarrow δ 31.1, 24.4; **Elemental Analysis** calculated for $\text{C}_8\text{H}_{11}\text{OBr}$: C, 47.32 %; H, 5.46 %; Found: C, 44.30 %; H, 5.13 %.

Dec-9-en-2-yn-1-ol (**178**)

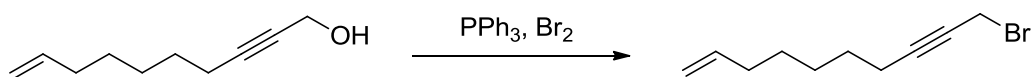


150 mL of dry ammonia was condensed into a 500 mL three-neck flask equipped with a dry-ice condenser, a glass stopper and a vacuum adapter at $-78\text{ }^\circ\text{C}$. A pinch of solid $\text{Fe}(\text{NO}_3)_3$ ($\sim 0.05\text{ g}$) was introduced to the flask *via* spatula, once the $\text{Fe}(\text{NO}_3)_3$ solid was dissolved, 0.435 g of Li wire (0.063 mol) was added in 7 portions over half an hour. During each addition of lithium wire, the color of the ammonia solution changed from dark blue to light brown with the expulsion of gas; this indicated that lithium amide had been formed. 1.8 mL of propargyl alcohol (0.031 mol) was added dropwise *via* plastic syringe to the lithium amide mixture, and was stirred for 1 hour; during this time a grayish-white solid formed. 5 g of 1-bromo-6-heptene (0.033 mol) was then added dropwise to the mixture *via* plastic syringe, and the mixture was stirred for 16 hours. During this time, the mixture was warmed to room temperature while allowing the ammonia to evaporate; a grey residue remained after the ammonia had evaporated. 100 mL of saturated $\text{NH}_4\text{Cl}_{(\text{aq})}$ was added to the white residue remaining in the flask and stirred for 1 hour. The aqueous solution was then transferred to a separatory funnel and extracted with diethyl ether (3 X 100 mL). The combined ether extracts were dried over MgSO_4 , filtered through filter paper then concentrated *in vacuo* resulting in a light yellow oil. The product was purified by flash chromatography (9:1, Hx:EtOAc) to yield 3.48 g (80 %) of product.

Spectroscopic data for **178**: **IR** (neat film, cm^{-1}): 3336 (s, br), 3077 (w), 2932 (s), 2858 (m), 2288 (w), 2226 (w), 1641 (m), 1457 (m), 1435 (m), 1256 (w), 1228 (w), 1136 (m), 1013 (m), 911 (m), 836 (w), 779 (w); **$^1\text{H NMR}$** (400 MHz, CDCl_3): δ 5.80 (ddt $J = 17.0, 10.2, 6.8\text{ Hz}$, 1H, $-\text{H}_2\text{CCH}=\text{CH}_2$), δ 4.99 (ddt $J = 17, 2.2, 1.6\text{ Hz}$, 1H, $-\text{H}_2\text{CCH}=\text{CH}_2$), δ 4.93 (ddt $J =$

10.2, 2.2, 1.3 Hz, 1H, $-H_2CCH=CH_2$), δ 4.24 (s, 2H, $-C\equiv CCH_2OH$), δ 2.21 (tt, $J = 6.8, 2.2$ Hz, 2H, $-CH_2C\equiv C-$), δ 2.05 (m, 2H, $-H_2CCH=CH_2$), δ 1.80 (s, 1H, $-C\equiv CCH_2OH$), δ 1.51 (m, 2H, $-CH_2CH_2CH_2-$), δ 1.40 (m, 4H, $-CH_2CH_2CH_2-$); $^{13}C \{^1H\}$ NMR (100 MHz, $CDCl_3$): δ 138.5 ($-H_2CCH=CH_2$), 113.9₅ ($-H_2CCH=CH_2$), 86.0 ($-C\equiv CCH_2OH$), 77.9₇ ($-C\equiv CCH_2OH$), 50.9 ($-C\equiv CCH_2OH$), 33.2 ($-H_2CCH=CH_2$), 28.0, 27.9₇, 27.9, ($-CH_2CH_2CH_2-$), 18.3 ($-CH_2C\equiv C$); COSY (400 MHz, $CHCl_3$): δ 5.80 \leftrightarrow δ 4.99, 4.93, 2.05; δ 4.99 \leftrightarrow δ 4.93, 2.05; δ 4.93 \leftrightarrow δ 2.05; δ 4.24 \leftrightarrow δ 2.21, 1.80; δ 2.21 \leftrightarrow δ 1.51; δ 2.05 \leftrightarrow δ 1.40, 1.51; δ 1.51 \leftrightarrow δ 1.41; HMQC (400 MHz, $CDCl_3$): δ 5.80 \leftrightarrow δ 138.5, δ 4.99, 4.93 \leftrightarrow δ 113.9₅, δ 4.24 \leftrightarrow δ 50.9, δ 2.21 \leftrightarrow δ 18.3, δ 2.05 \leftrightarrow δ 33.2; δ 1.51, 1.40 \leftrightarrow δ 28.0, 27.9₇, 27.9; EI-MS m/z calculated for: $C_{10}H_{15}O(M^+-H)$, 151.11229; Found: $C_{10}H_{15}O(M^+-H)$, 151.11208; No M^+ ion found; Elemental Analysis calculated for $C_{10}H_{16}O$: C, 78.90 %; H, 10.59 %; Found: C, 78.15 %; H, 10.58 %.

10-Bromo-dec-1-en-8-yne (180)



3.3 g of PPh_3 (0.013 mol) and 30 mL of CH_2Cl_2 were introduced into a 100 mL round bottom flask, which was cooled to 0 °C. 0.68 mL of Br_2 (0.013 mol) was then added dropwise *via* plastic syringe to the PPh_3/CH_2Cl_2 solution; the resulting mixture was stirred for 15 minutes; during this time a white suspension had formed. The white suspension was then added dropwise *via* glass pipette into a 100 mL round bottom flask which contains a cooled (0 °C) solution of 2.0 g of dec-9-en-2-yn-1-ol (0.013 mol) in 10 mL CH_2Cl_2 . The resulting mixture was stirred for 16 hours; during this time the mixture was warmed to room temperature. The volatiles were then removed *in vacuo* then 20 mL of diethyl ether was added to the crude product in order to precipitate triphenylphosphine oxide, which was removed by filtering the heterogeneous solution through celite. This process was repeated two more times until minimal white solid remained. The resulting residue was purified by flash chromatography (9:1, Hx:EtOAc) in which 2.76 g (98 %) of the desired product was obtained.

Spectroscopic data for **180**: **IR** (neat film, cm^{-1}): 3076 (w), 2998 (w), 2976 (w), 2940 (s), 2862 (w), 2841 (w), 2310 (w), 2233 (w), 1710 (w), 1641 (m), 1431 (m), 1330 (w), 1209 (s), 1153 (w), 993 (m), 915 (s), 863 (w); **^1H NMR** (500 MHz, CDCl_3): δ 5.83 (ddt, $J = 16.9, 10.2, 6.7$ Hz, 1H, $-\text{H}_2\text{CCH}=\text{CH}_2$), δ 5.02 (ddt $J = 16.9, 2.1, 1.5$ Hz, 1H, $-\text{H}_2\text{CCH}=\text{CH}_2$), δ 4.87 (ddt, $J = 10.2, 2.1, 1.3$ Hz, 1H, $-\text{H}_2\text{CCH}=\text{CH}_2$), δ 3.95 (t, $J = 2.4$ Hz, 2H, $-\text{C}\equiv\text{CCH}_2\text{Br}$), δ 2.26 (tt, $J = 7.0, 2.4$ Hz, 2H, $-\text{CH}_2\text{C}\equiv\text{C}-$), δ 2.08 (m, 2H, $-\text{H}_2\text{CCH}=\text{CH}_2$), δ 1.58-1.50 (m, 2H, $-\text{CH}_2\text{CH}_2\text{CH}_2-$), δ 1.45-1.39 (m, 4H, $-\text{CH}_2\text{CH}_2\text{CH}_2-$); **^{13}C $\{^1\text{H}\}$ NMR** (125 MHz, CDCl_3): δ 138.9 ($-\text{H}_2\text{CCH}=\text{CH}_2$), 114.4 ($-\text{H}_2\text{CCH}=\text{CH}_2$), 88.2 ($-\text{C}\equiv\text{CCH}_2\text{Br}$), 75.4 ($-\text{C}\equiv\text{CCH}_2\text{Br}$), 33.6 ($-\text{H}_2\text{CCH}=\text{CH}_2$), 28.4, 28.3, 28.2 ($-\text{CH}_2\text{CH}_2\text{CH}_2-$), 18.9 ($-\text{CH}_2\text{C}\equiv\text{C}-$), 15.8 ($-\text{C}\equiv\text{CCH}_2\text{Br}$); **COSY** (500 MHz, CHCl_3): δ 5.83 \leftrightarrow δ 5.02, 4.87, 2.08; δ 5.02 \leftrightarrow δ 4.87, 2.08; δ 4.87 \leftrightarrow δ 2.08; δ 3.95 \leftrightarrow δ 2.26; δ 2.26 \leftrightarrow δ 1.58-1.50; δ 2.08 \leftrightarrow δ 1.45-1.39; **HMQC** (500 MHz, CDCl_3): δ 5.83 \leftrightarrow δ 138.9, δ 5.02, 4.87 \leftrightarrow δ 114.4, δ 3.95 \leftrightarrow δ 15.8, δ 2.26 \leftrightarrow δ 18.9, δ 2.08 \leftrightarrow δ 33.6; δ 1.58-1.50, 1.45-1.39 \leftrightarrow δ 28.4, 28.3, 28.2; **EI-MS** m/z calculated for: $\text{C}_{10}\text{H}_{16}^{81}\text{Br}(\text{M}^+\text{+H})$, 217.04149; $\text{C}_{10}\text{H}_{16}^{79}\text{Br}(\text{M}^+\text{+H})$, 215.04353; Found: $\text{C}_{10}\text{H}_{16}^{81}\text{Br}(\text{M}^+\text{+H})$, 217.04183; $\text{C}_{10}\text{H}_{16}^{79}\text{Br}(\text{M}^+\text{+H})$, 215.04366; No M^+ ion found.

2-(8-Bromo-oct-6-ynyl)-oxirane (173)

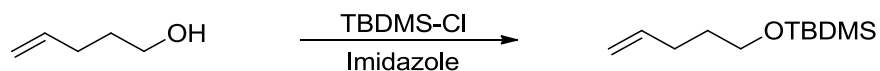


1.79 g of 10-bromo-dec-1-en-8-yne (8.32 mmol) and 30 mL of CH_2Cl_2 were introduced into a 250 mL round bottom flask, which was then cooled to 0°C . 3.2 g of solid *m*-CPBA (75 % by wt., 13.9 mmol) was then added in 4 portions over 30 minutes, then the mixture was stirred for 18 h; during this time the reaction was warmed to room temperature. The reaction mixture was filtered through celite to remove the insoluble benzoic acid which was formed during the reaction. The filtrate was then transferred to a separatory funnel and washed in sequence with saturated aqueous solutions of sodium metabisulfite (2 X 30 mL), $\text{NaHCO}_3(\text{aq})$ (2 X 30 mL) and then brine (1 X 30 mL). The organic layer was dried over MgSO_4 , filtered through filter paper then concentrated *in vacuo*. The product was purified by flash chromatography (9:1, Hx:EtOAc) in which

0.55 g (28 %) of the desired product is obtained. Note: The product yield is not accurate due to spillage of the product on the bench-top during workup.

Spectroscopic data for **173**: IR (neat film, cm^{-1}): 3045 (w), 2935 (s), 2859 (m), 2311 (w), 2233 (w), 1463 (w), 1429 (w), 1410 (w), 1259 (w), 1217 (m), 1129 (w), 1027 (w), 916 (w), 834 (m), 792 (w), 736 (w); $^1\text{H NMR}$ (400 MHz, CDCl_3): δ 3.91 (apparent t, $J = 2.4$ Hz, 2H, $-\text{C}\equiv\text{CCH}_2\text{Br}$), δ 2.90 (m, 1H, $-\text{CH}(\text{O})\text{CH}_2$), δ 2.74 (dd, $J = 5.2, 4.0$ Hz, 1H, $-\text{CH}(\text{O})\text{CH}_2$), δ 2.43 (dd, $J = 5.2, 2.7$ Hz, 1H, $-\text{CH}(\text{O})\text{CH}_2$), δ 2.24 (apparent tt, $J = 6.8, 2.4$ Hz, 2H, $-\text{CH}_2\text{C}\equiv\text{C}-$), δ 1.60-1.40 (m, 8H, $-\text{CH}_2\text{CH}_2\text{CH}_2\text{CH}_2-$); $^{13}\text{C}\{^1\text{H}\}$ NMR (100 MHz, CDCl_3): δ 87.6 ($-\text{C}\equiv\text{CCH}_2\text{Br}$), 75.0 ($-\text{C}\equiv\text{CCH}_2\text{Br}$), 51.9 ($-\text{CH}(\text{O})\text{CH}_2$), 46.7 ($-\text{CH}(\text{O})\text{CH}_2$), 31.9 ($-\text{CH}_2\text{CH}(\text{O})\text{CH}_2$), 28.1, 27.8, 25.1 ($-\text{CH}_2\text{CH}_2\text{CH}_2-$), 18.4 ($-\text{CH}_2\text{C}\equiv\text{C}-$), 15.3 ($-\text{C}\equiv\text{CCH}_2\text{Br}$); COSY (400 MHz, CHCl_3): δ 3.91 \leftrightarrow δ 2.43; δ 2.90 \leftrightarrow δ 2.74, 2.40, 1.59; δ 2.74 \leftrightarrow δ 2.40; δ 2.40 \leftrightarrow δ 1.59; HMQC (400 MHz, CDCl_3): δ 3.91 \leftrightarrow δ 15.3, δ 2.90 \leftrightarrow δ 51.9, δ 2.74, 2.43 \leftrightarrow δ 46.7, δ 1.60 - 1.40 \leftrightarrow δ 31.9, 27.8, 25.1; **Elemental Analysis** calculated for $\text{C}_{10}\text{H}_{15}\text{OBr}$: C, 51.97 %; H, 6.54 %; Found: C, 50.43 %; H, 6.29 %.

Tert-butyl-dimethyl-pent-4-enyloxy-silane²⁸⁰ (**182**)



30.0 g of solid TBDMS-Cl (0.200 mol), 14 g of solid Imidazole (0.206 mol) and 250 mL of CH_2Cl_2 were added to a 500 mL round bottom flask, the flask was then cooled to 0 °C. 20.0 mL of 4-penten-1-ol (0.193 mol) was then introduced dropwise over 20 min *via* plastic syringe to the cooled CH_2Cl_2 solution; this mixture was stirred for 6 hours where a white precipitate formed during this time. The resulting mixture was filtered through celite, and the filtrate was transferred to a separatory funnel. The organic layer was washed in sequence with saturated $\text{NH}_4\text{Cl}_{(\text{aq})}$ (3 X 50 mL) then brine (2 X 50 mL). The organic layer was dried over MgSO_4 , filtered through filter paper, and then concentrated *in vacuo*. The product was purified by vacuum distillation (35 °C at 0.1 mmHg) resulting in 36.9 g product (95 %). This was carried on to the next step without

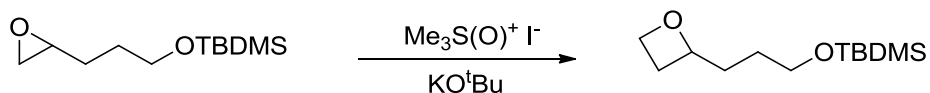
further purification. The ^1H NMR spectrum of the product exactly matches that of the ^1H NMR spectrum of **182** from previous characterization data.²⁸⁰

***Tert*-butyl-dimethyl-(3-oxiranyl-propoxy)-silane²⁸⁰ (183)**



36.9 g of the *tert*-butyl-dimethyl-pent-4-enyloxy-silane (0.184 mol) and 250 mL of CH_2Cl_2 were introduced into a 500 mL round bottom flask; this solution was cooled to $0\text{ }^\circ\text{C}$. 45.0 g of solid *m*-CPBA (75 % by wt, 0.200 mol) was then added in portions of 5 g *via* spatula over 1 hour. The resulting mixture was warmed to room temperature and stirred for 16 hours; during this time a white suspension had formed. The resulting mixture was filtered through celite to remove the insoluble benzoic acid formed during the reaction; the filtrate was then transferred to a separatory funnel where the organic layer was washed in sequence with saturated aqueous solutions of sodium metabisulfite (1 X 50 mL), $\text{NaHCO}_{3(\text{aq})}$ (2 X 50 mL), then brine (1 X 50 mL). The resulting organic layer was dried over MgSO_4 , filtered through filter paper, and concentrated *in vacuo*. The product was purified by vacuum distillation ($55\text{-}60\text{ }^\circ\text{C}$ at 0.1 mm Hg) giving 31.2 g (78 %) of the pure product. The ^1H NMR spectrum of the product exactly matches that of the ^1H NMR spectrum of **183** from previous characterization data.²⁸⁰

***Tert*-butyl-dimethyl-(3-oxetan-2-yl-propoxy)-silane (184)**

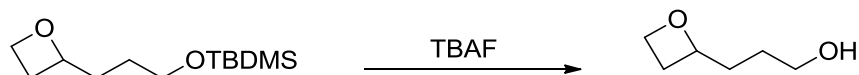


300 mL of $^t\text{BuOH}$ was added via plastic syringe into a 500 mL 3-necked round bottom flask, which was equipped with two rubber stoppers and a water condenser; the flask was then heated to $45\text{ }^\circ\text{C}$. 8.46 g of potassium metal (0.216 mol) was carefully added to the warmed $^t\text{BuOH}$ in 1.0 g portions over 6 hours. After all of the potassium had been added the mixture was then heated to $80\text{ }^\circ\text{C}$ overnight to insure complete

formation of potassium *tert*-butoxide salt. The resulting colorless mixture was cooled to 45 °C and 47.6 g of solid $\text{Me}_3\text{S}(\text{O})^+\text{I}^-$ (0.216 mol) was added *via* spatula; the mixture was stirred for 2 hours which afforded a white precipitate suspended in $^t\text{BuOH}$. 31.2 g of the epoxy-silyl ether (0.144 mol) was then added into the flask *via* syringe and the mixture was maintained at 45 °C for 2 days; during this time, the $^t\text{BuOH}$ solution became a faint yellow. The flask was then cooled to room temperature and 100 mL of distilled water was added to the $^t\text{BuOH}$ solution and was stirred for 1 hour. The mixture was then transferred to a separatory funnel, to which the aqueous layer was extracted with 3 X 100 mL of diethyl ether. The combined organic layers were combined, dried over MgSO_4 , filtered through filter paper and concentrated *in vacuo*. The product was purified by flash chromatography (9:1. Hx, EtOAc) in which 13.8 g (41.0 %) of the desired product was obtained.

Spectroscopic data for **184**: IR (neat film, cm^{-1}): 2954 (s), 2930 (s), 2883 (s), 2858 (s), 1472 (w), 1463 (w), 1388 (w), 1361 (w), 1256 (m), 1100 (s), 983 (m), 836 (s), 776 (m); ^1H NMR (400 MHz, CDCl_3): δ 4.83 (apparent pent, $J = 6.9$ Hz, 1H, $:\text{CHOCH}_2\text{CH}_2:$), 4.65 (ddd, $J = 8.4, 7.8, 5.9$ Hz, 1H, $:\text{CHOCH}_2\text{CH}_2:$), δ 4.49 (ddd, $J = 9.1, 5.9, 5.7$ Hz, 1H, $:\text{CHOCH}_2\text{CH}_2:$), δ 3.62 (apparent td, $J = 6.4, 1.8$ Hz, 2H, $-\text{OCH}_2\text{CH}_2\text{CH}_2-$), δ 2.64 (dddd, $J = 10.8, 8.4, 7.4, 5.7$ Hz, 1H, $:\text{CHOCH}_2\text{CH}_2:$), δ 2.33 (dddd, $J = 10.8, 9.1, 7.6, 6.9$ Hz, 1H, $:\text{CHOCH}_2\text{CH}_2:$), δ 1.86-1.68 (m, 2H, $-\text{OCH}_2\text{CH}_2\text{CH}_2-$), δ 1.62-1.45 (m, 2H, $-\text{OCH}_2\text{CH}_2\text{CH}_2-$), δ 0.99 (s, 9H, $-\text{SiMe}_2^t\text{Bu}$), δ 0.04 (s, 6H, $-\text{SiMe}_2^t\text{Bu}$); ^{13}C APT $\{^1\text{H}\}$ NMR (100 MHz, CDCl_3): δ 82.2 ($:\text{CHOCH}_2\text{CH}_2:$), 67.6 ($:\text{CHOCH}_2\text{CH}_2:$), 62.5 ($-\text{OCH}_2\text{CH}_2\text{CH}_2$), 33.9₆ ($-\text{OCH}_2\text{CH}_2\text{CH}_2$), 27.2 ($:\text{CHOCH}_2\text{CH}_2:$), 26.9₈ ($-\text{OCH}_2\text{CH}_2\text{CH}_2$), 25.5 ($-\text{SiMe}_2(\text{CMe}_3)$), 17.9 ($-\text{SiMe}_2(\text{CMe}_3)$), -5.7 ($-\text{SiMe}_2^t\text{Bu}$); COSY (400 MHz, CHCl_3): δ 4.83 \leftrightarrow δ 2.64, 2.33, 1.86-1.68; δ 4.65 \leftrightarrow δ 4.49, 2.64, 2.33; δ 3.62 \leftrightarrow δ 1.67-1.45; δ 2.64; \leftrightarrow δ 2.33; δ 1.86-1.68 \leftrightarrow δ 1.67-1.45; δ 3.62 \leftrightarrow δ 1.62-1.45; δ 1.96-1.74 \leftrightarrow δ 1.96-1.74; HMQC (400 MHz, CDCl_3): δ 4.83 \leftrightarrow 82.2, δ 4.65, 4.49 \leftrightarrow δ 67.6, δ 3.62 \leftrightarrow δ 62.7, δ 2.64, 2.33 \leftrightarrow δ 27.2, δ 1.86-1.68 \leftrightarrow δ 33.9₆, δ 1.62-1.45 \leftrightarrow δ 26.9₈, δ 0.99 \leftrightarrow δ 25.5, δ 0.04 \leftrightarrow δ -5.7; EI-MS m/z calculated for: $\text{C}_8\text{H}_{17}\text{O}_2\text{Si}(\text{M}^+-\text{C}_4\text{H}_9)$, 173.09978; $\text{C}_6\text{H}_{13}\text{SiO}_2(\text{M}^+-\text{C}_2\text{H}_2-\text{C}_4\text{H}_9)$, 145.06848; $\text{C}_7\text{H}_{15}\text{SiO}(\text{M}^+-\text{CH}_2\text{O}-\text{C}_4\text{H}_9)$, 143.08922; Found: $\text{C}_8\text{H}_{17}\text{O}_2\text{Si}(\text{M}^+-\text{C}_4\text{H}_9)$, 173.09986; $\text{C}_6\text{H}_{13}\text{SiO}_2(\text{M}^+-\text{C}_2\text{H}_2-\text{C}_4\text{H}_9)$, 145.06889; $\text{C}_7\text{H}_{15}\text{SiO}(\text{M}^+-\text{CH}_2\text{O}-\text{C}_4\text{H}_9)$, 107.08517; No M^+ ion found; Elemental Analysis calculated for $\text{C}_{12}\text{H}_{26}\text{O}_2\text{Si}$: C, 62.55 %; H, 11.37 %; Found: C, 61.38 %; H, 11.31 %.

3-Oxetan-2-yl-propan-1-ol (187)

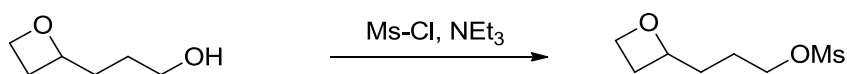


13.8 g of the oxetanylsilyl ether (59.9 mmol) and 40 mL of THF were introduced into a 250 one-necked round bottom flask; this solution was cooled to 0 °C. 67 mL of TBAF (1.0M in THF, 67 mmol) was then added *via* syringe to the cooled THF solution and the mixture stirred at room temperature overnight. The mixture was then concentrated and filtered through a plug of silica gel on a filter frit; and the frit was washed repeatedly with THF (3 X 10 mL). The solvents were removed *in vacuo* and the product was purified using flash chromatography (2:1, Hx, EtOAc) which gave 4.2 g (60 %) of the desired product.

Spectroscopic data for **187**: IR (neat film, cm^{-1}): 3395 (s, br), 2939 (s), 2884 (s), 1660 (w), 1451 (w), 1379 (w), 1229 (w), 1061 (m), 1020 (w), 959 (s); $^1\text{H NMR}$ (400 MHz, CDCl_3): δ 4.86 (apparent dq, $J = 4.6, 7.3$ Hz, 1H, : $\text{CHOCH}_2\text{CH}_2$:), 4.67 (ddd, $J = 8.4, 7.7, 5.9$ Hz, 1H, : $\text{CHOCH}_2\text{CH}_2$:), δ 4.52 (dt, $J = 9.1, 5.9$ Hz, 1H, : $\text{CHOCH}_2\text{CH}_2$:), δ 3.64 (apparent q, $J = 5.7$ Hz, 2H, $\text{HOCH}_2\text{CH}_2\text{CH}_2$ -), δ 2.68 (dddd, $J = 10.9, 8.4, 7.5, 5.9$ Hz, 1H, : $\text{CHOCH}_2\text{CH}_2$:), δ 2.39 (t, $J = 5.7$ Hz, 1H, $\text{HOCH}_2\text{CH}_2\text{CH}_2$ -), δ 2.33 (dddd, $J = 10.9, 9.1, 7.7, 7.0$ Hz, 1H, : $\text{CHOCH}_2\text{CH}_2$:), δ 1.89 (dq, 14.1, 7.6 Hz, 1H, $-\text{OCH}_2\text{CH}_2\text{CH}_2$ -), δ 1.77 (m, 1H, $-\text{OCH}_2\text{CH}_2\text{CH}_2$ -), δ 1.72-1.55 (m, 2H, $-\text{OCH}_2\text{CH}_2\text{CH}_2$ -); $^{13}\text{C APT } \{^1\text{H}\}$ NMR (100 MHz, CDCl_3): δ 82.7 (: $\text{CHOCH}_2\text{CH}_2$:), 68.1 (: $\text{CHOCH}_2\text{CH}_2$:), 62.5 ($-\text{OCH}_2\text{CH}_2\text{CH}_2$ -), 34.9₆ ($-\text{OCH}_2\text{CH}_2\text{CH}_2$ -), 28.1 ($-\text{OCH}_2\text{CH}_2\text{CH}_2$ -), 27.4 (: $\text{CHOCH}_2\text{CH}_2$:); COSY (400 MHz, CHCl_3): δ 4.86 \leftrightarrow δ 2.68, 2.33 1.89, 1.77; δ 4.67 \leftrightarrow δ 4.52, 2.68, 2.33; δ 4.52 \leftrightarrow δ 2.68, 2.33; δ 3.64; \leftrightarrow δ 1.72-1.55; δ 2.68 \leftrightarrow δ 2.33; δ 1.89 \leftrightarrow δ 1.77, 1.72-1.55; δ 1.77 \leftrightarrow δ 1.72-1.55; δ 1.72-1.55 \leftrightarrow δ 1.72-1.55; HMQC (400 MHz, CDCl_3): δ 4.86 \leftrightarrow 82.7, δ 4.67, 4.52 \leftrightarrow δ 68.1, δ 3.64 \leftrightarrow δ 62.5, δ 2.68, 2.33 \leftrightarrow δ 27.4, δ 1.89, 1.77 \leftrightarrow δ 34.9₆, δ 1.72-1.55 \leftrightarrow δ 28.1; EI-MS m/z calculated for: $\text{C}_6\text{H}_{11}\text{O}_2(\text{M}^+-\text{H})$, 115.07590; $\text{C}_6\text{H}_{10}\text{O}(\text{M}^+-\text{H}_2\text{O})$, 98.07317; $\text{C}_6\text{H}_9\text{O}(\text{M}^+-\text{H}_2\text{O}-\text{H})$, 97.06534; $\text{C}_4\text{H}_8\text{O}_2(\text{M}^+-\text{C}_2\text{H}_2-\text{H})$, 89.06026; $\text{C}_5\text{H}_{10}\text{O}(\text{M}^+-\text{CH}_2\text{O})$, 86.07317; $\text{C}_5\text{H}_9\text{O}(\text{M}^+-\text{CH}_2\text{O}-\text{H})$, 85.06534; Found: $\text{C}_6\text{H}_{11}\text{O}_2(\text{M}^+-\text{H})$, 115.07600; $\text{C}_6\text{H}_{10}\text{O}(\text{M}^+-\text{H}_2\text{O})$, 98.07288; $\text{C}_6\text{H}_9\text{O}(\text{M}^+-\text{H}_2\text{O}-\text{H})$, 97.06539; $\text{C}_4\text{H}_8\text{O}_2(\text{M}^+-\text{C}_2\text{H}_2-\text{H})$, 89.06013; $\text{C}_5\text{H}_{10}\text{O}(\text{M}^+-\text{CH}_2\text{O})$, 86.07318; $\text{C}_5\text{H}_9\text{O}(\text{M}^+-$

CH₂O-H), 85.06538; No M⁺ ion found; **Elemental Analysis** calculated for C₆H₁₂O₂: C, 62.04 %; H, 10.41 %; Found: C, 60.76 %; H, 10.32 %.

Methanesulfonic acid 3-oxetan-2-yl-propyl ester

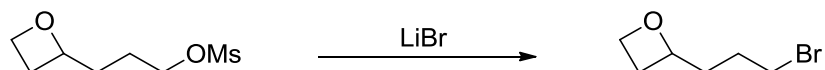


1.11 g of the oxetanyl alcohol (9.55 mmol) and 10 mL of CH₂Cl₂ were introduced into a 50 mL round bottom flask and the resulting solution was cooled to 0 °C. 1.3 mL of NEt₃ (14.0 mmol) was added to the CH₂Cl₂ solution followed by 1.1 mL of Ms-Cl (14.2 mmol) which was added dropwise *via* plastic syringe over 5 minutes; the mixture was stirred overnight and afforded a yellow solution with a white precipitate. The mixture was filtered through celite and the filtrate was washed with distilled water (2 X 30 mL). The organic layer was dried over MgSO₄, filtered through filter paper and concentrated *in vacuo*. The product was purified by flash chromatography (1:1 Hx:EtOAc) in which 0.75 g (34 %) of the desired product was obtained. The yield is poor due to a portion of the product solution that was spilt during purification.

Spectroscopic data: **IR** (neat film, cm⁻¹): 2939 (s), 2833 (s), 1472 (w), 1449 (w), 1417 (w), 1351 (s), 1229 (w), 1174 (s), 1126 (w), 1080 (w), 956 (s), 832 (w); **¹H NMR** (500 MHz, CDCl₃): δ 4.86 (apparent dq, *J* = 4.8, 7.4 Hz, 1H, :CHOCH₂CH₂:), 4.67 (ddd, *J* = 8.4, 7.6, 6.1 Hz, 1H, :CHOCH₂CH₂:), δ 4.51 (dt, *J* = 9.1, 5.9 Hz, 1H, :CHOCH₂CH₂:), δ 4.32-4.24 (m, 2H, (-OCH₂CH₂CH₂-), δ 3.02 (s, 3H, -SO₂Me), δ 2.70 (dddd, *J* = 11.0, 8.4, 7.4, 5.9 Hz, 1H, :CHOCH₂CH₂:), δ 2.36 (dddd, *J* = 11.0, 9.1, 7.6, 6.9 Hz, 1H, :CHOCH₂CH₂:), δ 1.96-1.74 (m, 4H, -OCH₂CH₂CH₂-); **¹³C APT {¹H} NMR** (125 MHz, CDCl₃): δ 81.9 (:CHOCH₂CH₂:), 69.8 (-OCH₂CH₂CH₂-), 68.1 (:CHOCH₂CH₂:), 37.4 (-SO₂Me), 32.7 (-OCH₂CH₂CH₂-), 27.4 (:CHOCH₂CH₂:), 24.4 (-OCH₂CH₂CH₂-); **COSY** (500 MHz, CHCl₃): δ 4.86 ↔ δ 2.70, 2.36, 1.96-1.74; δ 4.67 ↔ δ 4.51, 2.70, 2.36; δ 4.51 ↔ δ 2.70, 2.36; δ 4.27 ↔ δ 1.96-1.74; δ 2.70 ↔ δ 2.36; δ 1.96-1.74 ↔ δ 1.96-1.74; **HMQC** (500 MHz, CDCl₃): δ 4.86 ↔ 81.9, δ 4.67, 4.51 ↔ δ 68.1, δ 4.27 ↔ δ 69.8, δ 3.02 ↔ δ 37.4, δ 2.70, 2.36 ↔ δ 27.4, δ 1.96-1.74 ↔ 32.7, 24.4; **EI-MS** *m/z* calculated for: C₇H₁₄O₄S(M⁺), 194.06128; C₅H₁₀O₄S(M⁺-

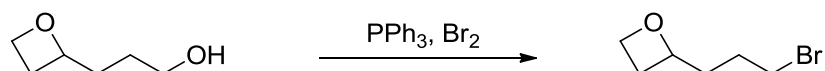
C₂H₂), 166.02998; Found: C₇H₁₄O₄S(M⁺), 194.06308; C₅H₁₀O₄S(M⁺-C₂H₂), 166.02969;
Elemental Analysis calculated for C₇H₁₄O₄S: C, 43.28 %; H, 7.26 %; Found: C, 43.39 %;
H, 7.31 %.

2-(3-Bromo-propyl)-oxetane (188)



Procedure 1: 0.73 g of the oxetanyl mesylate (3.76 mmol) and 10 mL of acetone were added to a 50 mL round bottom flask and the solution was cooled to 0 °C. 0.35 g of solid LiBr (40 mmol) was added to the acetone solution *via* spatula and the mixture was stirred for 3 hours, during this time it had warmed to room temperature. The mixture was concentrated *in vacuo*, redissolved in CH₂Cl₂ and filtered through celite to remove residual white solids. This procedure was repeated two more times until minimal white solid was present in the filtrate. The crude product was purified by flash chromatography (3:1 Hx:EtOAc) to which 0.67 g (97 %) of the purified product was obtained. Spectroscopic Data for this compound is listed in the experimental section below.

2-(3-Bromo-propyl)-oxetane (188)

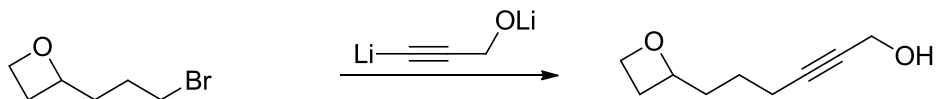


Alternative Procedure: 10.0 g of PPh₃ (38.1 mmol) and 80 mL of CH₂Cl₂ were introduced into a 250 mL round bottomed flask, then the resulting solution was cooled to 0 °C. 1.9 mL of Br₂ (37.1 mmol) was carefully added dropwise *via* plastic syringe to the cooled CH₂Cl₂ solution and the resulting mixture was stirred for 30 minutes at 0 °C. 2.6 g of solid imidazole (38.2 mmol) was added *via* spatula to the reaction flask, this was followed by the dropwise addition of 4.2 g of the oxetanyl alcohol (36.2 mmol) *via* plastic syringe. The resulting mixture was stirred for 16 hours where the reaction

mixture was warmed to room temperature. The crude product mixture was concentrated *in vacuo*. Diethyl ether (30 mL) was added to the crude residue in order to precipitate triphenylphosphine oxide which was generated during the reaction; this mixture was then filtered through celite and concentrated *in vacuo*. The concentrate was redissolved into diethyl ether, filtered through celite and concentrated two more times. This work up procedure furnished a colorless oil after removal of diethyl ether. The product was purified by flash chromatography (5:1, Hx, EtOAc) resulting in 2.1 g (32 %) of the desired product.

Spectroscopic data for **188**: IR (neat film, cm^{-1}): 2992 (m), 2936 (s), 2879 (s), 1440 (w), 1382 (w), 1245 (m), 1228 (w), 1106 (w), 980 (s), 956 (s), 917 (w), 871 (w); $^1\text{H NMR}$ (400 MHz, CDCl_3): δ 4.84 (apparent dq, $J = 5.1, 7.4$ Hz, 1H, $:\text{CHOCH}_2\text{CH}_2:$), 4.65 (ddd, $J = 8.4, 7.6, 5.8$ Hz, 1H, $:\text{CHOCH}_2\text{CH}_2:$), δ 4.50 (dt, $J = 9.1, 5.8$ Hz, 1H, $:\text{CHOCH}_2\text{CH}_2:$), δ 3.37 (apparent dt, $J = 0.9, 6.4$ Hz, 2H, $-\text{CH}_2\text{CH}_2\text{CH}_2\text{Br}$), δ 2.67 (dddd, $J = 10.9, 8.4, 7.4, 5.8$ Hz, 1H, $:\text{CHOCH}_2\text{CH}_2:$), δ 2.34 (dddd, $J = 10.9, 9.1, 7.4, 7.0$ Hz, 1H, $:\text{CHOCH}_2\text{CH}_2:$), δ 2.40-1.76 (m, 4H, $-\text{CH}_2\text{CH}_2\text{CH}_2\text{Br}$); $^{13}\text{C } \{^1\text{H}\}$ NMR (100 MHz, CDCl_3): δ 81.3 ($:\text{CHOCH}_2\text{CH}_2:$), 67.7 ($:\text{CHOCH}_2\text{CH}_2:$), 36.0 ($-\text{CH}_2\text{CH}_2\text{CH}_2\text{Br}$), 33.1 ($-\text{CH}_2\text{CH}_2\text{CH}_2\text{Br}$), 27.3 ($:\text{CHOCH}_2\text{CH}_2:$), 27.0 ($-\text{CH}_2\text{CH}_2\text{CH}_2\text{Br}$); $^1\text{H}-^1\text{H}$ (400 MHz, CHCl_3): δ 4.84 \leftrightarrow δ 2.67, 2.34; δ 4.65 \leftrightarrow δ 4.50, 2.67, 2.34; δ 3.37 \leftrightarrow δ 2.40-1.76; **HMQC** (400 MHz, CDCl_3): δ 4.84 \leftrightarrow 81.3, δ 4.65, 4.50 \leftrightarrow δ 67.7, δ 3.37 \leftrightarrow δ 33.1, δ 2.67, 2.34 \leftrightarrow δ 27.3, δ 2.40-1.76 \leftrightarrow δ 27.0, 36.0; **EI-MS** m/z calculated for: $\text{C}_4\text{H}_8\text{O}^{79}\text{Br}(\text{M}^+-\text{H})$, 160.99658; $\text{C}_4\text{H}_8\text{O}^{81}\text{Br}(\text{M}^+-\text{C}_2\text{H}_2-\text{H})$, 152.97380; $\text{C}_4\text{H}_8\text{O}^{79}\text{Br}(\text{M}^+-\text{C}_2\text{H}_2-\text{H})$, 150.97585; $\text{C}_6\text{H}_{11}\text{O}(\text{M}^+-\text{Br})$, 99.08099; $\text{C}_6\text{H}_{10}\text{O}(\text{M}^+-\text{Br}-\text{H})$, 98.07317; Found: $\text{C}_4\text{H}_8\text{O}^{79}\text{Br}(\text{M}^+-\text{H})$, 160.99669; $\text{C}_4\text{H}_8\text{O}^{81}\text{Br}(\text{M}^+-\text{C}_2\text{H}_2-\text{H})$, 152.97392; $\text{C}_4\text{H}_8\text{O}^{79}\text{Br}(\text{M}^+-\text{C}_2\text{H}_2-\text{H})$, 150.97592; $\text{C}_6\text{H}_{11}\text{O}(\text{M}^+-\text{Br})$, 99.08080; $\text{C}_6\text{H}_{10}\text{O}(\text{M}^+-\text{Br}-\text{H})$, 98.07303; No M^+ ion found; **Elemental Analysis** calculated for $\text{C}_6\text{H}_{11}\text{OBr}$: C, 40.25 %; H, 6.19 %; Found: C, 40.03 %; H, 6.40 %.

6-Oxetan-2-yl-hex-2-yn-1-ol (189)

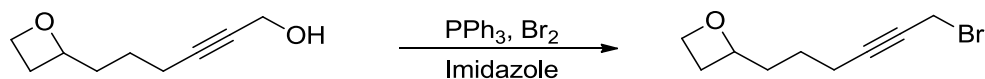


100 mL of anhydrous ammonia was condensed into a three necked round bottomed flask equipped with a dry-ice condenser at $-78\text{ }^{\circ}\text{C}$. A small amount ($\sim 0.05\text{ g}$) of solid $\text{Fe}(\text{NO}_3)_3$ was added to the ammonia solution; when the $\text{Fe}(\text{NO}_3)_3$ solid had dissolved, 0.205 g of lithium wire (0.030 mol) was added in 5 portions over 2 hours. During the addition of lithium wire, the color of the ammonia solution changed from dark blue to light brown and was accompanied with vigorous gas evolution. The color change indicated that the lithium amide had been successfully formed. 0.78 mL of propargyl alcohol (13.4 mmol) was then added dropwise at $-78\text{ }^{\circ}\text{C}$ to the liquid ammonia solution *via* plastic syringe, and the mixture was stirred for 1 hour; during this time a grayish-white suspension had formed. 2.0 g of the oxetanyl-bromide (11.2 mmol) was then added to the ammonia solution *via* plastic syringe and stirred overnight; during this time the reaction flask was warmed to room temperature and the ammonia was allowed to evaporate from the flask. After 16 hours, a white residue was left on the bottom of the flask. 100 mL of distilled water was added to the white residue and was stirred for one hour until the solids dissolved. The aqueous solution was transferred to a separatory funnel and extracted with diethyl ether (3 X 100 mL). The combined organic extracts were dried over MgSO_4 , filtered through filter paper, and concentrated *in vacuo* which afforded a colorless oil. The product was purified using flash chromatography (4:1, Hx:EtOAc) which resulted in 1.2 g (70 %) of the desired product.

Spectroscopic data for **189**: IR (neat film, cm^{-1}): 3399 (s, br), 2937 (s), 2882 (s), 2286.8 (w), 2222 (w), 1452 (m), 1433 (m), 1382 (m), 1356 (m), 1329 (m), 1229 (m), 1134 (m), 1021 (s), 977 (s), 914 (m), 880 (m); $^1\text{H NMR}$ (400 MHz, CDCl_3): δ 4.85 (apparent dq, $J=5.7, 7.2\text{ Hz}$, 1H, $:\text{CHOCH}_2\text{CH}_2:$), δ 4.67 (ddd, $J=8.4, 7.8, 6.0\text{ Hz}$, 1H, $:\text{CHOCH}_2\text{CH}_2:$), δ 4.51 (ddd, $J=9.0, 6.0, 5.7\text{ Hz}$, 1H, $:\text{CHOCH}_2\text{CH}_2:$), δ 4.24 (apparent dt, $J=6.0, 2.3\text{ Hz}$, 2H, $-\text{C}\equiv\text{CCH}_2\text{OH}$), δ 2.66 (dddd, $J=10.9, 8.4, 7.4, 5.7\text{ Hz}$, 1H, $:\text{CHOCH}_2\text{CH}_2:$), δ 2.36 (dddd, $J=10.9, 9.0, 7.8, 6.7\text{ Hz}$, 1H, $:\text{CHOCH}_2\text{CH}_2:$), δ 2.27 (apparent tt, $J=7.0, 2.3\text{ Hz}$, 2H, $-\text{CH}_2\text{CH}_2\text{CH}_2\text{C}\equiv\text{C}-$), δ 1.89 (apparent dddd, $J=12.0, 9.9, 6.5, 5.5\text{ Hz}$, 1H, $-\text{CH}_2\text{CH}_2\text{CH}_2\text{C}\equiv\text{C}-$), δ

1.77 (apparent ddt, $J = 12.0, 9.8, 5.9$ Hz, 1H, $-\underline{C}H_2CH_2CH_2C\equiv C-$), δ 1.70 (broad t, $J = 6.0$, Hz, 1H, $(-C\equiv CCH_2OH)$), δ 1.55 (m, 2H, $-CH_2CH_2CH_2C\equiv C-$); ^{13}C { 1H } NMR (100 MHz, $CDCl_3$): δ 86.1 ($-C\equiv CCH_2OH$), 82.4 ($:\underline{C}HOCH_2CH_2:$), 78.9₈ ($-\underline{C}\equiv CCH_2OH$), 68.3 ($:\underline{C}HOCH_2CH_2:$), 51.5 ($-C\equiv CCH_2OH$), 37.1 ($-\underline{C}H_2CH_2CH_2C\equiv C-$), 27.7 ($:\underline{C}HOCH_2CH_2:$), 23.4 ($-CH_2CH_2CH_2C\equiv C-$), 18.8 ($-CH_2CH_2CH_2C\equiv C-$); **COSY** (400 MHz, $CHCl_3$): δ 4.85 \leftrightarrow δ 2.66, 2.36, 1.89, 1.77; δ 4.67 \leftrightarrow δ 4.51, 2.66, 2.36; δ 4.51 \leftrightarrow δ 2.66, 2.36; δ 4.24 \leftrightarrow δ 2.27, 1.70; δ 2.66 \leftrightarrow δ 2.36; δ 2.27 \leftrightarrow δ 1.77, 1.55; δ 1.89 \leftrightarrow δ 1.77, 1.55; δ 1.77 \leftrightarrow δ 1.55; **HMQC** (500 MHz, $CDCl_3$): δ 4.85 \leftrightarrow 82.4, δ 4.67, 4.51 \leftrightarrow δ 68.3, δ 4.24 \leftrightarrow δ 51.5, δ 2.66, 2.36 \leftrightarrow δ 27.7, δ 2.27 \leftrightarrow δ 18.8, δ 1.77, 1.70 \leftrightarrow δ 37.1, δ 1.55 \leftrightarrow δ 23.4; **EI-MS** m/z calculated for: $C_9H_{13}O_2(M^+-H)$, 153.09155; $C_9H_{11}O(M^+-H_2O)$, 135.08099; $C_7H_9O_2(M^+-C_2H_2-H)$, 125.06026; $C_8H_{11}O(M^+-CH_2O-H)$, 123.08099; $C_7H_8O(M^+-C_2H_2)$, 108.05752; $C_7H_8O(M^+-C_2H_2)$, 107.04969; Found: $C_9H_{13}O_2(M^+-H)$, 153.09108; $C_9H_{11}O(M^+-H_2O)$, 135.08139; $C_7H_9O_2(M^+-C_2H_2-H)$, 125.06008; $C_8H_{11}O(M^+-CH_2O-H)$, 123.08076; $C_7H_8O(M^+-C_2H_2-H_2O)$, 108.05760; $C_7H_8O(M^+-C_2H_2-H_2O-H)$, 107.04991; No M^+ ion found; **Elemental Analysis** calculated for $C_9H_{14}O_2$: C, 70.10 %; H, 9.15 %; Found: C, 70.32 %; H, 9.32 %.

2-(6-Bromo-hex-4-ynyl)-oxetane (172)



Procedure 1: 1.81 g of PPh_3 (6.90 mmol) and 10 mL of CH_2Cl_2 were introduced into a 50 mL round bottom flask; this mixture was cooled to 0 °C. 0.35 mL of Br_2 (6.83 mmol) was then added dropwise to the cooled CH_2Cl_2 solution *via* plastic syringe and the resulting mixture was stirred for 15 minutes; during this time a white suspension had formed. In another 50 mL round bottom flask, 0.47 g of imidazole (6.90 mmol), 20 mL of CH_2Cl_2 and 1.08 g of 6-oxetan-2-yl-hex-2-yn-1-ol (7.00 mmol) were combined in the described order; this flask was also cooled to 0 °C. Once both solutions were cooled, the heterogeneous $CH_2Cl_2/PPh_3/Br_2$ mixture was introduced dropwise *via* glass pipette into the imidazole; the combined mixture was then stirred overnight. The volatile solvents were then removed *in vacuo* from the combined reaction mixture. 20 mL of diethyl ether was added to the residue in order to precipitate triphenylphosphine oxide

which was produced during the reaction. The diethyl ether solution was filtered through celite and then concentrated *in vacuo*. The product was purified by flash chromatography (5:1, Hx:EtOAc) and 0.605 g (40 %) of product was obtained.

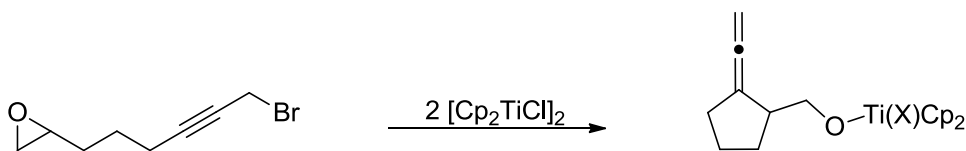
Procedure 2: 88 mg of 6-oxetan-2-yl-hex-2-yn-1-ol (0.057 mmol), 2 mL of CH₂Cl₂, and 0.08 mL of NEt₃ (0.086 mmol) were added to a 10 mL round bottom flask; this mixture was cooled to 0 °C. 0.05 mL of Ms-Cl (0.065 mol) was then added dropwise *via* plastic syringe to the cooled CH₂Cl₂ solution, and the resulting solution was stirred for 16 hours; during this time, the reaction mixture warmed to room temperature. An additional 2 mL of CH₂Cl₂ was added to the reaction mixture and then was transferred to a separatory funnel. The CH₂Cl₂ layer was washed sequentially with of saturated NaHCO_{3(aq)} (1 X 2 mL), then distilled water (2 X 2 mL). The organic layer was dried over MgSO₄, filtered through filter paper, and concentrated *in vacuo*.

The crude product and 1 mL of THF were introduced into a 10 mL round bottom flask and was cooled to 0 °C. A solution of 0.182 g of LiBr (2.10 mmol) in 3 mL of THF was added dropwise *via* plastic syringe and the mixture was stirred overnight. 5 mL of diethyl ether was then added to the mixture and was transferred to a separatory funnel where it was washed with distilled water (3 X 5 mL). The organic layer was dried over MgSO₄, filtered through filter paper, and concentrated giving 91 mg (55 %) of the desired product. The spectroscopic analysis is identical to the product obtained when using method A.

Spectroscopic data for **172**: IR (neat film, cm⁻¹): 2993 (s), 2936 (s), 2880 (s), 2310 (w), 2232 (m), 1451 (m), 1430 (m), 1380 (w), 1355 (w), 1329 (w), 1272 (w), 1218 (s), 1151 (w), 1114 (w), 977 (s), 917 (w), 873 (w); ¹H NMR (500 MHz, CDCl₃): δ 4.85 (apparent dq, *J*= 5.8, 7.1 Hz, 1H, :CHOCH₂CH₂:), δ 4.68 (dt, *J*= 5.8, 7.8 Hz, 1H, :CHOCH₂CH₂:), δ 4.52 (dt, *J*= 9.1, 5.8 Hz, 1H, :CHOCH₂CH₂:), δ 3.94 (apparent t, *J*= 2.6 Hz, 2H, -C≡CCH₂Br), δ 2.69 (dddd, *J*= 10.9, 8.3, 7.8, 5.8 Hz, 1H, :CHOCH₂CH₂:), δ 2.37 (dddd, *J*= 10.9, 9.1, 7.8, 7.0 Hz, 1H, :CHOCH₂CH₂:), δ 2.31 (apparent tt, *J*= 7.1, 2.6, Hz, 2H, -CH₂CH₂CH₂C≡C-), δ 1.90 (apparent dddd, *J*= 13.0, 10.0, 7.2, 5.8 Hz, 1H, -CH₂CH₂CH₂C≡C-), δ 1.88 (apparent ddt, *J*= 13.0, 10.0, 5.8 Hz, 1H, -CH₂CH₂CH₂C≡C-), δ 1.66-1.49 (m, 2H, -CH₂CH₂CH₂C≡C-); ¹³C APT {¹H} NMR (125 MHz, CDCl₃): δ 87.7 (-C≡CCH₂Br), 82.2 (:CHOCH₂CH₂:), 75.8 (-C≡CCH₂Br),

68.1 (:CHOCH₂CH₂:), 36.9₆ (-CH₂CH₂CH₂C≡C-), 27.6 (:CHOCH₂CH₂:), 23.1 (-CH₂CH₂CH₂C≡C-), 18.8 (-CH₂CH₂CH₂C≡C-), 15.6 (-C≡CCH₂Br); **COSY** (500 MHz, CHCl₃): δ 4.85 ↔ δ 2.69, 2.33, 1.90, 1.88; δ 4.68 ↔ δ 4.52, 2.69, 2.33; δ 4.52 ↔ δ 2.69, 2.33; δ 3.94 ↔ δ 2.31; δ 2.69 ↔ δ 2.33; δ 2.31 ↔ δ 1.66-1.49; δ 1.90 ↔ δ 1.88, 1.66-1.49; δ 1.88 ↔ δ 1.66-1.49; δ 1.66-1.49 ↔ δ 1.66-1.49; **HMQC** (500 MHz, CDCl₃): δ 4.85 ↔ δ 82.2, δ 4.68, 4.52 ↔ δ 68.1, δ 3.94 ↔ δ 15.6, δ 2.69, 2.33 ↔ δ 27.6, δ 2.31 ↔ δ 18.8, δ 1.90, 1.88 ↔ δ 36.9₆, δ 1.66, 1.49 ↔ δ 23.1; **EI-MS** *m/z* calculated for: C₉H₁₃O(M⁺-Br), 137.09663; C₇H₉O(M⁺-C₂H₂-Br), 109.06534; C₈H₁₁(M⁺-CH₂O-Br), 107.08607; Found: C₉H₁₃O(M⁺-Br), 137.09657; C₇H₉O(M⁺-C₂H₂-Br), 109.06434; C₈H₁₁(M⁺-CH₂O-Br), 107.08517; No M⁺ ion found; **Elemental Analysis** calculated for C₉H₁₃OBr: C, 49.79 %; H, 6.04 %; Found: C, 48.84 %; H, 5.97 %.

((2-Vinylidene-cyclopentyl)-methoxy)titanocene(IV) monobromide (190) or monochloride (191)



0.136 g of solid [Cp₂TiCl]₂ (1.09 mmol) and 3 mL THF were introduced into a 5 dram vial, which was then placed in the drybox freezer (-30 °C) for 1 hour. The vial was removed and quickly treated with a solution containing 64.7 mg of 2-(6-bromo-hex-4-ynyl)-oxirane (0.319 mmol) in 1 mL THF; this mixture was placed back in the drybox freezer (-30 °C) and left there for 16 hours. The vial was removed from the freezer and warmed to room temperature over 4 hours; this gave a dark red solution. The volatiles were removed *in vacuo*; the red residue was then extracted with toluene and filtered through celite, the volatiles were removed from the filtrate *in vacuo* resulting in 108.5 mg of the crude products (95 %, based on 1:1 product ration X = Br, Cl). Attempts to purify the product were unsuccessful, however, minimal impurities are observed by ¹H NMR spectroscopy.

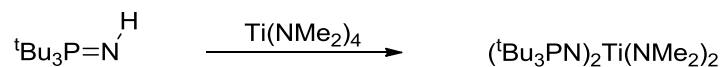
Spectroscopic data for **190** and **191**: **IR** (neat film, cm^{-1}): 3467 (m, br), 3110 (m), 2950 (s), 2867 (s), 1956 (m), 1730.6, (w), 1639 (w), 1441 (s), 1361 (m), 1262 (w), 1083 (s, br), 1024 (s), 921 (w), 829 (s, br), 726 (s);

Major isomer: $^1\text{H NMR}$ (500 MHz, C_6D_6): δ 5.95 (s, 5H, Cp-H), δ 5.93 (s, 5H, Cp-H), δ 4.75 (m, 2H, $>\text{C}=\text{C}=\text{CH}_2$), δ 4.49 (dd, $J=11.2, 5.1$ Hz, 1H, $-\text{CH}_2\text{OH}$), δ 4.29 (dd, $J=11.2, 8.1$ Hz, 1H, $-\text{CH}_2\text{OH}$), δ 2.75 (m, 1H, $:\text{CH}_2\text{CH}_2\text{CH}_2\text{CHC:}$), δ 2.35 (m, 2H, $:\text{CH}_2\text{CH}_2\text{CH}_2\text{CHC:}$), δ 1.75 (m, 1H, $:\text{CH}_2\text{CH}_2\text{CH}_2\text{CHC:}$), δ 1.63 (m, 1H, $:\text{CH}_2\text{CH}_2\text{CH}_2\text{CHC:}$), δ 1.54 (m, 1H, $:\text{CH}_2\text{CH}_2\text{CH}_2\text{CHC:}$), δ 1.46 (m, 1H, $:\text{CH}_2\text{CH}_2\text{CH}_2\text{CHC:}$); $^{13}\text{C APT } \{^1\text{H}\} \text{NMR}$ (125 MHz, C_6D_6): δ 203.5 ($>\text{C}=\text{C}=\text{CH}_2$), 116.9₇ (Cp), 116.9 (Cp), 105.1 ($>\text{C}=\text{C}=\text{CH}_2$), 85.8 ($-\text{CH}_2\text{OH}$), 77.1 ($>\text{C}=\text{C}=\text{CH}_2$), 46.9 ($:\text{CH}_2\text{CH}_2\text{CH}_2\text{CHC:}$), 32.4 ($:\text{CH}_2\text{CH}_2\text{CH}_2\text{CHC:}$), 31.5 ($:\text{CH}_2\text{CH}_2\text{CH}_2\text{CHC:}$), 26.3₃ ($:\text{CH}_2\text{CH}_2\text{CH}_2\text{CHC:}$); **COSY** (500 MHz, C_6D_6): δ 4.75 \leftrightarrow δ 2.75, 2.35; δ 4.49 \leftrightarrow δ 4.29, 2.75; δ 4.29 \leftrightarrow δ 2.75; δ 2.75 \leftrightarrow δ 1.75, 1.54; δ 2.35 \leftrightarrow δ 1.63, 1.46; δ 1.75 \leftrightarrow δ 1.54; δ 1.63 \leftrightarrow δ 1.46; **HMQC** (500 MHz, C_6D_6): δ 5.95, 5.93 \leftrightarrow δ 116.9₇, 116.9; δ 4.75 \leftrightarrow δ 77.1, δ 4.49, 4.29 \leftrightarrow δ 85.8, δ 2.75 \leftrightarrow δ 46.9, δ 2.35 \leftrightarrow δ 32.4, δ 1.75, 1.54 \leftrightarrow δ 31.5, δ 1.63, 1.46 \leftrightarrow δ 26.3₃;

Minor isomer: $^1\text{H NMR}$ (500 MHz, C_6D_6): δ 5.97 (s, 5H, Cp-H), δ 5.94 (s, 5H, Cp-H), δ 4.75 (m, 2H, $>\text{C}=\text{C}=\text{CH}_2$), δ 4.43 (dd, $J=11.3, 4.9$ Hz, 1H, $-\text{CH}_2\text{OH}$), δ 4.23 (dd, $J=11.3, 8.0$ Hz, 1H, $-\text{CH}_2\text{OH}$), δ 2.75 (m, 1H, $:\text{CH}_2\text{CH}_2\text{CH}_2\text{CHC:}$), δ 2.35 (m, 2H, $:\text{CH}_2\text{CH}_2\text{CH}_2\text{CHC:}$), δ 1.75 (m, 1H, $:\text{CH}_2\text{CH}_2\text{CH}_2\text{CHC:}$), δ 1.63 (m, 1H, $:\text{CH}_2\text{CH}_2\text{CH}_2\text{CHC:}$), δ 1.54 (m, 1H, $:\text{CH}_2\text{CH}_2\text{CH}_2\text{CHC:}$), δ 1.46 (m, 1H, $:\text{CH}_2\text{CH}_2\text{CH}_2\text{CHC:}$); $^{13}\text{C APT } \{^1\text{H}\} \text{NMR}$ (125 MHz, C_6D_6): δ 203.5 ($>\text{C}=\text{C}=\text{CH}_2$), 116.7 (Cp), 116.6 (Cp), 105.0 ($>\text{C}=\text{C}=\text{CH}_2$), 86.2 ($-\text{CH}_2\text{OH}$), 77.1 ($>\text{C}=\text{C}=\text{CH}_2$), 46.8₆ ($:\text{CH}_2\text{CH}_2\text{CH}_2\text{CHC:}$), 32.4 ($:\text{CH}_2\text{CH}_2\text{CH}_2\text{CHC:}$), 31.5 ($:\text{CH}_2\text{CH}_2\text{CH}_2\text{CHC:}$), 26.3 ($:\text{CH}_2\text{CH}_2\text{CH}_2\text{CHC:}$); **COSY** (500 MHz, C_6D_6): δ 4.75 \leftrightarrow δ 2.75, 2.35; δ 4.43 \leftrightarrow δ 4.23, 2.75; δ 4.23 \leftrightarrow δ 2.75; δ 2.75 \leftrightarrow δ 1.75, 1.54; δ 2.35 \leftrightarrow δ 1.63, 1.46; δ 1.75 \leftrightarrow δ 1.54; δ 1.63 \leftrightarrow δ 1.46; **HMQC** (500 MHz, C_6D_6): δ 5.97, 5.94 \leftrightarrow δ 116.7, 116.6; δ 4.75 \leftrightarrow δ 77.1, δ 4.43, 4.23 \leftrightarrow δ 86.2, δ 2.75 \leftrightarrow δ 46.8₆, δ 2.35 \leftrightarrow δ 32.4, δ 1.75, 1.54 \leftrightarrow δ 31.5, δ 1.63, 1.46 \leftrightarrow δ 26.3;

6.5.2 Chapter 4 Experimental Section

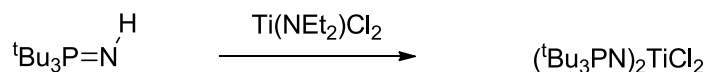
Bis(diethylamido)titanium(IV) bis(tri(tert-butyl)phosphinimide) (296)



1.08 g of titanium(IV) tetrakis(dimethylamide) (4.81 mmol) and 3 mL of toluene were combined in a 50 mL round bottom flask. The mixture was then treated with a solution containing 1.99 g of tri(*tert*-butyl)phosphinimine (9.11 mmol) and 4 mL of toluene; the combined mixture was then stirred at room temperature for 16 hours. During this time the solution color became dark yellow. The solution was concentrated to 1 mL and placed in the drybox freezer (-30 °C) where after 5 crystallizations, 0.3 g (11 %) of pure material was obtained.

Spectroscopic data for **298**: IR (neat film, cm^{-1}): 2963 (m), 1591 (w, br), 1260 (s), 1091 (s), 1019 (s), 799 (s), 703 (w); ${}^1\text{H}$ $\{{}^{31}\text{P}\}$ NMR (400 MHz, C_6D_6): δ 3.56 (s, 12H, NMe_2), δ 1.39 (d, $J = 12$ Hz, 54H, CMe_3); ${}^{13}\text{C}$ $\{{}^1\text{H}\}$ NMR (100 MHz, C_6D_6): δ 48.0 (CMe_3), 40.5 (NMe_2), 40.0 (NMe_2), 29.9 (CMe_3); ${}^{31}\text{P}$ $\{{}^1\text{H}\}$ NMR (162 MHz, C_6D_6): δ 26.4.

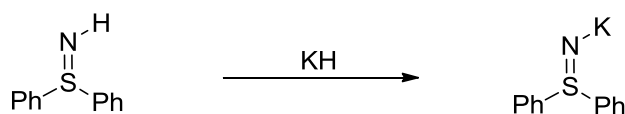
Dichlorotitanium(IV) bis(tri(tert-butyl)phosphinimide) (293)



0.65 g of $\text{Ti}(\text{NEt}_2)_2\text{Cl}_2$ (2.46 mmol) and 5 mL of THF were combined in a 50 mL round bottom flask. This mixture was treated with a solution containing 1.08 g of (*tert*-butyl)phosphinimine (4.94 mmol) in 10 mL of THF; the resultant mixture was then stirred for 16 hours at room temperature. During this time the color of the solution changed from dark red to grayish-green. The volatiles were removed in vacuo and the resulting residue was washed with hexanes to give 1.22 g (89.7 %) of an off-white powder. The ${}^1\text{H}$ NMR and ${}^{31}\text{P}$ NMR spectra of the product exactly matched that of the ${}^1\text{H}$ NMR and ${}^{31}\text{P}$ NMR spectrum of **295** from previous characterization data.²¹⁷ Single

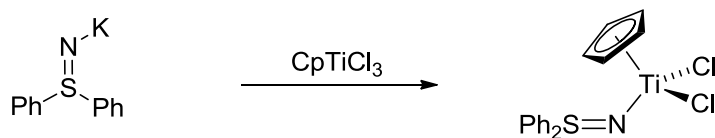
crystals suitable for X-ray diffraction were grown from a saturated solution of the compound in toluene at -30 °C.

N-potassium-S,S-diphenylsulfimide (326)



3.53 g of diphenylsulfilimine (17.6 mmol) and 20 mL of THF were combined in a 50 mL round bottom flask. 0.74 g of washed KH (18.4 mmol) was added to the THF solution *via* spatula. The resulting mixture was then stirred for 16 hours; during this time the color of the reaction mixture changed from colorless to yellow while evolving a colorless gas. The yellow solution was filtered through celite and the volatiles were removed *in vacuo* resulting in 3.52 g (83.0 %) of an orange powder. The solid was carried forward without purification.

(η^5 -Cyclopentadienyl)(S,S-diphenylsulfimido)titanium(IV) dichloride (313)

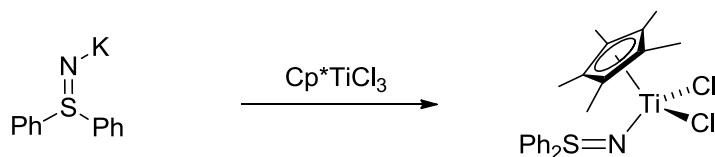


3.21 g of CpTiCl₃ (14.6 mmol) and 25 mL toluene were combined in a 50 mL round bottom flask. The mixture was then treated with a solution containing 3.52 g of [Ph₂S=NK] (14.7 mmol) in 10 mL toluene. The resulting mixture was stirred for 16 hours at room temperature; during this time the color of the solution changed from yellow to dark-orange. The orange mixture was concentrated to 5 mL of toluene and filtered through celite; the volatiles were then removed *in vacuo*. The product was purified by crystallization at low-temperature; this involved cooling a saturated toluene solution to -30 °C in the drybox freezer. Over two days, yellow crystals were formed then the

mother liquor was decanted off giving 3.12 g (60.9 %) of yellowish-orange crystals which were suitable for X-ray diffraction. These crystals were also analytically pure.

Spectroscopic data for **315**: IR (cast film, cm^{-1}): 3057 (w, br), 1654 (w), 1577 (w), 1472 (m), 1441 (m), 1329 (w), 1082 (s), 1020 (s), 999 (m), 836 (w), 814 (s), 747 (s), 733 (s), 685 (s); $^1\text{H NMR}$ (500 MHz, C_6D_6): δ 7.52 (m, 2H, Ar-H), δ 6.87 (m, 2H, Ar-H), δ 6.82 (m, 1H, Ar-H), δ 6.23 (s, 5H, C_5H_5); $^{13}\text{C } \{^1\text{H}\}$ NMR (125 MHz, C_6D_6): δ 142.1 (Ph), 132.1 (Ph), 130.2 (Ph), 126.2 (Ph), 115.8 (C_5H_5); **Elemental Analysis** calculated for $\text{C}_{17}\text{H}_{15}\text{NSTiCl}_2$: C, 52.72 %; H, 4.12 %; N, 3.84; S, 8.58; Found: C, 52.79 %; H, 4.10 %; N, 3.84 %; S, 8.32 %.

(η^5 -Pentamethylcyclopentadienyl)(S,S-diphenylsulfimido)titanium(IV) dichloride (314)

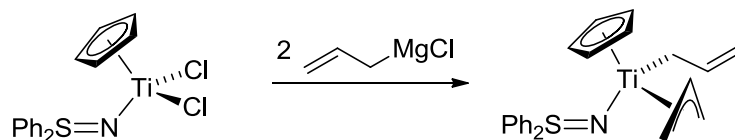


1.20 g of Cp^*TiCl_3 (4.18 mmol) and 25 mL of THF were combined in a 50 mL round bottom flask at room temperature. This mixture was treated with a solution containing 1.00 g of $[\text{Ph}_2\text{S}=\text{N}K]$ (4.18 mmol) in 10 mL THF *via* glass pipette. The resulting mixture was stirred at room temperature for 16 hours; during this time the color of the solution changed from red to dark-orange. The reaction mixture was concentrated to 5 mL and was filtered through celite; the volatiles were then removed *in vacuo*. The product was purified by low temperature recrystallization; this involved making a saturated solution in toluene and placing in the $-30\text{ }^\circ\text{C}$ freezer. Over two days, orange crystals formed and the mother liquor was decanted off. 1.89 g (99.5 %) of analytically pure dark-orange crystals was obtained; these were also suitable for X-ray diffraction.

Spectroscopic data for **316**: IR (cast film, cm^{-1}): 3060 (s), 2978 (s), 2914 (s), 1817 (m), 1581 (m), 1473 (s), 1443 (s), 1378 (s), 1308 (s), 1157 (m), 1103 (m), 1061 (m), 1020 (m), 998 (m), 928 (w), 743 (w); $^1\text{H NMR}$ (400 MHz, C_6D_6): δ 7.68 (m, 4H, Ar-H), δ 6.88 (m, 4H, Ar-H), δ 6.79 (m, 2H, Ar-H), δ 2.08 (s, 15H, C_5Me_5); $^{13}\text{C } \{^1\text{H}\}$ NMR (100 MHz, C_6D_6): δ

143.5 (Ph), 131.5 (Ph), 129.9 (Ph), 126.5 (Ph), 125.8 (C₅Me₅), 12.9 (C₅Me₅); **HMQC** (400 MHz, CDCl₃): δ 7.68 ↔ 126.5, δ 6.88 ↔ δ 129.9, δ 6.79 ↔ δ 131.5, δ 2.08 ↔ δ 12.9; **Elemental Analysis** calculated for C₂₂H₂₅NSTiCl₂: C, 58.16 %; H, 5.55 %; N, 3.08; S, 7.06; Found: C, 57.88 %; H, 5.51 %; N, 3.13 %; S, 6.75 %.

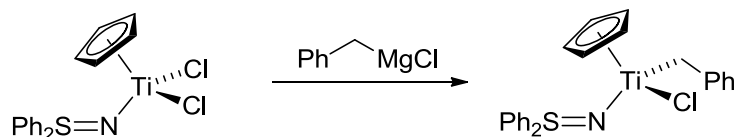
(η⁵-Cyclopentadienyl)mono(diphenylsulfilimido)titanium(IV) bis(allyl) (327)



110 mg of the starting titanium material (0.286 mmol) and 2 mL THF were combined in a flame-dried 5 dram vial; the vial was then placed in the drybox freezer (-30 °C) for 1 hour. The vial was removed from the freezer and treated with a 0.3 mL solution of allyl magnesium chloride (2.0 M in THF, 0.60 mmol) which was added dropwise *via* glass pipette. The reaction mixture was stirred for 1.5 hours; during this time it was warmed to room temperature. The volatiles were removed *in vacuo* which afforded a reddish-orange solid. The solid was extracted first with benzene and filtered through celite, the volatiles were removed *in vacuo*. The reddish-orange solid was extracted with diethyl ether and filtered through celite; the volatiles were removed *in vacuo*. 132 mg of the crude reddish-orange oil (107 %) was isolated, but could not be purified due to the decomposition of the product while in the solid state.

Spectroscopic data for **329**: ¹H NMR (400 MHz, C₆D₆): δ 7.40 (m, 2H, Ar-H), δ 6.98-6.83 (m, 4H, Ar-H), δ 6.18 (pent, *J*= 9.2 Hz, 2H, CH₂CHCH₂), δ 5.75 (s, 5H, C₅H₅), δ 3.61 (apparent d, *J*= 9.2 Hz, 8H, CH₂CHCH₂);

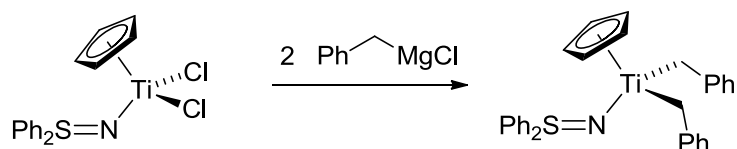
Benzyl(η^5 -cyclopentadienyl)(S,S-diphenylsulfimido)titanium(IV) chloride (328)



30 mg of the starting titanium material (0.078 mmol) and 2 mL THF were combined in a flame-dried 5 dram vial, this was placed in the drybox freezer (-30 °C) for 1 hour. The vial was removed from the freezer, and was treated with 42 μL of a solution containing benzyl magnesium chloride (2.0M in THF, 0.084 mmol), which was added dropwise *via* glass pipette. The resulting solution was then warmed to room temperature over 1 hour then stirred for an additional 16 hours. The volatiles were removed *in vacuo* resulting in a reddish-orange solid; this was extracted with diethyl ether and filtered through celite; and the volatiles were then removed from the filtrate *in vacuo*. Crude spectroscopic analysis reveals that the mono-benzyl product was formed. The product was taken on to the next step without further purification.

Spectroscopic data for **331**: ¹H NMR (400 MHz, C₆D₆): δ 7.68 (m, 4H, Ar-H), δ 6.88 (m, 4H, Ar-H), δ 6.79 (m, 2H, Ar-H), δ 5.76 (s, 5H, C₅H₅), δ 3.40 (d, *J* = 9.4 Hz, 1H, CH₂Ph), δ 3.21 (d, *J* = 9.4 Hz, 1H, CH₂Ph), partial data was reported due to contamination.

(η⁵-Cyclopentadienyl)(S,S-diphenylsulfimido)titanium(IV) bis(benzyl) (329)



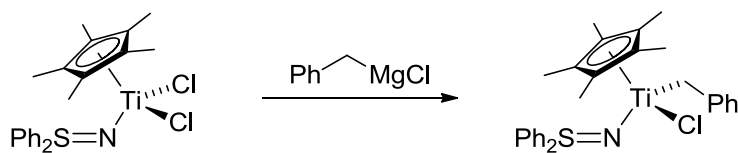
Procedure 1: 51mg (0.133 mmol) of the starting titanium material and 5 mL THF were combined in a flame-dried 5 dram vial which was then placed in the drybox freezer (-30 °C) for 1 hour. The vial was then removed from the freezer and then treated with 0.14 μL of a solution containing benzyl magnesium chloride (2.0M in THF, 0.28 mmol) which was added dropwise *via* glass pipette. The reaction was warmed to room temperature over 1 hour, then stirred for an additional 2 hours. The volatiles were

removed *in vacuo* which afforded a reddish-orange solid. This solid was extracted with benzene, filtered through celite and then the filtrate was concentrated *in vacuo*. The solid was then extracted with diethyl ether, filtered through celite and then the filtrate was concentrated *in vacuo*. 47.5 mg of a reddish-orange oil was obtained that contains roughly around 38 mg (60 %) of the desired product; this was based on the relative integrations of the benzyl proton signals in the ^1H NMR spectrum. The product was purified by recrystallization at $-30\text{ }^\circ\text{C}$ from a saturated solution in diethyl ether. During the course of one week, red-crystals had grown. The mother liquor was decanted and the red crystals were subjected to the crystallization same process. The second iteration afforded analytically pure red crystals, which were suitable for X-ray analysis.

Procedure 2: The crude residue containing the mono-benzylated species **331** was dissolved in 2 mL THF in a flame-dried 5 dram vial; this solution was placed in the drybox freezer ($-30\text{ }^\circ\text{C}$) for 1 hour. The vial was removed and was treated with 42 μL of a solution containing benzyl magnesium chloride (2.0M in THF, 0.84 mmol) which was added dropwise *via* glass pipette. The reaction mixture was warmed to room temperature over 1 hour, then stirred for an additional 16 hours. The volatiles were removed *in vacuo* which afforded a reddish-orange solid; this was extracted with diethyl ether and filtered through celite and the resulting filtrate was concentrated *in vacuo*. The ^1H NMR spectrum of the crude reaction mixture revealed that the di-benzyl product was formed cleanly.

Spectroscopic data for **332**: ^1H NMR (400 MHz, C_6D_6): δ 7.40 (m, 4H, Ar-H), δ 7.80-7.13 (m, 4H, Ar-H), δ 7.08 (m, 4H, Ar-H), δ 6.98-6.84 (m, 8H, Ar-H), δ 5.78 (s, 5H, C_5H_5), δ 3.00 (d, $J=9.2$ Hz, 2H, CH_2Ph), δ 2.68 (d, $J=9.2$ Hz, 2H, CH_2Ph); ^{13}C $\{^1\text{H}\}$ NMR (100 MHz, C_6D_6): δ 151.9, 145.0, 131.0, 129.7, 126.8, 125.8, 120.7, 113.4, 72.9₅; **Elemental Analysis** calculated for $\text{C}_{31}\text{H}_{29}\text{NSTi}$: C, 75.14 %; H, 5.90 %; N, 2.83; Found: C, 74.75 %; H, 5.94 %; N, 2.93 %.

Benzyl(η^5 -pentamethylcyclopentadienyl)(S,S-diphenylsulfimido)titanium(IV) chloride (330)

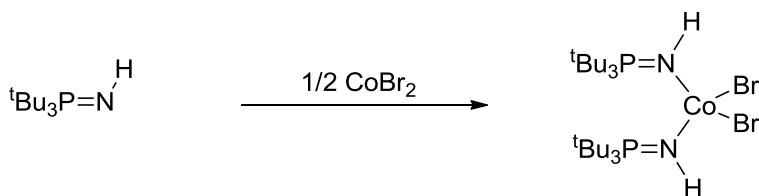


30 mg of the titanium starting material (0.061 mmol) and 2 mL of THF were added to a flame-dried 5 dram vial and placed in the drybox freezer (-30 °C) for 1 hour. The vial was removed from the freezer and was treated with 0.05 mL of a solution containing benzyl magnesium chloride (2.0 M in THF, 0.10 mmol) which was added dropwise *via* glass pipette. The solution was warmed to room temperature for 1 hour, then stirred for an additional 2 hours; during this time, the solution color changed from dark red to light reddish-orange. The volatiles were removed *in vacuo* and the residue was extracted in benzene, filtered through celite, and the filtrate was concentrated *in vacuo*. 50 mg (150 %) of crude material was isolated. Single crystals of the product were grown by low temperature recrystallization from a saturated solution in diethyl ether at -30 °C. The red crystals obtained were analytically pure.

Spectroscopic data for **333**: ¹H NMR (400 MHz, C₆D₆): δ 7.47-7.36 (m, 6H, Ar-H), δ 7.10 (m, 2H, Ar-H), δ 6.96-6.72 (m, 7H, Ar-H), δ 2.53 (d, *J* = 10.8 Hz, 1H, CH₂Ph), δ 2.38 (d, *J* = 10.8 Hz, 1H, CH₂Ph), δ 1.94 (s, 15H, C₅Me₅); ¹³C {¹H} NMR (100 MHz, C₆D₆): δ 154.1 (Ph), 145.0 (Ph), 144.8 (Ph), 130.9 (Ph), 130.6 (Ph), 129.6 (Ph), 129.5₇ (Ph), 128.6 (Ph), 128.4 (Ph), 125.8 (Ph), 125.5 (Ph), 122.4 (C₅(CH₃)₅), 121.1 (Ph), 77.8 (CH₂Ph), 12.3 (C₅(CH₃)₅); **Elemental Analysis** calculated for C₂₉H₃₂NSTi: C, 68.30 %; H, 6.32 %; N, 2.75; Found: C, 68.03 %; H, 6.28 %; N, 2.83 %.

6.5.3 Chapter 5 Experimental Section

Bis[tri(*tert*-butyl)phosphinimine]cobalt(II) dibromide (356)

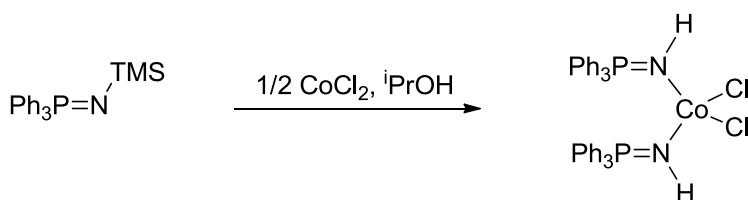


1.27 g of tri(*tert*-butyl)phosphinimine (5.84 mmol) was added to a mixture of 0.64 g of CoCl_2 (2.92 mmol) in 4 mL of THF. The resulting solution was stirred for 16 hours; during this time the solution color became dark blue. The resulting mixture was filtered through celite and the solvent was then removed *in vacuo*. The residue was dissolved in a minimal amount of benzene and layered with an equal amount of hexanes; after 16 hours, crystals were obtained that were suitable for analysis. Repeating the procedure from the supernatant two more times results in 1.30 g (80 %) of purified compound.

Spectroscopic Data for **358**: IR (neat film, cm^{-1}): 3306 (w), 2999 (m), 2972 (m), 2907 (m), 1473 (m), 1395 (m), 1373 (m), 1180 (m), 1129 (m), 1024 (w), 982 (s), 930 (m), 806 (m);

Elemental Analysis calculated for $\text{C}_{24}\text{H}_{56}\text{N}_2\text{P}_2\text{Br}_2\text{Co}$: C, 44.12 %; H, 8.64 %; N, 4.29 %; Found: C, 44.03 %; H, 8.58 %; N, 4.28 %.

Bis(triphenylphosphinimine)cobalt(II) dichloride (357)

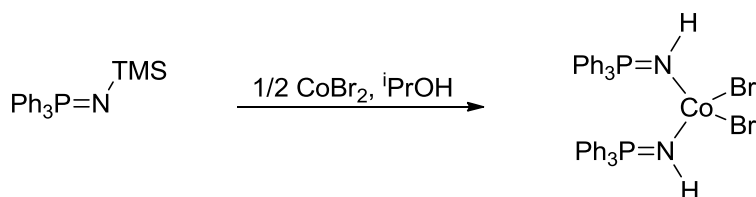


In a flame-dried 5 dram vial, 3.23 g of N-(trimethylsilyl)triphenylphosphinimine (9.24 mmol) was added to a mixture of 0.6 g of CoCl_2 (4.62 mmol) in 4 mL of THF; this solution was stirred at room temperature for 2 hours. During this time the color of the

solution changed from light to dark blue. 5 mL of ⁱPrOH (65.3 mol) was then added to the vial *via* glass pipette, and the mixture was stirred at room temperature for 2 days. The solvents were removed *in vacuo* and the remaining residue was extracted with 5 mL of acetonitrile and filtered through celite. 1 mL of THF was then added to the solution and placed in the drybox freezer (-30 °C) for 2 days; during this time, dark blue crystals formed on the sides of the vial. The supernatant was taken off and the dark blue crystals were washed with 2 mL of cold acetonitrile. The solid was then placed on the high vacuum line overnight resulting in 1.8 g (57 %) of a dark blue powder.

Spectroscopic Data for **359**: IR (neat film, cm⁻¹): 3349 (w), 3319 (w), 3263 (w), 3075 (w), 3052 (w), 3020 (w), 2973 (w), 2868 (w), 1975 (w), 1904 (w), 1824 (w), 1588 (w), 1483 (w), 1435 (m), 1316 (w), 1110 (s), 1065 (m), 1010 (s), 995 (s), 754 (m), 715 (s), 693 (s); **Elemental Analysis** calculated for C₃₆H₃₂N₂P₂Cl₂Co : C, 63.17 %; H, 4.71 %; N, 4.09 %; Found: C, 63.44 %; H, 4.72 %; N, 4.13 %.

Bis(triphenylphosphinimine)cobalt(II) dibromide (**358**)

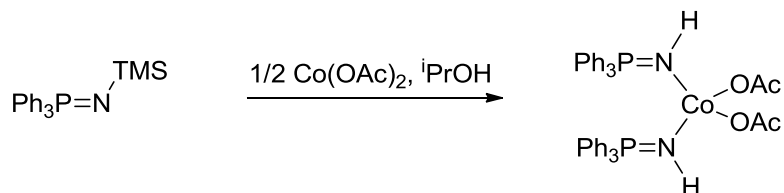


In a flame-dried 5 dram vial, 1.92 g (5.49 mmol) of N-(trimethylsilyl)triphenylphosphinimine was added to a mixture of 0.6 g of CoBr₂ (2.74 mmol) in 10 mL of THF, then the solution was stirred for 4 hours; during this time the solution color changed from light to dark blue. 1 mL of ⁱPrOH (13.1 mmol) was then added *via* glass pipette and the mixture was stirred for an additional 16 hours; during this time a dark blue solid appeared. The supernatant liquid was decanted and the solid was washed with 3 mL THF; the remaining solid was then placed on the high vacuum line overnight which results in 1.43 g (56 %) of a dark blue powder.

Spectroscopic Data for **360**: IR (neat film, cm⁻¹): 3266 (m, br), 3074 (w), 3051 (m), 3020 (m), 2001 (w), 1972 (w), 1901 (w), 1821 (w), 1588 (m), 1574 (w), 1484 (m), 1436 (s),

1398 (w), 1339 (w), 1315 (w), 1185 (w), 1159 (w), 1111 (s), 1035 (s), 1016 (s), 997 (s), 754 (s), 717 (s), 694 (s); **Elemental Analysis** calculated for $C_{36}H_{32}N_2P_2Br_2Co$: C, 55.91 %; H, 4.17 %; N, 3.62 %; Found: C, 56.06 %; H, 4.25 %; N, 3.68 %.

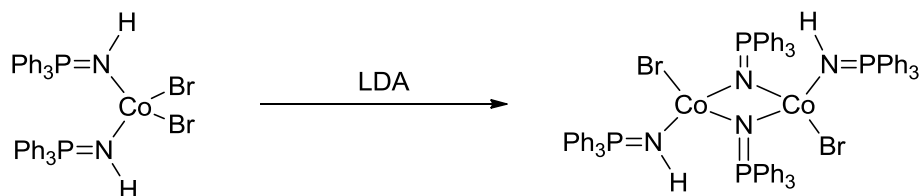
Bis(triphenylphosphinimine)cobalt(II) bis(acetate) (359)



3.02 g of N-(trimethylsilyl)triphenylphosphinimine (8.64 mmol), 0.76 g of $Co(OAc)_2$ (4.29 mmol), 50 mL of toluene and 12 mL of $iPrOH$ (0.157 mmol) were combined in a 50 mL Schlenk flask. The flask was removed from the drybox and heated to 60 °C for 16 hours. The solvents were removed *in vacuo* and the residue was rinsed repeatedly with toluene until a dark blue solid remained. The remaining volatiles were removed *in vacuo*. The product was recrystallized by creating a saturated solution of the blue solid in THF and layering with pentane. The result was 2.04 g (65 %) of dark blue crystals which were suitable for X-ray diffraction.

Spectroscopic Data for **361**: IR (neat film, cm^{-1}): 3706 (w), 3400-2800 (s, br), 3045 (s), 2923 (s), 2701 (m), 2647 (w), 2326 (w), 2287 (w), 2231 (w), 1984 (m), 1951 (w), 1921 (m), 1902 (m), 1833 (m), 1779 (m), 1592 (s, br), 1487 (s), 1432 (s, br), 1338 (s), 1233 (m), 1187 (s), 1005 (s, br), 941 (s), 916 (s), 859 (m), 748 (s), 667 (s); **Elemental Analysis** calculated for $C_{40}H_{38}N_2P_2O_4Co$: C, 65.67 %; H, 5.24 %; N, 3.85 %; Found: C, 65.66 %; H, 5.03 %; N, 3.87 %.

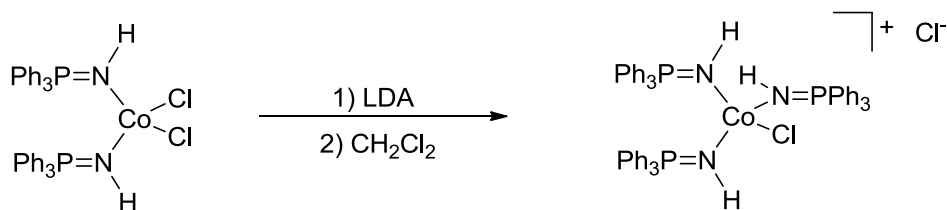
Bis(μ -triphenylphosphinimide)bis(triphenylphosphinimine)cobalt(II) dibromide (361)



80 mg of the starting cobalt phosphinimine coordination compound (0.103 mmol) and 5 mL of THF were added to a 50 mL Schlenk flask. The flask was removed from the drybox and cooled to -78 °C. This mixture was then treated with a solution containing 19 mg of LDA•THF (0.105 mmol) in 3 mL of THF, which was added dropwise *via* plastic syringe. The mixture was stirred for 30 minutes at -78 °C, then warmed to room temperature over 16 hours; during this time, the color of the solution evolved from green to black to blue. The volatiles were removed *in vacuo* then the residue was dissolved in acetonitrile and filtered through celite. The solution was then concentrated to 2 mL of acetonitrile and layered with 2 mL of THF, then 4 mL of benzene. After 3 days, light blue crystals were obtained at the THF interface. These single crystals were suitable for X-ray diffraction. Placing the crystals on a high vacuum line afforded an analytically pure product. As a result, 41.1 mg (29 %) of a pure light blue powder was obtained.

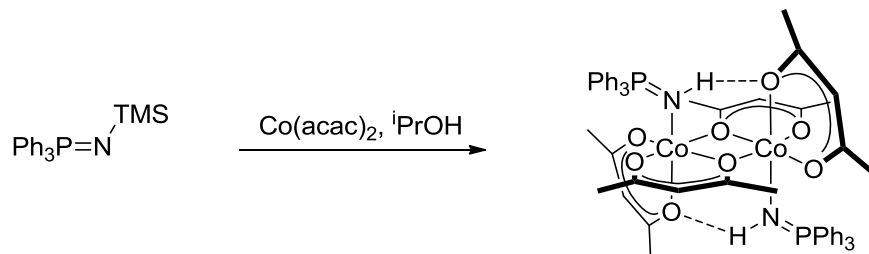
Spectroscopic Data for **364**: IR (neat film, cm⁻¹): 3331 (w), 3192 (m), 3144 (m), 3052 (m), 3013 (w), 2989 (w), 2009 (w), 1986 (w), 1897 (w), 1824 (w), 1774 (w), 1684 (w), 1587 (m), 1574 (w), 1482 (m), 1433 (s), 1342 (w), 1311 (w), 1162 (m), 1104 (s), 1068 (m), 1031 (m), 995 (s), 925 (m), 747 (s), 715 (s), 690 (s); **Elemental Analysis** calculated for C₇₂H₆₂N₄P₄Br₂Co₂: C, 62.54 %; H, 4.37 %; N, 4.05 %; Found: C, 62.63 %; H, 4.63 %; N, 3.99 %.

Chlorotris(triphenylphosphinimine)cobalt(II) chloride (363)



400 mg of the starting cobalt phosphinimine coordination compound (5.84 mmol) and 15 mL of THF were combined in a Schlenk flask. The flask was removed from the drybox and was cooled to $-78\text{ }^{\circ}\text{C}$. The mixture was then treated with a solution containing 104.8 mg of LDA•THF (5.84 mmol) in 3 mL of THF, which was added dropwise *via* plastic syringe. The mixture was then stirred for 30 minutes at $-78\text{ }^{\circ}\text{C}$, then warmed to room temperature over 16 hours; during this time, the color of the solution became light blue. The volatiles were removed *in vacuo* then the residue was dissolved in CH_2Cl_2 and filtered through celite. The solution was then concentrated to 4 mL of CH_2Cl_2 and layered with 8 mL of hexane. Light and dark blue crystals were obtained which were suitable for X-ray diffraction.

(Triphenylphosphinimine)cobalt(II) bis(acetylacetonate) (365)

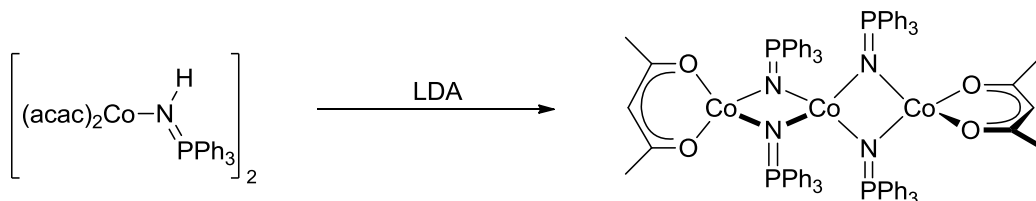


3.01 g of N-(trimethylsilyl)triphenylphosphinimine (8.61 mmol), 2.21 g of $\text{Co}(\text{acac})_2$ (8.49 mmol) and 25 mL of toluene were added to a 50 mL Schlenk flask. 15 mL of $i\text{PrOH}$ (0.196 mol) was added to this solution *via* glass pipette and the flask was removed from the drybox and heated to $60\text{ }^{\circ}\text{C}$ for 4 hours. The volatiles were then removed *in vacuo* which affords a pink oil. The flask was brought back into the drybox and 50 mL of hexane was added to the resulting residue while scraping the pink solid

from the sides of the flask; this mixture was stirred vigorously for 16 hours to isolate the rest of the pink powder. The mixture was filtered through a glass frit to collect the pink solid. The impure pink solid was recrystallized by making a saturated solution in THF and layering with an equal amount of hexanes; this furnished dark purple crystals which were placed under on a high vacuum line for 16 hours. As a result 4.59 g (82 %) of purified product was obtained in analytical purity.

Spectroscopic Data for **365**: IR (neat film, cm^{-1}): 3217 (m, br), 3057 (m), 3015 (m), 2921 (m), 1608 (s), 1433 (s, br), 1312 (m), 1253 (s), 1188 (s), 1157 (m), 1107 (s), 1013 (s), 921 (s), 844 (m), 787 (m), 754 (s), 721 (s), 696 (s); **Elemental Analysis** calculated for $\text{C}_{56}\text{H}_{60}\text{N}_2\text{P}_2\text{O}_8\text{Co}_2$: C, 62.92 %; H, 5.66 %; N, 2.62 %; Found: C, 63.17 %; H, 5.99 %; N, 2.75 %.

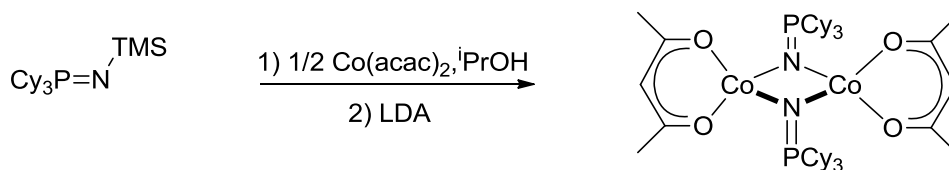
Tetrakis(μ^2 -phosphinimido)tricobalt(II) bis(acetylacetonate) (**366**)



1.03 g of the starting cobalt phosphinimine compound (1.92 mmol) and 25 mL of THF were added to a 50 mL Schlenk flask. The flask was removed from the drybox and cooled to $-78\text{ }^\circ\text{C}$. The mixture was then treated with a solution containing 0.36 g of LDA•THF (2.01 mmol) in 10 mL, which was added dropwise *via* plastic syringe. The reaction mixture was stirred at $-78\text{ }^\circ\text{C}$ for 6 hours then warmed to room temperature over 12 hours; during this time the color of the solution changed from pink to dark blue. The volatiles were removed *in vacuo* then the flask was brought back into the drybox where the residue was dissolved in toluene and filtered through celite. The volatiles were removed from the filtrate *in vacuo* giving a blue solid; the impure product was then recrystallized by creating a saturated toluene solution and layering with hexanes. 0.65 g (87 %) of analytically pure material was obtained, and was also suitable for X-ray diffraction.

Spectroscopic Data **368**: IR (neat film, cm^{-1}): 3143 (w), 3053 (s), 3021 (m), 3004 (m), 2960 (m), 2920 (m), 1959 (w), 1897 (w), 1822 (w), 1773 (w), 1671 (w), 1589 (m), 1574 (m), 1519 (s), 1482 (s), 1433 (s), 1364 (s), 1309 (m), 1267 (m), 1186 (s), 1109 (s), 1026 (s), 999 (m), 924 (m), 853 (w), 746 (s), 710 (s), 694 (s); **Elemental Analysis** calculated for $\text{C}_{89}\text{H}_{82}\text{N}_4\text{P}_4\text{O}_4\text{Co}_3$: C, 66.54 %; H, 5.04 %; N, 3.60 %; Found: C, 66.72 %; H, 4.93 %; N, 3.63 %

Bis(tri(cyclohexyl)phosphinimido)dicobalt(II) bis(acetylacetonate) (369)

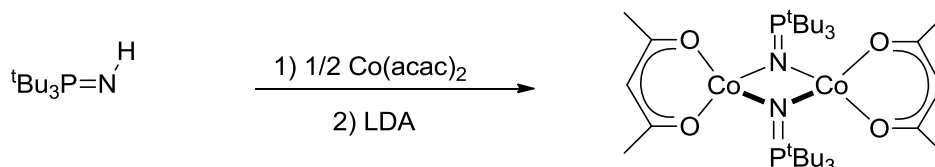


300 mg of N-(trimethylsilyl)tricyclohexylphosphinimine (8.16 mmol), 220 mg of $\text{Co}(\text{acac})_2$ (8.46 mmol) and 10 mL of toluene were combined in a 50 mL Schlenk flask and stirred from 30 minutes at room temperature. 1 mL of $i\text{PrOH}$ (13.0 mmol) was added to the mixture *via* glass pipette. The flask was removed from the drybox and heated to 60 $^\circ\text{C}$ for 16 hours; during this time the solution became maroon in color. The volatiles were removed *in vacuo*. 10 mL of THF was then added to the flask *via* plastic syringe and the flask was cooled to -78°C . The cooled mixture was then treated with a solution containing 153 mg $\text{LDA}\cdot\text{THF}$ (0.853 mmol) in 10 mL THF; this solution was added dropwise *via* plastic syringe. The resulting mixture was stirred for 30 minutes at -78°C ; during this time the color of the reaction mixture changed from dark blue to dark green. The mixture was then warmed to room temperature and stirred for 16 hours. The volatiles were removed *in vacuo* and the flask was brought back into the drybox. The green residue was extracted into hexanes and filtered through celite then the volatiles were removed from the filtrate *in vacuo*. The product was purified by layering a THF (3 mL) solution containing the compound with 7 mL of acetonitrile resulting in green crystals. As a result 201 mg (55 %) of product was obtained of analytical purity.

Spectroscopic Data for **371**: IR (neat film, cm^{-1}): 3071 (w), 2922 (s), 2850 (s), 2666 (w), 1584 (m), 1518 (s), 1443 (s), 1260 (m), 1126 (s), 1111 (s), 1079 (s), 1008 (s), 915 (m), 896

(m), 848(m), 764 (m), 752 (w), 653 (w); **Elemental Analysis** calculated for $C_{46}H_{40}N_2P_2O_4Co_2$: C, 61.05 %; H, 8.91 %; N, 3.10 %; Found: C, 60.95 %; H, 8.59 %; N, 3.33 %.

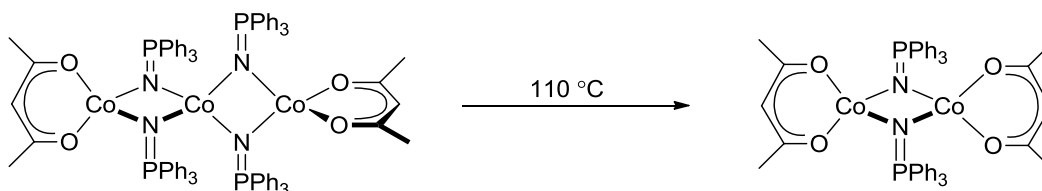
Bis(tri(*tert*-butyl)phosphinimido)dicobalt(II) bis(acetylacetonate) (370)



437 mg of tri(*tert*-butyl)phosphinimine (2.01 mmol), 517 mg of $Co(acac)_2$ (1.99 mmol), and 10 mL of toluene were added to a 50 mL Schlenk flask. The mixture was stirred for 30 minutes then 2 mL of $iPrOH$ was added *via* glass pipette. The flask was then removed from the drybox and heated to 60 °C for 16 hours which afforded a dark blue solution. The flask was then cooled to -78 °C and the mixture was treated with a solution containing 367 mg LDA•THF (2.04 mmol) in 10 mL of THF, which was added dropwise. The mixture was then stirred at -78 °C for 0.5 hours; during this time the color of the reaction mixture changed from dark blue to dark green. The mixture was then warmed to room temperature and stirred for 16 hours. The volatiles were removed *in vacuo* and the flask was brought back into the drybox. The green residue was extracted into toluene and filtered through celite; the volatiles were removed from the filtrate *in vacuo*. After drying the solid on the high vacuum line overnight, 635 mg of product (84 %) was obtained of analytical purity. Single crystals suitable for X-ray crystallographic analysis were produced by cooling a saturated solution of the compound in toluene to -30 °C.

Spectroscopic Data for **372**: IR (neat film, cm^{-1}): 3700-2700 (v, br), 3319 (s), 3050-2700 (s, br), 2965 (s), 2060 (s, br), 1594 (s), 1550-1300 (s, br), 1255 (s), 1189 (s), 1004 (s), 928 (s), 804 (m), 809 (s), 761 (s); **Elemental Analysis** calculated for $C_{34}H_{68}N_2P_2O_4Co_2$: C, 54.54 %; H, 9.15 %; N, 3.74 %; Found: C, 54.38 %; H, 9.15 %; N, 3.80 %.

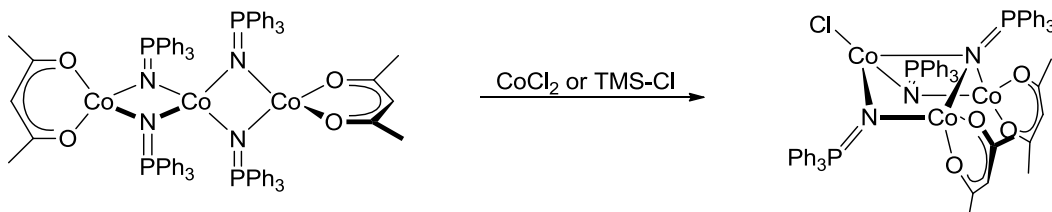
Bis(triphenylphosphinimido)dicobalt(II) bis(acetylacetonate) (**371**)



30 mg of the linear tricobalt phosphinimide complex (0.020 mmol) and 1 mL of toluene was added to a 3 mL reaction bomb. The bomb was removed from the drybox and to 110 °C for 3 days; during this time no significant physical changes in solution color were observed. The reaction mixture was cooled and brought back into the drybox. The volatiles were removed *in vacuo* and the blue residue was crystallized through dissolving the crude in 2 mL of THF and layering it with 10 mL of hexanes; as a result 16 mg (92 %) of dark blue crystals were obtained in analytical purity. The crystals were also suitable for X-ray analysis.

Spectroscopic Data for **373**: IR (neat film, cm^{-1}): 3142 (w), 3076 (m), 3056 (m), 3005 (m), 2985 (w), 2955 (w), 2918 (w), 2868 (w), 1969 (w), 1951(w), 1899 (w), 1883 (w), 1826 (w), 1810 (w), 1778 (w), 1676 (w), 1513 (s), 1433 (s), 1382 (s), 1307 (m), 1269 (m), 1159 (m), 1086 (s), 1048 (s), 1024 (s), 997 (s), 930 (s), 858 (w), 776 (m), 746 (s), 709 (s), 692 (s); **Elemental Analysis** calculated for $\text{C}_{46}\text{H}_{44}\text{N}_2\text{P}_2\text{O}_4\text{Co}_2$: C, 63.60 %; H, 5.11 %; N, 3.22 %; Found: C, 63.90 %; H, 5.27 %; N, 6.59 %.

Chlorobis(μ^2 -triphenylphosphinimido)mono(μ^3 -triphenylphosphinimido)tricobalt(II) bis(acetylacetonate) (**373**)



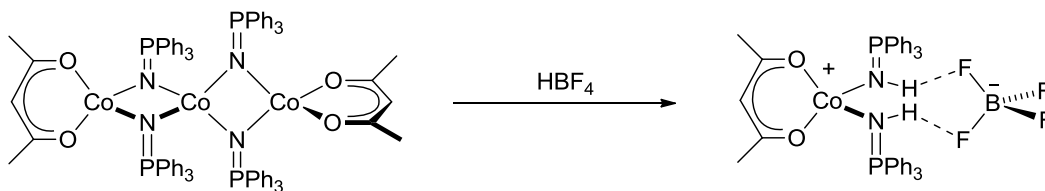
Procedure 1: 30 mg of the linear tri-cobalt phosphinimide compound (0.020 mmol) and 3 mL of THF were combined in a flame-dried 5 dram vial. 3 mg of CoCl_2 (0.023 mmol) was added to this THF solution *via spatula* and the mixture was stirred for

2 hours at room temperature. The resulting blue solution was filtered through celite and concentrated to 1 mL *in vacuo*; the THF layer was then layered with 6 mL of hexanes. As a result, 10 mg (40 %) of the purified product was obtained; the crystals grown from this vial were suitable for X-ray diffraction.

Procedure 2: 30 mg of the cobalt phosphinimide compound (0.020 mmol) and 3 mL of THF were combined in a flame-dried 5 dram vial. 2.5 mg of TMS-Cl was added to the THF solution *via* micro syringe and the mixture was stirred for 16 hours at room temperature. The resulting blue solution was filtered through celite then concentrated to 1 mL *in vacuo*. The THF solution was then layered with 6 mL of hexanes. As a result, 12 mg (48 %) of the purified product were obtained; the crystals grown from this vial were suitable for X-ray diffraction.

Spectroscopic Data for **375**: IR (neat film, cm^{-1}): 3145 (m), 3051 (s), 3006 (s), 2986 (s), 2917 (s), 2863 (m), 2695 (w), 2616 (w), 2584 (w), 2459 (w), 2315 (w), 2285 (w), 1965 (m), 1889 (m), 1823 (m), 1772 (w), 1671 (m), 1600-1300 (s, br), 1519 (s), 1436 (s), 1311 (s), 1270 (s), 1109 (s), 1021 (s), 998 (s), 926 (s), 850 (m), 756 (s), 718 (s), 652 (m); **Elemental Analysis** calculated for $\text{C}_{64}\text{H}_{59}\text{N}_3\text{P}_3\text{O}_4\text{Co}_3\text{Cl}$: C, 62.02 %; H, 4.80 %; N, 3.41%; Found: C, 61.65 %; H, 4.88 %; N, 3.40 %.

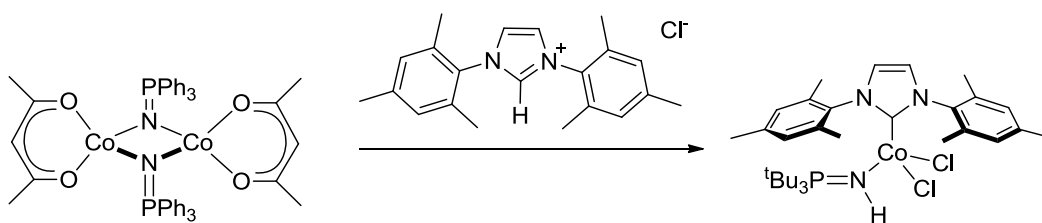
Acetylacetonato-bis(triphenylphosphinimido)cobalt(II) tetrafluoroborate (374)



30 mg of the tricobalt phosphinimide compound (0.021 mmol), 170 mg (1.57 mmol), 1,5-cyclooctadiene and 2 mL of diethyl ether were combined in a flame-dried 5 dram vial. The vial was then placed in the drybox freezer (-30 °C) for 1 hour. The vial was removed from the freezer and 6 mg of $\text{HBF}_4 \cdot \text{OEt}_2$ (0.037 mmol) was added to the vial *via* micro syringe; immediately a light blue precipitate formed. The resulting mixture was warmed to room temperature over 2 hours. During this time the light blue

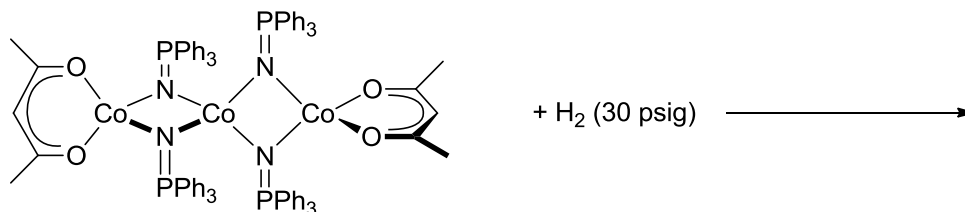
precipitate dissolved and the solution color became light purple; the mixture was then stirred for an additional 4 hours at room temperature. The volatiles were removed *in vacuo* and the resulting pink residue was dissolved in THF and layered with hexanes; this afforded purplish-pink crystals which were good enough for X-ray crystallographic analysis.

((N,N-Dimesityl)imidazole-2-yl)(tri(*tert*-butyl)phosphinimine)cobalt(II) dichloride (376)



30 mg of the cobalt phosphinimide compound (0.040 mmol) and 3 mL of THF were combined in a flame-dried 5 dram vial. A heterogeneous mixture containing 27 mg of the protonated NHC ligand (0.081 mmol) in 2 mL THF was then added dropwise to the 5 dram vial via glass pipette and the resulting mixture was stirred at room temperature for 16 hours. The solution was filtered through celite and concentrated to 1 mL then the THF solution was layered with 8 mL of hexanes. The crystals that were isolated from the recrystallization mixture were suitable for X-ray diffraction.

General procedure for test hydrogenation reactions:

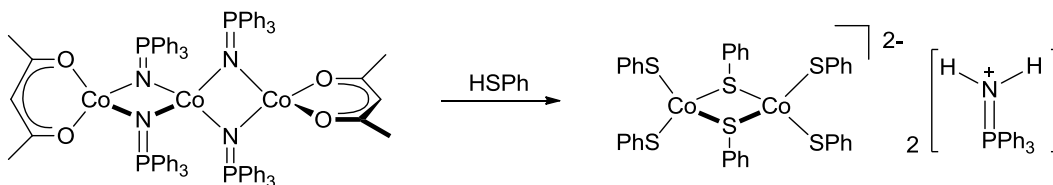


General Procedure 1: 20 mg of the linear tri-cobalt phosphinimide compound **366** (0.014 mmol) and 2 mL of THF were combined in a flame-dram 5 dram vial; this

mixture was then transferred to a Fisher-Porter bottle. 1 (0.014 mmol) or 10 (0.140 mmol) equivalents of either: diphenylacetylene, cyclohexene, cinnamaldehyde, dibenzothiophene, benzophenone or N-benzylcinnamylimine²⁸¹ was added to the Fisher-Porter bottle. The atmosphere was then filled to 30 psig of hydrogen and released; this was repeated 4 times in order to have the reaction mixture under a sufficient atmosphere of hydrogen gas. The container was then pressurized with hydrogen up to 30 psi and stirred at room temperature for 16 hours; during this time the solution became light brown. The hydrogen gas was then vented and the resulting brown mixture was concentrated to 0.5 mL. This mixture was filtered through a small plug of silica and washed with 2 mL of THF; brown and blue color bands remained on the silica. The filtrate was removed of all volatiles *in vacuo*. The resulting colorless residue was dissolved in C₆D₆ and analyzed by NMR spectroscopy which revealed only the presence of starting materials.

General Procedure 2: 20 mg of the linear tri-cobalt phosphinimide compound **366** (0.014 mmol) and 1 mL of C₆D₆ was combined in a flame-dried 5 dram vial; this mixture was then transferred into a Fisher-Porter bottle. 1 (0.014 mmol) or 10 (0.140 mmol) equivalents of either: diphenylacetylene, cyclohexene, cinnamaldehyde, dibenzothiophene, benzophenone or N-benzylcinnamylimine²⁸¹ was added to the Fisher-Porter bottle. The atmosphere was filled to 30 psi of hydrogen and released; this was repeated 4 times in order to place the reaction mixture under a sufficient atmosphere of hydrogen gas. The container was then pressurized with hydrogen up to 30 psi and stirred at room temperature for 16 hours; during this time the mixture became light brown. The mixture was filtered through a plug of silica leaving the brown and blue bands on the silica; this afforded a colorless filtrate.

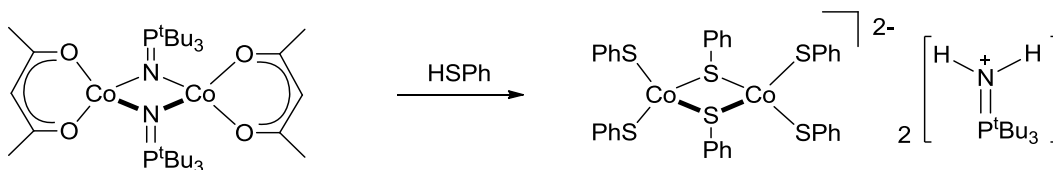
**Bis(triphenylphosphiniminium)bis(μ^2 -phenylthiolato)tetrakis(phenylthiolato)
dicobaltate (**381**)**



97 mg of the linear tri-cobalt phosphinimide compound (0.068 mmol) and 10 mL of THF were combined in a flame-dried 5 dram vial. 0.60 mL of thiophenol (5.84 mmol) was added dropwise to the vial *via* micro syringe and the resulting solution was stirred for 16 hours at room temperature; during this time the reaction mixture became dark brown. The volatiles were removed *in vacuo* and the resulting brown residue was extracted with benzene and filtered through celite. Over four days, the benzene solution was allowed to concentrate to 1 mL, which afforded dark brown crystals. The mother liquor was decanted then the residual solids were rinsed with 3 mL of hexanes. This resulted in the isolation of 78 mg (93 %) of **383** in analytical purity.

Spectroscopic Data for **383**: IR (neat film, cm^{-1}): 3200-2800 (s, br), 3040 (s), 2567 (w, br), 1999 (w), 1971 (w), 1943 (w), 1898 (w), 1850 (w), 1812 (w), 1778 (w), 1681 (w), 1587 (s), 1576 (s), 1483 (s), 1474 (s), 1436 (s), 1389 (w), 1182 (m), 1164 (m), 1115 (s), 1085 (s), 1021 (s), 998 (s), 951 (m), 891 (w), 843 (w), 740 (s), 728 (s), 694 (s); **Elemental Analysis** calculated for $\text{C}_{72}\text{H}_{64}\text{N}_2\text{P}_2\text{S}_6\text{Co}_2$: C, 65.04 %; H, 4.85 %; N, 2.11 %; S, 14.47; Found: C, 65.22 %; H, 4.87 %; N, 2.14 %; S, 14.61 %.

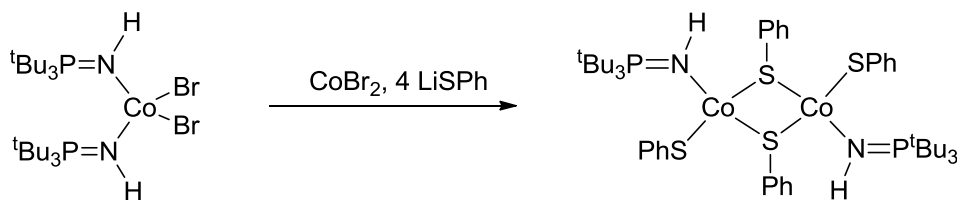
Bis(tri(*tert*-butyl)phosphiniminium)bis(μ^2 -phenylthiolato)tetrakis(phenylthiolato)dicobaltate (382)



45 mg of the linear tri-cobalt phosphinimide compound (0.060 mmol) and 4 mL of THF were combined in a flame-dried 5 dram vial. 0.15 mL of thiophenol (1.46 mmol) was added dropwise to the THF solution *via* micro syringe. The resulting solution was stirred for 16 hours at room temperature; during this time the reaction mixture became dark brown. The volatiles were removed *in vacuo*. The residue was then extracted with benzene and filtered through celite. Over four days, the benzene solution was concentrated to 1 mL which afforded dark brown crystals. The mother liquor was decanted and the brown crystals were rinsed with 3 mL hexanes resulting in 28.9 mg (40 %) of **381** in analytical purity.

Spectroscopic Data for **381**: IR (neat film, cm^{-1}): 3400-2900 (s, br), 2528 (w), 2387 (w), 2312 (w), 2175 (w), 1939 (m), 1923 (m), 1867 (m), 1843 (m), 1812 (m), 1778 (w), 1747 (w), 1719 (w), 1575 (s), 1550 (s), 1401 (s), 1375 (s), 1180 (s), 1122 (m), 1083 (s), 1068 (s), 1023 (s), 910 (s), 810 (s), 741 (s), 692 (s); **Elemental Analysis** calculated for $\text{C}_{60}\text{H}_{88}\text{N}_2\text{P}_2\text{S}_6\text{Co}_2$: C, 59.98 %; H, 7.33 %; N, 2.32 %; Found: C, 59.59 %; H, 6.97 %; N, 2.35 %.

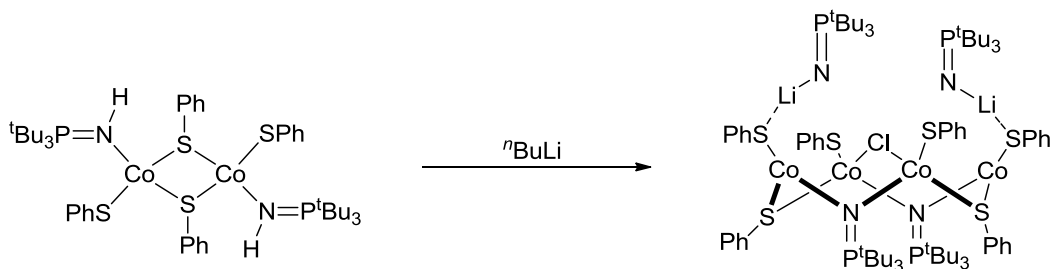
Bis(tri(*tert*-butyl)phosphinimine)dicobalt(II) hexakis(thiophenolate) (383)



0.39 g of CoBr_2 (1.78 mmol) and 0.40 g of tri(*tert*-butyl)phosphinimine (1.84 mmol) were stirred in 10 mL of THF for 10 minutes; the color of the solution at this point was dark blue. A solution of 0.41 g of LiSPh (3.53 mmol) in 10 mL of THF was then introduced dropwise to the original THF mixture over 2 minutes; this afforded a dark green solution. The green solution was stirred for an additional 16 hours. The volatiles were removed *in vacuo*, redissolved in toluene and filtered through celite. The resulting toluene solution was layered with the same volume of hexane; after one week dark green rods resulted that were suitable for various analyses. As a result 0.40 g (91 %) of the purified product was obtained in spectral purity.

Spectroscopic Data for **385**: IR (neat film, cm^{-1}): 3301 (m), 3034 (s), 3001 (s), 2974 (s), 2957 (s), 2916 (s), 1938 (w), 1866 (w), 1801 (w), 1575 (s), 1476 (s), 1434 (s), 1397 (w), 1373 (m), 1180 (m), 1142 (m), 1024 (m), 1014 (m), 940 (m), 929 (m), 895 (w), 807 (m), 738 (s), 693 (s); **Elemental Analysis** calculated for $\text{C}_{48}\text{H}_{76}\text{N}_2\text{P}_2\text{S}_4\text{Co}_2$: C, 58.28 %; H, 7.74 %; N, 2.83 %; S, 12.97 %; Found: C, 57.89 %; H, 7.74 %; N, 2.83 %; S, 12.90 %.

(μ^3 -Chloro)bis(μ -lithiumphosphinimido)bis(μ^2 -phenylthiolato)tetrakis(thiolato)bis(μ^2 -tri(*tert*-butyl)phosphinimido)tricobalt(II)monocobalt(I) (384)



118 mg (1.25 mmol) of the cobalt phosphinimine compound was dissolved in 5 mL of THF and cooled to $-78\text{ }^{\circ}\text{C}$. 0.1 mL of a 2.5M solution of ${}^n\text{BuLi}$ in hexanes (2.50 mmol) was added dropwise to the cooled THF solution and stirred at $-78\text{ }^{\circ}\text{C}$ for 2 hours. After this time, the mixture was allowed to warm to room temperature and stir for 16 hours; during this time the reaction mixture became dark brown. The volatiles were removed *in vacuo* and the brown residue was extracted with 20 mL of pentane and filtered through celite. By allowing the pentane solution to evaporate over one week, dark green crystals were formed on the side of the flask. 30 mg (14 %) of analytically pure compound was obtained.

Spectroscopic Data for **386**: IR (neat film, cm^{-1}): 3047 (w), 2977 (m), 2912 (w), 1932 (w), 1855 (w), 1793 (w), 1575 (s), 1470 (s), 1434 (m), 1392 (m), 1368 (m), 1265 (w), 1179 (m), 991 (s), 932 (s), 807 (s), 737 (s), 695 (s); **Elemental Analysis** calculated for $\text{C}_{84}\text{H}_{128}\text{N}_4\text{P}_4\text{S}_6\text{Co}_4\text{ClLi}_2$: C, 55.88 %; H, 7.70 %; N, 3.10 %; S, 10.67 %; Found: C, 55.80 %; H, 7.77 %; N, 3.09 %; S, 10.53.

Notes and References

- (1) Morita, M.; Bauer, R. C.; Stryker, J. M. In *Comprehensive Heterocyclic Chemistry III*; Alan, R. K., Christopher, A. R., Eric, F. V. S., Richard, J. K. T., Eds.; Elsevier: Oxford, 2008, p 555-621.
- (2) McNaught, A. D. *Adv. Heterocycl. Chem.* **1976**, *20*, 175-319.
- (3) Chen, J. Ph.D Dissertation, University of Alberta, 1999.
- (4) Tiege, P. Ph.D. Dissertation, University of Alberta, 2001.
- (5) Ogoshi, S.; Nishida, T.; Tsutsumi, K.; Ooi, M.; Shinagawa, T.; Akasaka, T.; Yamane, M.; Kurosawa, H. *J. Am. Chem. Soc.* **2001**, *123*, 3223-3228.
- (6) Bauer, R. C. Ph.D. Dissertation, University of Alberta, 2009.
- (7) McKinney, R. J.; Tulip, T. H.; Thorn, D. L.; Coolbaugh, T. S.; Tebbe, F. N. *J. Am. Chem. Soc.* **1981**, *103*, 5584-5586.
- (8) Binger, P.; Müller, P.; Benn, R.; Mynott, R. *Angew. Chem. Int. Ed.* **1989**, *28*, 610-611.
- (9) Teuben, J. H. *J. Organomet. Chem.* **1969**, *17*, 87-93.
- (10) Brownwensley, K. A.; Buchwald, S. L.; Cannizzo, L.; Clawson, L.; Ho, S.; Meinhardt, D.; Stille, J. R.; Straus, D.; Grubbs, R. H. *Pure Appl. Chem.* **1983**, *55*, 1733-1744.
- (11) Stille, J. R.; Grubbs, R. H. *J. Am. Chem. Soc.* **1983**, *105*, 1664-1665.
- (12) Tebbe, F. N.; Harlow, R. L. *J. Am. Chem. Soc.* **1980**, *102*, 6149-6151.
- (13) Tebbe, F. N.; Parshall, G. W.; Reddy, G. S. *J. Am. Chem. Soc.* **1978**, *100*, 3611-3613.
- (14) Howard, T. R.; Lee, J. B.; Grubbs, R. H. *J. Am. Chem. Soc.* **1980**, *102*, 6876-6878.
- (15) Anslyn, E. V.; Grubbs, R. H. *J. Am. Chem. Soc.* **1987**, *109*, 4880-4890.
- (16) Hoffmann, R.; Woodward, R. B. *J. Am. Chem. Soc.* **1965**, *87*, 2046-2048.
- (17) Shono, T.; Nagasawa, T.; Tsubouchi, A.; Noguchi, K.; Takeda, T. *Chem. Commun.* **2008**, 3537-3539.
- (18) Oishi, S.; Shono, T.; Nagasawa, T.; Inoue, T.; Tsubouchi, A.; Takeda, T. *Tetrahedron Lett.* **2008**, *49*, 6426-6428.
- (19) Hawkins, J. M.; Grubbs, R. H. *J. Am. Chem. Soc.* **1988**, *110*, 2821-2823.
- (20) Beckhaus, R.; Sang, J.; Wagner, T.; Ganter, B. *Organometallics* **1996**, *15*, 1176-1187.
- (21) Dennehy, R. D.; Whitby, R. J. *J. Chem. Soc., Chem. Commun.* **1990**, 1060-1062.
- (22) Sekutowski, D. G.; Stucky, G. D. *J. Am. Chem. Soc.* **1976**, *98*, 1376-1382.
- (23) Horáček, M.; Bazyakina, N.; Stepnicka, P.; Gyepes, R.; Cisarová, I.; Bredeau, S.; Meunier, P.; Kubista, J.; Mach, K. *J. Organomet. Chem.* **2001**, *628*, 30-38.
- (24) Rosenthal, U.; Ohff, A.; Tillack, A.; Baumann, W.; Görls, H. *J. Organomet. Chem.* **1994**, *468*, C4-C8.
- (25) Bruneau, C.; Dixneuf, P. H. *Acc. Chem. Res.* **1998**, *32*, 311-323.
- (26) Wakatsuki, Y. *J. Organomet. Chem.* **2004**, *689*, 4092-4109.
- (27) de Boer, H. J. R.; Akkermann, O. S.; Bickelhaupt, F.; Erker, G.; Czisch, P.; Mynott, R.; Wallis, J. M.; Krüger, C. *Angew. Chem. Int. Ed.* **1986**, *25*, 639-640.
- (28) Petasis, N. A.; Fu, D. K. *Organometallics* **1993**, *12*, 3776-3780.

- (29) Doxsee, K. M.; Juliette, J. J. J.; Zientara, K.; Nieckarz, G. *J. Am. Chem. Soc.* **1994**, *116*, 2147-2148.
- (30) Doxsee, K. M.; Juliette, J. J. J.; Mouser, J. K. M.; Zientara, K. *Organometallics* **1993**, *12*, 4682-4686.
- (31) Shono, T.; Kurashige, R.; Mukaiyama, R.; Tsubouchi, A.; Takeda, T. *Chemistry – A European Journal* **2007**, *13*, 4074-4080.
- (32) Binger, P.; Müller, P.; Herrmann, A. T.; Philipps, P.; Gabor, B.; Langhauser, F.; Krüger, C. *Chem. Ber.* **1991**, *124*, 2165-2170.
- (33) Huang, T. M.; Chen, J. T.; Lee, G. H.; Wang, Y. *J. Am. Chem. Soc.* **1993**, *115*, 1170-1171.
- (34) Casey, C. P.; Yi, C. S. *J. Am. Chem. Soc.* **1992**, *114*, 6597-6598.
- (35) Casey, C. P.; Nash, J. R.; Yi, C. S.; Selmecky, A. D.; Chung, S.; Powell, D. R.; Hayashi, R. K. *J. Am. Chem. Soc.* **1998**, *120*, 722-733.
- (36) Taits, E.; Petrovskii, P.; Krivykh, V. *Russ. Chem. Bull.* **1999**, *48*, 1774-1781.
- (37) Krivykh, V. V.; Taits, E. S.; Petrovskii, P. V.; Struchkov, Y. T.; Yanovskii, A. I. *Mendeleev Commun.* **1991**, *1*, 103-104.
- (38) Morita, M.; Stryker, J. M., Unpublished Work, University of Alberta; Edmonton, 2004.
- (39) Ephritikhine, M.; Francis, B. R.; Green, M. L. H.; Mackenzie, R. E.; Smith, M. J. *J. Chem. Soc., Dalton Trans.* **1977**, 1131-1135.
- (40) Periana, R. A.; Bergman, R. G. *J. Am. Chem. Soc.* **1986**, *108*, 7346-7355.
- (41) Tjaden, E. B.; Stryker, J. M. *J. Am. Chem. Soc.* **1990**, *112*, 6420-6422.
- (42) McGhee, W. D.; Bergman, R. G. *J. Am. Chem. Soc.* **1985**, *107*, 3388-3389.
- (43) Tjaden, E. B.; Casty, G. L.; Stryker, J. M. *J. Am. Chem. Soc.* **1993**, *115*, 9814-9815.
- (44) Huang, T.-M.; Hsu, R.-H.; Yang, C.-S.; Chen, J.-T.; Lee, G.-H.; Wang, Y. *Organometallics* **1994**, *13*, 3657-3663.
- (45) Casty, G. L.; Stryker, J. M. *J. Am. Chem. Soc.* **1995**, *117*, 7814-7815.
- (46) Carter, C. A. G.; McDonald, R.; Stryker, J. M. *Organometallics* **1999**, *18*, 820-822.
- (47) Greidanus, G.; McDonald, R.; Stryker, J. M. *Organometallics* **2001**, *20*, 2492-2504.
- (48) Ogoshi, S.; Stryker, J. M. *J. Am. Chem. Soc.* **1998**, *120*, 3514-3515.
- (49) Quesnel, J. M. Sc. Dissertation, University of Alberta, 2009.
- (50) C. Green, *J. Chem. Soc. Rev.* **1998**, *27*, 263-272.
- (51) Lauher, J. W.; Hoffmann, R. *J. Am. Chem. Soc.* **1976**, *98*, 1729-1742.
- (52) Curtis, M. D.; Eisenstein, O. *Organometallics* **1984**, *3*, 887-895.
- (53) Negishi, E.-i.; Kondakov, D. Y.; Van Horn, D. E. *Organometallics* **1997**, *16*, 951-957.
- (54) Tumas, W.; Suriano, J. A.; Harlow, R. L. *Angew. Chem. Int. Ed.* **1990**, *29*, 75-76.
- (55) Qiu, X. Ph.D. Dissertation, University of Alberta, 2000.
- (56) Doxsee, K. M.; Wood, N. P.; Hanawalt, E. M.; Weakley, T. J. R. *Heteroat. Chem* **1996**, *7*, 383-389.
- (57) Avarvari, N.; Le Floch, P.; Charrier, C.; Mathey, F. *Heteroat. Chem* **1996**, *7*, 397-402.
- (58) Meinhardt, J. D.; Santarsiero, B. D.; Grubbs, R. H. *J. Am. Chem. Soc.* **1986**, *108*, 3318-3323.
- (59) Carter, C. A. G.; Casty, G. L.; Stryker, J. M. *Synlett* **2001**, 1046-1049.

- (60) Carter, C. A. G.; Greidanus, G.; Chen, J. X.; Stryker, J. M. *J. Am. Chem. Soc.* **2001**, *123*, 8872-8873.
- (61) Dennehy, R. D.; Whitby, R. J. *J. Chem. Soc., Chem. Commun.* **1992**, 35-36.
- (62) Chamberlain, L. R.; Durfee, L. D.; Fanwick, P. E.; Kobriger, L. M.; Latesky, S. L.; McMullen, A. K.; Steffey, B. D.; Rothwell, I. P.; Foltin, K.; Huffman, J. C. *J. Am. Chem. Soc.* **1987**, *109*, 6068-6076.
- (63) Fandos, R.; Meetsma, A.; Teuben, J. H. *Organometallics* **1991**, *10*, 2665-2671.
- (64) Meinhart, J. D.; Grubbs, R. H. *Bull. Chem. Soc. Jpn.* **1988**, *61*, 171-180.
- (65) Doxsee, K. M.; Mouser, J. K. M. *Tetrahedron Lett.* **1991**, *32*, 1687-1690.
- (66) Doxsee, K. M.; Mouser, J. K. M. *Organometallics* **1990**, *9*, 3012-3014.
- (67) Doxsee, K. M.; Juliette, J. J. J.; Weakley, T. J. R.; Zientara, K. *Inorg. Chim. Acta* **1994**, *222*, 305-315.
- (68) Petasis, N. A.; Staszewski, J. P.; Fu, D.-K. *Tetrahedron Lett.* **1995**, *36*, 3619-3622.
- (69) Doxsee, K. M.; Juliette, J. J. J.; Mouser, J. K. M.; Zientara, K. *Organometallics* **1993**, *12*, 4742-4744.
- (70) van der Heijden, H.; Hessen, B. *Inorg. Chim. Acta* **2003**, *345*, 27-36.
- (71) Horikawa, Y. N., Tadahiro; Watanabe, Mikako; Fujiwara, Tooru; Takeda, Takeshi *J. Org. Chem.* **1997**, *62*, 3678-3682.
- (72) Yatsumonji, Y.; Atake, Y.; Tsubouchi, A.; Takeda, T. *Chem. Commun.* **2009**, 3375-3377.
- (73) Holland, R. L.; Bunker, K. D.; Chen, C. H.; DiPasquale, A. G.; Rheingold, A. L.; Baldrige, K. K.; O'Connor, J. M. *J. Am. Chem. Soc.* **2008**, *130*, 10093-+.
- (74) Procter, D. J. F., R.A.; Skrydstrup, T. *Organic Synthesis Using Samarium Diiodide: A Practical Guide*; The Royal Society of Chemistry, 2009.
- (75) Girard, P.; Namy, J. L.; Kagan, H. B. *J. Am. Chem. Soc.* **1980**, *102*, 2693-2698.
- (76) Shabangi, M.; Flowers, R. A. *Tetrahedron Lett.* **1997**, *38*, 1137-1140.
- (77) Zhan, Z.-P.; Yang, R.-F.; Lang, K. *Tetrahedron Lett.* **2005**, *46*, 3859-3862.
- (78) Van de Weghe, P.; Collin, J. *Tetrahedron Lett.* **1995**, *36*, 1649-1652.
- (79) Barrero, A. F.; Herrador, M. M.; del Moral, J. F. Q.; Arteaga, P.; Akssira, M.; El Hanbali, F.; Arteaga, J. F.; Dieguez, H. R.; Sanchez, E. M. *J. Org. Chem.* **2007**, *72*, 2251-2254.
- (80) Parrish, J. D.; Shelton, D. R.; Little, R. D. *Org. Lett.* **2003**, *5*, 3615-3617.
- (81) Sancho-Sanz, I.; Miguel, D.; Millán, A.; Estévez, R. E.; Oller-López, J. L.; Álvarez-Manzaneda, E.; Robles, R.; Cuerva, J. M.; Justicia, J. *J. Org. Chem.* **2010**, *76*, 732-735.
- (82) Diéguez, H. R.; López, A.; Domingo, V.; Arteaga, J. s. F.; Dobado, J. A.; Herrador, M. M.; Quílez del Moral, J. F.; Barrero, A. F. *J. Am. Chem. Soc.* **2009**, *132*, 254-259.
- (83) Gansäuer, A.; Ndene, N.; Lauterbach, T.; Justicia, J.; Winkler, I.; Muck-Lichtenfeld, C.; Grimme, S. *Tetrahedron* **2008**, *64*, 11839-11845.
- (84) Gansäuer, A.; Bluhm, H.; Pierobon, M. *J. Am. Chem. Soc.* **1998**, *120*, 12849-12859.
- (85) Furstner, A.; Shi, N. Y. *J. Am. Chem. Soc.* **1996**, *118*, 12349-12357.
- (86) Coutts, R. S. P.; Wailes, P. C.; Martin, R. L. *J. Organomet. Chem.* **1973**, *47*, 375-382.
- (87) Birmingham, J. M.; Fischer, A. K.; Wilkinson, G. *Naturwissenschaften* **1955**, *42*, 96-96.
- (88) Sekutowski, D. G.; Stucky, G. D. *Inorg. Chem.* **1975**, *14*, 2192-2199.

- (89) Alt, H. G.; Engelhardt, H. E.; Rausch, M. D.; Kool, L. B. *J. Am. Chem. Soc.* **1985**, *107*, 3717-3718.
- (90) Kool, L. B.; Rausch, M. D.; Alt, H. G.; Herberhold, M.; Thewalt, U.; Wolf, B. *Angew. Chem. Int. Ed.* **1985**, *24*, 394-401.
- (91) Kool, L. B.; Rausch, M. D.; Alt, H. G.; Herberhold, M.; Wolf, B.; Thewalt, U. *J. Organomet. Chem.* **1985**, *297*, 159-169.
- (92) Girolami, G. S.; Wilkinson, G.; Thorntonpett, M.; Hursthouse, M. B. *J. Chem. Soc., Dalton Trans.* **1984**, 2347-2350.
- (93) Concellón, J. M.; Rodríguez-Solla, H.; del Amo, V. *Chem. Eur. J.* **2008**, *14*, 10184-10191.
- (94) Oshima, K. *J. Organomet. Chem.* **1999**, *575*, 1-20.
- (95) Takai, K.; Ueda, T.; Hayashi, T.; Moriwake, T. *Tetrahedron Lett.* **1996**, *37*, 7049-7052.
- (96) Hojo, M.; Harada, H. *Chem. Commun.* **1997**, 2077-2078.
- (97) Cahiez, G.; Marquais, S. *Tetrahedron Lett.* **1996**, *37*, 1773-1776.
- (98) Cahiez, G.; Marquais, S. *Pure Appl. Chem.* **1996**, *68*, 53-60.
- (99) Donkervoort, J. G.; Vicario, J. L.; Jastrzebski, J.; Cahiez, G.; vanKoten, G. *Recl. Trav. Chim. Pays-Bas* **1996**, *115*, 547-548.
- (100) Riguet, E.; Klement, I.; Reddy, C. K.; Cahiez, G.; Knochel, P. *Tetrahedron Lett.* **1996**, *37*, 5865-5868.
- (101) Layfield, R. A. *Chemical Society Reviews* **2008**, *37*, 1098-1107.
- (102) Kim, S.-H.; Rieke, R. D. *J. Org. Chem.* **2000**, *65*, 2322-2330.
- (103) Gansäuer, A. *J. Org. Chem.* **1998**, *63*, 2070-2071.
- (104) Brasen, W. R.; Holmquist, H. E.; Benson, R. E. *J. Am. Chem. Soc.* **1961**, *83*, 3125-3135.
- (105) RajanBabu, T. V.; Nugent, W. A. *J. Am. Chem. Soc.* **1989**, *111*, 4525-4527.
- (106) Friedrich, J.; Walczak, K.; Dolg, M.; Piestert, F.; Lauterbach, T.; Worgull, D.; Gansauer, A. *J. Am. Chem. Soc.* **2008**, *130*, 1788-1796.
- (107) Barrero, A. F.; del Moral, J. F. Q.; Sanchez, E. M.; Arteaga, J. F. *Eur. J. Org. Chem.* **2006**, 1627-1641.
- (108) RajanBabu, T. V.; Nugent, W. A.; Beattie, M. S. *J. Am. Chem. Soc.* **1990**, *112*, 6408-6409.
- (109) Nugent, W. A.; RajanBabu, T. V. *J. Am. Chem. Soc.* **1988**, *110*, 8561-8562.
- (110) *Titanium and Zirconium in Organic Synthesis*; Marek, I., Ed.; Wiley-VCH: Weinheim, 2002.
- (111) Gansäuer, A.; Barchuk, A.; Keller, F.; Schmitt, M.; Grimme, S.; Gerenkamp, M.; Mück-Lichtenfeld, C.; Daasbjerg, K.; Svith, H. *J. Am. Chem. Soc.* **2007**, *129*, 1359-1371.
- (112) Gansäuer, A.; Ndene, N.; Lauterbach, T.; Justicia, J.; Winkler, I.; Mück-Lichtenfeld, C.; Grimme, S. *Tetrahedron* **2008**, *64*, 11839-11845.
- (113) Kraus, G. A.; Landgrebe, K. *Synthesis* **1984**, 885-885.
- (114) Page, P. C. B.; Rayner, C. M.; Sutherland, I. O. *J. Chem. Soc., Chem. Commun.* **1988**, 356-358.
- (115) Sylvester, K. T.; Chirik, P. J. *J. Am. Chem. Soc.* **2009**, *131*, 8772-8774.
- (116) Sonnet, P. E.; Oliver, J. E. *J. Org. Chem.* **1976**, *41*, 3279-3283.
- (117) König, B.; Pitsch, W.; Thondorf, I. *J. Org. Chem.* **1996**, *61*, 4258-4261.
- (118) Baumstark, A. L.; Vasquez, P. C. *J. Org. Chem.* **1988**, *53*, 3437-3439.
- (119) Kwon, D. W.; Kim, Y. H.; Lee, K. *J. Org. Chem.* **2002**, *67*, 9488-9491.

- (120) Johnson, A. W.; LaCount, R. B. *J. Am. Chem. Soc.* **1961**, *83*, 417-423.
- (121) Okuma, K.; Tanaka, Y.; Kaji, S.; Ohta, H. *J. Org. Chem.* **1983**, *48*, 5133-5134.
- (122) Yamaguchi, M.; Nobayashi, Y.; Hirao, I. *Tetrahedron* **1984**, *40*, 4261-4266.
- (123) Bagdasaryan, G. B.; Pogosyan, P. S.; Panosyan, G. A.; Indzhikyan, M. G. *Russ. J. Gen. Chem.* **2008**, *78*, 1177-1183.
- (124) Asandei, A. D.; Moran, I. W. *J. Polym. Sci., Part A: Polym. Chem.* **2006**, *44*, 1060-1070.
- (125) Gansäuer, A.; Lauterbach, T.; Narayan, S. *Angew. Chem. Int. Ed.* **2003**, *42*, 5556-5573.
- (126) Rendler, S.; MacMillan, D. W. C. *J. Am. Chem. Soc.* **2010**, *132*, 5027-5029.
- (127) Gansäuer, A.; Rosales, A.; Justicia, J. *Synlett* **2006**, 927-929.
- (128) Elchenbroich, C. *Organometallics*; 3 ed.; Wiley-VCH: Marburg, 2006.
- (129) Schoeller, W. W. *Z. Anorg. Allg. Chem.* **2003**, *629*, 816-827.
- (130) Siemeling, U.; Kölling, L.; Kuhnert, O.; Neumann, B.; Stammler, A.; Stammler, H. G.; Fink, G.; Kaminski, E.; Kiefer, A.; Schrock, R. R. *Z. Anorg. Allg. Chem.* **2003**, *629*, 781-792.
- (131) Weber, K.; Korn, K.; Schorm, A.; Kipke, J.; Lemke, M.; Khvorost, A.; Harms, K.; Sundermeyer, J. *Z. Anorg. Allg. Chem.* **2003**, *629*, 744-754.
- (132) Wolczanski, P. T. *Polyhedron* **1995**, *14*, 3335-3362.
- (133) Glueck, D. S.; Green, J. C.; Michelman, R. I.; Wright, I. N. *Organometallics* **1992**, *11*, 4221-4225.
- (134) Williams, D. S.; Schofield, M. H.; Schrock, R. R.; Davis, W. M.; Anhaus, J. T. *J. Am. Chem. Soc.* **1991**, *113*, 5480-5481.
- (135) Dehnicke, K.; Krieger, M.; Massa, W. *Coord. Chem. Rev.* **1999**, *182*, 19-65.
- (136) Dehnicke, K.; Strähle, J. *Polyhedron* **1989**, *8*, 707-726.
- (137) Stephan, D. W. In *Adv. Organomet. Chem.*; R. West., A. F. Hill, Eds.; Academic Press: 2006; Vol. Volume 54, p 267-291.
- (138) Dehnicke, K.; Weller, F. *Coord. Chem. Rev.* **1997**, *158*, 103-169.
- (139) Dehnicke, K.; Greiner, A. *Angew. Chem. Int. Ed.* **2003**, *42*, 1340-1354.
- (140) Sundermann, A.; Schoeller, W. W. *J. Am. Chem. Soc.* **2000**, *122*, 4729-4734.
- (141) Diefenbach, A.; Bickelhaupt, F. M. *Z. Anorg. Allg. Chem.* **1999**, *625*, 892-900.
- (142) Stephan, D. W.; Stewart, J. C.; Guérin, F.; Courtenay, S.; Kickham, J.; Hollink, E.; Beddie, C.; Hoskin, A.; Graham, T.; Wei, P.; Spence, R. E. v. H.; Xu, W.; Koch, L.; Gao, X.; Harrison, D. G. *Organometallics* **2003**, *22*, 1937-1947.
- (143) Tolman, C. A. *J. Am. Chem. Soc.* **1970**, *92*, 2956-2965.
- (144) Tolman, C. A. *Chem. Rev.* **1977**, *77*, 313-348.
- (145) Lu, W. C.; Sun, C. C. *J. Mol. Struct.* **2002**, *593*, 1-7.
- (146) Beddie, C.; Hollink, E.; Wei, P.; Gault, J.; Stephan, D. W. *Organometallics* **2004**, *23*, 5240-5251.
- (147) Latham, I. A.; Leigh, G. J.; Huttner, G.; Jibril, I. *J. Chem. Soc., Dalton Trans.* **1986**, 377-383.
- (148) Bakir, M.; White, P. S.; Dovletoglou, A.; Meyer, T. J. *Inorg. Chem.* **1991**, *30*, 2835-2836.
- (149) Huynh, M. H. V.; Jameson, D. L.; Meyer, T. J. *Inorg. Chem.* **2001**, *40*, 5062-5063.
- (150) Bennett, B. K.; Saganic, E.; Lovell, S.; Kaminsky, W.; Samuel, A.; Mayer, J. M. *Inorg. Chem.* **2003**, *42*, 4127-4134.

- (151) Fang, G.-S.; Huang, J.-S.; Zhu, N.; Che, C.-M. *Eur. J. Inorg. Chem.* **2004**, 2004, 1341-1348.
- (152) Yi, Lam, T. C. H.; Sau, Y.-K.; Zhang, Q.-F.; Williams, I. D.; Leung, W.-H. *Inorg. Chem.* **2007**, 46, 7193-7198.
- (153) Besson, C.; Geletii, Y. V.; Villain, F. o.; Villanneau, R.; Hill, C. L.; Proust, A. *Inorg. Chem.* **2009**, 48, 9436-9443.
- (154) Morello, L.; Yu, P.; Carmichael, C. D.; Patrick, B. O.; Fryzuk, M. D. *J. Am. Chem. Soc.* **2005**, 127, 12796-12797.
- (155) Adhikari, D.; Basuli, F.; Fan, H.; Huffman, J. C.; Pink, M.; Mindiola, D. J. *Inorg. Chem.* **2008**, 47, 4439-4441.
- (156) Scepaniak, J. J.; Fulton, M. D.; Bontchev, R. P.; Duesler, E. N.; Kirk, M. L.; Smith, J. M. *J. Am. Chem. Soc.* **2008**, 130, 10515-10517.
- (157) Strahle, J. Z. *Anorg. Allg. Chem.* **1974**, 405, 139-152.
- (158) Klein, H. F.; Haller, S.; Koenig, H.; Dartiguenave, M.; Dartiguenave, Y.; Menu, M. *J. J. Am. Chem. Soc.* **1991**, 113, 4673-4675.
- (159) Kyba, E. P.; Abramovitch, R. A. *J. Am. Chem. Soc.* **1980**, 102, 735-740.
- (160) Buschhorn, D.; Pink, M.; Fan, H.; Caulton, K. G. *Inorg. Chem.* **2008**, 47, 5129-5135.
- (161) Mronga, N.; Weller, F.; Dehnicke, K. Z. *Anorg. Allg. Chem.* **1983**, 502, 35-44.
- (162) Bottomley, F.; Brooks, W. V. F.; Clarkson, S. G.; Tong, S.-B. *J. Chem. Soc., Chem. Commun.* **1973**, 919-920.
- (163) Sellmann, D.; Keller, J.; Moll, M.; Beck, H. P.; Milius, W. *Z. Naturforsch., B: Chem. Sci.* **1986**, 41, 1551-1560.
- (164) Eberhardt, U.; Mattern, G.; Schiller, G. *Chem. Ber. Recl.* **1988**, 121, 1525-1529.
- (165) Pannell, K. H.; Chen, Y. S.; Belknap, K.; Wu, C. C.; Bernal, I.; Creswick, M. W.; Huang, H. N. *Inorg. Chem.* **1983**, 22, 418-427.
- (166) Schmidba.H; Wolfsber.W *Chem. Ber. Recl.* **1967**, 100, 1000-1015.
- (167) Schmidba.H; Wolfsber.W *Chem. Ber. Recl.* **1967**, 100, 1016-1022.
- (168) Masnadi, M.; Jamjah, R.; Ahmadjo, S.; Nekoomanesh, M. *Synth. React. Inorg. Met.-Org. Chem.* **2006**, 36, 543-547.
- (169) Abram, S.; Abram, U.; Kocker, R. M. Z.; Dehnicke, K. Z. *Anorg. Allg. Chem.* **1996**, 622, 867-872.
- (170) Ackermann, H.; Leo, R.; Massa, W.; Neumuller, B.; Dehnicke, K. Z. *Anorg. Allg. Chem.* **2000**, 626, 284-289.
- (171) Krieger, M.; Gould, R. O.; Pebler, J.; Dehnicke, K. Z. *Anorg. Allg. Chem.* **1998**, 624, 781-786.
- (172) Mai, H. J.; Kang, H. C.; Wocadlo, S.; Massa, W.; Dehnicke, K. Z. *Anorg. Allg. Chem.* **1995**, 621, 1963-1968.
- (173) Mai, H. J.; Kocker, R. M. Z.; Wocadlo, S.; Massa, W.; Dehnicke, K. *Angew. Chem. Int. Ed.* **1995**, 34, 1235-1236.
- (174) Riese, U.; Faza, N.; Harms, K.; Massa, W.; Neumuller, B.; Dehnicke, K. *Phosphorus Sulfur and Silicon and the Related Elements* **1997**, 125, 315-321.
- (175) Riese, U.; Faza, N.; Massa, W.; Harms, K.; Breyhan, T.; Knochel, P.; Ensling, J.; Ksenofontov, V.; Gutlich, P.; Dehnicke, K. Z. *Anorg. Allg. Chem.* **1999**, 625, 1494-1499.
- (176) Riese, U.; Harms, K.; Pebler, J.; Dehnicke, K. Z. *Anorg. Allg. Chem.* **1999**, 625, 746-754.

- (177) Krieger, M.; Gould, R. O.; Neumuller, B.; Harms, K.; Dehnicke, K. *Z. Anorg. Allg. Chem.* **1998**, *624*, 1434-1442.
- (178) Krieger, M.; Neumuller, B.; Dehnicke, K. *Z. Anorg. Allg. Chem.* **1998**, *624*, 1563-1564.
- (179) Mai, H. J.; Neumuller, B.; Dehnicke, K. *Z. Naturforsch., B: Chem. Sci.* **1996**, *51*, 433-436.
- (180) Riese, U.; Harms, K.; Neumuller, B.; Dehnicke, K. *Z. Anorg. Allg. Chem.* **1998**, *624*, 1279-1284.
- (181) Rolle, U.; Harms, K.; Dehnicke, K. *Z. Anorg. Allg. Chem.* **2003**, *629*, 936-938.
- (182) Krieger, M.; Gould, R. O.; Harms, K.; Parsons, S.; Dehnicke, K. *Chem. Ber. Recl.* **1996**, *129*, 1621-1625.
- (183) Krieger, M.; Gould, R. O.; Neumüller, B.; Harms, K.; Dehnicke, K. *Z. Anorg. Allg. Chem.* **1998**, *624*, 1434-1442.
- (184) Dilworth, J. R.; de Liefde Meijer, H. J.; Teuben, J. H. *J. Organomet. Chem.* **1978**, *159*, 47-52.
- (185) Cabrera, L.; Hollink, E.; Stewart, J. C.; Wei, P.; Stephan, D. W. *Organometallics* **2005**, *24*, 1091-1098.
- (186) Stephan, D. W.; Guérin, F.; Spence, R. E. v. H.; Koch, L.; Gao, X.; Brown, S. J.; Swabey, J. W.; Wang, Q.; Xu, W.; Zoricak, P.; Harrison, D. G. *Organometallics* **1999**, *18*, 2046-2048.
- (187) Hlatky, G. G. *Coord. Chem. Rev.* **1999**, *181*, 243-296.
- (188) Hlatky, G. G. *Coord. Chem. Rev.* **2000**, *199*, 235-329.
- (189) Stephan, D. W. *Organometallics* **2005**, *24*, 2548-2560.
- (190) Katti, K. V.; Cavell, R. G. *Organometallics* **1988**, *7*, 2236-2238.
- (191) Katti, K. V.; Cavell, R. G. *Organometallics* **1989**, *8*, 2147-2153.
- (192) Katti, K. V.; Roesky, H. W.; Rietzel, M. *Z. Anorg. Allg. Chem.* **1987**, *553*, 123-126.
- (193) Roesky, H. W.; Hesse, D.; Rietzel, M.; Noltemeyer, M. *Z. Naturforsch., B: Chem. Sci.* **1990**, *45*, 72-76.
- (194) Rentschler, E.; Nußhär, D.; Weller, F.; Dehnicke, K. *Z. Anorg. Allg. Chem.* **1993**, *619*, 999-1003.
- (195) Hecht, M.; Anaya, S. S.; Hagenbach, A.; Abram, U. *Inorg. Chem.* **2005**, *44*, 3172-3180.
- (196) Nusshar, D.; Weller, F.; Dehnicke, K. *Z. Anorg. Allg. Chem.* **1993**, *619*, 1121-1126.
- (197) Hollink, E.; Wei, P.; Stephan, D. W. *Organometallics* **2004**, *23*, 1562-1569.
- (198) Birkofer, L.; Kim, S. M. *Chem. Ber. Recl.* **1964**, *97*, 2100-2101.
- (199) Appel, R.; Hauss, A. *Angew. Chem. Int. Ed.* **1959**, *71*, 626-626.
- (200) Appel, R.; Hauss, A. *Chem. Ber. Recl.* **1960**, *93*, 405-411.
- (201) Appel, R.; Kohnlein, G.; Schollho, R. *Chem. Ber. Recl.* **1965**, *98*, 1355-&.
- (202) LePichon, L.; Stephan, D. W.; Gao, X.; Wang, Q. *Organometallics* **2002**, *21*, 1362-1366.
- (203) Dietrich, A.; Neumüller, B.; Dehnicke, K. *Z. Anorg. Allg. Chem.* **1998**, *624*, 1247-1249.
- (204) Ravi, P.; Gröb, T.; Dehnicke, K.; Greiner, A. *Macromolecules* **2001**, *34*, 8649-8653.
- (205) Pattacini, R.; Predieri, G.; Tiripicchio, A.; Mealli, C.; Phillips, A. D. *Chem. Commun.* **2006**, 1527-1529.

- (206) Süss-Fink, G.; Bodensieck, U.; Hoferkamp, L.; Rheinwald, G.; Stoeckli-Evans, H. J. *Cluster Sci.* **1992**, *3*, 469-478.
- (207) Bodensieck, U.; Stoeckli-Evans, H.; Süss-Fink, G. *Chem. Ber.* **1990**, *123*, 1603-1606.
- (208) Belletti, D.; Braunstein, P.; Messaoudi, A.; Pattacini, R.; Predieri, G.; Tiripicchio, A. *Chem. Commun.* **2007**, 141-143.
- (209) Zu Köcker, R. M.; Frenzen, G.; Neumüller, B.; Dehnicke, K.; Magull, J. Z. *Anorg. Allg. Chem.* **1994**, *620*, 431-437.
- (210) Sgro, M. J.; Stephan, D. W. *Dalton Transactions* **2011**, *40*, 2419-2421.
- (211) Spannhoff, K.; Kehr, G.; Kehr, S.; Fohlich, R.; Erker, G. *Dalton Transactions* **2008**, 7036-7036.
- (212) Babu, R. P. K.; McDonald, R.; Cavell, R. G. *Organometallics* **2000**, *19*, 3462-3465.
- (213) Ma, G. B.; McDonald, R.; Cavell, R. G. *Organometallics* **2010**, *29*, 52-60.
- (214) Mast, C.; Krieger, M.; Dehnicke, K.; Greiner, A. *Macromol. Rapid Commun.* **1999**, *20*, 232-235.
- (215) Tjaden, E. B.; Zizelman, P. M.; Stryker, J. M. *Abstracts of Papers of the American Chemical Society* **1989**, *198*, 137.
- (216) Stephan, D. W.; Stewart, J. C.; Guérin, F.; Spence, R. E. v. H.; Xu, W.; Harrison, D. G. *Organometallics* **1999**, *18*, 1116-1118.
- (217) Guérin, F.; Stewart, J. C.; Beddie, C.; Stephan, D. W. *Organometallics* **2000**, *19*, 2994-3000.
- (218) Benzing, E.; Kornicker, W. *Chem. Ber. Recl.* **1961**, *94*, 2263-2267.
- (219) Larsen, J.; Enemaerke, R. J.; Skrydstrup, T.; Daasbjerg, K. *Organometallics* **2006**, *25*, 2031-2036.
- (220) Enemaerke, R. J.; Larsen, J.; Skrydstrup, T.; Daasbjerg, K. *J. Am. Chem. Soc.* **2004**, *126*, 7853-7864.
- (221) Graham, T. W.; Kickham, J.; Courtenay, S.; Wei, P.; Stephan, D. W. *Organometallics* **2004**, *23*, 3309-3318.
- (222) Caballo, J.; García-Castro, M. a.; Martín, A.; Mena, M.; Pérez-Redondo, A. n.; Yélamos, C. *Inorg. Chem.* **2011**, *50*, 6798-6808.
- (223) Gröb, T.; Seybert, G.; Massa, W.; Dehnicke, K. Z. *Anorg. Allg. Chem.* **1999**, *625*, 1897-1903.
- (224) Otte, R.; Fröhlich, R.; Wibbeling, B.; Hoppe, D. *Angew. Chem. Int. Ed.* **2005**, *44*, 5492-5496.
- (225) Denomme, D. R.; Dumbris, S. M.; Hyatt, I. F. D.; Abboud, K. A.; Ghiviriga, I.; McElwee-White, L. *Organometallics* **2010**, *29*, 5252-5256.
- (226) Suzuki, M.; Morita, Y.; Noyori, R. *J. Org. Chem.* **1990**, *55*, 441-449.
- (227) Li, J. S.; Stahl, M.; Faza, N.; Massa, W.; Dehnicke, K. Z. *Anorg. Allg. Chem.* **1997**, *623*, 1035-1036.
- (228) Voth, P.; Fraser, C.; Graham, T.; Zhu, C.; Gauld, J.; Stephan, D. W. *Organometallics* **2006**, *25*, 4779-4786.
- (229) Ariyaratne, K.; Cramer, R. E.; Jameson, G. B.; Gilje, J. W. *J. Organomet. Chem.* **2004**, *689*, 2029-2032.
- (230) Ariyaratne, K. A. N. S.; Cramer, R. E.; Gilje, J. W. *Organometallics* **2002**, *21*, 5799-5802.
- (231) Roesky, H. W.; Zimmer, M.; Noltemeyer, M.; Sheldrick, G. M. *Chem. Ber. Recl.* **1988**, *121*, 1377-1379.

- (232) Roesky, H. W.; Zimmer, M.; Schmidt, H. G.; Noltemeyer, M. *Z. Naturforsch., B: Chem. Sci.* **1988**, *43*, 1490-1494.
- (233) Williams, V. C.; Müller, M.; Leech, M. A.; Denning, R. G.; Green, M. L. H. *Inorg. Chem.* **2000**, *39*, 2538-2541.
- (234) Pichierri, F. *Chem. Phys. Lett.* **2010**, *487*, 315-319.
- (235) Furukawa, N.; Oae, S. *Ind. Eng. Chem. Res.* **1981**, *20*, 260-270.
- (236) Gilchrist, T. L.; Moody, C. J. *Chem. Rev.* **1977**, *77*, 409-435.
- (237) Claridge, R. P.; Millar, R. W.; Sandall, J. P. B.; Thompson, C. J. *Chem. Res., Synop.* **1999**, 520.
- (238) Mann, F. G.; Pope, W. J. *J. Chem. Soc.* **1922**, *121*, 1052-1055.
- (239) Yoshimura, T.; Omata, T.; Furukawa, N.; Oae, S. *J. Org. Chem.* **1976**, *41*, 1728-1733.
- (240) Martin, H. A.; Lemair, P. J.; Jellinek, F. *J. Organomet. Chem.* **1968**, *14*, 149-156.
- (241) Reetz, M. T. *Top. Curr. Chem.* **1982**, *106*, 1-54.
- (242) Gomezsal, P.; Martin, A.; Mena, M.; Yelamos, C. *J. Chem. Soc., Chem. Commun.* **1995**, 2185-2186.
- (243) Roesky, H. W.; Bai, Y.; Noltemeyer, M. *Angew. Chem. Int. Ed.* **1989**, *28*, 754-755.
- (244) Sarasa, J.; Poblet, J. M.; Bénard, M. *Organometallics* **2000**, *19*, 2264-2272.
- (245) *Organometallic Modeling of the Hydrodesulfurization and Hydrodenitrogenation Reactions*; Sanchez-Delgado, R., A., Ed.; Kluwer Academic Publishers: Hingham, Ma, USA, 2002.
- (246) Sanchez-Delgado, R., A. In *Comprehensive Organometallic Chemistry III*; Crabtree, R. H. M., D. M. P., Ed.; Elsevier: Oxford, 2006; Vol. 1, p 759-900.
- (247) Jones, W. D.; Chin, R. M. *Organometallics* **1992**, *11*, 2698-2700.
- (248) Jones, W. D.; Chin, R. M. *J. Organomet. Chem.* **1994**, *472*, 311-316.
- (249) Ylijoki, K. E. O.; Witherell, R. D.; Kirk, A. D.; Böcklein, S.; Lofstrand, V. A.; McDonald, R.; Ferguson, M. J.; Stryker, J. M. *Organometallics* **2009**, *28*, 6807-6822.
- (250) Witherell, R. D.; Ylijoki, K. E. O.; Stryker, J. M. *J. Am. Chem. Soc.* **2008**, *130*, 2176-2177.
- (251) Jonas, K. *Angew. Chem. Int. Ed.* **1985**, *24*, 295-311.
- (252) Chan, B. Ph.D Dissertation, University of Alberta, 2010.
- (253) Ackermann, H.; Weller, F.; Dehnicke, K. *Z. Naturforsch., B: Chem. Sci.* **2000**, *55*, 448-451.
- (254) Abram, S.; Abram, U.; zu Köcker, R. M.; Dehnicke, K. *Z. Anorg. Allg. Chem.* **1996**, *622*, 867-872.
- (255) Ackermann, H.; Leo, R.; Massa, W.; Dehnicke, K. *Z. Naturforsch., B: Chem. Sci.* **1998**, *53*, 1241-1243.
- (256) Ackermann, H.; Leo, R.; Massa, W.; Dehnicke, K. *Z. Anorg. Allg. Chem.* **2000**, *626*, 608-610.
- (257) Riese, U.; Harms, K.; Neumüller, B.; Dehnicke, K. *Z. Anorg. Allg. Chem.* **1998**, *624*, 1279-1284.
- (258) Grün, M.; Harms, K.; Köcker, R. M. Z.; Dehnicke, K.; Goesmann, H. *Z. Anorg. Allg. Chem.* **1996**, *622*, 1091-1096.
- (259) Rankin, D. W. H.; Robertson, H. E.; Seip, R.; Schmidbaur, H.; Blaschke, G. *J. Chem. Soc., Dalton Trans.* **1985**, 827-830.
- (260) Kim, Y. J.; Bernstein, M. P.; Roth, A. S. G.; Romesberg, F. E.; Williard, P. G.; Fuller, D. J.; Harrison, A. T.; Collum, D. B. *J. Org. Chem.* **1991**, *56*, 4435-4439.

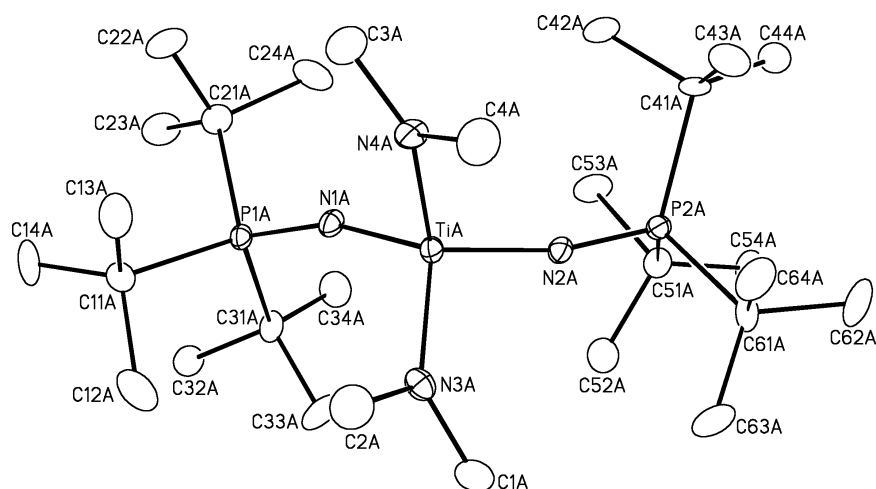
- (261) Cotton, F. A.; Elder, R. C. *Inorg. Chem.* **1965**, *4*, 1145-1151.
- (262) Mandal, D.; Mikuriya, M.; Fun, H.-K.; Ray, D. *Inorg. Chem. Commun.* **2007**, *10*, 657-660.
- (263) Zhu, Y.; Li, W.-H. *Transition Met. Chem.* **2010**, *35*, 745-749.
- (264) Boonmak, J.; Nakano, M.; Youngme, S. *Dalton Transactions* **2011**, *40*, 1254-1260.
- (265) Zhang, Y.-Z.; Wernsdorfer, W.; Pan, F.; Wang, Z.-M.; Gao, S. *Chem. Commun.* **2006**, 3302-3304.
- (266) Burlov, A. S.; Kuznetsova, L. I.; Uraev, A. I.; Kurbatov, V. P.; Bondarenko, G. I.; Vasil'chenko, I. S.; Garnovskii, A. D. *Russ. J. Gen. Chem.* **2003**, *73*, 1190-1197.
- (267) Jia, Q.-X.; Tian, H.; Zhang, J.-Y.; Gao, E.-Q. *Chemistry – A European Journal* **2011**, *17*, 1040-1051.
- (268) Rieke, R. D.; Hudnall, P. M. *J. Am. Chem. Soc.* **1972**, *94*, 7178-7179.
- (269) Liu, H.-J.; Yip, J.; Shia, K.-S. *Tetrahedron Lett.* **1997**, *38*, 2253-2256.
- (270) Ungváry, F.; Babos, B.; Markó, L. *J. Organomet. Chem.* **1967**, *8*, 329-337.
- (271) S, T. *J. Organomet. Chem.* **1973**, *59*, 365-378.
- (272) A. Roth, J.; Wiseman, P. *J. Organomet. Chem.* **1981**, *217*, 231-234.
- (273) Yamada, T. *Synthesis* **2008**, *2008*, 1628,1640.
- (274) Leutenegger, U.; Madin, A.; Pfaltz, A. *Angew. Chem. Int. Ed.* **1989**, *28*, 60-61.
- (275) Dance, I. G. *J. Am. Chem. Soc.* **1979**, *101*, 6264-6273.
- (276) Crisp, G. T.; Turner, P. D.; Stephens, K. A. *J. Organomet. Chem.* **1998**, *570*, 219-224.
- (277) Tamura, Y.; Matsushima, H.; Minamikawa, J.; Ikeda, M. *Tetrahedron* **1975**, *31*, 3035-3040.
- (278) Llinas, G. H.; Mena, M.; Palacios, F.; Royo, P.; Serrano, R. *J. Organomet. Chem.* **1988**, *340*, 37-40.
- (279) Bradley, D. C.; Thomas, I. M. *J. Chem. Soc.* **1960**, 3857-3861.
- (280) Zhang, K.; Curran, D. P. *Synlett* **2010**, 667-671.
- (281) Colby, D. A.; Bergman, R. G.; Ellman, J. A. *J. Am. Chem. Soc.* **2008**, *130*, 3645-3651.

Appendix: Crystallographic Data

Selected crystallographic data for all compound are presented in this section, any further information regarding additional structural factors can be obtained by contacting Dr. Robert McDonald or Dr. Michael Ferguson of the University of Alberta X-ray Laboratory, University of Alberta, Department of Chemistry, Edmonton, AB, Canada, T6G 2G2. Request either the report number (JMSXXXX) or the .cif file.

6.1 Chapter 4 X-Ray Crystallographic Data:

A. JMS0718 (296)



A. Crystal Data

formula	$C_{28}H_{66}N_4P_2Ti$
formula weight	568.69
crystal dimensions (mm)	$0.43 \times 0.29 \times 0.21$
crystal system	monoclinic
space group	$P2_1$ (No. 4)
unit cell parameters ^a	
<i>a</i> (Å)	8.6840 (7)
<i>b</i> (Å)	16.0667 (12)
<i>c</i> (Å)	12.5192 (10)
β (deg)	97.6300 (10)
<i>V</i> (Å ³)	1731.3 (2)

Z	2
ρ_{calcd} (g cm ⁻³)	1.091
μ (mm ⁻¹)	0.361
<i>B. Data Collection and Refinement Conditions</i>	
diffractometer	Bruker PLATFORM/SMART 1000 CCD ^b
radiation (λ [Å]) (0.71073)	graphite-monochromated Mo K α
temperature (°C)	-80
scan type	ω scans (0.3°) (20 s exposures)
data collection 2θ limit (deg)	54.98
total data collected ≤ 16)	14642 ($-11 \leq h \leq 11, -20 \leq k \leq 20, -16 \leq l$
independent reflections	7856 ($R_{\text{int}} = 0.0244$)
number of observed reflections (NO)	7225 [$F_o^2 \geq 2\sigma(F_o^2)$]
structure solution method	direct methods (SHELXS-97 ^c)
refinement method 97 ^d)	full-matrix least-squares on F^2 (SHELXL-
absorption correction method	multi-scan (SADABS)
range of transmission factors	0.9281-0.8604
data/restraints/parameters	7856 [$F_o^2 \geq -3\sigma(F_o^2)$] / 0 / 613
Flack absolute structure parameter ^e	-0.013(19)
goodness-of-fit (S) ^f	1.042 [$F_o^2 \geq -3\sigma(F_o^2)$]
final R indices ^g	
R_1 [$F_o^2 \geq 2\sigma(F_o^2)$]	0.0373
wR_2 [$F_o^2 \geq -3\sigma(F_o^2)$]	0.0946
largest difference peak and hole	0.325 and -0.234 e Å ⁻³

^aObtained from least-squares refinement of 8015 reflections with $5.08^\circ < 2\theta < 54.52^\circ$.

^bPrograms for diffractometer operation, data collection, data reduction and absorption correction were those supplied by Bruker.

^cSheldrick, G. M. *Acta Crystallogr.* **1990**, A46, 467-473.

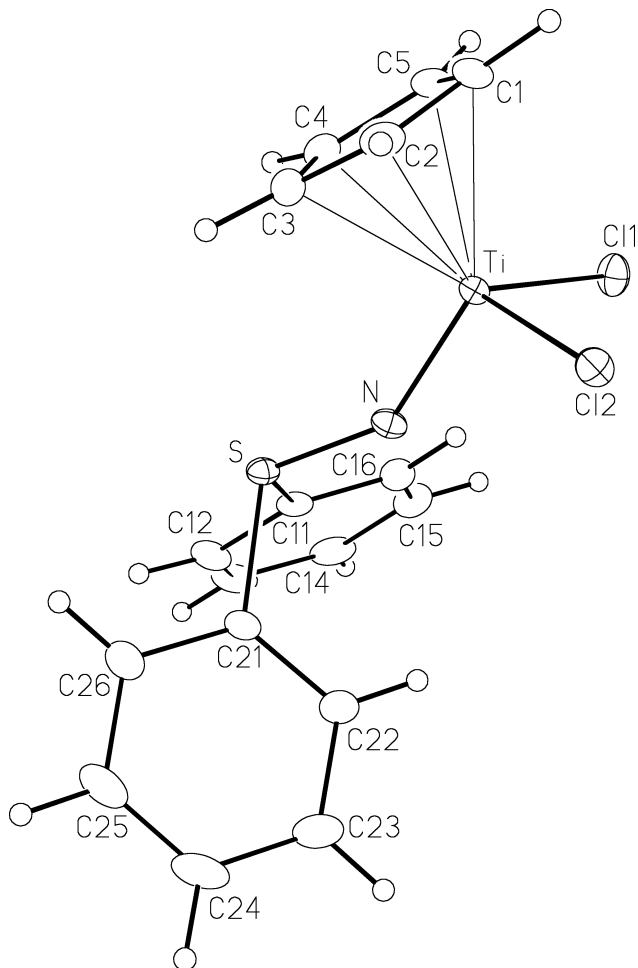
^dSheldrick, G. M. SHELXL-97. Program for crystal structure determination. University of Göttingen, Germany, 1997.

^eFlack, H. D. *Acta Crystallogr.* **1983**, A39, 876-881; Flack, H. D.; Bernardinelli, G. *Acta Crystallogr.* **1999**, A55, 908-915; Flack, H. D.; Bernardinelli, G. *J. Appl. Cryst.* **2000**, 33, 1143-1148. The Flack parameter will refine to a value near zero if the structure is in the correct configuration and will refine to a value near one for the inverted configuration.

$fS = [\sum w(F_o^2 - F_c^2)^2 / (n - p)]^{1/2}$ (n = number of data; p = number of parameters varied; $w = [\sigma^2(F_o^2) + (0.0604P)^2]^{-1}$ where $P = [\text{Max}(F_o^2, 0) + 2F_c^2] / 3$).

$gR_1 = \sum ||F_o| - |F_c|| / \sum |F_o|$; $wR_2 = [\sum w(F_o^2 - F_c^2)^2 / \sum w(F_o^4)]^{1/2}$.

B. JMS0749 (313)



A. Crystal Data

formula	C ₁₇ H ₁₅ Cl ₂ NSTi
formula weight	384.16
crystal dimensions (mm)	0.53 × 0.29 × 0.19
crystal system	monoclinic
space group	<i>P</i> 2 ₁ / <i>c</i> (No. 14)
unit cell parameters ^a	
<i>a</i> (Å)	11.5981 (11)
<i>b</i> (Å)	6.3449 (6)
<i>c</i> (Å)	24.027 (2)
β (deg)	102.3660 (10)
<i>V</i> (Å ³)	1727.1 (3)
<i>Z</i>	4
ρ _{calcd} (g cm ⁻³)	1.477

μ (mm ⁻¹)	0.920
<i>B. Data Collection and Refinement Conditions</i>	
diffractometer	Bruker PLATFORM/SMART 1000 CCD ^b
radiation (λ [Å]) (0.71073)	graphite-monochromated Mo K α
temperature (°C)	-80
scan type	ω scans (0.3°) (20 s exposures)
data collection 2θ limit (deg)	55.00
total data collected 30)	14025 ($-15 \leq h \leq 15$, $-8 \leq k \leq 8$, $-30 \leq l \leq 30$)
independent reflections	3951 ($R_{\text{int}} = 0.0160$)
number of observed reflections (<i>NO</i>)	3625 [$F_o^2 \geq 2\sigma(F_o^2)$]
structure solution method	direct methods (<i>SHELXS-97</i> ^c)
refinement method <i>97</i> ^d)	full-matrix least-squares on F^2 (<i>SHELXL-97</i> ^d)
absorption correction method	multi-scan (<i>SADABS</i>)
range of transmission factors	0.8446–0.6413
data/restraints/parameters	3951 [$F_o^2 \geq -3\sigma(F_o^2)$] / 0 / 199
goodness-of-fit (<i>S</i>) ^e	1.057 [$F_o^2 \geq -3\sigma(F_o^2)$]
final <i>R</i> indices ^f	
R_1 [$F_o^2 \geq 2\sigma(F_o^2)$]	0.0263
wR_2 [$F_o^2 \geq -3\sigma(F_o^2)$]	0.0742
largest difference peak and hole	0.361 and -0.213 e Å ⁻³

^aObtained from least-squares refinement of 6817 reflections with $4.44^\circ < 2\theta < 54.96^\circ$.

^bPrograms for diffractometer operation, data collection, data reduction and absorption correction were those supplied by Bruker.

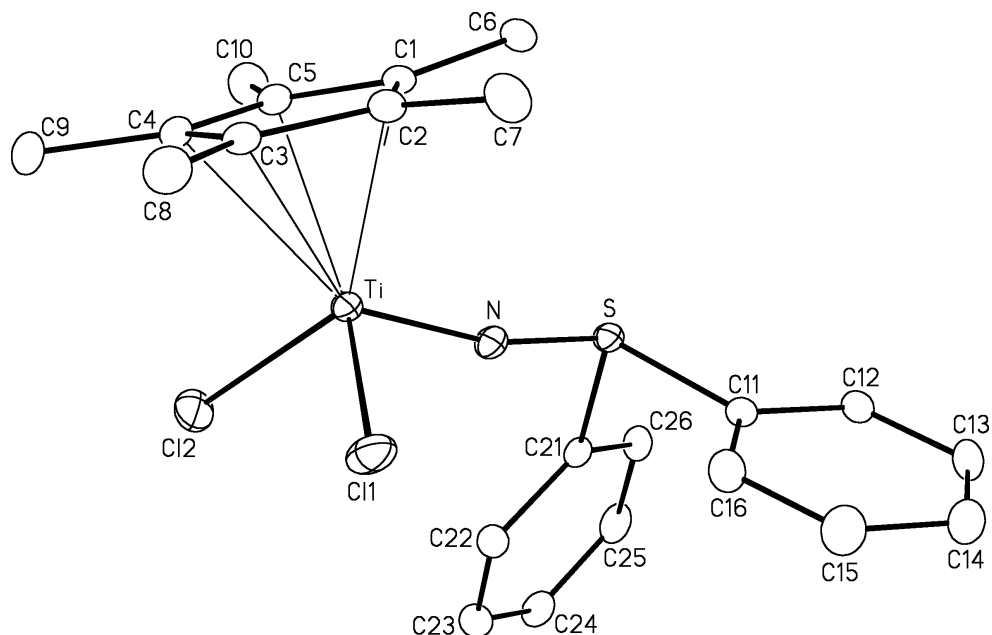
^cSheldrick, G. M. *Acta Crystallogr.* **1990**, *A46*, 467–473.

^dSheldrick, G. M. *SHELXL-97*. Program for crystal structure determination. University of Göttingen, Germany, 1997.

^e $S = [\sum w(F_o^2 - F_c^2)^2 / (n - p)]^{1/2}$ (n = number of data; p = number of parameters varied; $w = [\sigma^2(F_o^2) + (0.0410P)^2 + 0.6268P]^{-1}$ where $P = [\text{Max}(F_o^2, 0) + 2F_c^2] / 3$).

^f $R_1 = \sum ||F_o| - |F_c|| / \sum |F_o|$; $wR_2 = [\sum w(F_o^2 - F_c^2)^2 / \sum w(F_o^4)]^{1/2}$.

C. JMS0817 (314)



A. Crystal Data

formula	C ₂₂ H ₂₅ Cl ₂ NSTi
formula weight	454.29
crystal dimensions (mm)	0.54 × 0.11 × 0.10
crystal system	monoclinic
space group	<i>P</i> 2 ₁ / <i>n</i> (an alternate setting of <i>P</i> 2 ₁ / <i>c</i>)
[No. 14])	
unit cell parameters ^a	
<i>a</i> (Å)	13.0213 (12)
<i>b</i> (Å)	10.2856 (9)
<i>c</i> (Å)	17.8078 (16)
β (deg)	109.6820 (10)
<i>V</i> (Å ³)	2245.7 (3)
<i>Z</i>	4
ρ _{calcd} (g cm ⁻³)	1.344
μ (mm ⁻¹)	0.719

B. Data Collection and Refinement Conditions

diffractometer	Bruker PLATFORM/SMART 1000 CCD ^b
radiation (λ [Å])	graphite-monochromated Mo Kα
(0.71073)	
temperature (°C)	-80

scan type	ω scans (0.3°) (20 s exposures)
data collection 2θ limit (deg)	54.98
total data collected ≤ 23)	17623 ($-16 \leq h \leq 16, -13 \leq k \leq 12, -23 \leq l$)
independent reflections	5142 ($R_{\text{int}} = 0.0408$)
number of observed reflections (NO)	3849 [$F_o^2 \geq 2\sigma(F_o^2)$]
structure solution method	direct methods (<i>SHELXS-97</i> ^c)
refinement method	full-matrix least-squares on F^2 (<i>SHELXL-97</i> ^c)
absorption correction method	multi-scan (<i>SADABS</i>)
range of transmission factors	0.9316–0.6975
data/restraints/parameters	5142 [$F_o^2 \geq -3\sigma(F_o^2)$] / 0 / 249
goodness-of-fit (S) ^d	1.040 [$F_o^2 \geq -3\sigma(F_o^2)$]
final R indices ^e	
R_1 [$F_o^2 \geq 2\sigma(F_o^2)$]	0.0381
wR_2 [$F_o^2 \geq -3\sigma(F_o^2)$]	0.0987
largest difference peak and hole	0.443 and $-0.225 \text{ e } \text{\AA}^{-3}$

^aObtained from least-squares refinement of 5523 reflections with $4.74^\circ < 2\theta < 54.64^\circ$.

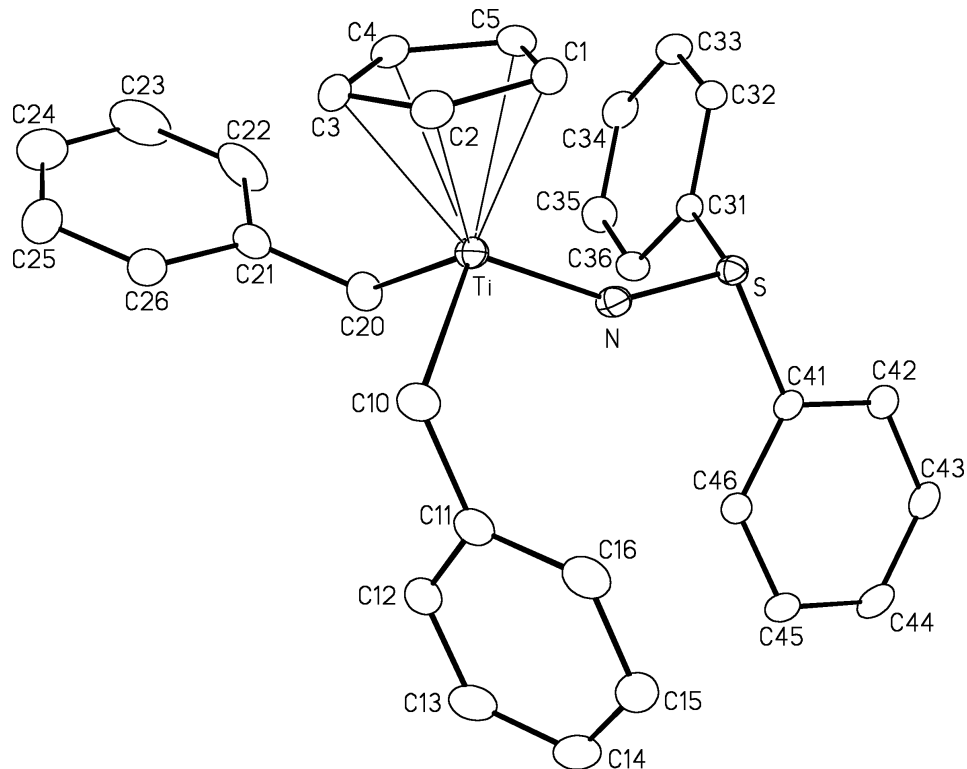
^bPrograms for diffractometer operation, data collection, data reduction and absorption correction were those supplied by Bruker.

^cSheldrick, G. M. *Acta Crystallogr.* **2008**, *A64*, 112–122.

^d $S = [\sum w(F_o^2 - F_c^2)^2 / (n - p)]^{1/2}$ (n = number of data; p = number of parameters varied;
 $w = [\sigma^2(F_o^2) + (0.0486P)^2 + 0.5844P]^{-1}$ where $P = [\text{Max}(F_o^2, 0) + 2F_c^2] / 3$).

^e $R_1 = \sum ||F_o| - |F_c|| / \sum |F_o|$; $wR_2 = [\sum w(F_o^2 - F_c^2)^2 / \sum w(F_o^4)]^{1/2}$.

D. JMS0811 (329)



A. Crystal Data

formula	C ₃₁ H ₂₉ NSTi
formula weight	495.51
crystal dimensions (mm)	0.38 × 0.15 × 0.03
crystal system	monoclinic
space group	<i>P</i> 2 ₁ / <i>c</i> (No. 14)
unit cell parameters ^a	
<i>a</i> (Å)	10.8434 (15)
<i>b</i> (Å)	18.843 (3)
<i>c</i> (Å)	13.4947 (18)
β (deg)	113.425 (2)
<i>V</i> (Å ³)	2530.0 (6)
<i>Z</i>	4
ρ _{calcd} (g cm ⁻³)	1.301
μ (mm ⁻¹)	0.441

B. Data Collection and Refinement Conditions

diffractometer	Bruker PLATFORM/SMART 1000 CCD ^b
radiation (λ [Å])	graphite-monochromated Mo Kα

(0.71073)	
temperature (°C)	−80
scan type	ω scans (0.3°) (30 s exposures)
data collection 2θ limit (deg)	50.50
total data collected	16057 ($-13 \leq h \leq 13, -21 \leq k \leq 22, -16 \leq l \leq 16$)
independent reflections	4574 ($R_{\text{int}} = 0.0649$)
number of observed reflections (NO)	3129 [$F_o^2 \geq 2\sigma(F_o^2)$]
structure solution method	direct methods (<i>SIR97</i> ^c)
refinement method	full-matrix least-squares on F^2 (<i>SHELXL-97</i> ^d)
absorption correction method	multi-scan (<i>SADABS</i>)
range of transmission factors	0.9869–0.8505
data/restraints/parameters	4574 [$F_o^2 \geq -3\sigma(F_o^2)$] / 0 / 307
goodness-of-fit (S) ^e	1.006 [$F_o^2 \geq -3\sigma(F_o^2)$]
final R indices ^f	
R_1 [$F_o^2 \geq 2\sigma(F_o^2)$]	0.0463
wR_2 [$F_o^2 \geq -3\sigma(F_o^2)$]	0.1180
largest difference peak and hole	0.330 and $-0.264 \text{ e } \text{Å}^{-3}$

^aObtained from least-squares refinement of 2790 reflections with $4.62^\circ < 2\theta < 41.92^\circ$.

^bPrograms for diffractometer operation, data collection, data reduction and absorption correction were those supplied by Bruker.

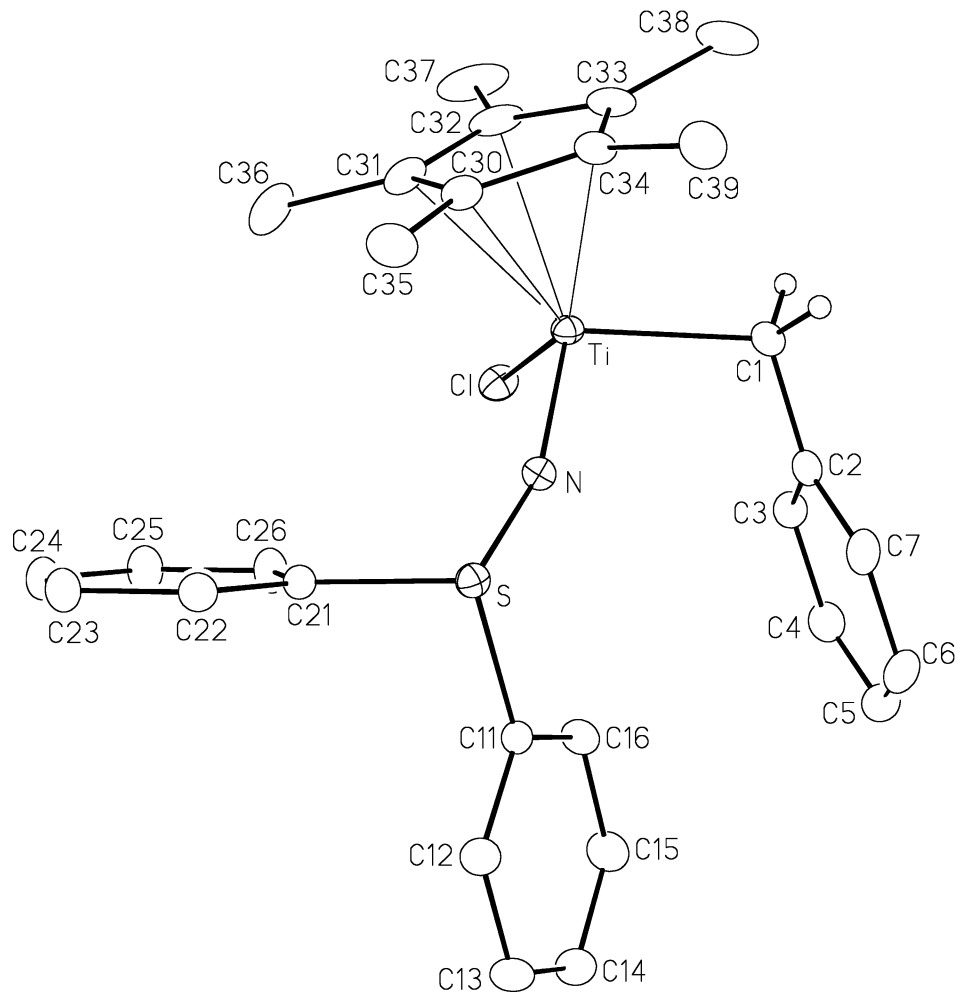
^cAltomare, A.; Burla, M. C.; Camalli, M.; Cascarano, G. L.; Giacovazzo, C.; Guagliardi, A.; Moliterni, A. G. G.; Polidori, G.; Spagna, R. *J. Appl. Cryst.* **1999**, *32*, 115–119.

^dSheldrick, G. M. *Acta Crystallogr.* **2008**, *A64*, 112–122.

^e $S = [\sum w(F_o^2 - F_c^2)^2 / (n - p)]^{1/2}$ (n = number of data; p = number of parameters varied; $w = [\sigma^2(F_o^2) + (0.0568P)^2 + 0.7355P]^{-1}$ where $P = [\text{Max}(F_o^2, 0) + 2F_c^2] / 3$).

^f $R_1 = \sum ||F_o| - |F_c|| / \sum |F_o|$; $wR_2 = [\sum w(F_o^2 - F_c^2)^2 / \sum w(F_o^4)]^{1/2}$.

E. JMS0972 (330)



A. Crystal Data

formula	$C_{29}H_{32}ClNSTi$
formula weight	509.97
crystal dimensions (mm)	$0.59 \times 0.56 \times 0.41$
crystal system	monoclinic
space group	$P2_1/n$ (an alternate setting of $P2_1/c$
[No. 14])	
unit cell parameters ^a	
a (Å)	15.3995 (11)
b (Å)	10.0126 (7)
c (Å)	17.9327 (13)
β (deg)	105.0580 (10)
V (Å ³)	2670.1 (3)
Z	4

ρ_{calcd} (g cm ⁻³)	1.269
μ (mm ⁻¹)	0.516

B. Data Collection and Refinement Conditions

diffractometer	Bruker D8/APEX II CCD ^b
radiation (λ [Å]) (0.71073)	graphite-monochromated Mo K α
temperature (°C)	-100
scan type	ω scans (0.4°) (10 s exposures)
data collection 2θ limit (deg)	55.08
total data collected ≤ 22)	18667 ($-19 \leq h \leq 19, -13 \leq k \leq 13, -22 \leq l$
independent reflections	6072 ($R_{\text{int}} = 0.0290$)
number of observed reflections (NO)	5190 [$F_o^2 \geq 2\sigma(F_o^2)$]
structure solution method	direct methods (SHELXS-97 ^c)
refinement method	full-matrix least-squares on F^2 (SHELXL-97 ^c)
absorption correction method	multi-scan (SADABS)
range of transmission factors	0.8144–0.7520
data/restraints/parameters	6072 [$F_o^2 \geq -3\sigma(F_o^2)$] / 0 / 303
goodness-of-fit (S) ^d	1.037 [$F_o^2 \geq -3\sigma(F_o^2)$]
final R indices ^e	
R_1 [$F_o^2 \geq 2\sigma(F_o^2)$]	0.0326
wR_2 [$F_o^2 \geq -3\sigma(F_o^2)$]	0.0908
largest difference peak and hole	0.539 and -0.213 e Å ⁻³

^aObtained from least-squares refinement of 9932 reflections with $4.70^\circ < 2\theta < 55.02^\circ$.

^bPrograms for diffractometer operation, data collection, data reduction and absorption correction were those supplied by Bruker.

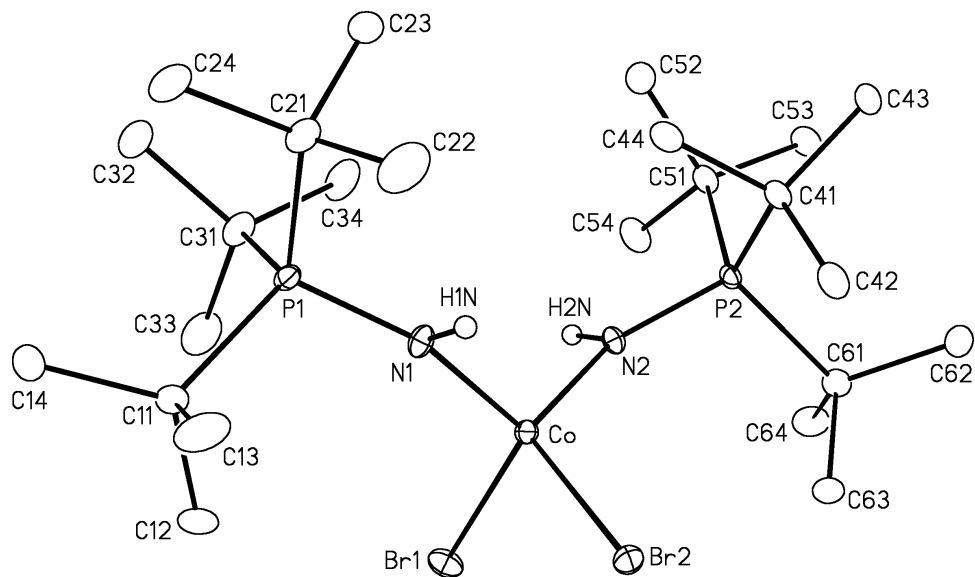
^cSheldrick, G. M. *Acta Crystallogr.* **2008**, A64, 112–122.

^d $S = [\sum w(F_o^2 - F_c^2)^2 / (n - p)]^{1/2}$ (n = number of data; p = number of parameters varied; $w = [\sigma^2(F_o^2) + (0.0438P)^2 + 0.9463P]^{-1}$ where $P = [\text{Max}(F_o^2, 0) + 2F_c^2] / 3$).

^e $R_1 = \sum ||F_o| - |F_c|| / \sum |F_o|$; $wR_2 = [\sum w(F_o^2 - F_c^2)^2 / \sum w(F_o^4)]^{1/2}$.

6.2 Chapter 5 X-Ray Crystallographic Data

F. JMS0837 (356)



A. Crystal Data

formula	C ₂₄ H ₅₆ Br ₂ CoN ₂ P ₂
formula weight	653.40
crystal dimensions (mm)	0.76 × 0.17 × 0.05
crystal system	orthorhombic
space group	<i>Pca</i> 2 ₁ (No. 29)
unit cell parameters ^a	
<i>a</i> (Å)	15.7945 (10)
<i>b</i> (Å)	15.2264 (10)
<i>c</i> (Å)	26.2072 (16)
<i>V</i> (Å ³)	6302.7 (7)
<i>Z</i>	8
ρ_{calcd} (g cm ⁻³)	1.377
μ (mm ⁻¹)	3.196

B. Data Collection and Refinement Conditions

diffractometer	Bruker D8/APEX II CCD ^b
radiation (λ [Å]) (0.71073)	graphite-monochromated Mo K α
temperature (°C)	−100
scan type	ω scans (0.3°) (20 s exposures)
data collection 2θ limit (deg)	54.98
total data collected ≤ 34)	53444 ($-20 \leq h \leq 20, -19 \leq k \leq 19, -34 \leq l$
independent reflections	14430 ($R_{\text{int}} = 0.0402$)
number of observed reflections (NO)	12913 [$F_o^2 \geq 2\sigma(F_o^2)$]
structure solution method (<i>DIRDIF-99</i> ^c)	Patterson search/structure expansion
refinement method <i>97</i> ^d)	full-matrix least-squares on F^2 (<i>SHELXL-97</i> ^d)
absorption correction method	Gaussian integration (face-indexed)
range of transmission factors	0.8565–0.1961
data/restraints/parameters	14430 [$F_o^2 \geq -3\sigma(F_o^2)$] / 0 / 560
Flack absolute structure parameter ^e	0.461 (4)
goodness-of-fit (S) ^f	1.041 [$F_o^2 \geq -3\sigma(F_o^2)$]
final R indices ^g	
R_1 [$F_o^2 \geq 2\sigma(F_o^2)$]	0.0281
wR_2 [$F_o^2 \geq -3\sigma(F_o^2)$]	0.0657
largest difference peak and hole	1.063 and $-0.326 \text{ e } \text{Å}^{-3}$

^aObtained from least-squares refinement of 9793 reflections with $4.84^\circ < 2\theta < 54.34^\circ$.

^bPrograms for diffractometer operation, data collection, data reduction and absorption correction were those supplied by Bruker.

^cBeurskens, P. T.; Beurskens, G.; de Gelder, R.; Garcia-Granda, S.; Israel, R.; Gould, R. O.; Smits, J. M. M. (1999). The *DIRDIF-99* program system. Crystallography Laboratory, University of Nijmegen, The Netherlands.

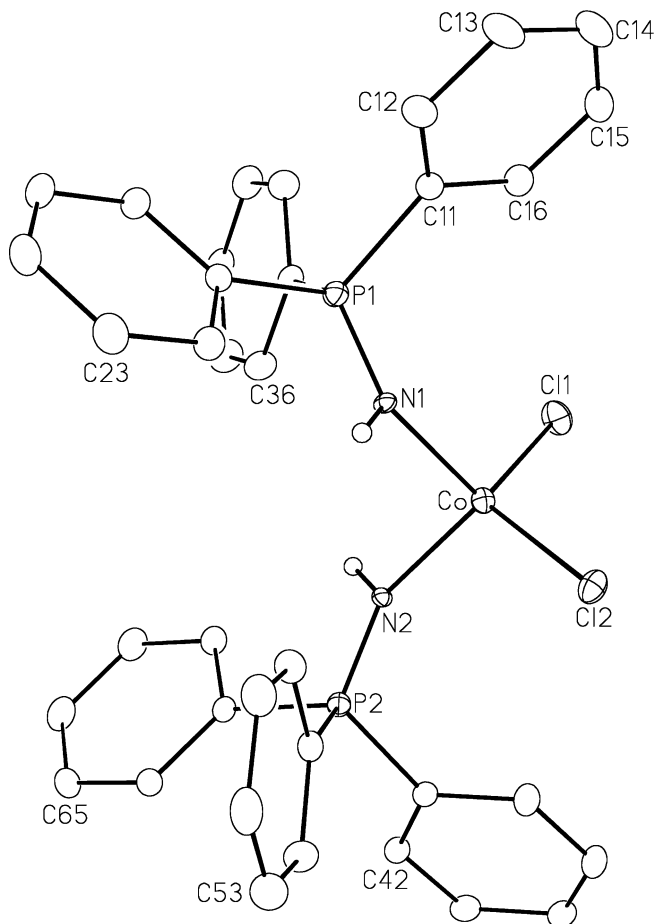
^dSheldrick, G. M. *Acta Crystallogr.* **2008**, *A64*, 112–122.

^eFlack, H. D. *Acta Crystallogr.* **1983**, *A39*, 876–881; Flack, H. D.; Bernardinelli, G. *Acta Crystallogr.* **1999**, *A55*, 908–915; Flack, H. D.; Bernardinelli, G. *J. Appl. Cryst.* **2000**, *33*, 1143–1148. The Flack parameter will refine to a value near zero if the structure is in the correct configuration and will refine to a value near one for the inverted configuration. The value observed herein is indicative of racemic twinning, and was accommodated during the refinement (using the *SHELXL-93* TWIN instruction [see reference *d*]).

^f $S = [\sum w(F_o^2 - F_c^2)^2 / (n - p)]^{1/2}$ (n = number of data; p = number of parameters varied; $w = [\sigma^2(F_o^2) + (0.0380P)^2]^{-1}$ where $P = [\text{Max}(F_o^2, 0) + 2F_c^2] / 3$).

^g $R_1 = \sum ||F_o| - |F_c|| / \sum |F_o|$; $wR_2 = [\sum w(F_o^2 - F_c^2)^2 / \sum w(F_o^4)]^{1/2}$.

G. JMS0826 (357)



A. Crystal Data

formula	$C_{44}H_{48}Cl_2CoN_2O_2P_2$
formula weight	828.61
crystal dimensions (mm)	$0.58 \times 0.17 \times 0.16$
crystal system	triclinic
space group	$P\bar{1}$ (No. 2)
unit cell parameters ^a	
<i>a</i> (Å)	11.8064 (17)
<i>b</i> (Å)	13.0368 (19)
<i>c</i> (Å)	15.519 (2)
α (deg)	110.672 (2)
β (deg)	110.327 (2)
γ (deg)	92.648 (2)
<i>V</i> (Å ³)	2056.6 (5)
<i>Z</i>	2
ρ_{calcd} (g cm ⁻³)	1.338

μ (mm⁻¹) 0.664

B. Data Collection and Refinement Conditions

diffractometer	Bruker PLATFORM/SMART 1000 CCD ^b
radiation (λ [Å]) (0.71073)	graphite-monochromated Mo K α
temperature (°C)	-80
scan type	ω scans (0.3°) (20 s exposures)
data collection 2θ limit (deg)	54.92
total data collected 20)	17507 ($-15 \leq h \leq 14, -16 \leq k \leq 15, 0 \leq l \leq 20$)
independent reflections	17507 ($R_{\text{int}} = 0.0000$)
number of observed reflections (NO)	14052 [$F_o^2 \geq 2\sigma(F_o^2)$]
structure solution method	direct methods (<i>SIR97</i> ^c)
refinement method <i>97</i> ^d)	full-matrix least-squares on F^2 (<i>SHELXL-97</i> ^d)
absorption correction method	multi-scan (<i>TWINABS</i>)
range of transmission factors	0.9012–0.6994
data/restraints/parameters	17507 [$F_o^2 \geq -3\sigma(F_o^2)$] / 0 / 479
goodness-of-fit (S) ^e	1.056 [$F_o^2 \geq -3\sigma(F_o^2)$]
final R indices ^f	
R_1 [$F_o^2 \geq 2\sigma(F_o^2)$]	0.0492
wR_2 [$F_o^2 \geq -3\sigma(F_o^2)$]	0.1515
largest difference peak and hole	0.790 and $-1.013 \text{ e } \text{Å}^{-3}$

^aObtained from least-squares refinement of 4398 reflections with $4.78^\circ < 2\theta < 55.62^\circ$.

^bPrograms for diffractometer operation, data collection, data reduction and absorption correction were those supplied by Bruker. The crystal used for data collection was found to display non-merohedral twinning. Both components of the twin were indexed with the program *CELL_NOW* (Bruker AXS Inc., Madison, WI, 2004). The second twin component can be related to the first component by 180° rotation about the [1 -0.79 0.03] axis in real space and about the [-1 1 0] axis in reciprocal space. Integrated intensities for the reflections from the two components were written into a *SHELXL-93* HKLF 5 reflection file with the data integration program *SAINTE* (version 7.06A), using all reflection data (exactly overlapped, partially overlapped and non-overlapped).

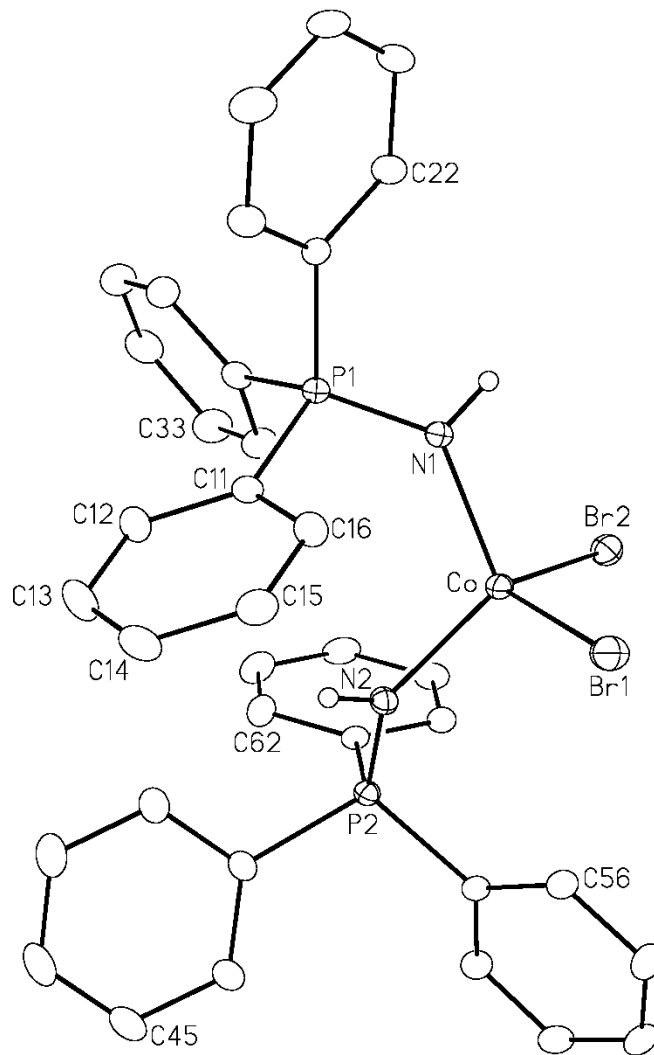
^cAltomare, A.; Burla, M. C.; Camalli, M.; Cascarano, G. L.; Giacovazzo, C.; Guagliardi, A.; Moliterni, A. G. G.; Polidori, G.; Spagna, R. *J. Appl. Cryst.* **1999**, *32*, 115–119.

^dSheldrick, G. M. *Acta Crystallogr.* **2008**, *A64*, 112–122.

^e $S = [\sum w(F_o^2 - F_c^2)^2 / (n - p)]^{1/2}$ (n = number of data; p = number of parameters varied; $w = [\sigma^2(F_o^2) + (0.0907P)^2 + 0.7228P]^{-1}$ where $P = [\text{Max}(F_o^2, 0) + 2F_c^2] / 3$).

^f $R_1 = \sum ||F_o| - |F_c|| / \sum |F_o|$; $wR_2 = [\sum w(F_o^2 - F_c^2)^2 / \sum w(F_o^4)]^{1/2}$.

H. JMS0823 (358)



A. Crystal Data

formula	C ₃₆ H ₃₂ Br ₂ CoN ₂ P ₂
formula weight	773.33
crystal dimensions (mm)	0.41 × 0.38 × 0.20
crystal system	orthorhombic
space group	<i>Pca</i> 2 ₁ (No. 29)
unit cell parameters ^a	
<i>a</i> (Å)	19.2482 (18)
<i>b</i> (Å)	10.3563 (10)
<i>c</i> (Å)	17.0995 (16)
<i>V</i> (Å ³)	3408.6 (6)

Z	4
ρ_{calcd} (g cm ⁻³)	1.507
μ (mm ⁻¹)	2.969
B. Data Collection and Refinement Conditions	
diffractometer	Bruker PLATFORM/SMART 1000 CCD ^b
radiation (λ [Å]) (0.71073)	graphite-monochromated Mo K α
temperature (°C)	-80
scan type	ω scans (0.3°) (20 s exposures)
data collection 2θ limit (deg)	55.00
total data collected (≤ 22)	28215 ($-25 \leq h \leq 24, -13 \leq k \leq 13, -22 \leq l \leq 22$)
independent reflections	7790 ($R_{\text{int}} = 0.0238$)
number of observed reflections (NO)	7220 [$F_o^2 \geq 2\sigma(F_o^2)$]
structure solution method	direct methods (SIR97 ^c)
refinement method (97 ^d)	full-matrix least-squares on F^2 (SHELXL-97 ^d)
absorption correction method	Gaussian integration (face-indexed)
range of transmission factors	0.5881–0.3757
data/restraints/parameters	7790 [$F_o^2 \geq -3\sigma(F_o^2)$] / 0 / 388
Flack absolute structure parameter ^e	0.008(4)
goodness-of-fit (S) ^f	1.022 [$F_o^2 \geq -3\sigma(F_o^2)$]
final R indices ^g	
R_1 [$F_o^2 \geq 2\sigma(F_o^2)$]	0.0251
wR_2 [$F_o^2 \geq -3\sigma(F_o^2)$]	0.0577
largest difference peak and hole	0.469 and -0.207 e Å ⁻³

^aObtained from least-squares refinement of 5746 reflections with $4.76^\circ < 2\theta < 54.32^\circ$.

^bPrograms for diffractometer operation, data collection, data reduction and absorption correction were those supplied by Bruker.

^cAltomare, A.; Burla, M. C.; Camalli, M.; Cascarano, G. L.; Giacovazzo, C.; Guagliardi, A.; Moliterni, A. G. G.; Polidori, G.; Spagna, R. *J. Appl. Cryst.* **1999**, *32*, 115–119.

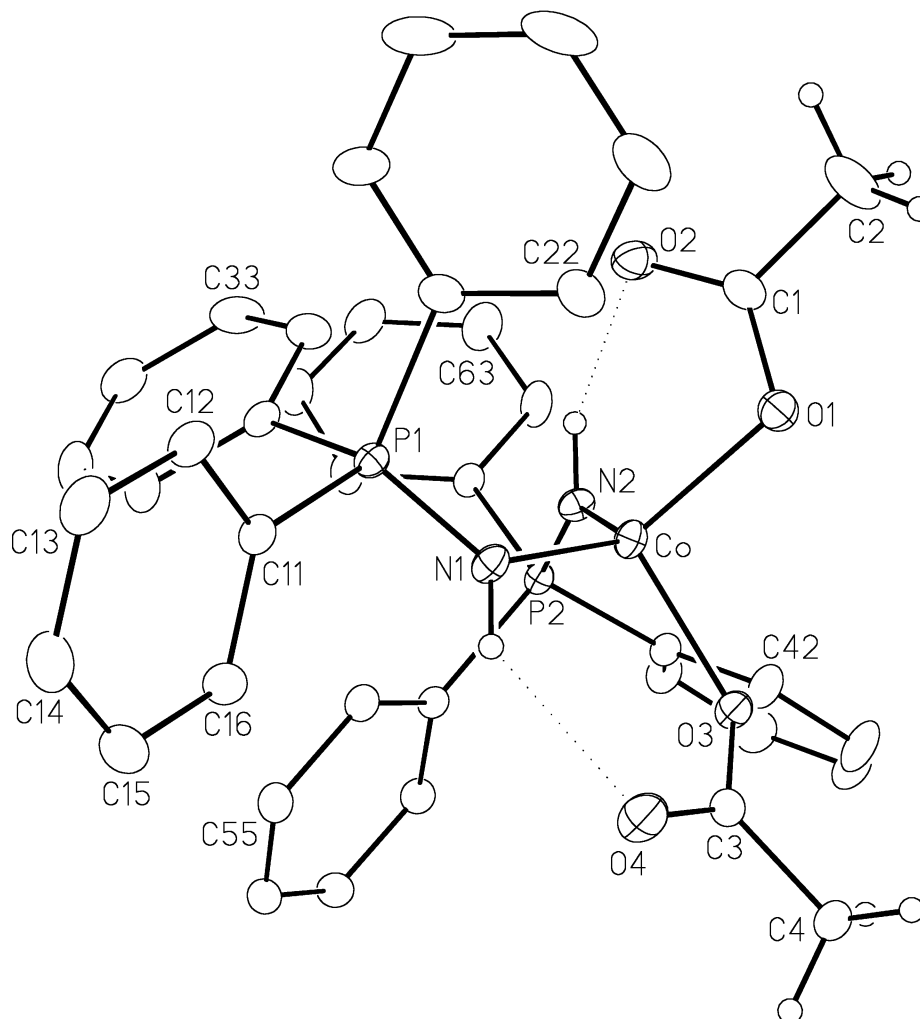
^dSheldrick, G. M. *Acta Crystallogr.* **2008**, *A64*, 112–122.

^eFlack, H. D. *Acta Crystallogr.* **1983**, *A39*, 876–881; Flack, H. D.; Bernardinelli, G. *Acta Crystallogr.* **1999**, *A55*, 908–915; Flack, H. D.; Bernardinelli, G. *J. Appl. Cryst.* **2000**, *33*, 1143–1148. The Flack parameter will refine to a value near zero if the structure is in the correct configuration and will refine to a value near one for the inverted configuration.

$fS = [\sum w(F_o^2 - F_c^2)^2 / (n - p)]^{1/2}$ (n = number of data; p = number of parameters varied; $w = [\sigma^2(F_o^2) + (0.0272P)^2]^{-1}$ where $P = [\text{Max}(F_o^2, 0) + 2F_c^2]/3$).

$gR_1 = \sum ||F_o| - |F_c|| / \sum |F_o|$; $wR_2 = [\sum w(F_o^2 - F_c^2)^2 / \sum w(F_o^4)]^{1/2}$.

I. JMS0930 (359)



A. Crystal Data

formula	$C_{40}H_{38}CoN_2O_4P_2$
formula weight	731.59
crystal dimensions (mm)	$0.51 \times 0.39 \times 0.32$
crystal system	triclinic
space group	$P\bar{1}$ (No. 2)
unit cell parameters ^a	
a (Å)	9.5895 (6)
b (Å)	12.8575 (8)
c (Å)	16.9049 (11)
α (deg)	104.4741 (7)
β (deg)	99.5703 (7)
γ (deg)	108.9694 (6)

V (Å ³)	1837.5 (2)
Z	2
ρ_{calcd} (g cm ⁻³)	1.322
μ (mm ⁻¹)	0.597

B. Data Collection and Refinement Conditions

diffractometer	Bruker PLATFORM/SMART 1000 CCD ^b
radiation (λ [Å]) (0.71073)	graphite-monochromated Mo K α
temperature (°C)	-100
scan type	ω scans (0.3°) (20 s exposures)
data collection 2θ limit (deg)	55.12
total data collected ≤ 22)	15907 ($-12 \leq h \leq 12$, $-16 \leq k \leq 16$, $-21 \leq l$
independent reflections	8304 ($R_{\text{int}} = 0.0120$)
number of observed reflections (NO)	7441 [$F_o^2 \geq 2\sigma(F_o^2)$]
structure solution method	direct methods (SHELXS-97 ^c)
refinement method	full-matrix least-squares on F^2 (SHELXL-97 ^c)
absorption correction method	Gaussian integration (face-indexed)
range of transmission factors	0.8320–0.7506
data/restraints/parameters	8304 [$F_o^2 \geq -3\sigma(F_o^2)$] / 0 / 444
goodness-of-fit (S) ^d	1.059 [$F_o^2 \geq -3\sigma(F_o^2)$]
final R indices ^e	
R_1 [$F_o^2 \geq 2\sigma(F_o^2)$]	0.0328
wR_2 [$F_o^2 \geq -3\sigma(F_o^2)$]	0.0912
largest difference peak and hole	0.364 and -0.229 e Å ⁻³

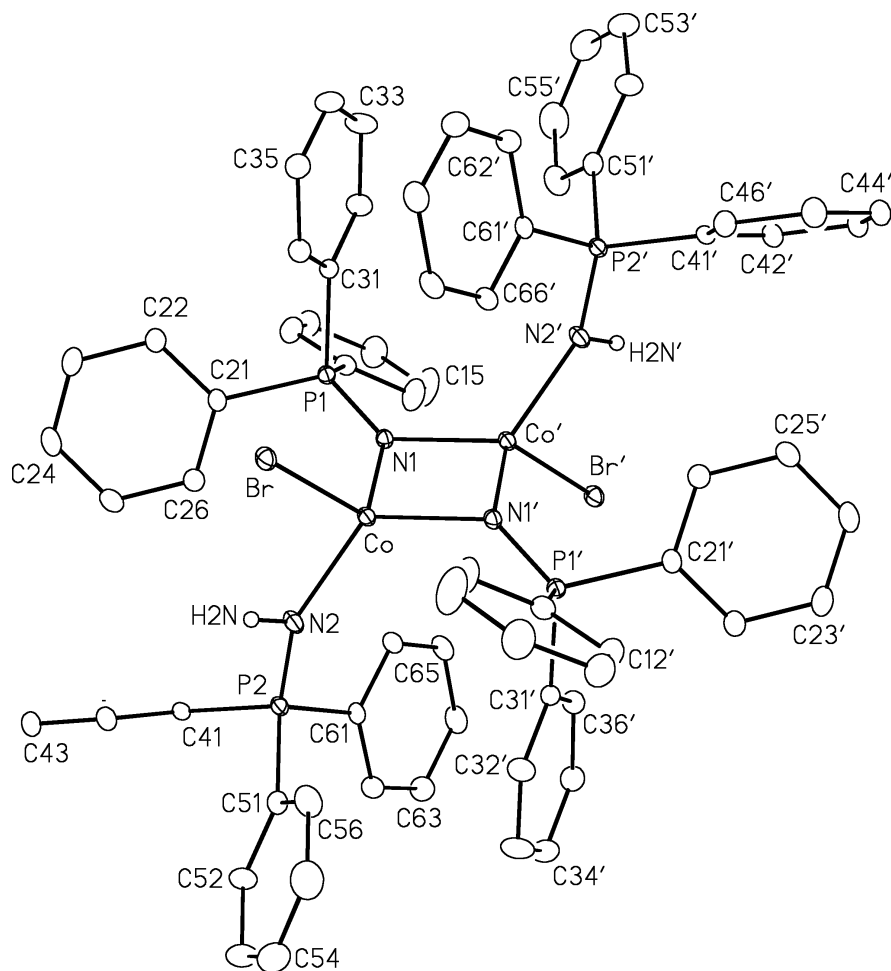
^aObtained from least-squares refinement of 8101 reflections with $4.66^\circ < 2\theta < 55.12^\circ$.

^bPrograms for diffractometer operation, data collection, data reduction and absorption correction were those supplied by Bruker.

^cSheldrick, G. M. *Acta Crystallogr.* **2008**, A64, 112–122.

^d $S = [\sum w(F_o^2 - F_c^2)^2 / (n - p)]^{1/2}$ (n = number of data; p = number of parameters varied; $w = [\sigma^2(F_o^2) + (0.0545P)^2 + 0.4481P]^{-1}$ where $P = [\text{Max}(F_o^2, 0) + 2F_c^2]/3$).

^e $R_1 = \sum ||F_o| - |F_c|| / \sum |F_o|$; $wR_2 = [\sum w(F_o^2 - F_c^2)^2 / \sum w(F_o^4)]^{1/2}$.



A. Crystal Data

formula	C ₉₆ H ₈₆ Br ₂ Co ₂ N ₄ P ₄
formula weight	1697.25
crystal dimensions (mm)	0.78 × 0.26 × 0.17
crystal system	triclinic
space group	<i>P</i> $\bar{1}$ (No. 2)
unit cell parameters ^a	
<i>a</i> (Å)	11.5210 (7)
<i>b</i> (Å)	13.7020 (9)
<i>c</i> (Å)	14.4871 (9)
α (deg)	68.0282 (8)
β (deg)	78.3226 (8)
γ (deg)	74.2484 (8)
<i>V</i> (Å ³)	2028.1 (2)

Z	1
ρ_{calcd} (g cm ⁻³)	1.390
μ (mm ⁻¹)	1.523

B. Data Collection and Refinement Conditions

diffractometer	Bruker D8/APEX II CCD ^b
radiation (λ [Å]) (0.71073)	graphite-monochromated Mo K α
temperature (°C)	-100
scan type	ω scans (0.3°) (20 s exposures)
data collection 2θ limit (deg)	55.02
total data collected ≤ 18)	17779 ($-14 \leq h \leq 14$, $-17 \leq k \leq 17$, $-18 \leq l \leq 18$)
independent reflections	9170 ($R_{\text{int}} = 0.0159$)
number of observed reflections (NO)	7899 [$F_o^2 \geq 2\sigma(F_o^2)$]
structure solution method (DIRDIF-99 ^c)	Patterson search/structure expansion
refinement method 97 ^d)	full-matrix least-squares on F^2 (SHELXL-97 ^d)
absorption correction method	Gaussian integration (face-indexed)
range of transmission factors	0.7796–0.3836
data/restraints/parameters	9170 [$F_o^2 \geq -3\sigma(F_o^2)$] / 0 / 487
goodness-of-fit (S) ^e	1.053 [$F_o^2 \geq -3\sigma(F_o^2)$]
final R indices ^f	
R_1 [$F_o^2 \geq 2\sigma(F_o^2)$]	0.0287
wR_2 [$F_o^2 \geq -3\sigma(F_o^2)$]	0.0794
largest difference peak and hole	0.763 and -0.214 e Å ⁻³

^aObtained from least-squares refinement of 9913 reflections with $4.38^\circ < 2\theta < 54.98^\circ$.

^bPrograms for diffractometer operation, data collection, data reduction and absorption correction were those supplied by Bruker.

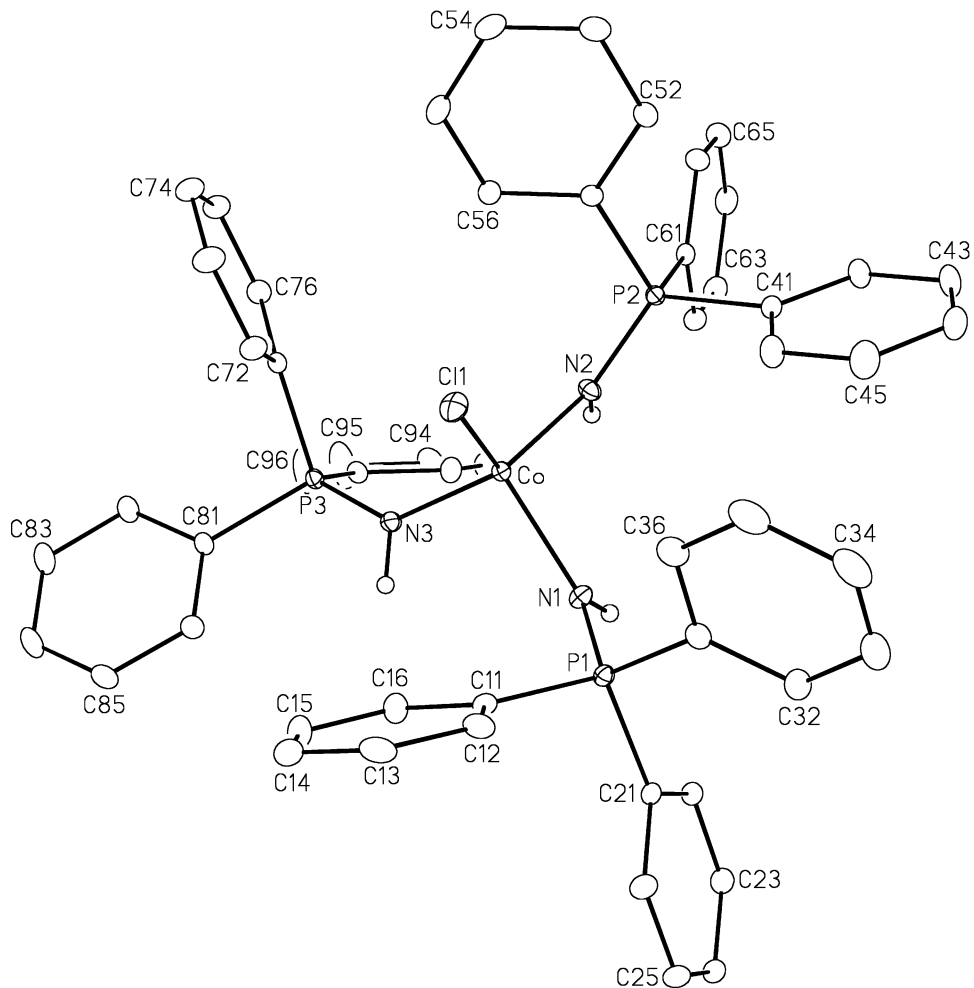
^cBeurskens, P. T.; Beurskens, G.; de Gelder, R.; Garcia-Granda, S.; Israel, R.; Gould, R. O.; Smits, J. M. M. (1999). The DIRDIF-99 program system. Crystallography Laboratory, University of Nijmegen, The Netherlands.

^dSheldrick, G. M. *Acta Crystallogr.* **2008**, A64, 112–122.

^e $S = [\sum w(F_o^2 - F_c^2)^2 / (n - p)]^{1/2}$ (n = number of data; p = number of parameters varied; $w = [\sigma^2(F_o^2) + (0.0440P)^2 + 0.5639P]^{-1}$ where $P = [\text{Max}(F_o^2, 0) + 2F_c^2] / 3$).

^f $R_1 = \sum ||F_o| - |F_c|| / \sum |F_o|$; $wR_2 = [\sum w(F_o^2 - F_c^2)^2 / \sum w(F_o^4)]^{1/2}$.

K. JMS0954 (363)



A. Crystal Data

formula	$C_{54}H_{48}Cl_2CoN_3P_3$
formula weight	961.69
crystal dimensions (mm)	$0.61 \times 0.56 \times 0.14$
crystal system	monoclinic
space group	$P2_1/n$ (an alternate setting of $P2_1/c$)
[No. 14]]	
unit cell parameters ^a	
a (Å)	12.148 (4)
b (Å)	18.729 (6)
c (Å)	20.570 (7)
β (deg)	91.402 (4)
V (Å ³)	4679 (3)
Z	4

ρ_{calcd} (g cm ⁻³)	1.365
μ (mm ⁻¹)	0.625

B. Data Collection and Refinement Conditions

diffractometer	Bruker D8/APEX II CCD ^b
radiation (λ [Å]) (0.71073)	graphite-monochromated Mo K α
temperature (°C)	-100
scan type	ω scans (0.3°) (20 s exposures)
data collection 2θ limit (deg)	55.02
total data collected ≤ 26)	40244 ($-15 \leq h \leq 15, -24 \leq k \leq 24, -26 \leq l$
independent reflections	10714 ($R_{\text{int}} = 0.0231$)
number of observed reflections (NO)	9756 [$F_o^2 \geq 2\sigma(F_o^2)$]
structure solution method	direct methods (SHELXS-97 ^c)
refinement method	full-matrix least-squares on F^2 (SHELXL-97 ^c)
absorption correction method	multi-scan (SADABS)
range of transmission factors	0.9188–0.7030
data/restraints/parameters	10714 [$F_o^2 \geq -3\sigma(F_o^2)$] / 0 / 568
goodness-of-fit (S) ^d	1.012 [$F_o^2 \geq -3\sigma(F_o^2)$]
final R indices ^e	
R_1 [$F_o^2 \geq 2\sigma(F_o^2)$]	0.0292
wR_2 [$F_o^2 \geq -3\sigma(F_o^2)$]	0.0808
largest difference peak and hole	0.526 and -0.492 e Å ⁻³

^aObtained from least-squares refinement of 9691 reflections with $4.42^\circ < 2\theta < 54.94^\circ$.

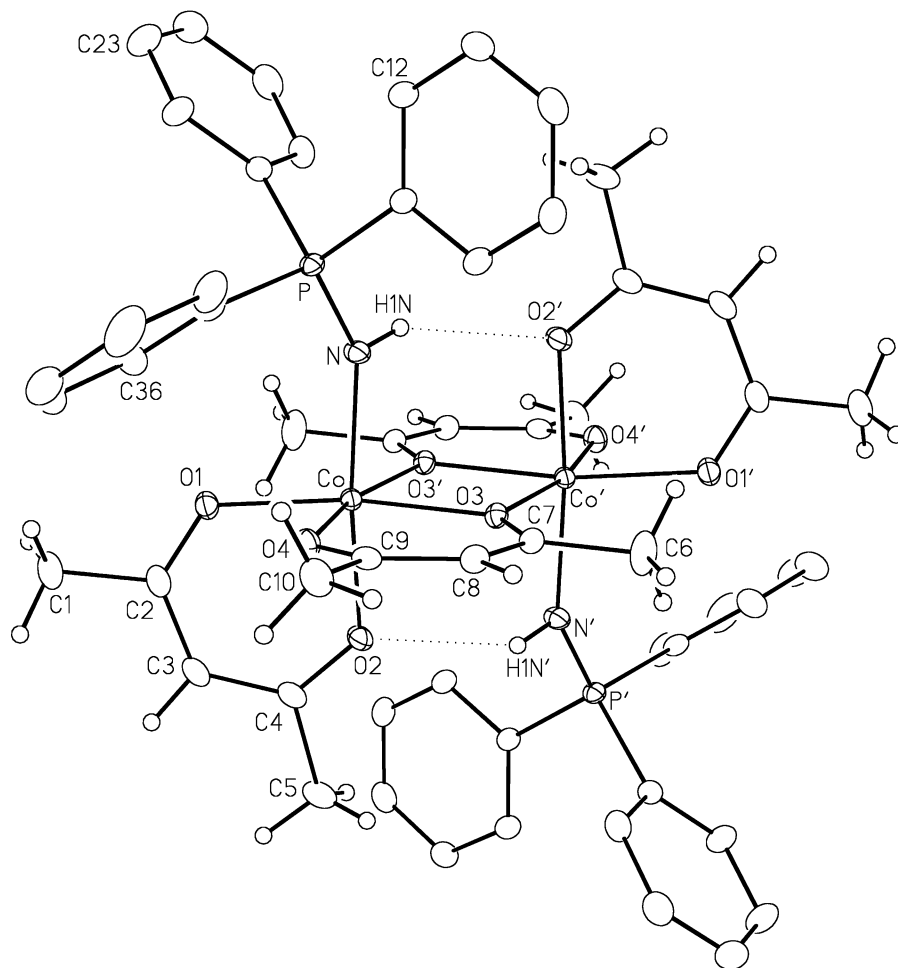
^bPrograms for diffractometer operation, data collection, data reduction and absorption correction were those supplied by Bruker.

^cSheldrick, G. M. *Acta Crystallogr.* **2008**, A64, 112–122.

^d $S = [\sum w(F_o^2 - F_c^2)^2 / (n - p)]^{1/2}$ (n = number of data; p = number of parameters varied; $w = [\sigma^2(F_o^2) + (0.0414P)^2 + 2.6297P]^{-1}$ where $P = [\text{Max}(F_o^2, 0) + 2F_c^2] / 3$).

^e $R_1 = \sum ||F_o| - |F_c|| / \sum |F_o|$; $wR_2 = [\sum w(F_o^2 - F_c^2)^2 / \sum w(F_o^4)]^{1/2}$.

L. JMS0853 (365)



A. Crystal Data

formula	C ₅₆ H ₆₀ Co ₂ N ₂ O ₈ P ₂
formula weight	1068.86
crystal dimensions (mm)	0.40 × 0.13 × 0.09
crystal system	monoclinic
space group	<i>P</i> 2 ₁ / <i>n</i> (an alternate setting of <i>P</i> 2 ₁ / <i>c</i>)
[No. 14]]	
unit cell parameters ^a	
<i>a</i> (Å)	9.4969 (5)
<i>b</i> (Å)	19.0110 (9)
<i>c</i> (Å)	15.0667 (7)
β (deg)	102.7360 (10)
<i>V</i> (Å ³)	2653.3 (2)
<i>Z</i>	2
ρ _{calcd} (g cm ⁻³)	1.338

μ (mm⁻¹) 0.740

B. Data Collection and Refinement Conditions

diffractometer	Bruker D8/APEX II CCD ^b
radiation (λ [Å]) (0.71073)	graphite-monochromated Mo K α
temperature (°C)	-100
scan type	ω scans (0.3°) (20 s exposures)
data collection 2θ limit (deg)	54.24
total data collected ≤ 19)	22520 ($-12 \leq h \leq 12, -24 \leq k \leq 24, -19 \leq l \leq 19$)
independent reflections	5863 ($R_{\text{int}} = 0.0234$)
number of observed reflections (NO)	5095 [$F_o^2 \geq 2\sigma(F_o^2)$]
structure solution method	direct methods (SHELXS-97 ^c)
refinement method	full-matrix least-squares on F^2 (SHELXL-97 ^c)
absorption correction method	multi-scan (SADABS)
range of transmission factors	0.9364–0.7546
data/restraints/parameters	5863 [$F_o^2 \geq -3\sigma(F_o^2)$] / 0 / 320
goodness-of-fit (S) ^d	1.045 [$F_o^2 \geq -3\sigma(F_o^2)$]
final R indices ^e	
R_1 [$F_o^2 \geq 2\sigma(F_o^2)$]	0.0313
wR_2 [$F_o^2 \geq -3\sigma(F_o^2)$]	0.0892
largest difference peak and hole	0.422 and -0.306 e Å ⁻³

^aObtained from least-squares refinement of 9937 reflections with $4.90^\circ < 2\theta < 54.20^\circ$.

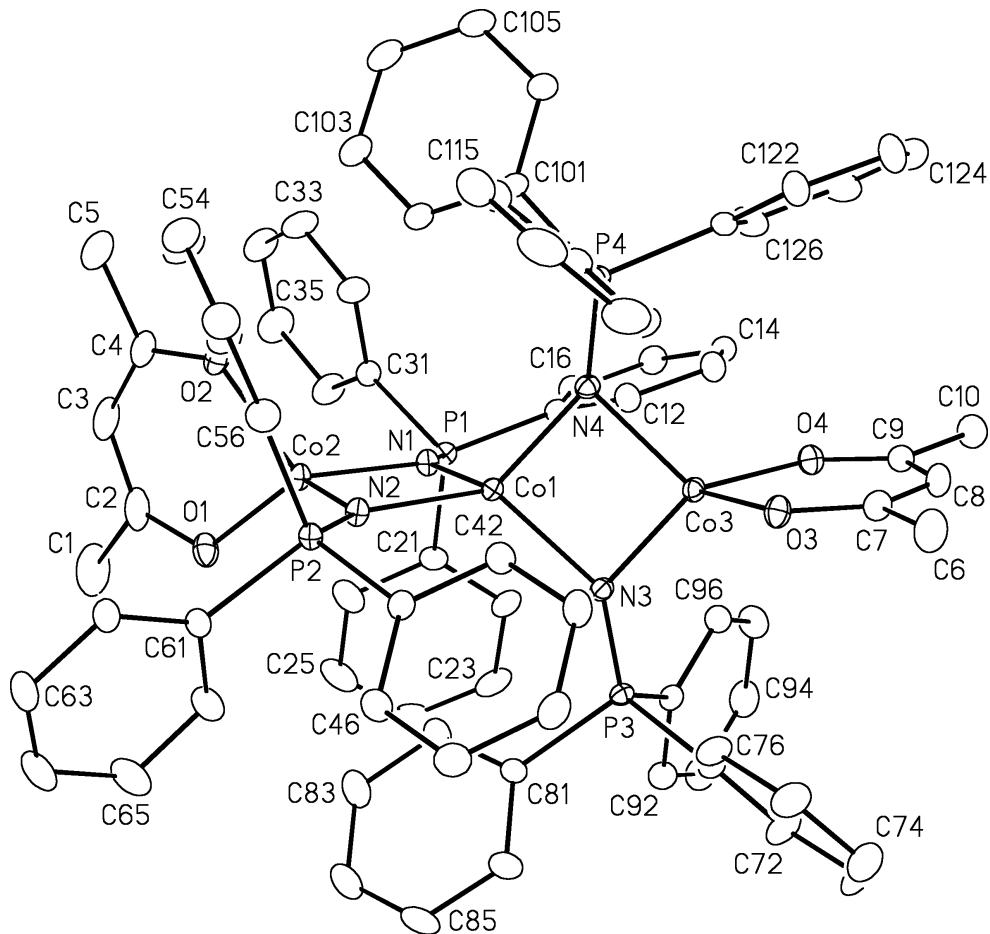
^bPrograms for diffractometer operation, data collection, data reduction and absorption correction were those supplied by Bruker.

^cSheldrick, G. M. *Acta Crystallogr.* **2008**, A64, 112–122.

^d $S = [\sum w(F_o^2 - F_c^2)^2 / (n - p)]^{1/2}$ (n = number of data; p = number of parameters varied; $w = [\sigma^2(F_o^2) + (0.0512P)^2 + 0.9281P]^{-1}$ where $P = [\text{Max}(F_o^2, 0) + 2F_c^2] / 3$).

^e $R_1 = \sum ||F_o| - |F_c|| / \sum |F_o|$; $wR_2 = [\sum w(F_o^2 - F_c^2)^2 / \sum w(F_o^4)]^{1/2}$.

M. JMS0863 (366)



A. Crystal Data

formula	C ₈₉ H ₈₂ Co ₃ N ₄ O ₄ P ₄
formula weight	1572.26
crystal dimensions (mm)	0.66 × 0.37 × 0.37
crystal system	triclinic
space group	$P\bar{1}$ (No. 2)
unit cell parameters ^a	
<i>a</i> (Å)	13.4762 (14)
<i>b</i> (Å)	13.8275 (15)
<i>c</i> (Å)	22.589 (2)
<i>α</i> (deg)	91.1153 (13)
<i>β</i> (deg)	91.2904 (13)
<i>γ</i> (deg)	112.3363 (12)
<i>V</i> (Å ³)	3890.6 (7)
<i>Z</i>	2

ρ_{calcd} (g cm ⁻³)	1.342
μ (mm ⁻¹)	0.769

B. Data Collection and Refinement Conditions

diffractometer	Bruker D8/APEX II CCD ^b
radiation (λ [Å]) (0.71073)	graphite-monochromated Mo K α
temperature (°C)	-100
scan type	ω scans (0.3°) (20 s exposures)
data collection 2θ limit (deg)	55.20
total data collected ≤ 29)	34146 ($-17 \leq h \leq 17, -17 \leq k \leq 17, -29 \leq l$
independent reflections	17683 ($R_{\text{int}} = 0.0214$)
number of observed reflections (NO)	15059 [$F_o^2 \geq 2\sigma(F_o^2)$]
structure solution method 2008 ^c)	Patterson/structure expansion (<i>DIRDIF-</i>
refinement method 97 ^d)	full-matrix least-squares on F^2 (<i>SHELXL-</i>
absorption correction method	Gaussian integration (face-indexed)
range of transmission factors	0.7667–0.6317
data/restraints/parameters	17683 [$F_o^2 \geq -3\sigma(F_o^2)$] / 0 / 942
goodness-of-fit (S) ^e	1.040 [$F_o^2 \geq -3\sigma(F_o^2)$]
final R indices ^f	
R_1 [$F_o^2 \geq 2\sigma(F_o^2)$]	0.0392
wR_2 [$F_o^2 \geq -3\sigma(F_o^2)$]	0.1167
largest difference peak and hole	0.745 and -0.968 e Å ⁻³

^aObtained from least-squares refinement of 9822 reflections with $4.79^\circ < 2\theta < 55.15^\circ$.

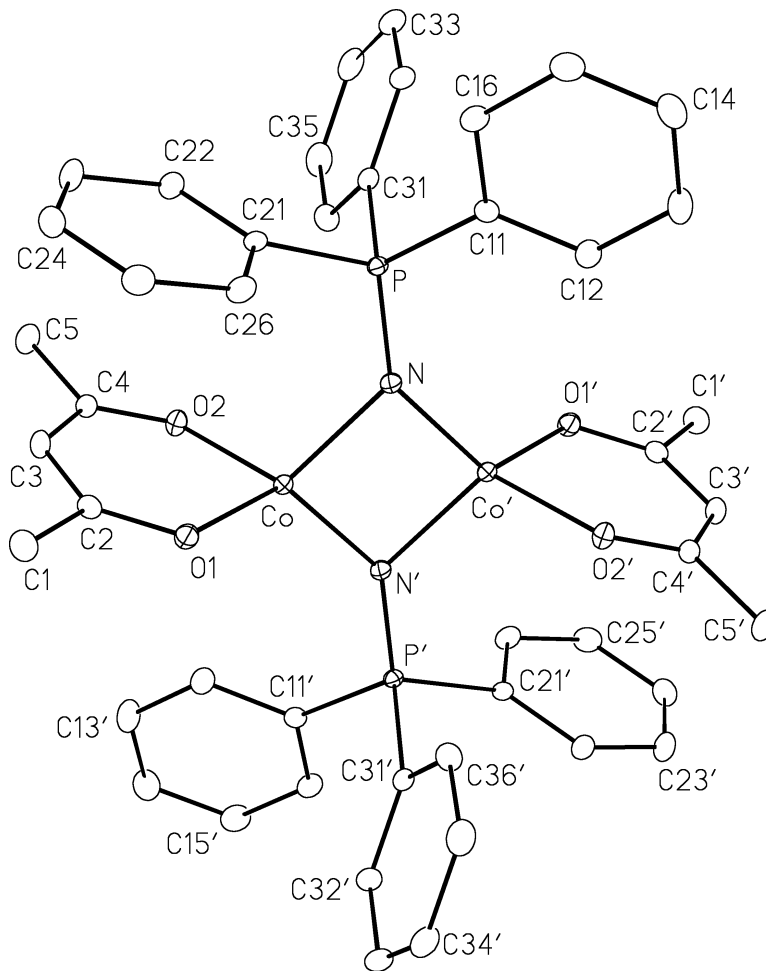
^bPrograms for diffractometer operation, data collection, data reduction and absorption correction were those supplied by Bruker.

^cBeurskens, P. T.; Beurskens, G.; de Gelder, R.; Smits, J. M. M.; Garcia-Granda, S.; Gould, R. O. (2008). The *DIRDIF-2008* program system. Crystallography Laboratory, Radboud University Nijmegen, The Netherlands.

^dSheldrick, G. M. *Acta Crystallogr.* **2008**, *A64*, 112–122.

^e $S = [\sum w(F_o^2 - F_c^2)^2 / (n - p)]^{1/2}$ (n = number of data; p = number of parameters varied);
 $w = [\sigma^2(F_o^2) + (0.0632P)^2 + 2.5344P]^{-1}$ where $P = [\text{Max}(F_o^2, 0) + 2F_c^2] / 3$.

^f $R_1 = \sum ||F_o| - |F_c|| / \sum |F_o|$; $wR_2 = [\sum w(F_o^2 - F_c^2)^2 / \sum w(F_o^4)]^{1/2}$.



A. Crystal Data

formula	$C_{46}H_{44}Co_2N_2O_4P_2$
formula weight	868.63
crystal dimensions (mm)	$0.43 \times 0.30 \times 0.27$
crystal system	monoclinic
space group	$P2_1/c$ (No. 14)
unit cell parameters ^a	
<i>a</i> (Å)	11.770 (2)
<i>b</i> (Å)	17.578 (3)
<i>c</i> (Å)	11.201 (2)
β (deg)	117.2154 (18)
<i>V</i> (Å ³)	2060.9 (6)
<i>Z</i>	2
ρ_{calcd} (g cm ⁻³)	1.400

μ (mm⁻¹) 0.928

B. Data Collection and Refinement Conditions

diffractometer	Bruker D8/APEX II CCD ^b
radiation (λ [Å]) (0.71073)	graphite-monochromated Mo K α
temperature (°C)	-100
scan type	ω scans (0.4°) (10 s exposures)
data collection 2θ limit (deg)	55.02
total data collected ≤ 14)	17732 ($-15 \leq h \leq 15, -22 \leq k \leq 22, -14 \leq l$
independent reflections	4724 ($R_{\text{int}} = 0.0270$)
number of observed reflections (NO)	4098 [$F_o^2 \geq 2\sigma(F_o^2)$]
structure solution method	direct methods (SHELXS-97 ^c)
refinement method	full-matrix least-squares on F^2 (SHELXL-97 ^c)
absorption correction method	Gaussian integration (face-indexed)
range of transmission factors	0.7897–0.6915
data/restraints/parameters	4724 [$F_o^2 \geq -3\sigma(F_o^2)$] / 0 / 255
goodness-of-fit (S) ^d	1.045 [$F_o^2 \geq -3\sigma(F_o^2)$]
final R indices ^e	
R_1 [$F_o^2 \geq 2\sigma(F_o^2)$]	0.0265
wR_2 [$F_o^2 \geq -3\sigma(F_o^2)$]	0.0736
largest difference peak and hole	0.387 and -0.311 e Å ⁻³

^aObtained from least-squares refinement of 9376 reflections with $4.52^\circ < 2\theta < 55.02^\circ$.

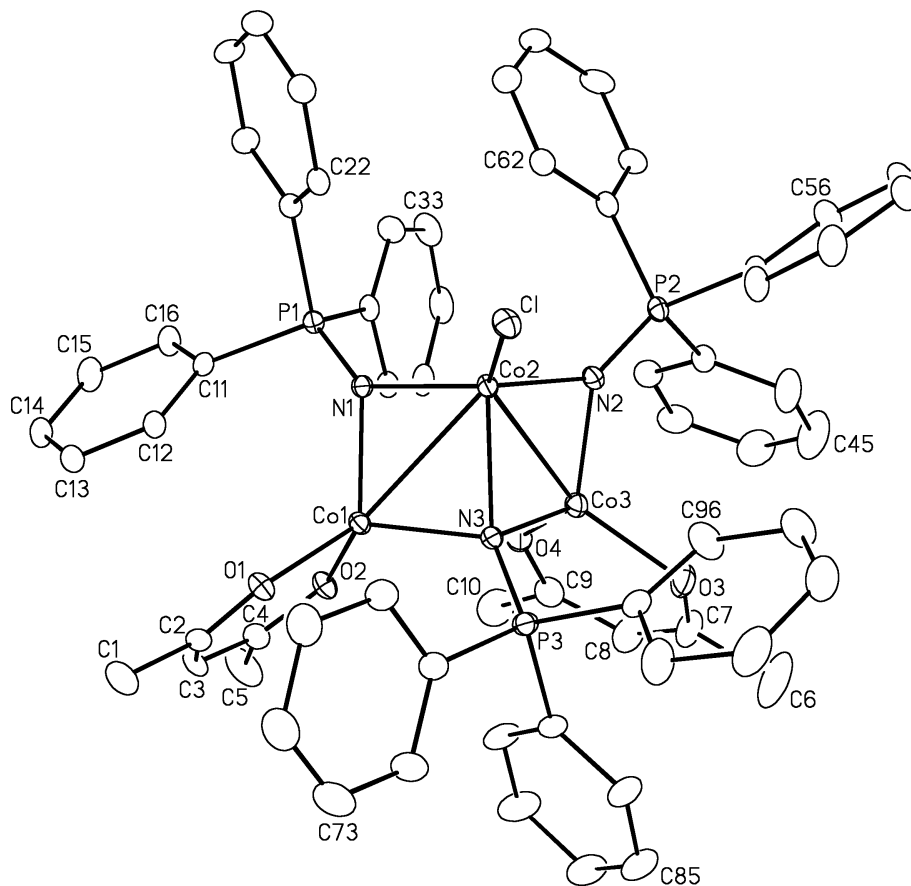
^bPrograms for diffractometer operation, data collection, data reduction and absorption correction were those supplied by Bruker.

^cSheldrick, G. M. *Acta Crystallogr.* **2008**, A64, 112–122.

^d $S = [\sum w(F_o^2 - F_c^2)^2 / (n - p)]^{1/2}$ (n = number of data; p = number of parameters varied;
 $w = [\sigma^2(F_o^2) + (0.0364P)^2 + 0.8600P]^{-1}$ where $P = [\text{Max}(F_o^2, 0) + 2F_c^2] / 3$).

^e $R_1 = \sum ||F_o| - |F_c|| / \sum |F_o|$; $wR_2 = [\sum w(F_o^2 - F_c^2)^2 / \sum w(F_o^4)]^{1/2}$.

O. JMS0869 (373)



A. Crystal Data

formula	C ₆₄ H ₅₉ ClCo ₃ N ₃ O ₄ P ₃
formula weight	1239.29
crystal dimensions (mm)	0.32 × 0.29 × 0.10
crystal system	monoclinic
space group	<i>P</i> 2 ₁ / <i>c</i> (No. 14)
unit cell parameters ^a	
<i>a</i> (Å)	33.0924 (16)
<i>b</i> (Å)	11.1565 (6)
<i>c</i> (Å)	31.5599 (16)
β (deg)	92.1050 (10)
<i>V</i> (Å ³)	11643.9 (10)
<i>Z</i>	8
ρ _{calcd} (g cm ⁻³)	1.414
μ (mm ⁻¹)	1.024

B. Data Collection and Refinement Conditions

diffractometer	Bruker D8/APEX II CCD ^b
radiation (λ [Å]) (0.71073)	graphite-monochromated Mo K α
temperature (°C)	−100
scan type	ω scans (0.3°) (20 s exposures)
data collection 2θ limit (deg)	52.78
total data collected ≤ 39)	91125 ($-41 \leq h \leq 41, -13 \leq k \leq 13, -39 \leq l \leq 39$)
independent reflections	23833 ($R_{\text{int}} = 0.0768$)
number of observed reflections (NO)	15787 [$F_o^2 \geq 2\sigma(F_o^2)$]
structure solution method	direct methods (<i>SIR97</i> ^c)
refinement method <i>97</i> ^d)	full-matrix least-squares on F^2 (<i>SHELXL</i> – <i>97</i> ^d)
absorption correction method	multi-scan (<i>SADABS</i>)
range of transmission factors	0.9010–0.7327
data/restraints/parameters	23833 [$F_o^2 \geq -3\sigma(F_o^2)$] / 0 / 1413
goodness-of-fit (S) ^e	1.013 [$F_o^2 \geq -3\sigma(F_o^2)$]
final R indices ^f	
R_1 [$F_o^2 \geq 2\sigma(F_o^2)$]	0.0419
wR_2 [$F_o^2 \geq -3\sigma(F_o^2)$]	0.1136
largest difference peak and hole	0.674 and $-0.357 \text{ e } \text{Å}^{-3}$

^aObtained from least-squares refinement of 9891 reflections with $4.40^\circ < 2\theta < 45.60^\circ$.

^bPrograms for diffractometer operation, data collection, data reduction and absorption correction were those supplied by Bruker.

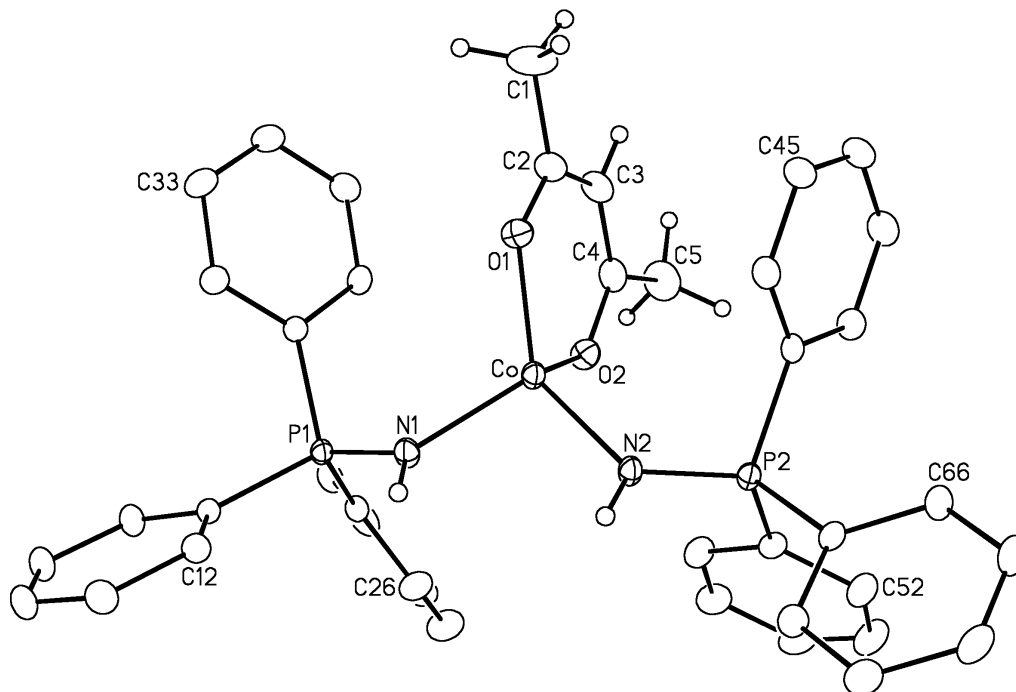
^cAltomare, A.; Burla, M. C.; Camalli, M.; Cascarano, G. L.; Giacovazzo, C.; Guagliardi, A.; Moliterni, A. G. G.; Polidori, G.; Spagna, R. *J. Appl. Cryst.* **1999**, *32*, 115–119.

^dSheldrick, G. M. *Acta Crystallogr.* **2008**, *A64*, 112–122.

^e $S = [\sum w(F_o^2 - F_c^2)^2 / (n - p)]^{1/2}$ (n = number of data; p = number of parameters varied; $w = [\sigma^2(F_o^2) + (0.0539P)^2 + 0.6940P]^{-1}$ where $P = [\text{Max}(F_o^2, 0) + 2F_c^2] / 3$).

^f $R_1 = \sum ||F_o| - |F_c|| / \sum |F_o|$; $wR_2 = [\sum w(F_o^2 - F_c^2)^2 / \sum w(F_o^4)]^{1/2}$.

P. JMS0868 (374)



A. Crystal Data

formula	C ₄₁ H ₃₉ BCoF ₄ N ₂ O ₂ P ₂
formula weight	799.42
crystal dimensions (mm)	0.57 × 0.29 × 0.08
crystal system	triclinic
space group	$P\bar{1}$ (No. 2)
unit cell parameters ^a	
<i>a</i> (Å)	13.206 (2)
<i>b</i> (Å)	13.395 (2)
<i>c</i> (Å)	13.724 (2)
<i>α</i> (deg)	93.643 (2)
<i>β</i> (deg)	112.751 (2)
<i>γ</i> (deg)	115.532 (2)
<i>V</i> (Å ³)	1941.2 (6)
<i>Z</i>	2
ρ_{calcd} (g cm ⁻³)	1.368
μ (mm ⁻¹)	0.581

B. Data Collection and Refinement Conditions

diffractometer Bruker D8/APEX II CCD^b

radiation (λ [Å]) (0.71073)	graphite-monochromated Mo K α
temperature (°C)	−100
scan type	ω scans (0.3°) (20 s exposures)
data collection 2θ limit (deg)	52.98
total data collected ≤ 17)	15685 ($-16 \leq h \leq 16, -16 \leq k \leq 16, -17 \leq l$
independent reflections	7974 ($R_{\text{int}} = 0.0277$)
number of observed reflections (NO)	6032 [$F_o^2 \geq 2\sigma(F_o^2)$]
structure solution method	direct methods (SHELXS-97 ^c)
refinement method	full-matrix least-squares on F^2 (SHELXL-97 ^c)
absorption correction method	Gaussian integration (face-indexed)
range of transmission factors	0.9561–0.7340
data/restraints/parameters	7974 [$F_o^2 \geq -3\sigma(F_o^2)$] / 0 / 480
goodness-of-fit (S) ^d	1.025 [$F_o^2 \geq -3\sigma(F_o^2)$]
final R indices ^e	
R_1 [$F_o^2 \geq 2\sigma(F_o^2)$]	0.0418
wR_2 [$F_o^2 \geq -3\sigma(F_o^2)$]	0.1177
largest difference peak and hole	0.767 and −0.402 e Å ^{−3}

^aObtained from least-squares refinement of 6871 reflections with $4.42^\circ < 2\theta < 50.88^\circ$.

^bPrograms for diffractometer operation, data collection, data reduction and absorption correction were those supplied by Bruker.

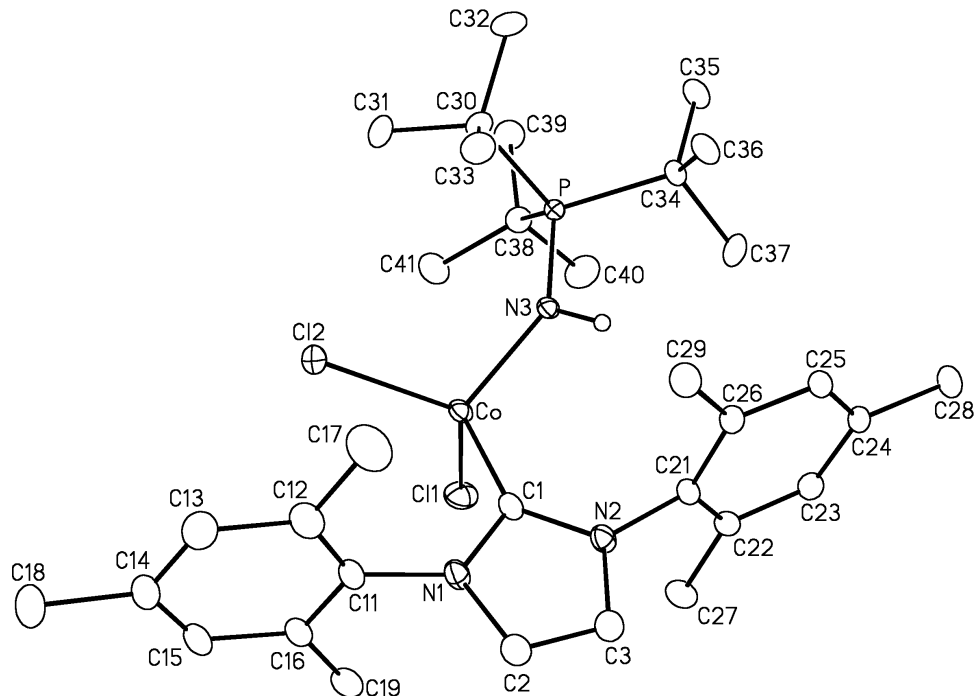
^cSheldrick, G. M. *Acta Crystallogr.* **2008**, A64, 112–122.

^d $S = [\sum w(F_o^2 - F_c^2)^2 / (n - p)]^{1/2}$ (n = number of data; p = number of parameters varied;

$w = [\sigma^2(F_o^2) + (0.0659P)^2 + 0.4078P]^{-1}$ where $P = [\text{Max}(F_o^2, 0) + 2F_c^2] / 3$).

^e $R_1 = \sum ||F_o| - |F_c|| / \sum |F_o|$; $wR_2 = [\sum w(F_o^2 - F_c^2)^2 / \sum w(F_o^4)]^{1/2}$.

Q. JMS0984 (376)



A. Crystal Data

formula	C ₃₃ H ₅₂ Cl ₂ CoN ₃ P
formula weight	651.58
crystal dimensions (mm)	0.55 × 0.24 × 0.05
crystal system	monoclinic
space group	<i>P</i> 2 ₁ / <i>c</i> (No. 14)
unit cell parameters ^a	
<i>a</i> (Å)	12.0681 (8)
<i>b</i> (Å)	15.6260 (10)
<i>c</i> (Å)	18.7051 (12)
β (deg)	90.8810 (10)
<i>V</i> (Å ³)	3526.9 (4)
<i>Z</i>	4
ρ _{calcd} (g cm ⁻³)	1.227
μ (mm ⁻¹)	0.708

B. Data Collection and Refinement Conditions

diffractometer	Bruker D8/APEX II CCD ^b
radiation (λ [Å])	graphite-monochromated Mo Kα
(0.71073)	

temperature (°C)	−100
scan type	ω scans (0.3°) (20 s exposures)
data collection 2θ limit (deg)	55.04
total data collected ≤ 23)	30649 ($-15 \leq h \leq 15, -20 \leq k \leq 20, -23 \leq l$
independent reflections	8104 ($R_{\text{int}} = 0.0295$)
number of observed reflections (NO)	6576 [$F_o^2 \geq 2\sigma(F_o^2)$]
structure solution method	direct methods (<i>SHELXS-97</i> ^c)
refinement method	full-matrix least-squares on F^2 (<i>SHELXL-97</i> ^c)
absorption correction method	Gaussian integration (face-indexed)
range of transmission factors	0.9681–0.6979
data/restraints/parameters	8104 [$F_o^2 \geq -3\sigma(F_o^2)$] / 0 / 376
goodness-of-fit (S) ^d	1.028 [$F_o^2 \geq -3\sigma(F_o^2)$]
final R indices ^e	
R_1 [$F_o^2 \geq 2\sigma(F_o^2)$]	0.0564
wR_2 [$F_o^2 \geq -3\sigma(F_o^2)$]	0.1660
largest difference peak and hole	2.397 and $-0.884 \text{ e } \text{\AA}^{-3}$

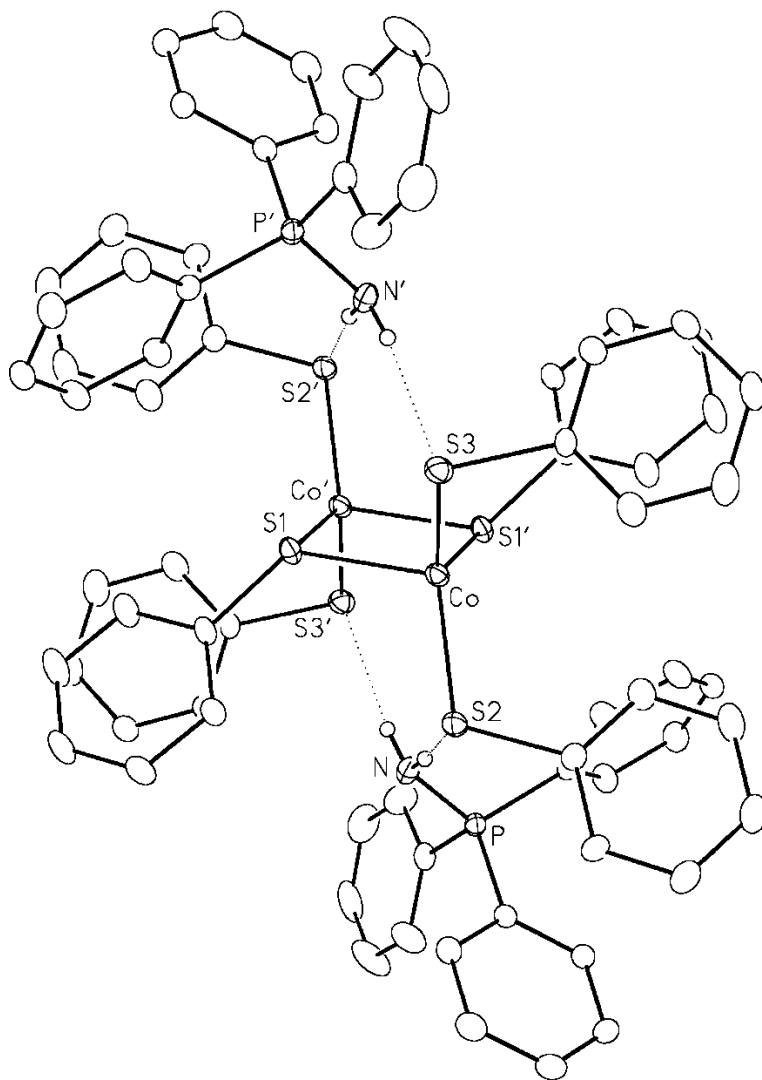
^aObtained from least-squares refinement of 9930 reflections with $4.36^\circ < 2\theta < 54.56^\circ$.

^bPrograms for diffractometer operation, data collection, data reduction and absorption correction were those supplied by Bruker.

^cSheldrick, G. M. *Acta Crystallogr.* **2008**, A64, 112–122.

^d $S = [\sum w(F_o^2 - F_c^2)^2 / (n - p)]^{1/2}$ (n = number of data; p = number of parameters varied;
 $w = [\sigma^2(F_o^2) + (0.0928P)^2 + 4.2481P]^{-1}$ where $P = [\text{Max}(F_o^2, 0) + 2F_c^2] / 3$).

^e $R_1 = \sum ||F_o| - |F_c|| / \sum |F_o|$; $wR_2 = [\sum w(F_o^2 - F_c^2)^2 / \sum w(F_o^4)]^{1/2}$.



A. Crystal Data

formula	C ₇₂ H ₆₄ Co ₂ N ₂ P ₂ S ₆
formula weight	1329.41
crystal dimensions (mm)	0.27 × 0.24 × 0.06
crystal system	triclinic
space group	<i>P</i> $\bar{1}$ (No. 2)
unit cell parameters ^a	
<i>a</i> (Å)	11.6624 (5)
<i>b</i> (Å)	12.1177 (5)
<i>c</i> (Å)	13.6444 (6)
<i>α</i> (deg)	68.3014 (5)
<i>β</i> (deg)	66.2099 (5)

γ (deg)	88.8029 (6)
V (Å ³)	1620.62 (12)
Z	1
ρ_{calcd} (g cm ⁻³)	1.362
μ (mm ⁻¹)	0.798

B. Data Collection and Refinement Conditions

diffractometer	Bruker D8/APEX II CCD ^b
radiation (λ [Å]) (0.71073)	graphite-monochromated Mo K α
temperature (°C)	-100
scan type	ω scans (0.3°) (20 s exposures)
data collection 2θ limit (deg)	53.08
total data collected ≤ 17)	13218 ($-14 \leq h \leq 14$, $-15 \leq k \leq 15$, $-17 \leq l$
independent reflections	6718 ($R_{\text{int}} = 0.0220$)
number of observed reflections (NO)	5367 [$F_o^2 \geq 2\sigma(F_o^2)$]
structure solution method	direct methods (SHELXS-97 ^c)
refinement method	full-matrix least-squares on F^2 (SHELXL-97 ^c)
absorption correction method	Gaussian integration (face-indexed)
range of transmission factors	0.9507–0.8121
data/restraints/parameters	6718 [$F_o^2 \geq -3\sigma(F_o^2)$] / 0 / 441
goodness-of-fit (S) ^d	1.024 [$F_o^2 \geq -3\sigma(F_o^2)$]
final R indices ^e	
R_1 [$F_o^2 \geq 2\sigma(F_o^2)$]	0.0351
wR_2 [$F_o^2 \geq -3\sigma(F_o^2)$]	00.0941
largest difference peak and hole	0.546 and -0.269 e Å ⁻³

^aObtained from least-squares refinement of 6945 reflections with $4.82^\circ < 2\theta < 52.04^\circ$.

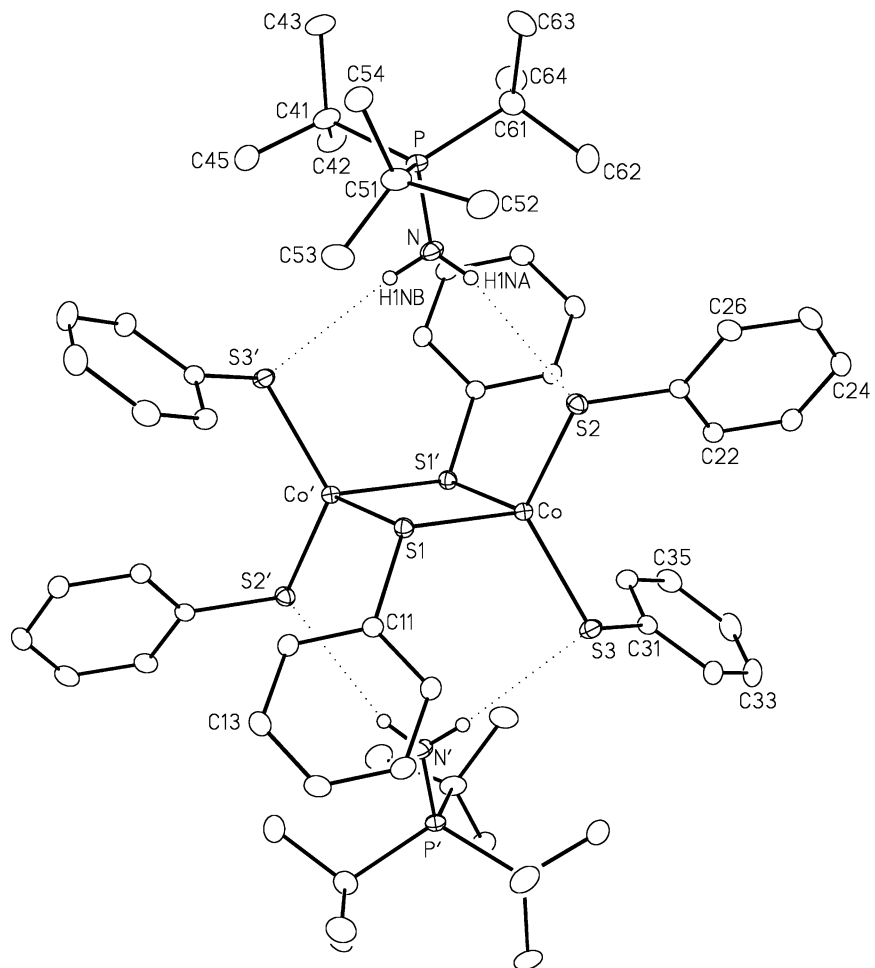
^bPrograms for diffractometer operation, data collection, data reduction and absorption correction were those supplied by Bruker.

^cSheldrick, G. M. *Acta Crystallogr.* **2008**, A64, 112–122.

^d $S = [\sum w(F_o^2 - F_c^2)^2 / (n - p)]^{1/2}$ (n = number of data; p = number of parameters varied; $w = [\sigma^2(F_o^2) + (0.0463P)^2 + 0.5547P]^{-1}$ where $P = [\text{Max}(F_o^2, 0) + 2F_c^2]/3$).

^e $R_1 = \sum ||F_o| - |F_c|| / \sum |F_o|$; $wR_2 = [\sum w(F_o^2 - F_c^2)^2 / \sum w(F_o^4)]^{1/2}$.

S. JMS0942 (382)



A. Crystal Data

formula	C ₆₀ H ₈₈ Co ₂ N ₂ P ₂ S ₆
formula weight	1209.48
crystal dimensions (mm)	0.42 × 0.22 × 0.15
crystal system	triclinic
space group	<i>P</i> $\bar{1}$ (No. 2)
unit cell parameters ^a	
<i>a</i> (Å)	10.4642 (3)
<i>b</i> (Å)	11.8311 (3)
<i>c</i> (Å)	12.8395 (4)
<i>α</i> (deg)	80.312 (1)
<i>β</i> (deg)	81.832 (1)
<i>γ</i> (deg)	84.871 (1)
<i>V</i> (Å ³)	1547.51 (8)
<i>Z</i>	1

ρ_{calcd} (g cm ⁻³)	1.298
μ (mm ⁻¹)	0.828

B. Data Collection and Refinement Conditions

diffractometer	Bruker D8/APEX II CCD ^b
radiation (λ [Å]) (0.71073)	graphite-monochromated Mo K α
temperature (°C)	-100
scan type	ω scans (0.3°) (20 s exposures)
data collection 2θ limit (deg)	54.34
total data collected ≤ 16)	13412 ($-13 \leq h \leq 13$, $-15 \leq k \leq 15$, $-16 \leq l$
independent reflections	6847 ($R_{\text{int}} = 0.0123$)
number of observed reflections (NO)	6186 [$F_o^2 \geq 2\sigma(F_o^2)$]
structure solution method	direct methods (SHELXS-97 ^c)
refinement method	full-matrix least-squares on F^2 (SHELXL-97 ^c)
absorption correction method	Gaussian integration (face-indexed)
range of transmission factors	0.8838–0.7213
data/restraints/parameters	6847 [$F_o^2 \geq -3\sigma(F_o^2)$] / 0 / 333
goodness-of-fit (S) ^d	1.057 [$F_o^2 \geq -3\sigma(F_o^2)$]
final R indices ^e	
R_1 [$F_o^2 \geq 2\sigma(F_o^2)$]	0.0311
wR_2 [$F_o^2 \geq -3\sigma(F_o^2)$]	0.0909
largest difference peak and hole	0.720 and -0.245 e Å ⁻³

^aObtained from least-squares refinement of 9896 reflections with $5.10^\circ < 2\theta < 54.28^\circ$.

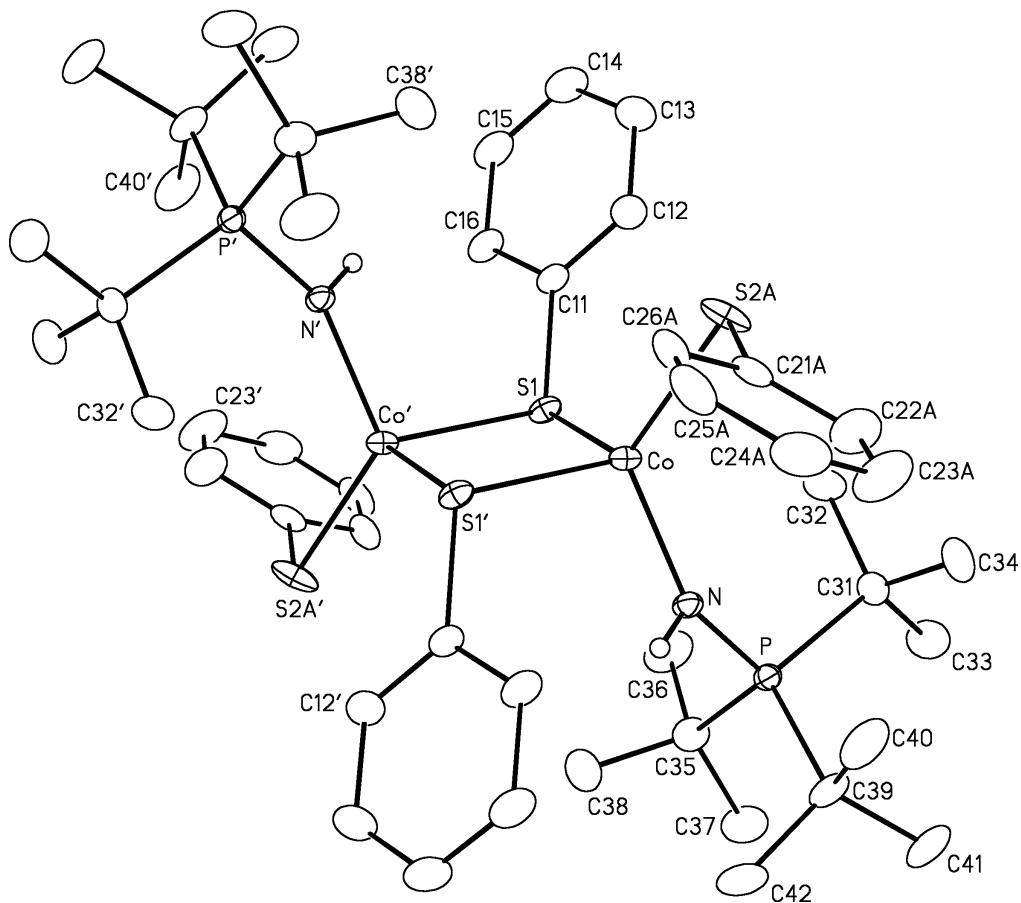
^bPrograms for diffractometer operation, data collection, data reduction and absorption correction were those supplied by Bruker.

^cSheldrick, G. M. *Acta Crystallogr.* **2008**, A64, 112–122.

^d $S = [\sum w(F_o^2 - F_c^2)^2 / (n - p)]^{1/2}$ (n = number of data; p = number of parameters varied; $w = [\sigma^2(F_o^2) + (0.0527P)^2 + 0.6445P]^{-1}$ where $P = [\text{Max}(F_o^2, 0) + 2F_c^2] / 3$).

^e $R_1 = \sum ||F_o| - |F_c|| / \sum |F_o|$; $wR_2 = [\sum w(F_o^2 - F_c^2)^2 / \sum w(F_o^4)]^{1/2}$.

T. JMS0971 (383)



A. Crystal Data

formula	C ₄₈ H ₇₆ Co ₂ N ₂ P ₂ S ₄
formula weight	989.15
crystal dimensions (mm)	0.62 × 0.51 × 0.43
crystal system	monoclinic
space group	<i>P</i> 2 ₁ / <i>n</i> (an alternate setting of <i>P</i> 2 ₁ / <i>c</i>)
[No. 14]	
unit cell parameters ^a	
<i>a</i> (Å)	11.0342 (5)
<i>b</i> (Å)	13.7706 (6)
<i>c</i> (Å)	16.9627 (7)
β (deg)	91.8050 (10)
<i>V</i> (Å ³)	2576.16 (19)
<i>Z</i>	2
<i>ρ</i> _{calcd} (g cm ⁻³)	1.275
<i>μ</i> (mm ⁻¹)	0.901

B. Data Collection and Refinement Conditions

diffractometer	Bruker D8/APEX II CCD ^b
radiation (λ [Å]) (0.71073)	graphite-monochromated Mo K α
temperature (°C)	–100
scan type	ω scans (0.4°) (10 s exposures)
data collection 2θ limit (deg)	55.10
total data collected ≤ 22)	16678 ($-14 \leq h \leq 12$, $-17 \leq k \leq 16$, $-22 \leq l$
independent reflections	5862 ($R_{\text{int}} = 0.0136$)
number of observed reflections (NO)	5189 [$F_o^2 \geq 2\sigma(F_o^2)$]
structure solution method	direct methods (SIR97 ^c)
refinement method 97 ^d)	full-matrix least-squares on F^2 (SHELXL–
absorption correction method	multi-scan (SADABS)
range of transmission factors	0.6819–0.5911
data/restraints/parameters	5862 [$F_o^2 \geq -3\sigma(F_o^2)$] / 13 ^e / 289
goodness-of-fit (S) ^f	1.027 [$F_o^2 \geq -3\sigma(F_o^2)$]
final R indices ^g	
R_1 [$F_o^2 \geq 2\sigma(F_o^2)$]	0.0302
wR_2 [$F_o^2 \geq -3\sigma(F_o^2)$]	0.0825
largest difference peak and hole	0.472 and –0.523 e Å ^{–3}

^aObtained from least-squares refinement of 9886 reflections with $4.80^\circ < 2\theta < 55.06^\circ$.

^bPrograms for diffractometer operation, data collection, data reduction and absorption correction were those supplied by Bruker.

^cAltomare, A.; Burla, M. C.; Camalli, M.; Cascarano, G. L.; Giacovazzo, C.; Guagliardi, A.; Moliterni, A. G. G.; Polidori, G.; Spagna, R. *J. Appl. Cryst.* **1999**, *32*, 115–119.

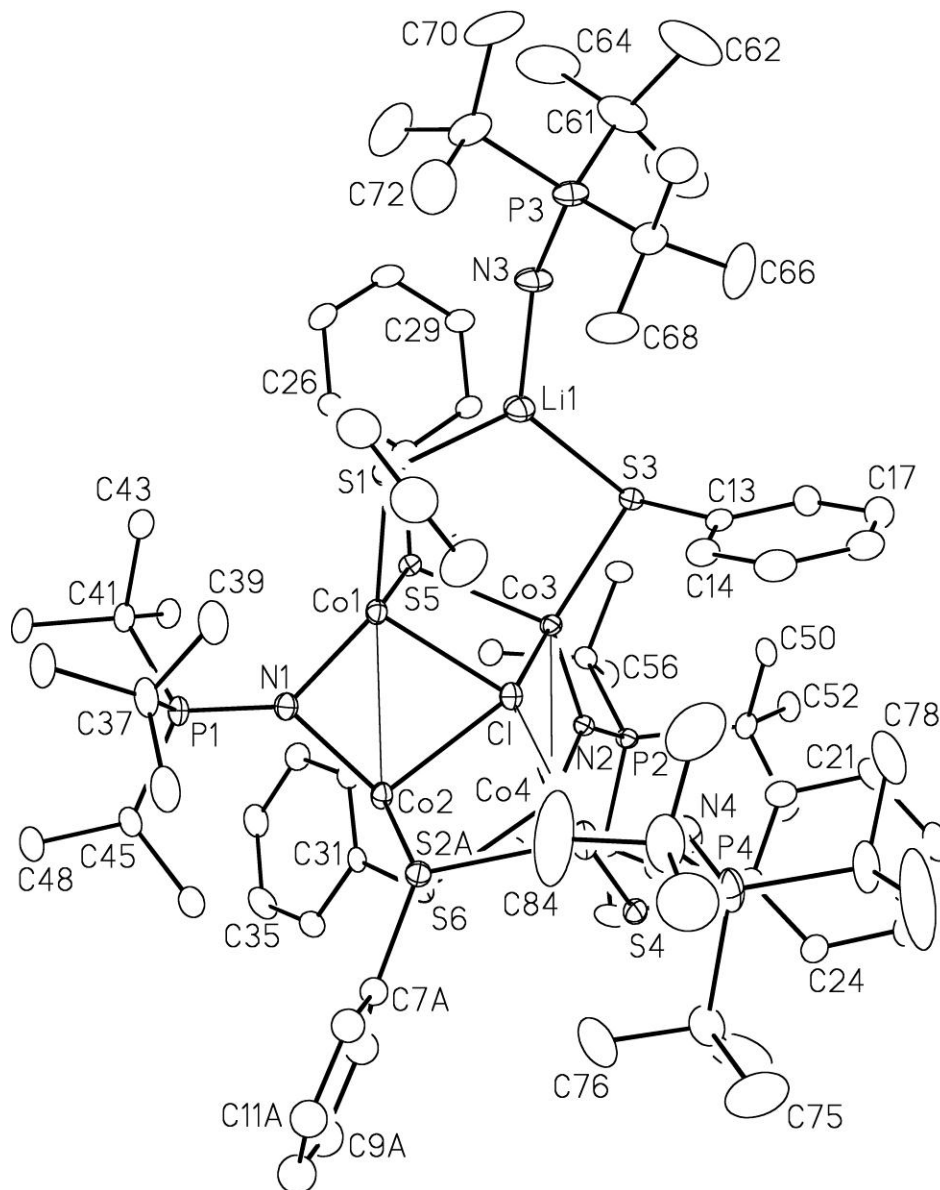
^dSheldrick, G. M. *Acta Crystallogr.* **2008**, *A64*, 112–122.

^eThe phenyl group in minor orientation for the disordered thiophenyl ligand was restrained to have the same geometry as that of the major orientation during refinement by use of the SHELXL **SAME** instruction. Additionally, the S2B..C22B distance was restrained to be 2.75 (1) Å.

$fS = [\sum w(F_o^2 - F_c^2)^2 / (n - p)]^{1/2}$ (n = number of data; p = number of parameters varied; $w = [\sigma^2(F_o^2) + (0.0403P)^2 + 1.3077P]^{-1}$ where $P = [\text{Max}(F_o^2, 0) + 2F_c^2] / 3$).

$gR_1 = \sum ||F_o| - |F_c|| / \sum |F_o|$; $wR_2 = [\sum w(F_o^2 - F_c^2)^2 / \sum w(F_o^4)]^{1/2}$.

U. JMS978 (384)



A. Crystal Data

formula	$C_{91.5}H_{156}ClCo_4Li_2N_4P_4S_6$
formula weight	1913.49
crystal dimensions (mm)	$0.27 \times 0.19 \times 0.17$
crystal system	monoclinic
space group	$P2_1/c$ (No. 14)
unit cell parameters ^a	
<i>a</i> (Å)	28.006 (3)
<i>b</i> (Å)	17.4021 (15)

c (Å)	23.091 (2)
β (deg)	113.8959 (12)
V (Å ³)	10289.3 (16)
Z	4
ρ_{calcd} (g cm ⁻³)	1.235
μ (mm ⁻¹)	0.886

B. Data Collection and Refinement Conditions

diffractometer	Bruker D8 /APEX II CCD ^b
radiation (λ [Å]) (0.71073)	graphite-monochromated Mo K α
temperature (°C)	−100
scan type	ω scans (0.3°) (20 s exposures)
data collection 2θ limit (deg)	51.66
total data collected ≤ 28)	75956 ($-34 \leq h \leq 34, -21 \leq k \leq 21, -28 \leq l$
independent reflections	19723 ($R_{\text{int}} = 0.0718$)
number of observed reflections (NO)	14668 [$F_o^2 \geq 2\sigma(F_o^2)$]
structure solution method	direct methods (<i>SHELXS-97</i> ^c)
refinement method <i>97c,d</i>)	full-matrix least-squares on F^2 (<i>SHELXL-</i>
absorption correction method	Gaussian integration (face-indexed)
range of transmission factors	0.8669–0.7966
data/restraints/parameters	19723 / 14 ^e / 940
goodness-of-fit (S) ^f [all data]	1.114
final R indices ^g	
R_1 [$F_o^2 \geq 2\sigma(F_o^2)$]	0.0720
wR_2 [all data]	0.1743
largest difference peak and hole	1.034 and −0.644 e Å ⁻³

^aObtained from least-squares refinement of 7410 reflections with $4.52^\circ < 2\theta < 43.98^\circ$.

^bPrograms for diffractometer operation, data collection, data reduction and absorption correction were those supplied by Bruker.

^cSheldrick, G. M. *Acta Crystallogr.* **2008**, *A64*, 112–122.

^dAttempts to refine peaks of residual electron density as disordered or partial-occupancy solvent *n*-pentane carbon atoms were unsuccessful. The data were corrected for disordered electron density through use of the SQUEEZE procedure (Sluis, P. van der; Spek, A. L. *Acta Crystallogr.* **1990**, *A46*, 194–201) as implemented in *PLATON* (Spek, A. L. *Acta Crystallogr.* **1990**, *A46*, C34; Spek, A. L. *J. Appl. Cryst.* **2003**, *36*, 7–13. *PLATON* - a multipurpose crystallographic tool. Utrecht University, Utrecht, The Netherlands). A total solvent-accessible void volume of 632.9 Å³ with a total electron count of 104 (consistent with 2 molecules of solvent *n*-pentane, or

0.5 molecules per formula unit of the tetracobalt complex molecule) was found in the unit cell, in addition to the disordered solvent *n*-pentane molecule that was located and refined.

^eDistances within the disordered solvent *n*-pentane molecule were restrained during refinement: $d(\text{C11S}-\text{C12S}) = d(\text{C12S}-\text{C13S}) = d(\text{C13S}-\text{C14S}) = d(\text{C14S}-\text{C15S}) = d(\text{C21S}-\text{C22S}) = d(\text{C22S}-\text{C23S}) = d(\text{C23S}-\text{C24S}) = d(\text{C24S}-\text{C15S}) = 1.52(1) \text{ \AA}$; $d(\text{C11S}\cdots\text{C13S}) = d(\text{C12S}\cdots\text{C14S}) = d(\text{C13S}\cdots\text{C15S}) = d(\text{C21S}\cdots\text{C23S}) = d(\text{C22S}\cdots\text{C14S}) = d(\text{C23S}\cdots\text{C25S}) = 2.52(1) \text{ \AA}$.

$fS = [\sum w(F_o^2 - F_c^2)^2 / (n - p)]^{1/2}$ (n = number of data; p = number of parameters varied; $w = [\sigma^2(F_o^2) + (0.0520P)^2 + 35.3683P]^{-1}$ where $P = [\text{Max}(F_o^2, 0) + 2F_c^2]/3$).

$gR_1 = \sum ||F_o| - |F_c|| / \sum |F_o|$; $wR_2 = [\sum w(F_o^2 - F_c^2)^2 / \sum w(F_o^4)]^{1/2}$.